ISSN 0021-9673

VOL. 607 NO. 2 AUGUST 28, 1992
THIS ISSUE COMPLETES VOL. 607

20th Sci. Meet. of the Spanish Group of Chromatography and Related Techniques San Sebastián-Donostia, Oct. 29–31, 1991

JOURNAL OF CHROMATOGRAPHY

INCLUDING ELECTROPHORESIS AND OTHER SEPARATION METHODS

SYMPOSIUM VOLUMES

ELSEVIER

JOURNAL OF CHROMATOGRAPHY

INCLUDING ELECTROPHORESIS AND OTHER SEPARATION METHODS

Scope. The *Journal of Chromatography* publishes papers on all aspects of chromatography, electrophoresis and related methods. Contributions consist mainly of research papers dealing with chromatographic theory, instrumental development and their applications. The section *Biomedical Applications*, which is under separate editorship, deals with the following aspects: developments in and applications of chromatographic and electrophoretic techniques related to clinical diagnosis or alterations during medical treatment; screening and profiling of body fluids or tissues with special reference to metabolic disorders; results from basic medical research with direct consequences in clinical practice; drug level monitoring and pharmacokinetic studies; clinical toxicology; analytical studies in occupational medicine.

Submission of Papers. Manuscripts (in English; *four* copies are required) should be submitted to: Editorial Office of *Journal of Chromatography*, P.O. Box 681, 1000 AR Amsterdam, Netherlands, Telefax (+31-20) 5862 304, or to: The Editor of *Journal of Chromatography, Biomedical Applications*, P.O. Box 681, 1000 AR Amsterdam, Netherlands. Review articles are invited or proposed by letter to the Editors. An outline of the proposed review should first be forwarded to the Editors for preliminary discussion prior to preparation. Submission of an article is understood to imply that the article is original and unpublished and is not being considered for publication elsewhere. For copyright regulations, see below.

Publication. The *Journal of Chromatography* (incl. *Biomedical Applications*) has 39 volumes in 1992. The subscription prices for 1992 are:

J. Chromatogr. (incl. *Cum. Indexes, Vols. 551–600*) + *Biomed. Appl.* (Vols. 573–611):
Dfl. 7722.00 plus Dfl. 1209.00 (p.p.h.) (total *ca.* US$ 4880.25)

J. Chromatogr. (incl. *Cum. Indexes, Vols. 551–600*) only (Vols. 585–611):
Dfl. 6210.00 plus Dfl. 837.00 (p.p.h.) (total *ca.* US$ 3850.75)

Biomed. Appl. only (Vols. 573–584):
Dfl. 2760.00 plus Dfl. 372.00 (p.p.h.) (total *ca.* US$ 1711.50).

Subscription Orders. The Dutch guilder price is definitive. The US$ price is subject to exchange-rate fluctuations and is given as a guide. Subscriptions are accepted on a prepaid basis only, unless different terms have been previously agreed upon. Subscriptions can be entered only by calender year (Jan.–Dec.) and should be sent to Elsevier Science Publishers, Journal Department, P.O. Box 211, 1000 AE Amsterdam, Netherlands, Tel. (+31-20) 5803 642, Telefax (+31-20) 5803 598, or to your usual subscription agent. Postage and handling charges include surface delivery except to the following countries where air delivery via SAL (Surface Air Lift) mail is ensured: Argentina, Australia, Brazil, Canada, China, Hong Kong, India, Israel, Japan*, Malaysia, Mexico, New Zealand, Pakistan, Singapore, South Africa, South Korea, Taiwan, Thailand, USA. *For Japan air delivery (SAL) requires 25% additional charge of the normal postage and handling charge. For all other countries airmail rates are available upon request. Claims for missing issues must be made within three months of our publication (mailing) date, otherwise such claims cannot be honoured free of charge. Back volumes of the *Journal of Chromatography* (Vols. 1–572) are available at Dfl. 217.00 (plus postage). Customers in the USA and Canada wishing information on this and other Elsevier journals, please contact Journal Information Center, Elsevier Science Publishing Co. Inc., 655 Avenue of the Americas, New York, NY 10010, USA, Tel. (+1-212) 633 3750, Telefax (+1-212) 633 3990.

Abstracts/Contents Lists published in Analytical Abstracts, Biochemical Abstracts, Biological Abstracts, Chemical Abstracts, Chemical Titles, Chromatography Abstracts, Clinical Chemistry Lookout, Current Awareness in Biological Sciences (CABS), Current Contents/Life Sciences, Current Contents/Physical, Chemical & Earth Sciences, Deep-Sea Research/Part B: Oceanographic Literature Review, Excerpta Medica, Index Medicus, Mass Spectrometry Bulletin, PASCAL-CNRS, Pharmaceutical Abstracts, Referativnyi Zhurnal, Research Alert, Science Citation Index and Trends in Biotechnology.

US Mailing Notice. *Journal of Chromatography* (main section ISSN 0021-9673, *Biomedical Applications* section ISSN 0378-4347) is published (78 issues/year) by Elsevier Science Publishers (Sara Burgerhartstraat 25, P.O. Box 211, 1000 AE Amsterdam, Netherlands). Annual subscription price in the USA US$ 4880.25 (subject to change), including air speed delivery. Application to mail at second class postage rate is pending at Jamaica, NY 11431. **USA POSTMASTERS:** Send address changes to *Journal of Chromatography*, Publications Expediting, Inc., 200 Meacham Avenue, Elmont, NY 11003. Airfreight and mailing in the USA by Publication Expediting.

See inside back cover for Publication Schedule, Information for Authors and information on Advertisements.

0021-9673/92/$05.00

Printed in the Netherlands

For Contents, see p. 171

SYMPOSIUM ISSUE

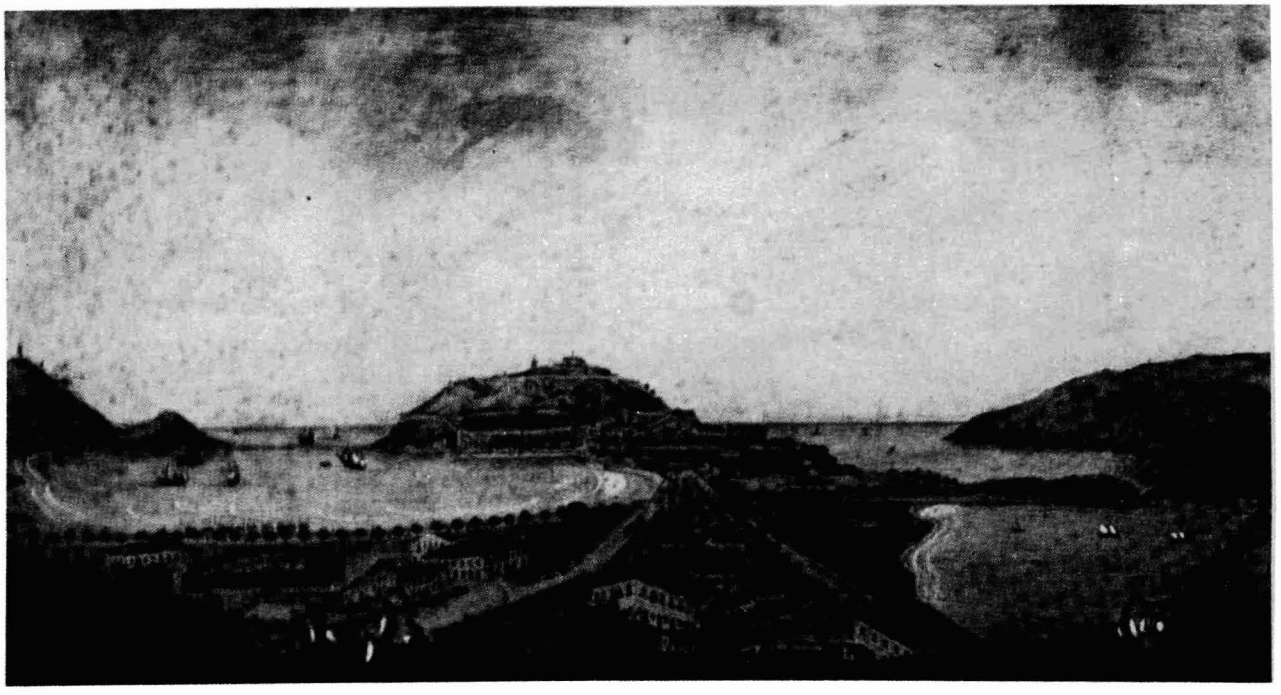

20TH SCIENTIFIC MEETING OF THE GROUP OF CHROMATOGRAPHY AND RELATED TECHNIQUES OF THE SPANISH ROYAL SOCIETY OF CHEMISTRY

San Sebastián-Donostia (Spain), October 29–31, 1991

Guest Editors

E. GELPÍ
(Barcelona)

J. O. GRIMALT
(Barcelona)

CONTENTS

In articles with more than one author, the name of the author to whom correspondence should be addressed is indicated in the article heading by a 6-pointed asterisk (*).

Journal of Chromatography, 607 (1992) 173
Elsevier Science Publishers B.V., Amsterdam

CHROM. 24 472

Foreword

The 20th Annual Scientific Meeting of the Grupo de Cromatografía y Técnicas Afines (GCTA or Group of Chromatography and Related Techniques) of the Spanish Royal Society of Chemistry was held from October 29 to 31, 1991, in the quiet and beautiful city of San Sebastián in Guipuzkoa, northern Spain. This historically rich city is known as a world famous tourist attraction, mostly for its beautiful bay and the surrounding coastal and mountain villages of Euskal Herria (Basque Country).

The meeting took place in the incomparable setting of the Palacio de Miramar which marks the historic origin of the city as well as the place where its two famous beaches Ondarreta and La Concha meet under the sentinel watch of Mounts Urgull and Igeldo. It was the 20th in a series of yearly meetings since the constitution of the GCTA which has now more than 600 members from academia and industry all over Spain. On this occasion it was attended by 200 chromatographers who presented a total of 108 communications and had the opportunity of listening to interesting invited lectures by R. Majors (Column technology), J. S. Sinninghe Damsté (Pyrolysis–gas chromatography–mass spectrometry), K. Grob (On-line liquid chromatography–gas chromatography) and A. F. Fell (Computer-aided liquid chromatography detection). These scientific presentations were complemented by round table and poster discussion sessions, which were well attended at all times. Perhaps one of the most noteworthy aspects to be underlined is the importance of the publication of this issue for Spanish chromatography. As part of an effort to elicit publications from attendees to these national meetings and to raise scientific standards, the call for papers issued before the meeting included for the first time an announcement explaining that all qualifying papers presented at the 20th GCTA meeting would be collected and published in the *Journal of Chromatography*. It is really gratifying to see that out of the 108 scientific communications presented at the meeting, a total of 40 were submitted for publication and that of these 27 have made it to the final stage and 26 are included in this issue. We have always been of the opinion that there is more chromatographic activity in Spain than is reflected in actual publications in journals. In this regard we feel that one of our most rewarding tasks is to bring potentially publishable contributions to light. We trust that this publication will encourage other authors engaged in high-quality research to publish their work and contribute to strengthen the position of the chromatographic sciences in our country.

Also, we would like to thank the Organizing Committee for their efforts to ensure a most enjoyable meeting both from a scientific and a social viewpoint, and we particularly wish to express our thanks and congratulations to Dr. Carmen Dorronsoro who, as Secretary of the event, demonstrated her superb organizational skills. Thanks are also due to all sponsoring organizations, specially those of the Basque Government and Institutions for their generous support.

Barcelona (Spain)

Emilio Gelpí
Joan Grimalt

Journal of Chromatography, 607 (1992) 175–181
Elsevier Science Publishers B.V., Amsterdam

CHROM. 24 142

Use of methyl and ethyl acetate as organic modifiers in reversed-phase high-performance liquid chromatography

Application to impurity control in bulk drug steroids

J. L. Bernal*, M. J. Del Nozal and G. A. García Buj

Department of Analytical Chemistry, Faculty of Sciences, University of Valladolid, E-47005 Valladolid (Spain)

J. Martín Juárez

Quality Control Department, CESQUISA, Apdo. 190, E-40154 Perogordo, Segovia (Spain)

ABSTRACT

We assayed methyl and ethyl acetate as organic modifiers for mobile phases used in reversed-phase high-performance liquid chromatography for the removal of impurities from steroids of pharmaceutical interest. By using ternary mobile phases consisting of one of the esters, water and a third component that was miscible with both and applying a systematic experimental methodology, we developed an optimal procedure for the isolation of the compound of interest (9α-fluoroprednisolone acetate) from the impurities resulting from its synthesis in a minimum time. Inclusion of an acetic ester in the reversed-phase high-performance liquid chromatographic mobile phase was found to improve the resolution of chemically similar substances.

INTRODUCTION

Methyl and particularly ethyl acetate have been frequently used in mobile phases for normal-phase high-performance liquid chromatography (HPLC) in order to modify the eluting power and selectivity of the technique, and hence facilitate separations [1–3]. However, they have only rarely been used as modifiers in reversed-phase (RP) HPLC.

One of the potential reasons for the infrequent use of acetic esters in RP-HPLC may be their marked absorption in a broad region of the ultraviolet spectrum. Methyl and ethyl acetate are virtually opaque to wavelengths below 256 nm, unlike other solvents commonly used in RP-HPLC [*e.g.* methanol (205 nm), acetonitrile (190 nm) and tetrahydrofuran (212 nm)] [4]. This implies that both solvents have to be used in amounts small enough to avoid interfering with the detection of the compounds of interest. As shown below, the high eluting power of these esters and the risk of forming immiscible phases compels the use of quite low concentrations in the mobile phase, which poses no technical problem on the analyses in our case.

The main reason why esters have systematically been avoided in RP-HPLC probably lies in their immiscibility with water, which is without doubt the most frequently employed eluent in this chromatographic mode. However, the miscibility of an ester–water system can be increased by using a third solvent provided that it is miscible with both the ester and water.

The third solvent in question is normally chosen in such a way as to ensure the maximum possible difference in selectivity between the three in order to obtain maximal differences in the behaviour of the mixtures to be dealt with and hence find the optimal conditions for their resolution. On Snyder's [5]

0021-9673/92/$05.00

selectivity triangle, aliphatic esters, like acetonitrile, belong to group VIa, while water belongs to group VII. Choosing methanol as the third solvent therefore seems appropriate inasmuch as it is fully miscible with the other two and belongs to selectivity group II, which is distant enough from the other two for the selectivity of the resulting mobile phase to vary markedly with its composition.

The effect of the acetic esters as organic modifiers was studied on the resolution of a mixture of nine steroids by RP-HPLC. Because of the synthetic procedure used for its preparation, 9α-fluoroprednisolone acetate (FPA) can be accompanied by the impurities shown in Fig. 1 [6]. In a previous work [7] we developed a procedure to determine the optimal composition of the ternary mobile phase and applied

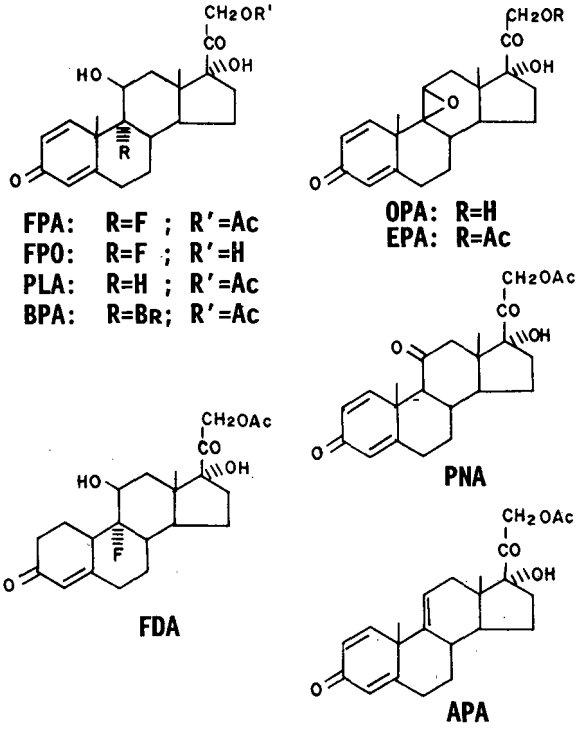

Fig. 1. Chemical structures of 9α-fluoroprednisolone and its related impurities resulting from its synthesis process. FPA = 9α-fluoroprednisolone acetate; FPO = 9α-fluoroprednisolone; PLA = prednisolone acetate; BPA = 9α-bromoprednisolone acetate; FDA = fludrocortisone acetate; PNA = prednisone acetate; OPA = 9β,11β-epoxy-17α,21-dihydroxypregne-1,4-dien-3,20-dione; EPA = 9β,11β-epoxy-17α-hydroxypregne-1,4-dien-3,20-dione 21-acetate; APA = 17α-hydroxypregne-1,4,9 (11)-trien-3,20-dione 21-acetate. Ac = Acetyl.

it to the acetonitrile–tetrahydrofuran–water system for the complete isolation of FPA from its related impurities. The reason for using the same type of sample here was the possibility of determining whether the acetic esters offer any advantages in terms of selectivity or rapidity. The procedure applied here was similar, but involved mobile phases including one of the acetic esters. Also, the impurities contest of the synthesized steroid must be reduced to less than 1 in 1000 in order to comply with the recommendations from most pharmacopeias [8,9].

EXPERIMENTAL

The chromatographic set-up used consisted of a CM4000 multiple solvent partitioning pump and an SM5000 photodiode-array detector, both from LDC Analytical (Riviera Beach, FL, USA). Data were processed and integrated with the aid of ThermoChrom PDA software, also from LDC Analytical. Samples were injected by means of a Rheodyne 7125 injector (Cotati, CA, USA) with a fixed-volume loop of 20 μl. The mobile phase was thoroughly homogenized prior to reaching the column by using a dynamic mixer (Dinamixer from LDC Analytical) immediately before the injector. Calculations were done and plots constructed with the aid of commercially available computer software.

The solvents used included methanol (Scharlau, Barcelona, Spain), ethyl acetate (SDS, Peypin, France) and methyl acetate (Fluka, Buchs, Switzerland), all of which were of HPLC grade. The water used was purified by passage through a Nanopure II system from Barnstead (Newton, MA, USA). All eluents were filtered through 0.5 μm mesh and degassed by bubbling with helium. The column used was a Spherisorb octadecylsilane (ODS) column, 5 μm particle size, 150 m × 0.46 mm I.D., supplied by Phenomenex (Torrance, CA, USA).

Chromatograms were recorded at a flow-rate of 1 ml/min and room temperature (*ca.* 20°C). The dead time (1.4 min) was the same for all the mobile phases assayed and was assigned to the first baseline distortion observed upon injection of pure acetonitrile. Steroids standards were supplied by Cesquisa (Segovia, Spain) and were dissolved in HPLC-grade acetonitrile (SDS) at a concentration of 1000 mg/l in

FPA and 1 mg/l in all of the other components except for 9β,11β-epoxy-17α,21-dihydroxypregne-1,4-dien-3,20-dione (OPA), the concentration of which was 0.1 mg/l.

RESULTS AND DISCUSSION

Construction of the phase diagrams

First, we determined which compositions of the mobile phase can be used. The range of useful concentrations was constrained by the partial immiscibility of the phase components. This involved examining the phase equilibrium diagrams of the systems as compiled by Sörensen and Artl [10]. We strived to maintain the retention of all the compounds to be resolved within a preset range given by $1 < k' < 100$, where k' is the so-called "capacity factor". The range in question was determined experimentally because the solvent strength parameter of the acetic acid esters in reversed phase was unknown.

The phase diagram of the ethyl acetate–methanol–water system was obtained by converting the experimental data reported by Beech and Glasstone [12] into percentage volumes by using the molecular masses and densities of the components at 20°C (Fig. 2).

We found no phase diagram in the literature for the methyl acetate–methanol–water system with the exception of an approximate description by Craw-

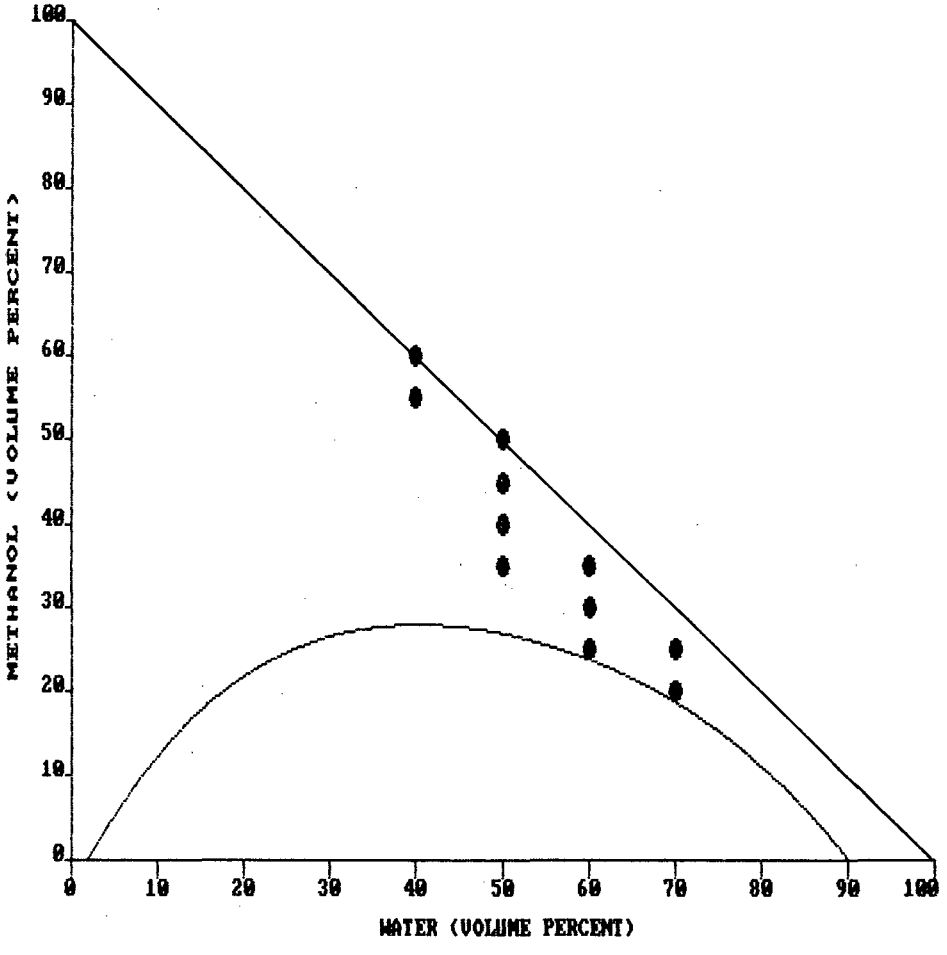

Fig. 2. Phase diagram and experimental design points for the ethyl acetate–methanol–water mobile phase.

ford *et al.* [13], which was used as a reference for precise construction of the diagram.

For convenience, we chose to use isoceles rectangular triangles, which can accommodate the Cartesian coordinates for two of the components, the composition of the third being obtained by difference.

Study of the ethyl acetate–methanol–water mobile phase

The optimization procedure used involved the construction of three-dimensional window diagrams. The response surface (*viz.* the minimal resolution *vs.* the composition of the mobile phase) was obtained from the equation of Schoenmaker *et al.* [11], which correlates retention and composition:

$$\log k' = A_1\varphi_1 + A_2\varphi_2 + B_1\varphi_1^2 + B_2\varphi_2^2 + C_{\varphi_1\varphi_2} + D \quad (1)$$

where φ_1 and φ_2 denote the volume fractions of methanol and ester, respectively, k' is the capacity factor for each solute in the sample and A–D are constants. The coefficients of eqn. 1 can be calculated by multiple regression from the data points obtained in the experimental design. From this point, one can develop a mathematical relation between the resolution (R_s) of the chromatographic peaks corresponding to two of the steroids assayed and the composition of the mobile phase since the resolution and the capacity factor are related through the well known equation:

$$R_s = \frac{1}{4}\sqrt{N}\left(\frac{\alpha - 1}{\alpha}\right)\left(\frac{k'_2}{1 + k'_2}\right) \quad (2)$$

where N is assumed to be constant for all compositions of the mobile phase and was estimated to be 4000 theoretical plates from several experimental determinations. By plotting the minimal resolution between FPA and each related impurity as a function of the composition of the ternary mobile phase a three-dimensional window diagram is obtained.

A window diagram features two essential parameters. One is the minimal resolution, which must be greater than 1.5 (*viz.* the limit for correct resolution of components present in a ratio of 1000:1). The other is the analysis time, which is taken as the time required for the last steroid to be eluted and should therefore be as short as possible.

We obtained the chromatograms of the mobile phases whose compositions and positions in the diagram are reflected in Fig. 2. Each composition yielded a chromatogram in which retention data obtained for each compound provided points for the experimental design and were used to calculate the coefficients of eqn. 1 by multiple regression analysis.

For a given water content in the mixture, the analysis time increases with decreasing proportion of ethyl acetate in the mixture. This is quite logical because ethyl acetate is less polar than methanol and hence has a higher reversed-phase eluting power. As regards the variation in the selectivity of the mobile phase with its composition, it occurs at peak overlapping. For a water content of 50%, 9α-bromoprednisolone acetate (BPA) is eluted before 9β,11β-epoxy-17α-hydroxypregne-1,4-dien-3,20-dione 21-acetate (EPA) at low methyl acetate contents then both peaks converge until co-elution, and EPA is eluted before BPA at high ethyl acetate content. Even more interesting is the variation pattern of the selectivity for the mobile phases containing 60% water since these involve the compound of interest (FPA). We studied no mobile phases containing 40% methanol and 60% water because they resulted in rather long retention times; however, in a previous work [7] we found that FPA is eluted before FDA, prednisolone acetate (PLA) and prednisone acetate (PNA) under these conditions. On increasing the proportion of ethyl acetate at the expense of methanol, the PLA and PNA peaks approach that of FPA to the point of co-elution and later both PLA and PNA are eluted before the steroid of interest.

From the experimental data gathered one can conclude that a 2:58:40 (v/v/v) ethyl acetate–methanol–water mixture provides a minimal resolution of 1.5 (estimated value, 1.6) between FPA and the other compounds in the shortest possible time (6.8 min) Fig. 3 shows the variation in the expected minimal resolution with the composition of the mobile phase. The chromatogram obtained with this mobile phase is shown in Fig. 4. As can be seen, the resolution of FPA is quite rapid and complete, at the expense of more extensive overlap between the other components.

Table I lists the estimated and experimental analysis times and minimal resolutions obtained with this mobile phase. As can be seen, the two sets of data are quite consistent, particularly at the

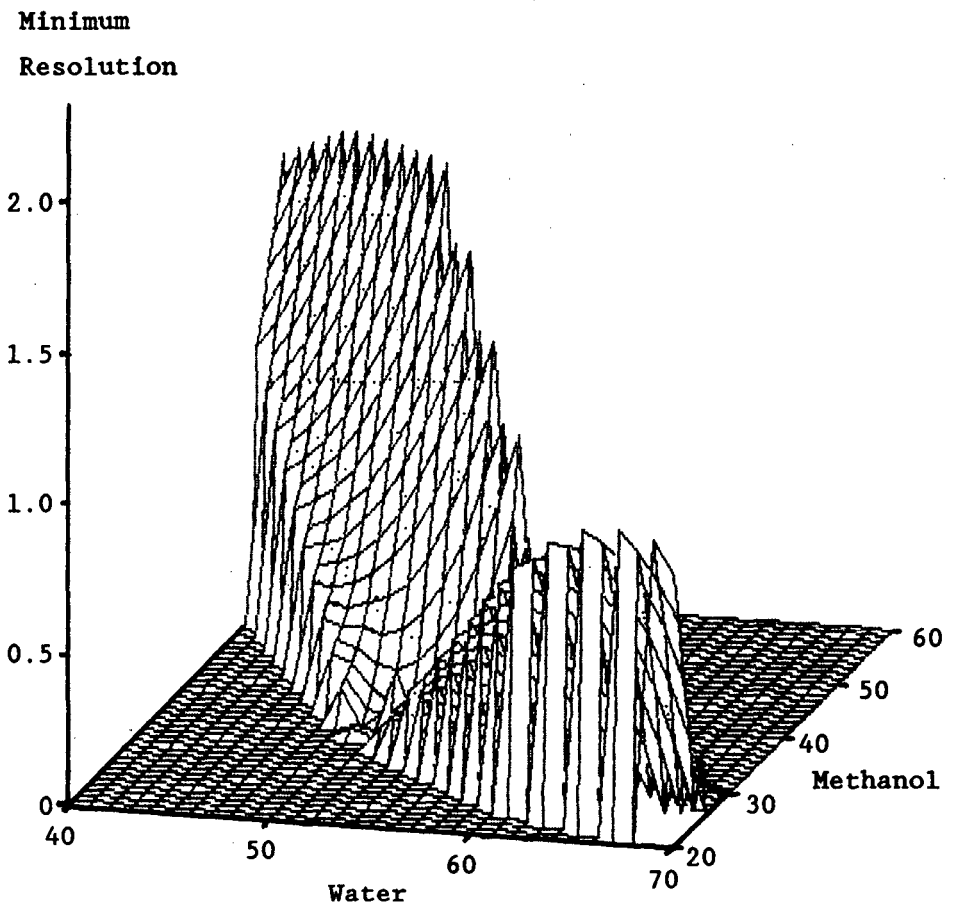

Fig. 3. Variation in the minimal resolution between FPA and its impurities as a function of the mobile phase composition for the ethyl acetate–methanol–water system. Water and methanol scales in %(v/v).

shorter analysis times. The divergences observed at very low resolution can be disregarded since resolution smaller than 0.5 result in a thorough peak overlap and hence prevent experimental determination of the minimal resolution.

Study of the methyl acetate–methanol–water mobile phase

The procedure used was identical to that followed for the previous phase. Like ethyl acetate, methyl acetate has reversed-phase eluting power that is slightly higher than that of methanol and slightly lower than that of the ethyl ester because of the higher polar character endowed by the methyl group compared with the ethyl group, which is somewhat bulkier. As far as the selectivity is concerned, peak overlap is similar, though less marked than that encountered with ethyl acetate, as one would expect from the chemical similarity between the two esters.

The optimal composition for this mobile phase was methyl acetate–methanol–water (3:57:40, v/v/v). This yielded a minimal resolution of 1.5 and an expected chromatographic analysis time of 6.6 min.

CONCLUSIONS

By including acetic esters as modifiers of mobile phases used in reversed-phase liquid chromatography, the analysis times can be substantially shortened, particularly if ethyl acetate is used. Also, they

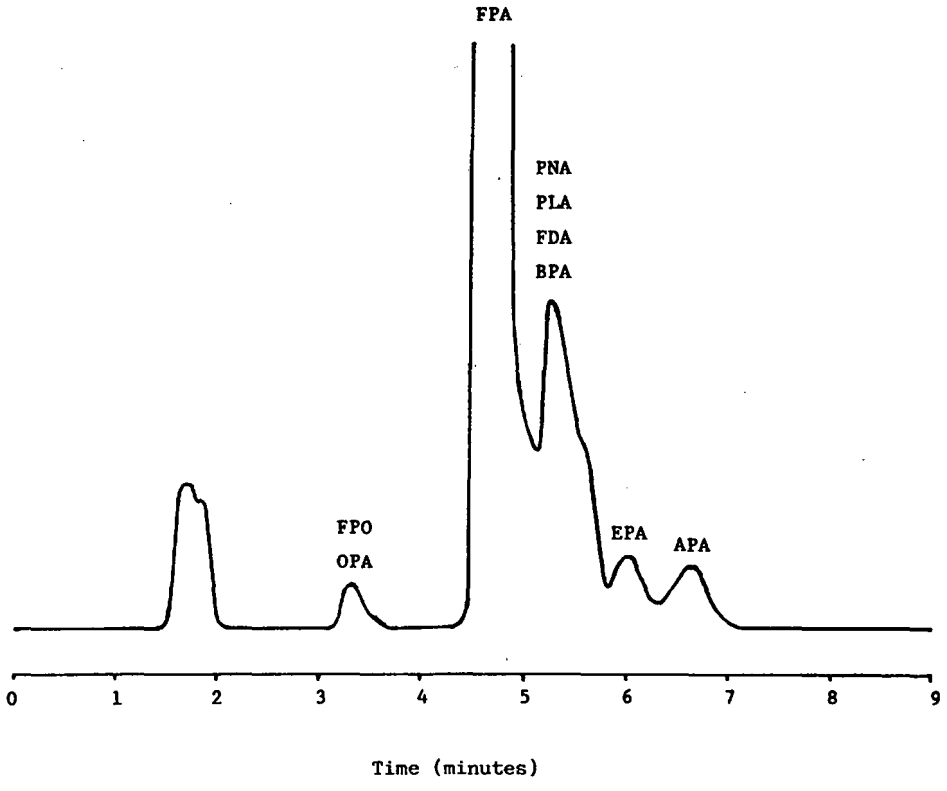

Fig. 4. Chromatogram obtained from a mixture of standards at 1000 mg/l in FPA and 1 mg/l in the other components (except OPA 0.1 mg/l). Mobile phase: ethyl acetate–methanol–water (2:58:40, v/v/v).

TABLE I

RETENTION TIMES AND MINIMUM RESOLUTION OBSERVED AND PREDICTED WITH THE MODEL OF EVERY COMPOSITION SPECIFIED IN FIG. 2

t_{obs} = Observed analysis time; t_{prd} = predicted analysis time with the model; R_{obs} = observed minimum resolution for FPA; R_{prd} = predicted minimum resolution with the model for FOA.

Eluent composition (%, v/v/v): ethyl acetate–methanol–water	t_{obs} (min)	t_{prd} (min)	R_{obs}	R_{prd}
00:60:40	8.3	8.8	1.81	1.94
05:55:40	5.2	5.0	1.44	1.19
00:50:50	24.1	23.1	2.15	2.23
05:45:50	10.9	11.2	0.98	0.96
10:40:50	7.5	7.3	0.00	0.21
15:35:50	5.9	6.0	0.00	0.04
05:35:60	26.0	27.6	0.00	0.30
10:30:60	15.7	15.9	0.00	0.49
15:25:60	12.1	12.0	0.89	0.99
05:25:70	69.2	70.2	0.49	0.29
10:20:70	38.3	36.8	1.40	1.22
2:58:40 (optimum)	6.5	6.8	1.88	1.63

modify the selectivity in the mobile phase. This additional asset was not exploited in our case because the optimal composition of the mobile phase involved a very low proportion of the ester and a high methanol content, which hindered the attainment of significant selectivity differences. Nevertheless, this could be of great use in resolving other types of mixtures.

As far as the isolation of FPA from its accompanying impurities is concerned, the resolution achieved by using a mobile phase including an acetic ester by a statistically optimized procedure was quite good and matched the experimental results. Also, the separation time was shortened in relation to the use of unmodified phases, which is of great interest with a view to improving product quality control procedures.

REFERENCES

1 J. E. Paanakker, J. C. Kraak and H. Poppe, *J. Chromatogr.*, 149 (1978) 111.

2 T. Dzido and E. Soczewinski, *J. Chromatogr.*, 395 (1987) 489.
3 J. D. Olsen and R. J. Hurtubise, *J. Chromatogr.*, 474 (1989) 347.
4 L. R. Snyder, *Techniques of Chemistry*, Vol. III, Part I, Wiley-Interscience, New York, 2nd ed., 1978, Ch. 2.
5 L. R. Snyder, *J. Chromatogr.*, 92 (1974) 223.
6 *Spanish Pat.* 520 070 (1983), 525 854 (1983), 528 910 (1984), 529 530 (1984) and 529 531 (1984).
7 J. Martin Juarez, A. Bermejo, J. L. Bernal, M. J. Del Nozal and G. A. Garcia, *Chromatographia*, 29 (1990) 338.
8 *United States Pharmacopeia XXI*, The United States Pharmacopeial Convention, Rockville, MD, 1988.
9 *British Pharmacopoeia*, Her Majesty's Stationary Office, London, 1988.
10 J. M. Sörensen and W. Artl, *Liquid–Liquid Equilibrium Data Collection. Ternary Systems*, Vol. V, Dechema, Frankfurt Main, 1980.
11 P. J. Schoenmakers, H. A. H. Billiet and L. De Galan, *J. Chromatogr.*, 218 (1981) 261.
12 D. G. Beech, and S. Glasstone, *J. Chem. Soc.*, (1938) 67.
13 A. G. Crawford, G. Edwards and D. S. Lindsay, *J. Chem. Soc.*, (1949) 1054.

Journal of Chromatography, 607 (1992) 183–189
Elsevier Science Publishers B.V., Amsterdam

CHROM. 24 207

Determination of 5-fluorouracil in vitreous gel and liquid by high-performance liquid chromatography

M. J. Del Nozal*, J. L. Bernal and A. Pampliega

Department of Analytical Chemistry, Faculty of Sciences, University of Valladolid, E-47005 Valladolid (Spain)

J. C. Pastor and M. I. Lopez

Institute for Applied Ophthalmobiology (IOBA), University of Valladolid, E-47005 Valladolid (Spain)

ABSTRACT

A high-performance liquid chromatographic method was developed for the determination of 5-fluorouracil (5-Fu) in vitreous gel and liquid. After addition of an internal standard (5-fluorocytosine), the vitreous humour samples were extracted with *n*-propanol–diethyl ether (16:84, v/v) with average recoveries of 95%. The extract was evaporated to dryness and the residue was reconstituted in 1 ml of mobile phase (0.05 *M* phosphate buffer, pH 3.5) and chromatographed isocratically on a C_{18} reversed-phase column coupled to an ultraviolet detector set at 254 nm. This method was applied to the pharmacokinetic study of 5-Fu in the vitreous gel and liquid of rabbit eyes after the injection of the drug.

INTRODUCTION

Over the last few years, 5-fluorouracil (5-Fu) has shown promise in the pharmacological treatment of proliferative vitreoretinopathy (PVR). The use of 5-Fu, however, is associated with a risk of retinal toxicity, which may be a consequence of high local drug concentrations. In order to avoid these effects, doses of 5-Fu must be fitted and the pharmacokinetics of the intravitreal injection of this drug must be studied correctly. Therefore, it is necessary to have an exact method in order to measure adequately the concentrations of 5-Fu in the vitreous cavity [1].

No methods have been described for measuring 5-Fu in vitreous gel and liquid. Nevertheless, different methods for determining this drug in other biological fluids such as plasma and urine have been developed and several procedures for extraction and determination have been proposed. Usually a previous deproteinization step, using different methods [2–5] is required, followed by extraction of the drug using, *e.g.*, ethyl acetate or *n*-propanol–diethyl ether mixtures [4].

The first reported methods for the determination of 5-Fu, based on the use of nuclear magnetic resonance [6,7] and radionuclides [8], showed poor sensitivity and resolution, so chromatographic methods were tried. Gas chromatography is not recommended because of the instability of the drug and also a laborious extraction procedure is required [4,9]. Currently most use high-performance liquid chromatography (HPLC) with fluorescence or UV detection [2,4,10–12]. Usually reversed-phase columns are employed [5,13] with phosphate mobile phases at different pH values [2–5,9,11,13]. We initially applied these HPLC methods to vitreous gel and liquid samples spiked with 5-Fu but adequate results were not obtained. However, this previous experience provided useful information for developing a satisfactory method for vitreous gel and liquid samples.

In this work, different methods of extraction and chromatographic columns were studied in order to

0021-9673/92/$05.00

establish a simple HPLC procedure for determining the concentration of 5-Fu in the vitreous gel and liquid in rabbit eyes after an initial dose of the drug.

EXPERIMENTAL

Chemicals

5-Fluorouracil (5-Fu) and 5-fluorocytosine (5-Fc) were obtained from Sigma (St. Louis, MO, USA). Monobasic ammonium phosphate and all other chemicals used for the preparation of buffers were of analytical-reagent grade (Merck, Darmstad, Germany). The water used was purified by passage through a Nanopure II system (Barnstead, Newton, MA, USA). Diethyl ether and *n*-propanol were obtained from SDS (Peypin, France).

Instrumentation and chromatographic conditions

The chromatographic set-up consisted of a CD4000 multiple solvent partitioning pump, a SM4000 UV–VIS variable-wavelength detector and a CI4000 integrator, all from LDC Analytical (Riviera Beach, FL, USA).

The columns adopted were Spherisorb 5 ODS 2 (25 × 0.46 cm I.D.), Ultramex C_{18} (25 × 0.2 cm I.D.) and Spherisorb SAX (15 × 0.4 cm I.D.) from Phenomenex (Torrance, CA, USA), Vydac C_{18} (25 × 0.46 cm I.D.) from The Separations Group (Hesperia, CA, USA) and Pinkerton GFF II (25 × 0.46 cm I.D.) from Regis Chemical (Morton Grove, IL, USA); all the packings were of 5-μm particle size. The mobile phase was 0.05 *M* phosphate buffer (pH 3.5) and was pumped at a flow-rate of 1.0 ml/min. Samples were injected by means of a Rheodyne (Berkeley, CA, USA) Model 7125 injector with a fixed-volume loop of 20 μl.

Animal study

The animals used were cared for and handled according to the ARVO Resolution on Use of Animals in Research. A total of 21 albino rabbits weighing between 2.0 and 3.0 kg were used.

All surgical procedures were performed under a combination of intramuscular ketamine (100 mg/kg) and diazepam (0.5/kg) anaesthesia using topical 1% cyclopentolate and 10% phenylephrine for mydriasis.

One eye of each animal was injected with 1 mg of commercial 5-Fu (Hoffmann la Roche, Basle, Switzerland) in a total volume of 0.05 ml using a tuberculin syringe and a 30-gauge needle. The needle was introduced through the proptosed globe at the equator under ophthalmoscopic control, taking great care to avoid damage to the lens, ciliary body and adjacent retina. The jet stream of fluid was directed towards the mid-vitreous gel and liquid. The intraocular pressure was allowed to equilibrate, the needle withdrawn and the perforation site covered for 30 s in order to avoid the reflux of the drug. Following drug administration samples were obtained at 0.1, 2, 6, 12, 24, 48 and 72 h. At each of the seven times three animals were killed and the treated eyes were immediately proptosed and enucleased, the adherent epiesclera being dissected. The vitreous gel and liquid was expressed, disrupted with a sonicator and the microtip was used for 30 s, centrifuged at 1000 *g* for 5 min and frozen.

Sample extraction

The extraction procedures using solid–liquid and liquid–liquid extraction were compared.

In the solid–liquid extraction, sample clean-up was done using solid-phase extraction (SPE) columns (Bond Elut, Analytichem, Harbor City, CA, USA). The cartridges were preconditioned by flushing with the appropriate solvent. The samples were loaded on the cartridges and the eluate was filtered on 0.2-μm filters (MFS, Dublin, CA, USA) and injected into the chromatographic system.

In the liquid–liquid extraction ethyl acetate or *n*-propanol–diethyl ether mixtures were added to samples of vitreous gel and liquid (0.2 ml), raw samples and samples spiked with 5-Fu, placed into separating funnels and shaken for 10 min. The organic phase was then separated and dried in a rotary evaporator from Büchi (Flawil, Switzerland). The residues obtained were dissolved in 1 ml of mobile phase and injected into the chromatographic system.

Internal standard calibration graph

Stock solutions of 5-Fu and 5-Fc were prepared in Nanopure water at a concentration of 100 μg/ml. They were stable for at least 3 months if stored at 4°C. Standard solutions were prepared from the stock solutions by sequential dilution with Nanopure water.

Drug-free vitreous gel and liquid samples spiked

with known amounts of 5-Fu and 5-Fc were analysed concurrently with each set of unknown samples. At least seven different concentrations of 5-Fu across the working range were measured in quintuplicate. Calibration graphs were calculated by the least-squares method. Peak-area ratios between 5-Fu and 5-Fc were used to generate the least-squares linear regression lines. Concentrations of 5-Fu in the vitreous samples were obtained by interpolation from these calibration graphs using peak-area ratios obtained from unknown samples. Vitreous blanks were used to monitor for interferences.

The recovery of 5-Fu was determined at concentrations between 1 and 100 μg/ml. Vitreous samples (0.2 ml) were spiked with appropriate volumes of 5-Fu solution and extracted. A constant concentration (25 μg/ml) of internal standard was added to each sample prior to extraction and analysis, completing to the final volume, always 1 ml, with Nanopure water.

Sample preparation

Homogenized vitreous gel and liquid (0.2 ml) was placed in a glass tube, 25 μg/ml of internal standard (5-Fc) were added and Nanopure water was added to a final volume of 1 ml. Then 50 μl of 0.1 *M* acetic acid–acetate buffer (pH 4.6) and 0.5 ml of a saturated solution of sodium sulphate were added. The mixture was placed in a 50-ml separating funnel and 15 ml of *n*-propanol–diethyl ether (16:84, v/v) were added and mechanically shaken for 15 min. The two layers were separated and the organic phase was concentrated to dryness in a rotary evaporator. The residue was dissolved in 1 ml of the mobile phase, the solution was filtered through a 0.2-μm filter and 20 μl were injected into the HPLC system.

RESULTS AND DISCUSSION

There are two bands between 190 and 300 nm in the molecular absorption spectra of 5-Fu and 5-Fc, which make the detection of these compounds possible over a wide range of wavelengths. In order to obtain an economical and simple procedure 254 nm was chosen although when working at 266 nm the sensitivity is multiplied by 1.4 and at 200 nm by 1.8, but at 200 and 266 nm there are more instrumental limitations and only a few mobile phases are useful.

Different types of columns were used in order to isolate the peaks of 5-Fu and 5-Fc: reversed-phase (Ultramex C_{18}, Vydac C_{18}, Spherisorb 5 ODS 2), exclusion reversed-phase (Pinkerton GFF II) and ion exchange (Spherisorb SAX), using mobile phases of acetic acid–acetate or phosphate solutions in different concentrations and pH values.

The best separation was obtained with the Sphe-

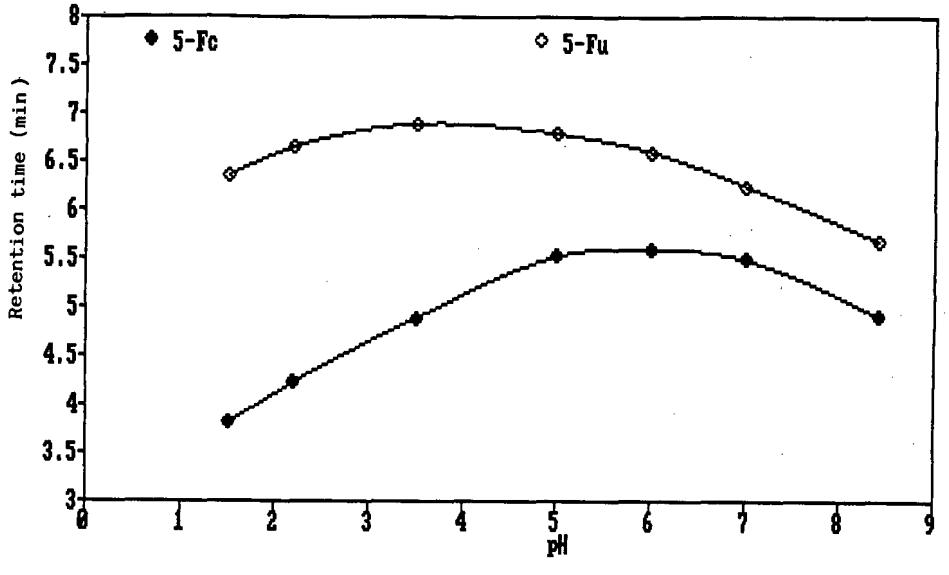

Fig. 1. Variations in the retention times of 5-Fu and 5-Fc *vs.* the pH of the mobile phase.

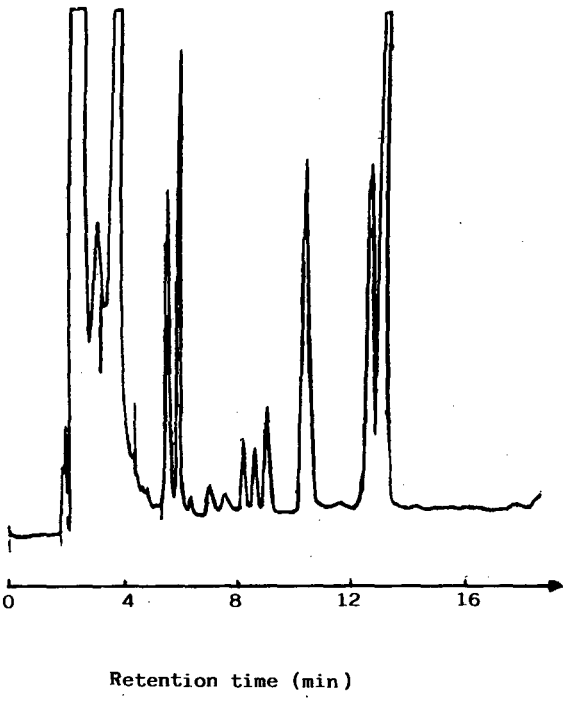

Fig. 2. Chromatogram of a drug-free vitreous gel and liquid sample after sonication, centrifugation and filtration.

risorb 5 ODS 2 column and 0.05 *M* phosphate solution. From these experiments it was found that the pH of the mobile phase affected the retention of different solutes considerably (Fig. 1). The most suitable pH seems to be 3.5, where the retention times are 4.89 min for 5-Fc and 6.89 min for 5-Fu.

Extraction clean-up

When a filtered vitreous sample without any other treatment is injected, various peaks that will coelute with 5-Fu (6.89 min) appear in the chromatogram (Fig. 2), so an extraction clean-up procedure is necessary. In order to obtain an appropriate method to determine 5-Fu without interferences, solid–liquid and liquid–liquid extractions were used.

In the solid–liquid extraction different minicolumns were used (C_{18}, C_8, NH_2, CN and phenyl). Using C_{18} cartridges most interfering compounds were retained and so was the 5-Fu (Fig. 3). However, it was not possible to carry out the selective elution of the compounds. With other cartridges it was also not possible to achieve the separation.

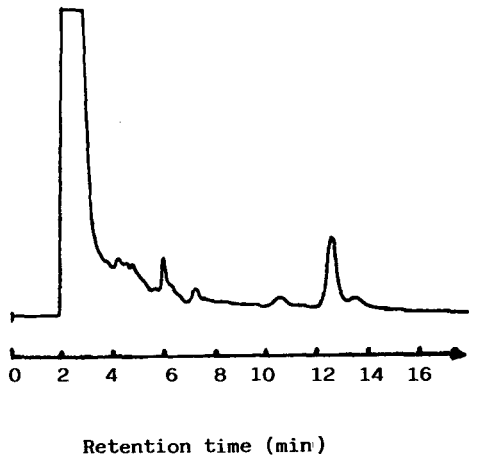

Fig. 3. Chromatogram of a vitreous gel and liquid sample spiked with 5-Fu and 5-Fc after clean-up through a C_{18} cartridge.

In the liquid–liquid extractions two solvents were used, ethyl acetate and *n*-propanol–diethyl ether.

In the former instance, the peaks that interfered with 5-Fu were eliminated (Fig. 4a) but the 5-Fu recovery was only about 30%. In order to increase the extraction yield, the influence of different parameters was studied: pH of the medium (2–9), volume of extractant (5–20 ml) and shaking time (10–30 min), but the recovery of the method was not improved.

With the latter solvent, in a first test 5 ml of *n*-propanol–diethyl ether (16:84, v/v) were added to a vitreous sample spiked with 5-Fu, shaking and rejecting the aqueous phase. Subsequently a new extraction of the organic phase was performed by adding 1 ml of phosphate buffer (pH 11), then the aqueous phase was separated, filtered and injected into the HPLC system. Many interfering peaks disappeared (Fig. 4b) but the efficiency of this procedure was only about 38%. To improve this, different volumes of acetic acid–acetate buffers at several pH values and different amounts of a sodium sulphate solution were also added to a vitreous sample prior to the extraction. When 0.1 *M* acetic acid–acetate buffer (pH 4.6) and 0.5 ml of the saturated solution of sodium sulphate were used, the recovery was about 55%. The effects of the volume of *n*-propanol–diethyl ether used and the shaking time were also studied, in addition to the influence of drying the organic phase from the first extraction

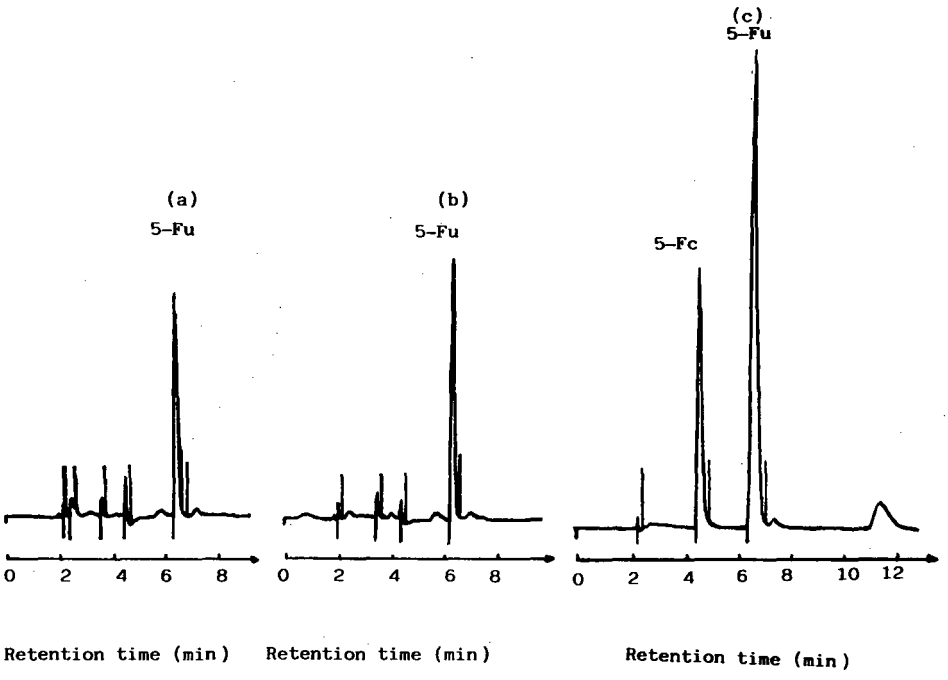

Fig. 4. Chromatogram of vitreous gel and liquid sample spiked with 5-Fu and 5-Fc (a) after extraction with ethyl acetate, (b) after extraction with *n*-propanol–diethyl ether followed by a second extraction with phosphate buffer and (c) after extraction according to sample preparation.

step and dissolving the residue in phosphate afterwards. The optimum conditions obtained, which were introduced in the sample preparation stage, were applied to different vitreous samples fortified with 5-Fu, giving recoveries around 95% (Table I), and the interfering peaks in the chromatogram disappeared, as can be seen in Fig. 4c.

Calibration graphs

The calibration graphs for 5-Fu obtained from the extraction of spiked vitreous samples was linear over the concentration range 0.5–100 μg/ml. The regression equation for this line was concentration = 0.28(peak area) − 2.68 with a correlation coefficient of 0.998. By using these conditions the detec-

TABLE I

EXTRACTION RECOVERY OF 5-Fu IN VITREOUS GEL AND LIQUID

Concentration (μg/ml)	Recovery (%) (mean ± S.D., n = 5)
1	94.61 ± 0.88
5	95.33 ± 0.91
10	94.96 ± 0.85
25	95.24 ± 0.95
50	94.91 ± 0.93
100	94.67 ± 0.89
Mean ± S.D.	94.95 ± 0.29

TABLE II

5-Fu CONCENTRATIONS IN VITREOUS GEL AND LIQUID AFTER A SINGLE 1-mg INTRAVITREAL INJECTION OF 5-Fu

Time after administration (h)	Concentration (μg/ml) (mean ± S.D., n = 3)
0.1	983.97 ± 41.87
2	609.69 ± 31.53
6	188.36 ± 3.63
12	9.21 ± 1.25
24	1.19 ± 0.18
48	0.39 ± 0.11
72	0.35 ± 0.10

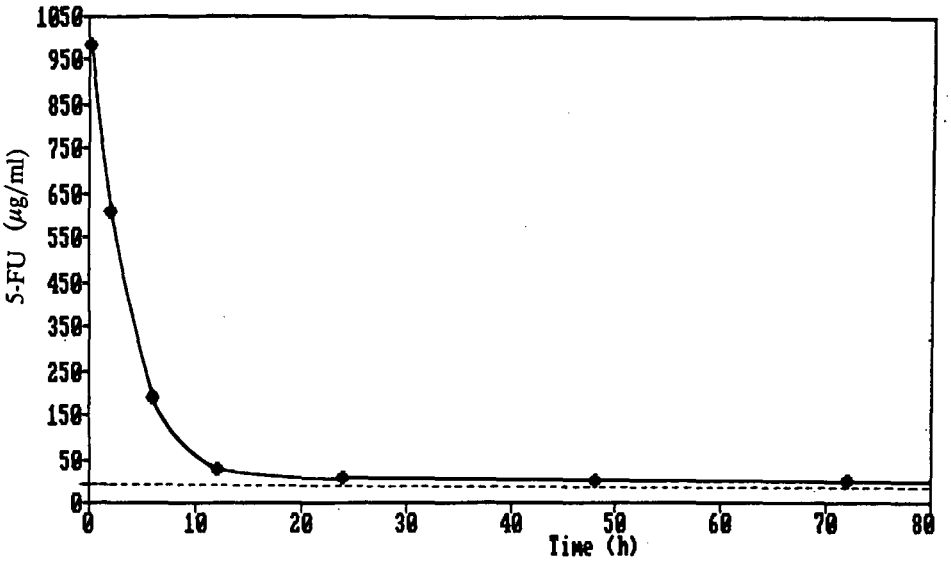

Fig. 5. Vitreous gel and liquid concentration–time profile of 5-Fu after a single 1-mg intravitreal injection of 5-Fu.

tion limit was 0.25 μg/ml and the limit of determination was 0.75 μg/ml.

Application to vitreous gel and liquid samples

The results obtained are given in Table II. The highest concentration of 5-Fu was obtained immediately after the injection of the drug. Data for vitreous sample clearance of 5-Fu *versus* time are plotted in Fig. 5 and suggest a biphasic character in which clearance is accelerated during the first 12 h and then is more moderate. Both phases closely approximate first-order kinetics, $\ln C = A - K_e t$, where C is the 5-Fu concentration in μg/ml, t is the time in which the samples were obtained and K_e is the elimination constant.

The pharmacokinetic parameters are given in Table III.

TABLE III

PHARMACOKINETIC PARAMETERS OF 5-Fu

Phase	Elimination constant, K_e (h^{-1})	Half-life time, $t_{1/2}$ (h)
First	0.282	2.45
Second	0.025	27.72

CONCLUSION

Reversed-phase HPLC is suitable for the determination of the remaining 5-Fu in vitreous gel and liquid samples after intravitreal therapy. The method requires a previous clean-up of the sample in which the addition of sodium sulphate solution and the drying step are extremely important.

This method is very useful for following the pharmacokinetic behaviour of intravitreal therapy with 5-Fu. There is almost no drug left in the vitreous cavity of rabbit eyes 12 h after injection of 5-Fu through this route.

REFERENCES

1 M. I. López, J. C. Pastor, J. I. Alonso, C. Mateu, L. A. Mate, M. J. Del Nozal and A. Pampliega, *Invest. Ophthalmol. Vis. Sci. (Suppl.)*, 32 (1991).
2 W. E. Wung and S. B. Howell *Clin. Chem.*, 26 (1980) 1704.
3 R. Kar, R. Cohen, M. Terem, M. Nahabadiam and A. Nile, *Cancer Res.*, 46 (1986) 4491.
4 N. Christophidis, G. Mihaldy, F. Vadja and W. Louis, *Clin. Chem.*, 25 (1979) 83.
5 F. La Greta and W. Williams, *J. Chromatogr.*, 414 (1987) 197.
6 J. A. Beteille, A. López, M. Bon, M. C. Malet-Martino and R. Martino, *Anal. Chim. Acta*, 171 (1985) 225.
7 J. L. Evelhoch, *Invest. New Drugs*, 7 (1989) 5.

8 D. Young, E. Wine, A. Ghanbarpour, J. Shani, J. K. Siemsen and W. Wolf, *Nucl. Med.*, 21 (1982) 1.
9 H. Odagiri, S. Ichichara, E. Semura, H. M. Utoh, M. Tatteshi and I. Kumura, *J. Pharmacobio-Dyn.*, 11 (1988) 234.
10 J. P. Sommadossi, D. A. Gewitz, R. B. Diasio, H. Aubert, J. P. Cano and I. D. Goldman, *J. Biol. Chem.*, 257 (1982) 8171.
11 A. A. Miller, E. D. Moore, R. B. Huyrlbert, J. A. Benvenuto and T. L. Loo, *Cancer Res.*, 43 (1983) 2565.
12 M. S. Didolkar, D. G. Covell, A. J. Jackson, A. D. Walker and J. R. Kalidindi, *Cancer Res.*, 44 (1984) 5105.
13 A. A. Miller, J. A. Benvenuto and T. L. Loo, *J. Chromatogr.*, 228 (1982) 165.

Journal of Chromatography, 607 (1992) 191–198
Elsevier Science Publishers B.V., Amsterdam

CHROM. 24 139

Post-column derivatization of carbohydrates with ethanolamine–boric acid prior to their detection by high-performance liquid chromatography

M. J. Del Nozal*, J. L. Bernal, F. J. Gomez, A. Antolin☆ and L. Toribio

Department of Analytical Chemistry, Faculty of Sciences, University of Valladolid, E-47005 Valladolid (Spain)

ABSTRACT

The influence of experimental variables such as the wavelength, composition of the fluorogenic reagent, reaction time, reaction and measurement temperatures, and concentration on the post-column derivatization of carbohydrates by reaction with an ethanolamine–boric acid mixture was studied. In order to enhance the signals given by di- and trisaccharides, they were hydrolysed, after elution, with *p*-toluenesulphonic acid, which also provided lower detection limits for monosaccharides. The procedure was applied to the determination of eleven carbohydrates in wines.

INTRODUCTION

Accurate determinations of individual sugars in foods and beverages are becoming more important every day because they not only provide compositional information on the samples, but also help to solve nutritional problems, and problems of adulteration, origin, manufacture, etc. Wine analyses involve some interesting aspects related to pentoses. These substances, which occur in grape juice as complex combinations from which they are released during fermentation [1], cannot be fermented by yeasts, so they are transferred to wine unchanged. Hence their analysis can be of great value in determining the grape variety used to produce a given wine. Confronted with the problem of evaluating both pentoses and other sugars [2] after fermentation, high-performance liquid chromatography (HPLC) with ion-exchange columns was chosen from the many types of HPLC to separate and evaluate carbohydrate samples [3] because of the selectivity of this technique. Taking into account the fact that pentose concentrations rarely exceeds 2 g/l in wines, anion exchange of carbohydrate–borate complexes [4] and fluorescence detection after post-column derivatization with ethanolamine-boric acid [5] was selected because of the simplicity, economy and sensitivity of this technique [6,7]. A preliminary application to some standards of pentoses and other carbohydrates revealed significant differences in analytical behaviour, so a more detailed study of the variables affecting the derivatization–detection process was carried out. This paper reports the results obtained in relation to the parameters with the most marked influence on the post-column fluorescence derivatization reaction between carbohydrates and an ethanolamine–boric acid mixture. The optimized conditions were applied to the analysis of several wines of different origin and manufacture.

EXPERIMENTAL

Reagents

Sugar stardards were purchased from Sigma Al-

☆ Present address: Glaxo S.A., Avda. de Extremadura, 3, E-09400 Aranda de Duero, Burgos, Spain.

0021-9673/92/$05.00

drich Química (Madrid, Spain). Boric acid, ethanolamine and *p*-toluenesulphonic acid were supplied by Fluka Chemie (Buchs, Switzerland). All other reagents required to prepare buffers and analytical solutions were pro analysis-grade chemicals purchased from Scharlau (Barcelona, Spain).

HPLC apparatus and conditions

The experimental set-up consisted of the following elements: a 6000A dual-piston pump from Waters Assoc. (Milford, MA, USA) that was used to propel the eluent, namely a 0.4 *M* borate buffer at pH 9.35, at a flow-rate of 1 ml/min; a Rheodyne 7125 injector with a fixed-volume (20 μl) loop. The separation was carried out on a glass chromatographic column of 50 cm × 0.3 cm I.D. that was packed with Aminex A-25 borate ion-exchange resin and wrapped in a water jacket. The working temperature was 69°C. Alternatively, a metal chassis of 30 cm × 0.46 cm I.D. packed with the same stationary phase which was customized by Bio Rad Labs. (Richardson, CA, USA) was used and was maintained at 69°C in an oven from Jones Chromatography (Wales, UK). An M-45 pump, from Waters Assoc., propelled the fluorogenic reagent (an aqueous solution containing 20% ethanolamine and 20% boric acid) at a rate of 0.5 ml min. After the merging point the reactants were conveyed into a PTFE capillary of 30 m × 0.3 mm I.D. which was immersed first in a reaction bath filled with glycerine at 140°C and then (1 m) in thermostated water at 20°C to cool the mixture. An SFM 25 fluorescence detector from Kontron Instruments (Zurich, Switzerland) furnished with a 15-μl flow cell was used. Measurements were made at excitation and emission wavelengths of 400 and 445 nm, respectively.

The hydrolysis involved a third pump (VS minipump from Milton Roy, Riviera Beach, FL, USA) to propel an aqueous solution of 1.6 *M* *p*-toluenesulphonic acid through a PTFE capillary (10 m × 0.3 mm I.D.) immersed in the bath at 140°C. Hydrolysis occurred after the carbohydrates were eluted from the column and before the derivatization reaction.

Reaction parameters

To study the influence of the reaction parameters and then to determine their optimal values, experiments were first carried out in non-continuous mode, and then the results were adapted to the chromatographic system and the chromatographic conditions were also studied.

For the non-continuous mode an LS-5 spectrofluorimeter from Perkin Elmer (Beaconsfield, UK) was used.

Wavelength. This was selected by reacting the different carbohydrates assayed with the fluorogenic reagent and recording the excitation and emission spectra of the products.

Reaction time. Volumes of 3 ml of 0.05% solutions of the carbohydrates were reacted with 5 ml of a 2% solution of the fluorogenic reagent in test tubes that were heated for different times and then allowed to cool before the fluorescence intensity was measured.

Fluorogenic reagent. The optimal composition of the ethanolamine–boric acid mixture was chosen from the intensity of the signal obtained for some carbohydrates (20 μg per 20-μl sample) on reaction with different mixtures containing a fixed amount of ethanolamine (15 g/l) and a concentration of boric acid that varied between 3 and 20 g/l. In order to obtain the proportion of mixed reagent to be used in the fluorogenic solution, contents between 2 and 30% in water were assayed.

Reaction temperature. Samples of 20 μg of each carbohydrate were injected and subjected to temperatures between 100 and 150°C, with no passage through the column. In this way the optimal reaction temperature was determined.

Measurement temperature. The mixture obtained after the reaction was cooled to different temperatures prior to arrival at the detector, to obtain the highest fluorescence response.

Hydrolysis. Different concentrations of *p*-toluenesulphonic acid, between 0.1 and 2 *M*, were assayed. In addition, the flow-rate was varied between 0.1 and 0.5 ml/min.

Internal standard calibration graphs

Melibiose was used as internal standard. Stock solutions of eleven carbohydrates (10 g/l) and melibiose (10 g/l) were prepared in nanopure water. Standard solutions were prepared from stock solutions by sequential dilution with nanopure water.

The calibration curves were calculated by the least-squares method. Peak-area ratios between the carbohydrates and melibiose were used to generate

the least-squares regression lines. Concentrations of carbohydrates in the wine samples were obtained by interpolation from these calibration curves using peak-area ratios obtained from unknown samples. A constant concentration (0.1 g/l) of internal standard was added to each sample prior to the analysis.

Wine sample

The proposed method was applied to the analysis of different wine samples from Castile and Leon winemakers, which belong to three Origin Denominations.

The white wines were from Rueda Origin Denomination, where the *V. vinifera* variety of grape most widely grown is *Verdejo*, native to this region. *Palomino* and *Viura* are other varieties grown to a lesser extent.

Rosé wines (Cigales Origin Denomination) are a mixture of *V. vinifera* varieties: *Tinta del Pais* (red), *Garnacha* (red), *Albillo* (white), *Verdejo* (white) and *Viura* (white).

The red wines were from Ribera del Duero Origin Denomination, where the most widespread *V. vinifera* variety is the *Tinta del Pais*, a variant of the classic fruity *Tempranillo*, usually mixed with *Cabernet, Merlot* or *Garnacha* in a small proportion.

Since in most samples the concentration of some carbohydrates was rather low the samples were concentrated ten-fold.

RESULTS AND DISCUSSION

Chromatographic column

Changing the column made by us to one customized in stainless steel provided better performance, though at the expense of longer retention times (Table I). Neither of the columns solved the problem of overlap between ribose and rhamnose.

Wavelength

In Table II the maximum excitation and emission wavelengths are shown. The optimal wavelengths were 400 and 445 nm, respectively.

Reaction time

Fig. 1 shows a typical curve for glucose. As can be seen, the fluorescence intensity increased markedly with increase in the heating time. In fact, appreciable signals were obtained after 15 min heating; this dictated the length and inner diameter of the reaction coil to be used for the post-column derivatization. In order to avoid too long reaction times, a PTFE capillary, 30 m × 0.3 mm I.D., was chosen and was stitched through a steel net with mesh openings to avoid peak broadening as far as possible [8].

TABLE I

RETENTION TIMES (t_R) OF CARBOHYDRATES IN BOTH COLUMNS

Carbohydrate	Retention time (min)	
	Home-made	Purchased from Bio-Rad
Melibiose	10.5	9.3
Sucrose	14.1	12.9
Maltose	17.4	16.3
Lactose	18.1	17.0
Rhamnose	19.6	18.2
Ribose	19.7	18.2
Mannose	25.9	29.9
Fructose	28.4	32.9
Arabinose	30.1	37.1
Galactose	34.7	43.3
Xylose	38.6	49.4
Glucose	51.0	67.7

Fluorogenic reagent

Fig. 2 shows the variation in the peak area as a function of the boric acid concentration. As can be seen, the maximum signal was obtained at a 1:1 ethanolamine/boric acid ratio. Fig. 3 shows that the increase was different for each carbohydrate, thus 20% concentration of each component was selected

TABLE II

OPTIMAL DETECTION WAVELENGTHS (λ) FOR SOME CARBOHYDRATES AFTER THEIR DERIVATIZATION WITH ETHANOLAMINE–BORIC ACID

Carbohydrate	$\lambda_{excitation}$ (nm)	$\lambda_{emission}$ (nm)
Galactose	397	447
Glucose	398	445
Xylose	403	449
Arabinose	398	453
Fructose	400	446

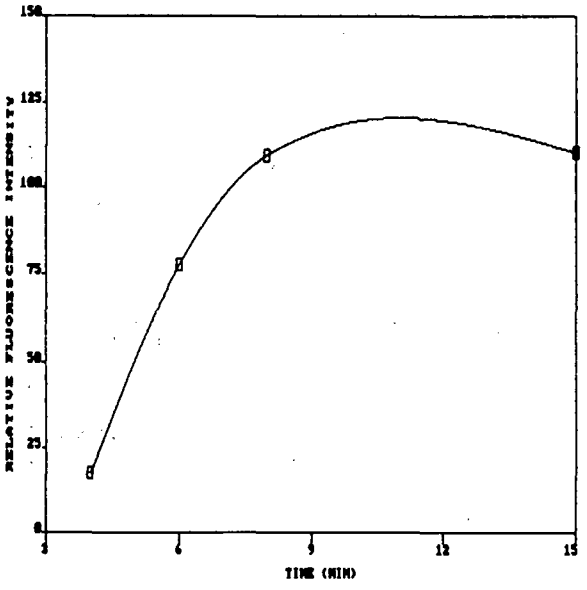

Fig. 1. Relative fluorescence intensity *versus* heating time for glucose.

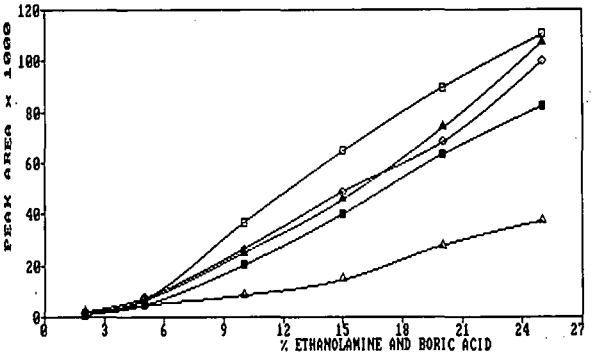

Fig. 3. Peak-area variation for some carbohydrates with the percentage ethanolamine and boric acid (1:1). △ = Lactose; □ = fructose; ◇ = xylose; ▲ = glucose; ■ = galactose.

for subsequent experiments since higher contents increased the mixture viscosity.

Reaction temperature

Figs. 4 and 5 show the results obtained. The peak area varies dissimilarly with temperature for each carbohydrate. As a rule, the maximum signals were obtained at about 140°C for monosaccharides and

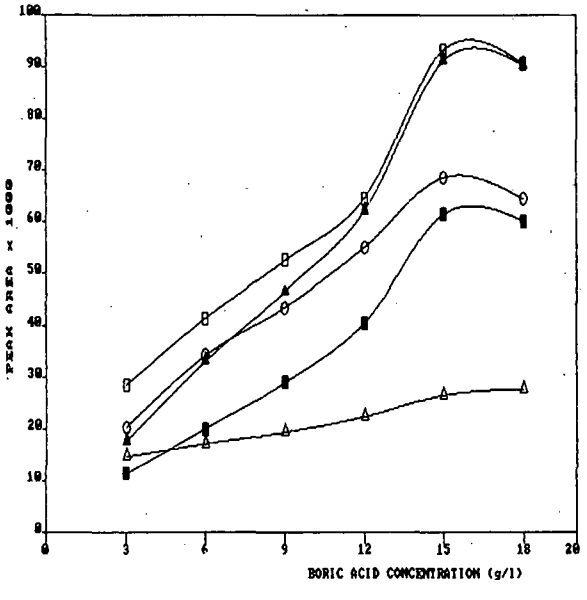

Fig. 2. Influence of boric acid concentration on the peak areas for different carbohydrates at a fixed ethanolamine content. △ = Lactose; □ = fructose; ○ = xylose; ▲ = glucose; ■ = galactose.

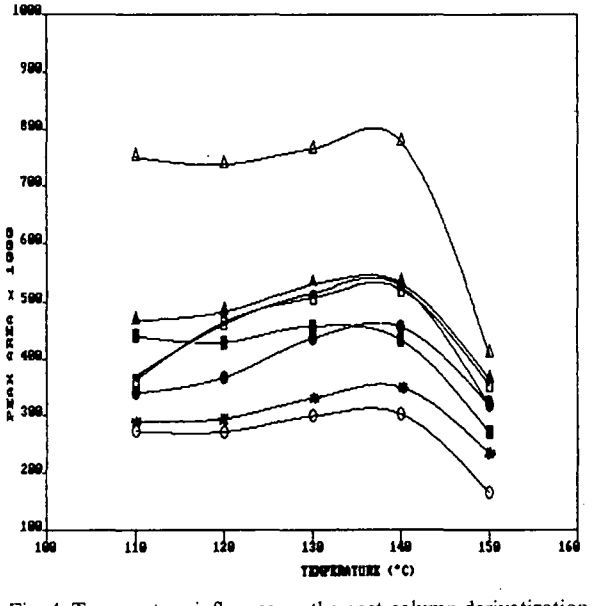

Fig. 4. Temperature influence on the post-column derivatization reaction for the monosaccharides assayed in relation to the peak area. ✳ = Ribose; ▲ = mannose; ■ = galactose; ● = xylose; △ = rhamnose; □ = fructose; ○ = arabinose; • = glucose.

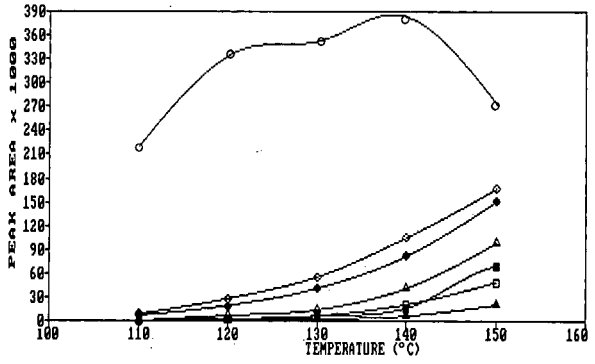

Fig. 5. Temperature influence on the post-column derivatization reaction for di- and trisaccharides assayed in relation to the peak area. ○ = Maltotriose; □ = rafinose; ◇ = lactose; ○ = melibiose; ▲ = melezitose; ■ = sucrose; ◆ = maltose.

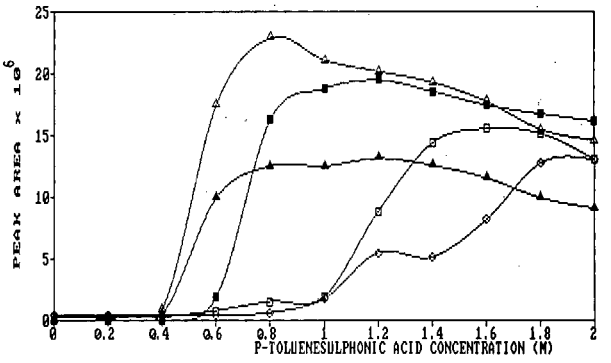

Fig. 7. Peak-area variation of some carbohydrates, with changes of the *p*-toluenesulphonic acid concentration for post-column hydrolysis. △ = Sucrose; ▲ = rafinose; □ = maltose; ■ = melezitose; ◇ = lactose.

occasionally above 150°C for di- and trisaccharides, which obviously featured higher detection limits.

Measurement temperature

As expected, cooling the reaction mixture prior to arrival at the detector resulted in increased fluorescence responses, as can be seen in Fig. 6. However, a temperature of 20°C was chosen for greater experimental convenience and in order to avoid problems in thermostating the flow cell.

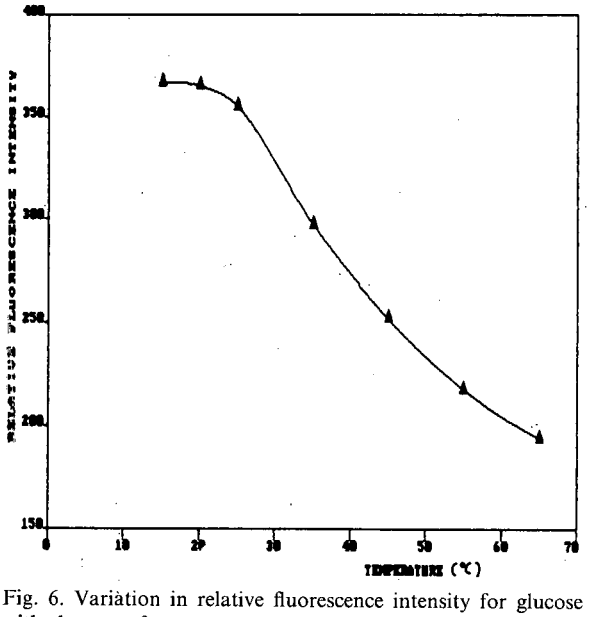

Fig. 6. Variation in relative fluorescence intensity for glucose with changes of measurement temperature.

Hydrolysis with p-toluenesulphonic acid

In Fig. 7 the different signals produced by the carbohydrates (4 μg per 20 μl sample) can be appreciated, but lactose and maltose behaved differently on hydrolysis. An acid concentration of 1.6 *M* was chosen because lactose and maltose signals were quite high and those of the other carbohydrates did not decrease to markedly.

As far as the reagent flow-rate is concerned (Fig. 8), lactose again behaved anomalously. In order to

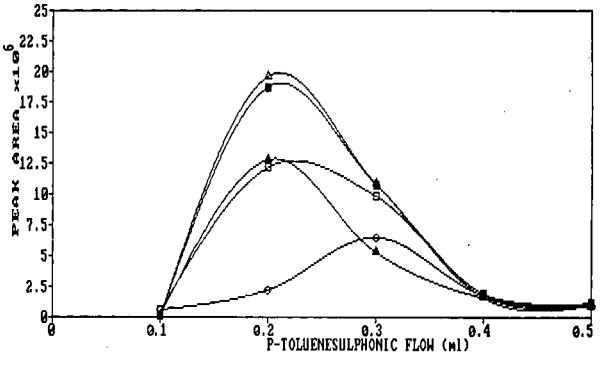

Fig. 8. Relation between the peak area for some carbohydrates and the flow-rate (ml/min) of *p*-toluenesulphonic acid. △ = Sucrose; ▲ = rafinose; □ = maltose; ■ = melezitose; ◇ = lactose.

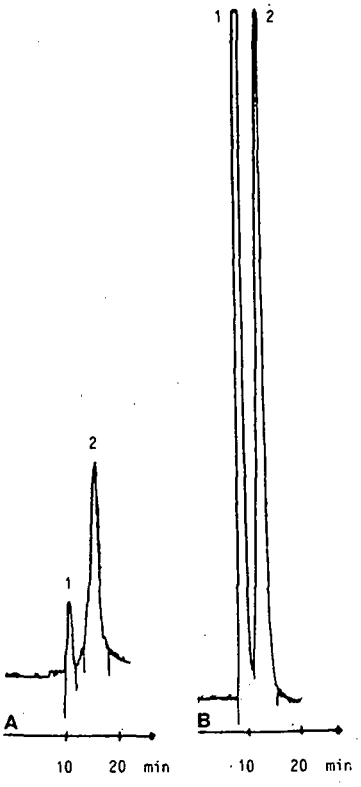

Fig. 9. Chromatogram showing the influence of acid hydrolysis on sucrose and maltose (A) without acid hydrolysis and (B) with acid hydrolysis for the same disaccharide concentration. Peaks: 1 = saccharose; 2 = maltose.

TABLE III

DETECTION LIMITS AND CONCENTRATION LINEARITY RANGES WITHOUT ACID HYDROLYSIS

Carbohydrate	Detection limits (mg/l)	Linearity range (mg/l)
Sucrose	111	100–300
Maltose	20	15–100
Lactose	20	15–100
Ribose	7	5–100
Rhamnose	7	5–100
Mannose	5	2.5–100
Fructose	10	7–100
Arabinose	10	7–100
Galactose	10	7–100
Xylose	8.5	5–100
Glucose	15	10–100

TABLE IV

DETECTION LIMITS AND CONCENTRATION LINEARITY RANGES WITH ACID HYDROLYSIS

Carbohydrate	Detection limit (mg/l)	Linearity range (mg/l)
Sucrose	40	20–200
Maltose	8.5	5–100
Lactose	8	5–100
Ribose	5	2–100
Rhamnose	5	2–100
Mannose	3	2–100
Fructose	6.5	4–100
Arabinose	6.5	4–100
Galactose	6.5	4–100
Xylose	5	2–100
Glucose	10	7–100

obtain the highest possible signal for this sugar an acid flow-rate of 0.3 ml/min was chosen.

Once the optimal acid concentration and flow-rate were selected, it was found by injecting a mix-

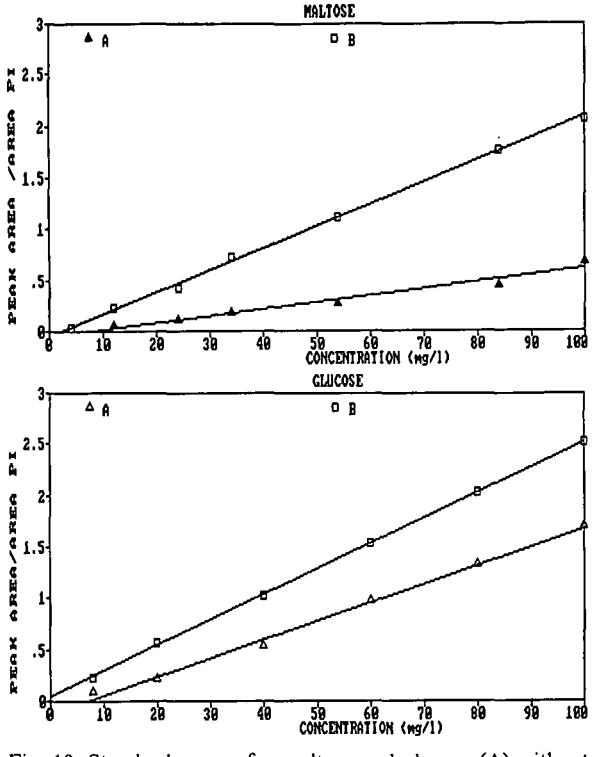

Fig. 10. Standard curves for maltose and glucose (A) without treatment with *p*-toluenesulphonic acid; (B) with treatment.

ture of carbohydrates that hydrolysis improved the signals given by mono-, di- and trisaccharides to such an extent as to make this advisable as pretreatment (Fig. 9).

Standard curves

In Tables III and IV the linearity ranges and detection limits obtained are shown. Fig. 10 shows examples of the standard curves of glucose (monosaccharide) and maltose (disaccharide).

Application

In Table V some of the results obtained are listed as an example. Of the white wines from the same winemaker and vintage, there are differences between V4 (fermented and finished from free-run juice) and V1 (cold settling), V2 (cold settling and treated with activated carbon) and V3 (press juice), indicating that V4 is monovarietal (*Verdejo*) and the others are obtained from a mixture of varieties. In particular, the high levels of fructose and the low levels of galactose are notable.

There are also significant differences between the rosé wine samples from two winemakers and three vintages. For example, from the same winemaker the oldest wine contains xylose, a high ratio of glucose to galactose and a high level of fructose. Comparing R1 and R5 samples (same vintage and different winemaker) reveals great differences in the fructose levels.

In the red wine samples from winemaker 5, note the lack of mannose and xylose and the very different glucose/galactose ratio (<1) in comparison with the results obtained from winemaker 4.

CONCLUSIONS

The use of a post-column fluorescence derivatization reaction between carbohydrates and ethanolamine-boric acid mixtures allows the detection of sugars in complex mixtures previously resolved by HPLC with ion-exchange columns. The reaction is

TABLE V

RESULTS OBTAINED FROM APPLYING THE OPTIMIZED METHOD FOR DIFFERENT WINES

Suc = Sucrose; Mal = maltose; Lac = lactose; Rib = ribose; Rham = rhamnose; Man = mannose; Fru = fructose; Ara = arabinose; Gal = galactose; Xyl = xylose; Glu = glucose.

Sample	Vintage	Carbohydrate concentration (mg/l)									
		Suc	Mal	Lac	Rib/Rham	Man	Fru	Ara	Gal	Xyl	Glu
White wines	*Winemaker 1*										
V1	1990	125	70	46	61	2.5	93	73	204	–	68
V2	1990	109	30	35	54	2.3	122	43	176	–	74
V3	1990	120	20	25	20	–	86	27	123	–	123
V4	1990	127	25	28	39	–	698	–	75	–	208
Rosé wines	*Winemaker 2*										
R1	1980	111	84	48	66	2.3	833	–	164	10	477
R2	1987	173	83	55	63	2.0	270	12	328	–	308
R3	1988	130	41	26	47	2.2	63	–	177	–	89
R4	1989	125	25	25	43	2.5	188	15	228	–	141
	Winemaker 3										
R5	1980	104	62	40	51	2.0	1186	–	227	–	181
Red wines	*Winemaker 4*										
T1	1984	125	102	68	73	6	297	20	109	10	467
T2	1985	127	103	76	95	3	170	60	199	59	221
T3	1986	115	117	79	63	2	160	15	241	–	132
	Winemaker 5										
T4	1984	120	39	26	47	–	106	–	222	–	117
T5	1985	125	60	46	94	–	182	–	316	–	200
T6	1986	111	56	38	64	–	218	–	207	–	143

quite sensitive, yet it is influenced by a number of variables in a continuous system. Thus, the working conditions must be optimized for the carbohydrates to be assayed and variations kept within margins as narrow as possible in order to obtain reliable analytical results.

Hydrolysis with *p*-toluenesulphonic acid before the post-column derivatization reaction markedly enhanced the sensitivity of the detection.

By applying the optimized reactions to wine samples from very similar winemaking practices, origin and vintages, interesting differences between the values for mannose, fructose, arabinose, glucose, xylose and for the glucose/galactose ratio were found.

ACKNOWLEDGEMENT

We thank Iberdrola S.A. (Spain) for financial suport.

REFERENCES

1 W. M. Kiliewer, *Am. J. Enol. Vitic.*, 18 (1967) 33.
2 P. Esau, *Am. J. Enol. Vitic.*, 15 (1967) 187.
3 A. A. Ben-Bassat and E. J. Grushka, *J. Liq. Chromatogr.*, 14 (1991) 1051.
4 J. K. Khym and L. P. Zill, *J. Am. Chem. Soc.*, 74 (1952) 2090.
5 R. Kamada and A. Ono, *Soil. Sci. Plant. Nutr.*, 30 (1984) 145.
6 T. Kato and T. Kinoshita, *Anal. Biochem.*, 106 (1980) 238.
7 V. R. Villanueva, M. Th. le Goff, M. Mardon and F. Moncelon, *J. Chromatogr.*, 393 (1987) 115.
8 B. Lilling and E. Heinz, in J. S. Krull (Editor), *Reaction Detection in Liquid Chromatography* (*Chromatographic Science Series*, Vol. 34), Marcel Dekker, New York, 1986, p. 27.

Journal of Chromatography, 607 (1992) 199–202
Elsevier Science Publishers B.V., Amsterdam

CHROM. 24 170

Determination of creatinine and purine derivatives in ruminants' urine by reversed-phase high-performance liquid chromatography

J. A. Resines

Departamento de Física, Química y Expresión Gráfica, Universidad de León, 24071-León (Spain)

M. J. Arín and M. T. Díez*

Departamento de Bioquímica y Biología Molecular, Universidad de León, 24071-León (Spain)

ABSTRACT

A procedure is described for the rapid and simultaneous determination of allantoin, creatinine, uric acid, hypoxanthine and xanthine in sheep urine. Separation was achieved on a Novapak C_{18} column under isocratic conditions. The mobile phase was potassium phosphate buffer (10 m*M*, pH 4.0). A flow-rate of 0.5 ml/min, detection at 218 nm and a column temperature of 25°C were employed with a total analysis time of less than 15 min. Detection limits for allantoin, creatinine, uric acid, hypoxanthine and xanthine were 1.0, 0.5, 0.5, 0.5 and 0.2 μg/ml, respectively, at a signal-to-noise ratio of 3 in a 20-μl injection volume of tenfold-diluted urine. This sensitivity permits the precise determination of these compounds in ruminants' urine.

INTRODUCTION

In ruminants, purines are metabolized in a series of reactions to form allantoin, uric acid, hypoxanthine and xanthine. These compounds, present in urinary excretion, were proposed as an index of their nutritive status in each phase of the productive cycle [1].

Allantoin is the main excretion product from purine metabolism and it has been shown [2] that urinary excretion in sheep was significantly correlated with the nucleic acid concentration in rumen fluid [3,4].

Urinary creatinine excretion was correlated with the live mass within a wide range of body mass [5]. Creatinine could be useful as an internal marker to make quantitative predictions of metabolic processes in intact animals [4].

Various methods have been described for the determination of allantoin and creatinine in biological fluids. Most procedures are based on colorimetric reactions. The traditional colorimetric analysis of allantoin in urine is based on the Rimini–Schryver reaction described by Young and Conway [6]. Lindberg and Jansson [7] and Chen *et al.* [8] described a method that adapted this reaction to the Technicon AutoAnalyzer.

For creatinine determination, the method most widely employed in clinical laboratories is the Jaffe alkaline picrate procedure [9,10]. This method requires several steps and it has been reported that it can give overestimated values of creatinine owing to interferences by endogenous and exogenous pseudo-creatinine chromogens [11].

Uric acid, hypoxanthine and xanthine have long been measured colorimetrically. More specific enzymatic techniques have been widely applied; both methods have problems [12,13] with intereferences from other compounds presents in biological fluids.

Reversed-phase high-performance liquid chromatographic (RP-HPLC) assays of allantoin in biological fluids proved to be good alternatives

0021-9673/92/$05.00

[14,15]. In recent years, several chromatographic methods for the determination of creatinine have been described. Approaches include cation-exchange column chromatography [16], ion-pair chromatography [17] and reversed-phase chromatography [18,19]. A series of papers reported HPLC methods for the determination of uric acid, hypoxanthine and xanthine. Particularly anion-exchange liquid column chromatography for routine clinical laboratory use appears far too time consuming [20].

Currently reversed-phase techniques have been most widely employed. Some workers have reported gradient elution techniques [21,22] while others recommended isocratic elution [23].

For the study of ruminant metabolism, a simple and rapid method is needed for measuring urinary allantoin, creatinine, uric acid, hypoxanthine and xanthine simultaneously. In this paper, an RP-HPLC method for this purpose is described.

EXPERIMENTAL

Reagents

Allantoin was obtained from Sigma (St. Louis, MO, USA). Creatinine, uric acid, hypoxanthine and xanthine were purchased from Merck (Darmstadt, Germany) and used without further purification. Other chemicals were of the highest purity commercially available. Methanol was of HPLC grade, obtained from Carlo Erba (Milan, Italy). Water was previously distilled and purified with a Milli-RO 15 reagent-grade water system (Millipore, Bedford, MA, USA).

Urine samples

Urine samples were centrifuged and filtered through a Millex-HV 0.45-μm pore size filter (Millipore) and diluted tenfold (or more when the concentrations in samples were high with distilled water. A 20-μl volume of the filtrate was injected into the HPLC column. Urine samles were stable for several weeks when stored at −20°C.

Standard solutions

Stock solutions of all compounds (1 mg/ml) were prepared by dissolving pure standards in water and were stored at 4°C for 1 month. Working standard solutions, were prepared weekly, 40 μg/ml for allantoin, 60 μg/ml for creatinine and 20 μg/ml for uric acid, hypoxanthine and xanthine, by diluting the stock solutions with water; a 20-μl aliquot of these solutions was used daily as a control to check the retention time and all other conditions of the HPLC procedure. A series of working standards were prepared by dilution of each of the stock solutions with water.

Calibration graphs were prepared over the concentration range 20–400 μg/ml for allantoin, 10–200 μg/ml for creatinine and 5–35 μg/ml for uric acid, hypoxanthine and xanthine.

Quantification was achieved by regression analysis of the peak areas of each compounds against concentration. Triplicate injections of each concentration were made.

Instruments

HPLC analyses were performed with a Waters (Milford, MA, USA) Model 600E system equipped with a Waters Model 484 UV detector. Quantification was based on integration of peak areas using a Waters Model 745B integrator.

Chromatographic conditions

A Novapak C_{18} reversed-phase column (30 cm × 3.9 mm I.D., 4-μm particles) (Waters) was used. The mobile phase was 10 m*M* potassium phosphate buffer (pH 4.0). Before use, the mobile phase was filtered through an HA 0.45-μm pore size filter (Millipore) and further degassed by sonication. The flow-rate was 0.5 ml/min, the column was maintained at 25°C and the absorbance detector was set at 218 nm.

Compound peaks were identified by their retention times and co-elution with authentic standards and quantified by comparison of the peak areas of the samples with those of authentic standards.

The purity of the compound peaks was tested by comparison of the peak areas obtained at wavelengths of 218 and 230 nm.

RESULTS AND DISCUSSION

Creatinine and allantoin have similar polarity and it is very difficult to separate them in biological fluids. In previous work [15] we found the optimum chromatographic conditions for the separation of the creatinine peak from the allantoin peak [mobile phase, 10 m*M* potassium phosphate buffer, (pH

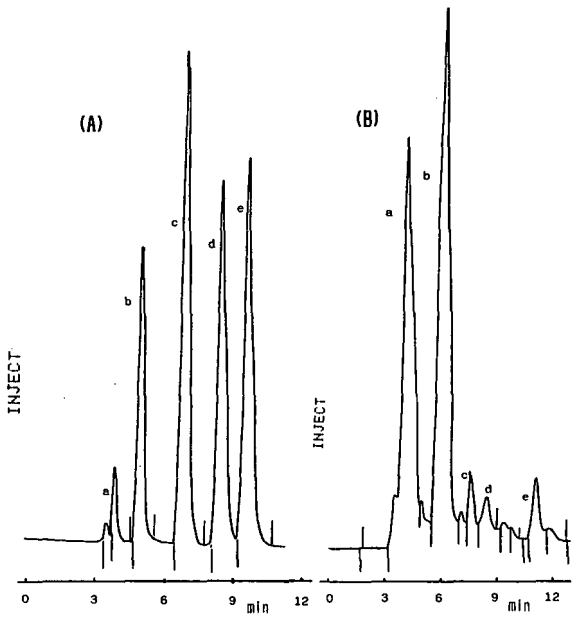

Fig. 1. (A) Chromatographic separation of standard solutions. (B) Chromatogram of tenfold-diluted sheep urine. Peaks: a = allantoin; b = creatinine; c = uric acid; d = hypoxanthine; e = xanthine.

4.0); flow-rate, 0.5 ml/min; temperature, 25°C; wavelength, 218 nm]. This method was applied successfully to the determination of uric acid, hypoxanthine and xanthine. Previously we have verified that there is little influence of the buffer concentration and column temperature on their separation. For this reason these conditions were applied to the simultaneous determination of the five metabolites with good resolution.

Fig. 1 shows chromatograms obtained for standard solutions and urine samples. The retention times for allantoin, creatinine, uric acid, hypoxanthine and xanthine were *ca.* 3.9, 5.7, 7.2, 8.3 and 10.8 min, respectively. At a signal-to-noise ratio of 3, the detection limits for tenfold diluted urine were 1.0, 0.5, 0.5, 0.5 and 0.2 μg/ml, respectively with a 20-μl injection.

In all instances, a linear relationship between the peak area and the concentration in urine was obtained for the ranges of concentrations tested, *i.e.*, 20–400 μg/ml for allantoin, 10–200 μg/ml for creatinine and 5–35 μg/ml for uric acid, hypoxanthine and xanthine. The equations calculated were $y = 0.029\,x + 0.263$ for allantoin [15], $y = 0.167\,x + 0.844$ for creatinine [15], $y = 0.058\,x - 0.009$ for uric acid, $y = 0.117\,x - 0.135$ for hypoxanthine and $y = 0.119\,x - 0.072$ for xanthine (y = peak area $\cdot 10^{-6}$; x = concentration). In all instances the correlation coefficients were greater than 0.99.

The standard addition method was used to check for chemical interferences. The equations calculated with the standard addition method applied to urine were $y = 0.026\,x + 14.091$ for allantoin [15], $y = 0.162\,x + 3.992$ for creatinine [15], $y = 0.057\,x + 0.969$ for uric acid, $y = 0.129\,x + 0.811$ for hypox-

TABLE I

INTER-DAY PRECISION AND ACCURACY OF THE DETERMINATION OF URIC ACID, HYPOXANTHINE AND XANTHINE IN SHEEP URINE

Compound	Concentration added (μg/ml)	Concentration found (μg/ml) (mean ± S.D.; n = 3)	R.S.D. (%)	Relative error (%)
Uric acid	10	10.9 ± 0.2	1.7	9.4
	15	15.9 ± 0.2	1.2	5.8
	20	20.7 ± 0.1	0.5	3.6
Hypoxanthine	10	11.0 ± 0.2	1.6	9.6
	15	15.7 ± 0.1	0.8	4.4
	20	21.1 ± 0.1	0.5	5.3
Xanthine	5	5.0 ± 0.1	2.1	1.2
	8	8.1 ± 0.1	1.2	1.0
	10	10.7 ± 0.1	0.9	6.9

anthine and $y = 0.126\ x + 0.203$ for xanthine. The slopes of the calibration and standard addition graphs were similar for each compound.

For each analyte, the inter-day precision and accuracy were determined by analysing three times per day for ten days diluted urine samples spiked at three concentrations. The results for uric acid, hypoxanthine and xanthine are given in Table I.

The results obtained for allantoin and creatinine were given in a previous paper [15]; for these two compounds, the relative standard deviation (R.S.D) varied between 1.2 and 2.2% for allantoin and between 1.1 and 2.5% for creatinine.

The recovery was determined by triplicate analyses of urine samples spiked with standards of the metabolites at concentrations ranging from 80 to 320 μg/ml for allantoin [15], from 20 to 120 μg/ml for creatinine [15], from 5 to 30 μg/ml for uric acid and hypoxanthine and from 2 to 15 μg/ml for xanthine. The recoveries were 97.9 ± 1.7% (R.S.D. = 1.8%) for allantoin [15], 99.1 ± 0.6% (R.S.D. = 0.6%) for creatinine [15], 93.6 ± 2.4% (R.S.D. = 2.5%) for uric acid, 106.5 ± 1.8% (R.S.D. = 1.7%) for hypoxanthine and 103.8 ± 1.2% (R.S.D. = 1.1%) for xanthine.

In conclusion, we have developed a sensitive RP-HPLC method for the simultaneous determination of allantoin, creatinine, uric acid, hypoxanthine and xanthine. The final chromatographic conditions adopted were a compromise between analysis time, peak shapes and symmetry and the resolution of these compounds from interefering substances. We consider that this method may be proposed as a possible reference method.

ACKNOWLEDGEMENTS

This study was supported by a Grant from CICYT (GAN 88/0071). We express our thanks and indebtedness to the Department of Animal Production, University of León, for their contribution.

REFERENCES

1 F. D. D. Hovell, E. R. Orksov, D. A. Grubb and N. A. MacLeod, *Br. J. Nutr.*, 50 (1983) 173.
2 J. H. Toppps and R. C. Elliot, *Nature (London)*, 205 (1985) 498.
3 A. M. Antoniewicz and P. M. Pisulewski, *Rocz. Nauk Zoot.*, 8 (1981) 49.
4 J. E. Lindberg, *Swed. J. Agric. Res.*, 15 (1985) 31.
5 S. Brody, *Bioenergetics and Growth*, Hafner, New York, 1964.
6 E. J. Young and C. F. Conway, *J. Biol. Chem.*, 142 (1942) 839.
7 J. E. Lindberg and C. Jansson, *Swed. J. Agric. Res.*, 19 (1989) 163.
8 X. B. Chen, J. Mathieson, F. Dickson and P. J. Reeds, *J. Sci. Food Agric.*, 53 (1990) 23.
9 J. Vasiliades, *Clin. Chem.*, 22 (1976) 1664.
10 M. H. Kroll, R. Chesler, C. Hagengruber, D. W.Blank, J. Kestner and M. Rawe, *Clin. Chem.*, 32 (1986) 446.
11 K. Spencer, *Ann. Clin. Biochem.*, 23 (1986) 1.
12 H. Dubois, *J. Clin. Chem. Clin. Biochem.*, 27 (1989) 151.
13 J. R. Klinenberg, S. Goldfinger, K. H. Bradley and J. E. Seegmiller, *Clin. Chem.*, 13 (1967) 834.
14 W.Tiemeyer and D. Giesecke, *Anal. Biochem.*, 123 (1982) 11.
15 M. T. Diez, M. J. Arin and J. A. Resines, *J. Liq. Chromatogr.*, in press.
16 G. P. Xue, R. C. Fishlock and A. M. Snoswell, *Anal. Biochem.*, 171 (1989) 135.
17 M. Ogata and T. Taguchi, *Ind. Health*, 25 (1987) 225.
18 D. H. Catlin and D. Starcevic, *J. Liq. Chromatogr.*, 14 (1991) 2399.
19 R. Paroni, C. Arcelloni, I. Fermo and A. Bonini, *Clin. Chem.*, 36 (1988) 830.
20 J. A. Milner and E. G. Perkins, *Anal. Biochem.*, 88 (1978) 560.
21 P. D. Schweinsberg and T. L. Loo, *J. Chromatogr.*, 181 (1980) 103.
22 M. J. Arin, M. T. Diez, J. A. Resines and M. T. Alemany, *J. Liq. Chromatogr.*, 13 (1990) 2465.
23 J. C. Crawhall, K. Itiaba and S. Katz, *Biochem. Med.*, 30 (1983) 261.

Journal of Chromatography, 607 (1992) 203–206
Elsevier Science Publishers B.V., Amsterdam

CHROM. 24 067

Short Communication

Carbosulfan in technical concentrates and formulated products

Liquid chromatographic determination with photodiode-array detection

C. de la Colina, A. Peña-Heras and F. Sánchez-Rasero*

Estación Experimental del Zaidín (CSIC), Profesor Albareda 1, 18008 Granada (Spain)

ABSTRACT

A reversed-phase high-performance liquid chromatographic method, based on the Food Machinery Corporation/Collaborative International Pesticides Analytical Council (FMC/CIPAC) method, has been developed for the determination of carbosulfan in technical and formulated products. With this method both time and solvents are saved and much more information on peak purity is obtained when compared with the FMC/CIPAC method. Accuracy, tested by application of the standard addition method, allowed recoveries from 99.0 to 101.3% of theoretical. Precision, determined by analysis of 22 samples prepared at concentrations of about 0.08 and 0.24 g/l, was 1.00 and 0.53%, respectively.

INTRODUCTION

Carbamate pesticides have been intensively used during recent years because of their broad spectrum, effectiveness and moderate mammalian toxicity.

Their thermal instability makes their analysis by gas chromatography difficult and thus numerous high-performance liquid chromatographic (HPLC) methods have been developed for this purpose [1–5]. Nevertheless, except for the Food Machinery Corporation/Collaborative International Pesticides Analytical Council (FMC/CIPAC) method [6], none has been found to be useful for the analysis of carbosulfan.

Carbosulfan is a systemic insecticide largely used in Spain to control soil-dwelling insects and foliar pests on maize, potatoes and sugar beet.

For the reasons indicated above and also because of a saving in both time and solvents compared with the FMC/CIPAC method, as well as to obtain more information on peak purity, we have developed an internal standard, reversed-phase HPLC method for the determination of carbosulfan.

EXPERIMENTAL

Apparatus

Filters. Millipore Type HAWP for water and Type FHLP for acetonitrile, pore size 0.5 μm (Millipore, Bedford, MA, USA).

0021-9673/92/$05.00

Liquid chromatograph. Hewlett-Packard 1090 as described in a previous paper [7].

Reagents

Solvents. Acetonitrile and water, both liquid chromatographic grade.

Eluent. Acetonitrile–water (85:15).

Internal standard solution. A 1.8-g aliquot of *n*-nonaphenone (Parish Chemical, Orem, UT, USA) was weighed into a 500-ml volumetric flask, dissolved and diluted to volume with acetonitrile.

Calibration solution. An aliquot of 100–110 mg of carbosulfan analytical standard of known purity (FMC Europe, Belgium) was weighed into a 50-ml flask. A 25.0-ml aliquot of the above internal standard solution was added and the carbosulfan dissolved quantitatively. A 5.0-ml volume of this solution was transferred to a 25-ml volumetric flask and diluted to volume with acetonitrile. A 2.0-ml volume of the latter solution was pipetted into a 20-ml volumetric flask and made up to volume with acetonitrile. The resulting solution was filtered through an appropriate Millipore filter into a small vial and capped.

Sample solutions

Sufficient sample (tehnical or formulated carbosulfan) to contain *ca.* 100–110 mg of carbosulfan was weighed and treated as described above for the calibration solution.

Chromatographic conditions

The chromatographic conditions were as follows: stainless-steel column, 100 × 2.1 mm I.D.; stationary phase, ODS-Hypersil 5 μm; guard column, 20 × 2.1 mm I.D. packed with ODS-Hypersil 30 μm; temperature, 40°C; flow-rate, 0.3 ml/min; stop time, 4.5 min; injected volume, 5 μl; detector wavelengths, 280–450 and 254–450 nm; spectra setting in apex, base and slope, from 240 to 350 nm; chart speed, 2 cm/min; attenuation, automatic.

The FMC/CIPAC method uses a 250 × 4.6 mm

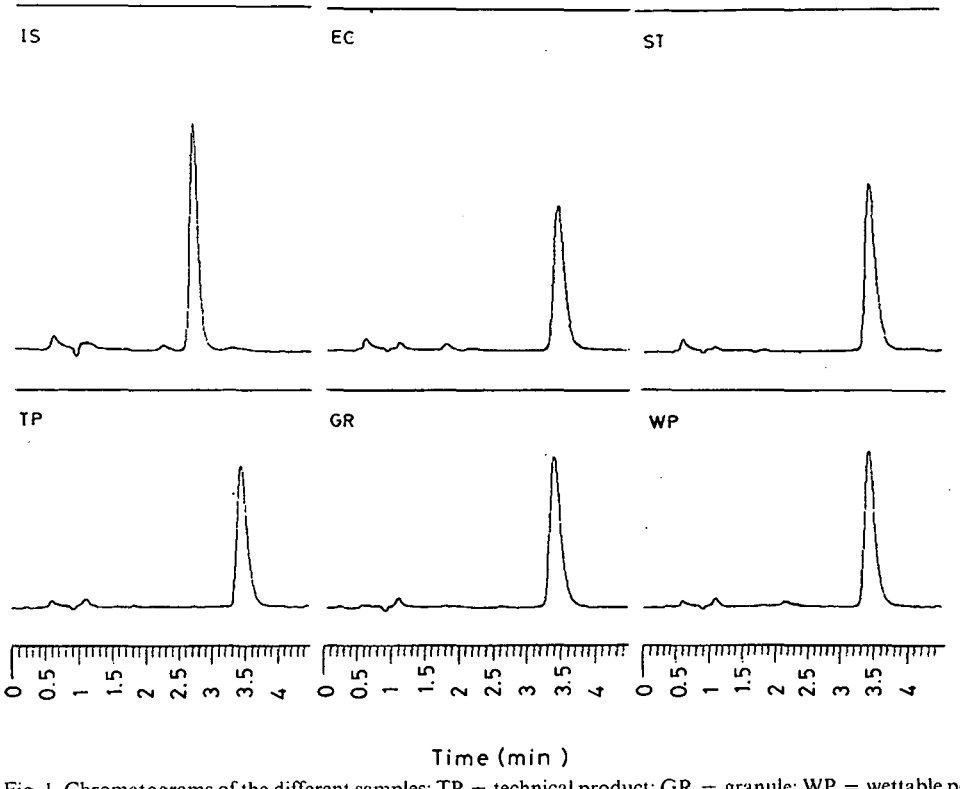

Fig. 1. Chromatograms of the different samples: TP = technical product; GR = granule; WP = wettable powder; ST = powder; EC = emulsifiable concentrate; IS = internal standard. See text for chromatographic conditions.

C_8 column and methanol–water (88:12) as eluent at a flow-rate of 1 ml/min. Detection is performed at 280 nm. The minimum chromatographic time is 13.5 min and it does not provide any test to prove peak purity.

Calibration and quantitation

The specified volumes of calibration solution were injected until the variation in peak areas did not deviate from the mean by more than 1%. After calibration, sample solutions were injected for analysis. Concentrations were proportional to peak areas at the concentration levels discussed in this paper.

RESULTS AND DISCUSSION

The calibration curve, obtained by plotting absorbance *versus* carbosulfan concentration, was linear over the range 0.02–0.34 g/l for 5-μl injections. The curve passed close to the origin and the data fitted the equation $y = 4700.0508x - 2.8067$, with a correlation coefficient of 0.9999.

Chromatograms of the different samples, technical product (TP), granule (GR), wettable powder (WP), powder (ST), emulsifiable concentrate (EC) and internal standard (IS) are shown in Fig. 1. It can be seen that in no case is here interference between samples and internal standard. In Figs. 1, 2 and 3 the y-axis shows absorbance.

Fig. 2 shows the signal plus spectra plot of a technical product added with internal standard. The identity of the three spectra, between 243 and 347 nm (each tick = 5 nm), for every peak, measured just prior to, at and after their respective maxima (upper left) shows their purities.

The carbosulfan spetrum shows a maximum absorbance at 280 nm, and both carbosulfan and *n*-nonaphenone present a considerable absorbance at 254 nm. These were the two wavelengths chosen for simultaneous integration. Fig. 3 shows the ratio of the signals obtained at those two wavelengths *versus* time for the same chromatogram as in Fig. 2. The linear relationship of the ratio of signals for

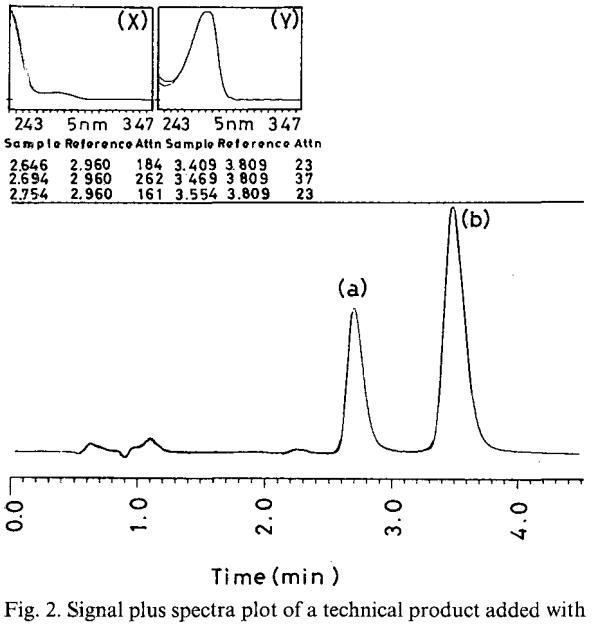

Fig. 2. Signal plus spectra plot of a technical product added with internal standard. (a) Internal standard peak; (b) carbosulfan peak; (X) three superimposed spectra obtained at different times of chromatographic peak a; (Y) three superimposed spectra obtained at different times of chromatographic peak b.

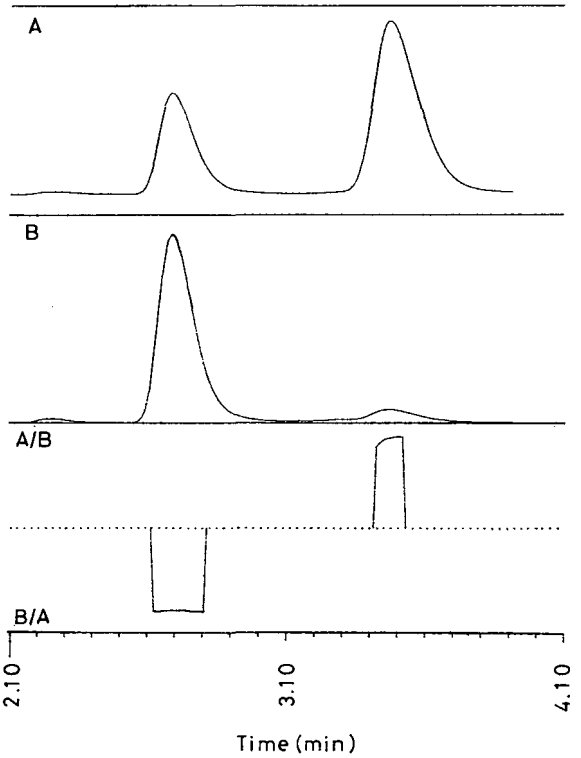

Fig. 3. Signals ratio of the chromatogram from Fig. 2, for both peaks, measured at (A) 280 nm and (B) 245 nm, and A/B ratio of the two signals.

TABLE I

RECOVERY OF CARBOSULFAN (STANDARD ADDITION METHOD)

Added (ng/5 μl)	Found (mean ± s_r)[b] (ng/5 μl)	Recovery (%)	R.S.D.[a] (%)
61.5	62.3 ± 6.0	101.3	2.25
122.9	121.7 ± 6.2	99.0	1.15
184.4	184.4 ± 7.9	100.0	0.98
245.8	244.6 ± 6.8	99.5	0.65

[a] Relative standard deviation of three determinations.
[b] $s_r = \sigma_{n-1} \cdot t_{n-1}$.

both peaks is a further demonstration of peak purity.

The standard addition method was used to test the accuracy of the method. To five 8-ml aliquots of a carbosulfan–nonaphenone solution in acetonitrile, at concentrations of 0.1121 and 0.1443 g/l, respectively, were added 0, 1, 2, 3 and 4 ml of a 0.1475 g/l carbosulfan solution in acetonitrile and, correspondingly 4, 3, 2, 1 and 0 ml of acetonitrile. Recoveries ranged from 99.0 to 101.3%. Details are given in Table I.

A total of 22 samples of a technical product were prepared and analysed. The details are given in Table II and they show that the relative standard deviation of the method is 1.00% for a carbosulfan concentration of about 0.08 g/l and 0.53% for a concentration of about 0.24 g/l.

It can be concluded that the method is specific, accurate and precise, provides a lot of information on peak purity and saves on operating costs (time and solvents).

TABLE II

CARBOSULFAN CONTENT IN A TECHNICAL PRODUCT, DETERMINED AT TWO DIFFERENT CONCENTRATIONS

0.08 g/l		0.24 g/l	
Weight (mg)	Percentage	Weight (mg)	Percentage
100.0	88.039	100.4	89.303
100.5	87.847	100.4	88.590
100.4	88.145	100.9	88.769
102.0	87.950	100.7	89.723
102.3	88.548	100.3	88.558
102.2	88.814	99.9	88.377
100.4	88.441	100.4	88.232
100.1	90.510	100.0	88.518
100.7	90.221	100.0	88.357
99.6	88.519	99.6	88.158
101.5	89.064	99.5	88.807
Mean ± s_r	88.736 ± 0.596		88.672 ± 0.317
R.S.D. (%)	1.00		0.53

ACKNOWLEDGEMENTS

We gratefully acknowledge FMC Europe, which supplied us with samples and standards. The valuable technical assistance of M. D. Maroto is acknowledged.

REFERENCES

1 C. M. Sparacino and J. W. Hines, *J. Chromatogr. Sci.*, 14 (1976) 549.
2 J. F. Lawrence and D. Turton, *J. Chromatogr.*, 159 (1978) 207.
3 R. T. Krause, *J. Chromatogr.*, 185 (1979) 615.
4 A. Peña-Heras and F. Sánchez-Rasero, *J. Liq. Chromatogr.*, 9 (1986) 3357.
5 J. Sherma, *Anal. Chem.*, 63 (1991) 118R.
6 *Document No. 3631*, CIPAC, Braunschweig, June 1991.
7 F. Sánchez-Rasero and A. Peña-Heras, *J. Assoc. Off. Anal. Chem.*, 71 (1988) 1064.

Journal of Chromatography, 607 (1992) 207–213
Elsevier Science Publishers B.V., Amsterdam

CHROM. 24 380

Separation and quantitation of some metal ions by reversed-phase high-performance liquid chromatography using *in situ* complexation with (±)-*trans*-1,2-diaminecyclohexane-N,N,N′,N′-tetraacetic acid

A. I. Valle

Departamento Química Analítica, Facultad de Ciencias, Universidad de Alcalá de Henares, 28871 Alcalá de Henares, Madrid (Spain)

M. J. González

Unidad de Contaminación Ambiental, Instituto de Química Orgánica (CSIC), C/Juan de la Cierva 3, 28006 Madrid (Spain)

M. L. Marina*

Departamento Química Analítica, Facultad de Ciencias, Universidad de Alcalá de Henares, 28871 Alcalá de Henares, Madrid (Spain)

ABSTRACT

(±)-*trans*-1,2-Diaminecyclohexane-N,N,N′,N′-tetraacetic acid (DCTA) was used as a mobile phase complexing agent to separate and quantitate the metal ions Fe(II), Fe(III), Cr(VI), Cu(II), Ni(II), Co(II), Pb(II) and Hg(II) in reversed-phase high-performance liquid chromatography. Cations were separated as metal–DCTA complexes formed in the chromatographic system and detected by UV spectrophotometry. Selectivity depended on the methanol content of the mobile phase and the pH. The method was fairly sensitive and detection limits for some metal ions were established at the nanogram level.

INTRODUCTION

Reversed-phase high-performance liquid chromatography (RP-HPLC) has proved to be an effective technique in the determination of inorganic species. The use of a non-polar chemically bonded phase as the stationary phase in HPLC can be applied to the determination of anions and cations. Ion-pair chromatography (IPC), which uses an ionic hydrophobic agent (counter ion) in the mobile phase, increases the retention of the ionic solutes with an opposite charge. With this method, many different parameters modify the retention of the solute and the selectivity of the separation.

The applications of HPLC using bonded phases to the determination of inorganic species has been reviewed [1]. For inorganic anions, separation is achieved by using tetraalkylammonium salts in the mobile phase and two different methods can be used to separate the metal ions. The first is the formation of an ion pair with the metal ion by placing an anionic counter ion in the mobile phase. This mode requires the detection of the metal ion by refractometry, atomic emission spectrometry or UV spectrophotometry with post-column derivatization. The second method is to form an ion pair consisting of a complex formed between the metal ion and a suitable complexing agent. This method is more often used because it allows detection of the metal ion with either UV–visible spectrophotometry or fluorimetry. The nature of the counter ion used is determined by the charge of the metal ion complex. If the

0021-9673/92/$05.00

complex has a negative charge, the simultaneous separation of metal ions that have been complexed from anions can be carried out with a positively charged counter ion.

Metal ion complexes can be made in one of two ways. (a) The complex is formed outside the chromatographic system (pre-column complexation); in this instance the complexing agent is not introduced into the mobile phase and the complexes are stable enough not to decompose when they are injected into the chromatographic system. Some prior techniques (such as solvent extraction) are often used to obtain the complexes. (b) Metal ion complexes are formed within the chromatographic system itself. In this method the complexing agent is introduced into the mobile phase and then the metal ions injected into the column dissolved in the mobile phase or even in water. This method is called *in situ* complexation and can also consist in injecting the metal ions as complexes if the complexing ligand must be present in the mobile phase to preclude complex decomposition.

Comparison of the two complexation methods shows that *in situ* complexation does not require prior extraction steps to obtain the complexes and thus has the advantage of a faster analysis time. However, this technique places some limitations on the complexing agent: it must be non-corrosive with respect to the chromatographic system and compatible with the detection system used.

Various papers on the separation of metal chelates by HPLC had been published before the review of Marina *et al.* [1]. Veening and Willeford [2–4] described the separation of metal ions as complexes using chemically bonded phases whereas Smith [5], O'Laughlin [6] and Steinbrech [7] reviewed the applications of HPLC in the separation of metal chelates.

All these papers give useful information on the characteristics of the complexing ligand that are required for metal complexation. First, to achieve separation of multielemental mixtures, the reagent must be able to form stable complexes with a great variety of metal ions. Second, the complexes obtained must present a strong UV–visible absorption or emission signal to allow their detection by UV–visible spectrophotometry or fluorimetry. As in the *in situ* complexation mode the metal complexes are formed in the chromatographic column, the formation of the metal complexes must be rapid.

Aminepolycarboxilic acids are known for their ability to form highly stable metal complexes with many different metal ions [8]. However, few reports have been published on the use of these reagents to separate metal ions in RP-HPLC. In fact, the reports that have been published used ethylenediaminetetraacetic acid (EDTA) as the complexing agent [9–11]. The interesting results obtained with this ligand suggest the possibility of using another aminepolycarboxylic acid, (±)-*trans*-1,2-diaminecyclohexanetetraacetic acid (DCTA), which also complexes with many different metal ions.

The purpose of the work reported here was to study the use of DCTA as a complexing agent in the mobile phase for the separation of metal ions by RP-HPLC.

EXPERIMENTAL

Reagents and solutions

All chemicals used were of analytical-reagent grade. Metal ion solutions were prepared from the following salts: $Pb(NO_3)_2$, $Co(NO_3)_2$, $Cu(NO_3)_2$, $FeSO_4$, $K_2Cr_2O_7$, $FeCl_3$, $NiCl_2$ and $HgCl_2$.

DCTA was obtained from Aldrich (Steinheim, Germany). Tetrabutylammonium bromide (TBA), tetrapropylammonium bromide (TPA), NaH_2PO_4 and Na_2HPO_4 were from Merck (Darmstadt, Germany). The methanol used for mobile phase preparation was of HPLC quality (Ferosa, Spain). Ultrapure Milli-Q water (Millipore, Belford, MA, USA) was also used.

Methanol–water mixtures containing DCTA, TBA or TPA and phosphate buffer at pH 4.15, 5.8 or 6.2 were used as mobile phases. These solutions were prepared by weighing the methanol and the aqueous solution and then calculating the percentage by volume. These mobile phases were filtered in a Millipore system with 0.47-μm filters and degassified in an ultrasonic bath.

Metal ion solutions were obtained by dissolving the correct amount of metal ion salt in the appropriate volume of mobile phase to reach the desired concentration.

Samples were eluted under isocratic conditions.

Apparatus

The components of the HPLC system (Perkin-Elmer, Beaconsfield, UK) were the following: a

Model 10 pump, a UV–visible LC-95 variable-wavelength detector and a Model 023 datarecorder. A 7125 Rheodyne injection valve with a 20-μl loop and a 25 cm × 4.5 mm I.D. Spherisorb ODS-2 column (particle diameter 10 μm) were also used.

The detection of the complexes was performed at 254 nm. Absorption spectra of the metal–DCTA complexes were obtained with a Model Lambda 2 UV–visible spectrophotometer (Perkin-Elmer).

Solution pH was measured with a Model M-501 pH meter (Orion Research, Cambridge, MA, USA) with a combined electrode.

Calibration graphs

The calibration graphs for metal ions were obtained by plotting the peak height against the concentration of the injected metal ion. An average of five injections were performed for measurements at each concentration of metal ions used.

RESULTS AND DISCUSSION

Detection of metal complexes

Absorption spectra of the metal complexes indicated an absorption maximum at wavelengths close to 230 nm for Ni(II) and Co(II), 245 nm for Pb(II), 265 nm for Fe(III) and two maxima for Cu(II) and Hg(II) at wavelengths of 230 and 265 nm and 230 and 255 nm, respectively. $Cr_2O_7^{2-}$ has almost the same absorption between 230 and 270 nm.

A wavelength of 254 nm was chosen to detect all the metal complexes investigated as it has a high absorption for most of the complexes, except Ni(II) and Co(II).

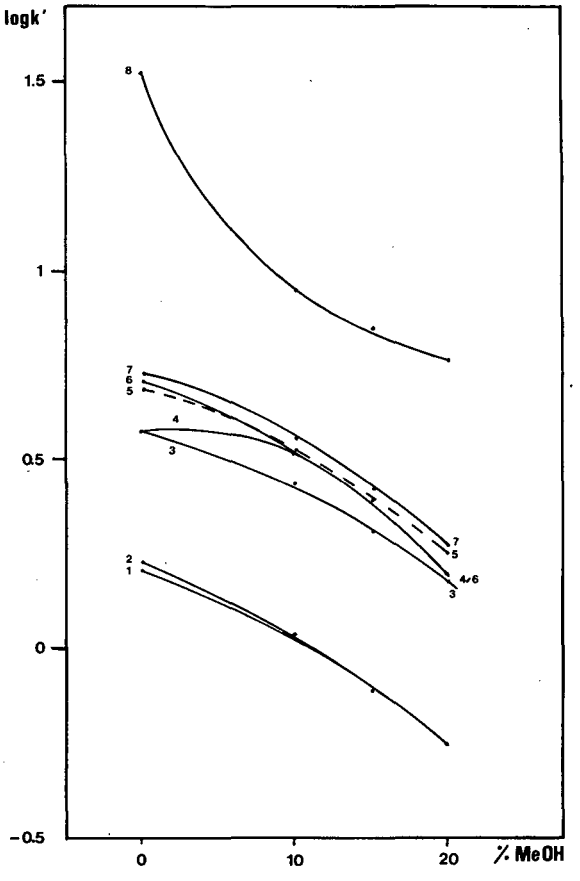

Fig. 1. Variation of the capacity factor logarithm (log k') of species as a function of percentage of methanol (MeOH) in the mobile phase. Mobile phase: methanol–water mixtures, $1 \cdot 10^{-2}$ M DCTA, $1 \cdot 10^{-2}$ M TBA, $1 \cdot 10^{-3}$ M phosphate buffer (pH 5.8). 1 = NO_3^-; 2 = Fe(II); Fe(III); 3 = Cu(II); 4 = Cr(VI); 5 = Ni(II); 6 = Pb(II); 7 = Co(II); and 8 = Hg(II).

Separation of metal complexes

To separate mixtures of the metal ions Fe(II), Fe(III), Cr(VI), Cu(II), Ni(II), Co(II), Pb(II) and Hg(II) as DCTA complexes by RP-HPLC, *in situ* complexation was chosen. This was because when a ligand similar to DCTA, such as EDTA, was used, it was found that the chromatographic peak widened when the concentration of ligand in the mobile phase was low (10^{-4} or 10^{-5} M) [9]. For this reason, the complexing agent DCTA was added to the mobile phase at a concentration of $1 \cdot 10^{-2}$ M. In this way, the formation equilibrium of the complex is favoured, allowing an optimum peak shape and conditions for maximum sensitivity at the wavelength at which the determination was performed.

As metal ions were separated as negatively charged DCTA complexes, a counter ion with a positive charge, TBA, was used to retain the complexes in the stationary phase. The choice of TBA should not only allow the separation of anionic metal–DCTA complexes, but also the separation of other species with a negative charge such as Cr(VI), found in solution as $Cr_2O_7^{2-}$, or of an inorganic anion such as NO_3^-. Preliminary experiments showed a good retention of the metal ions in the system when the concentration of TBA in the mobile phase was $1 \cdot 10^{-2}$ M. The TBA concentration was thus kept constant and equal to this value. The

percentage of organic modifier and the pH of the mobile phase were studied to determine their influence on system selectivity, thus establishing the best conditions for mixture separation.

Influence of percentage of organic modifier

Methanol was chosen as the organic modifier in the mobile phase and the variation of the capacity factor logarithm for either NO_3^-, Fe(II), Fe(III), Cr(VI), Cu(II), Ni(II), Co(II), Pb(II) or Hg(II) with the methanol content of the mobile phase was determined. The results obtained at pH 5.8 (phosphate buffer) are grouped in Fig. 1. Retention of species in the chromatographic system decreased when the methanol content increased, as expected, as when the methanol content increases the amount of counterion adsorbed in the stationary phase decreases, and this decreases the solute retention. Usually the logarithm for the capacity factor of the solutes in IPC decreases linearly with the percentage of methanol [12]. However, Fig. 1 shows that the curve obtained for Cr(VI), Pb(II), and Hg(II) does not concur with the considerations on the retention mechanism.

With respect to selectivity, there is no methanol percentage at which the selectivity is at a maximum as the selectivity depends on the kind of mixture to be separated. In fact, it can be observed (Fig. 1) that

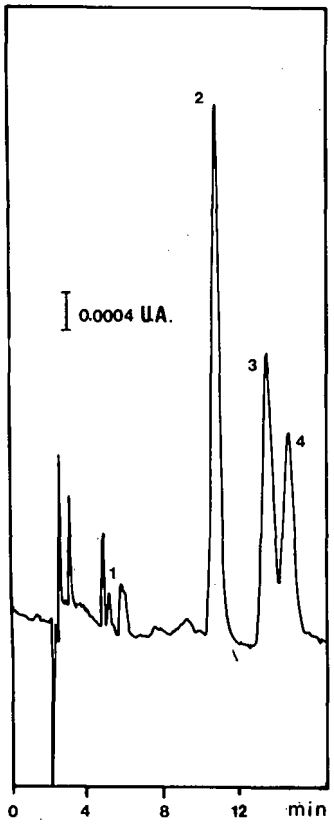

Fig. 2. Chromatogram showing the separation NO_3^-–Cu(II)–Ni(II)–Co(II). Mobile phase: water, $1 \cdot 10^{-2}$ *M* DCTA, $1 \cdot 10^{-2}$ *M* TBA, $1 \cdot 10^{-3}$ *M* phosphate buffer (pH 5.8). 1 = NO_3^-; 2 = Cu(II); 3 = Ni(II); and 4 = Co(II). U.A. = Absorbance units.

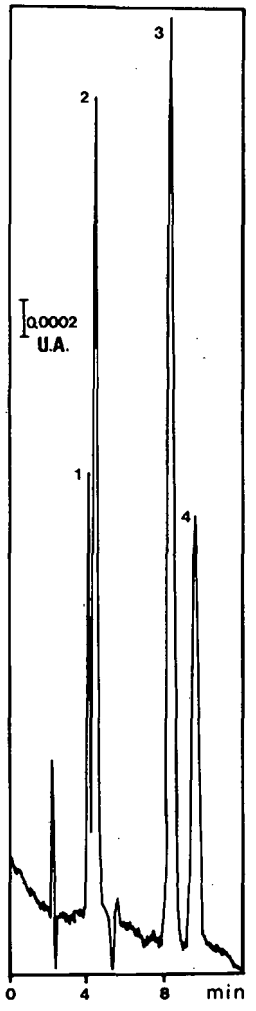

Fig. 3. Chromatogram showing the separation NO_3^-–Fe(II)–Cu(II)–Pb(II). Mobile phase: methanol–water (10:90), $1 \cdot 10^{-2}$ *M* DCTA, $1 \cdot 10^{-2}$ *M* TBA, $1 \cdot 10^{-3}$ *M* phosphate buffer (pH 5.8). 1 = NO_3^-; 2 = Fe(II); 3 = Cu(II); and 4 = Pb(II).

the separation of Ni(II)–Co(II), Cr(VI)–Pb(II) and Cu(II)–Pb(II) are favoured by low methanol contents (0%), the separation of Pb(II)–Ni(II) is favoured in mobile phase with a high methanol content (20%), and the separation of Cu(II)–Cr(VI) is favoured when the methanol content is intermediate (10%). Other separations are possible at any percentage of methanol: Cu(II)–Ni(II) and Cu(II)–Co(II). Finally, there are mixtures that could be separated at low or high methanol contents but not at intermediate ones (10%), such as the mixture Cr(VI)–Ni(II). The behaviour of these ions is roughly similar. However, for Fe(II), Fe(III) and Hg(II), the species Fe(II) as well as Fe(III) can be separated from Hg(II) and all three can be separated from any other ion because of their different retention behaviours. Fig. 1 includes NO_3^-, which can be separated from metal ion mixtures. These variations of selectivity can be illustrated with some simple separations such as those shown in Figs. 2 and 3, in which simply modifying the methanol content at a fixed pH of 5.8 separates the species in the chromatographic column. Fig. 2 shows the separation Cu(II)–Ni(II)–Co(II) at 0% methanol and Fig. 3 shows the separation Fe(II)–Cu(II)–Pb(II) at 10% methanol. It should be noted that although Hg(II) can be separated from all the other species, at this pH there is an important widening of its chromatographic peak.

Influence of mobile phase pH

To study the influence of pH on selectivity, the variation of the retention of the metal ions as a function of the pH of the mobile phase was determined. In these experiments the methanol content of the mobile phase was kept constant and equal to 10%. The results are shown in Fig. 4 in which the variation of the logarithm of the capacity factor for Fe(II), Fe(III), Cu(II), Cr(VI), Pb(II), Ni(II), Co(II) and Hg(II) is plotted for the three pH values studied (4.15, 5.8 and 6.2). It can be observed that the retention of metal ions generally decreases with an increase in the pH of the mobile phase. However, this decrease is more important between pH 5.8 and 6.2 [especially for Cr(VI)] as between pH 4.15 and 5.8, the influence of pH is low.

As the metal ions are retained in the chromatographic system through the formation of complexes with a negative charge, it might be expected that an increase in the pH of the mobile phase would increase the retention of metal ions because of the rise in the conditional complexation constant. However, the results can be explained by another effect. The mobile phase contained the complexing agent DCTA and phosphate buffer and both increase their negative charge with rising pH values. This implies greater retention in the chromatographic system through the formation of an ion pair with TBA and the competing effect provokes a decrease in the retention of the solutes. In fact, the decrease of the capacity factor for Cr(VI) with increasing pH is higher than for all the other metal ions for which the retention takes place by complexation. Regarding selectivity, Fig. 4 shows that it is similar at pH 4.15 and 5.8 whereas at pH 6.2 there is a change caused by the different behaviour of Cr(VI). However, the separations that can be made at pH 6.2 are, in general, also possible when the content of methanol is changed to pH 5.8; for instance, Cr(VI)–Pb(II) or Cr(VI)–Ni(II).

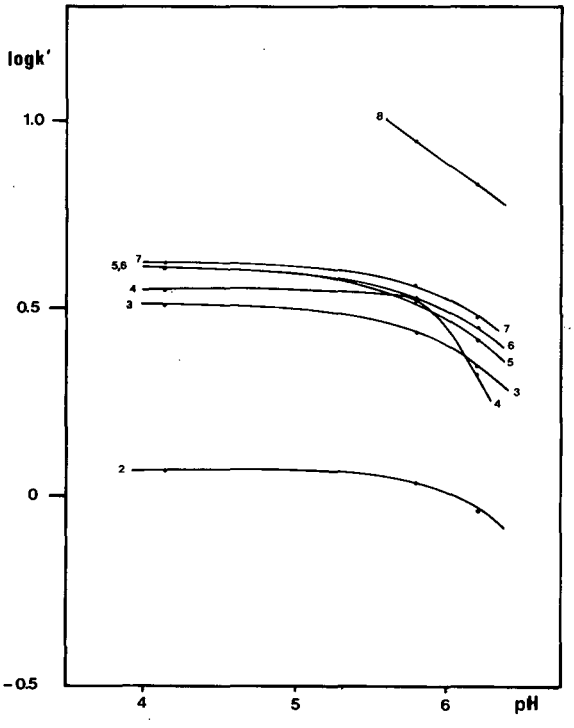

Fig. 4. Variation of the capacity factor logarithm (log k') of species as a function of the mobile phase pH. 2 = Fe(II), Fe(III); 3 = Cu(II); 4 = Cr(VI); 5 = Pb(II); 6 = Ni(II); 7 = Co(II); and 8 = Hg(II).

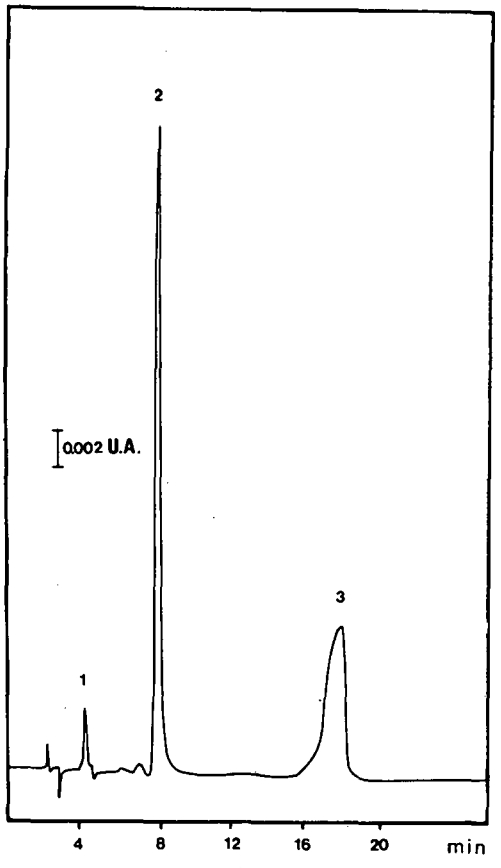

Fig. 5. Chromatogram showing the separation NO_3^-–Pb(II)–Hg(II). Mobile phase: methanol–water (10:90), $1 \cdot 10^{-2}$ *M* DCTA, $1 \cdot 10^{-2}$ *M* TBA, $1 \cdot 10^{-3}$ *M* phosphate buffer (pH 6.2). 1 = NO_3^-; 2 = Pb(II); and 3 = Hg(II).

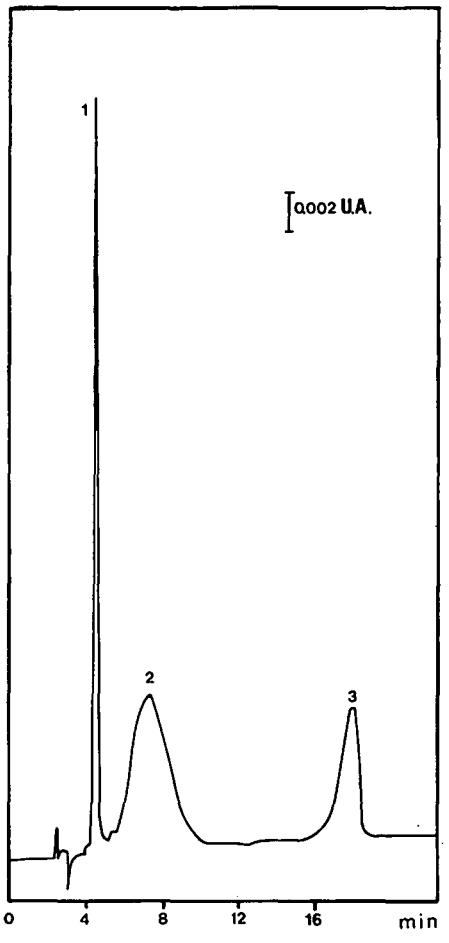

Fig. 6. Chromatogram showing the separation Fe(III)–Cr(VI)–Hg(II). Mobile phase as in Fig. 5. 1 = Fe(III); 2 = Cr(VI); and 3 = Hg(II).

The most interesting effect of a change in pH is the improvement of the peak shape, especially for Hg(II) and Cr(VI). For Hg(II), the peak shape improves considerably between pH 5.8 and 6.2. However, at pH 4.15, a peak for Hg(II) was not obtained. Figs. 5 and 6 show the peak of Hg(II) when it is separated from the others at pH 6.2. Fig. 5 shows the separation Hg(II)–Pb(II) and Fig. 6 shows the separation Fe(III)–Cr(VI)–Hg(II). In this last figure it is possible to observe the significant broadening that is observed for the Cr(VI) peak at pH 6.2. However, at pH 4.15 the peak shape for Cr(VI) improves, allowing separation from other metal ions with a similar retention, as illustrated in Fig. 7. This result for Cr(VI) may be explained by the higher stability of the anion $Cr_2O_7^{2-}$ when the acidity of the medium increases. For Hg(II) the improvement of the peak shape at pH 6.2 could be due to an increase in the conditional complexation constant wiht DCTA that occurs when the pH of the solution is increased.

Quantitation of species

To illustrate the sensitivity of the method, the detection limits (calculated by using a signal-to-noise ratio of 2:1) have been determined for some species. The results are shown in Table I, which groups detection limits in mass as well as in concentration units for Cu(II), Pb(II), Cr(VI) and Hg(II). Table I specifies the mobile phases used to obtain the given

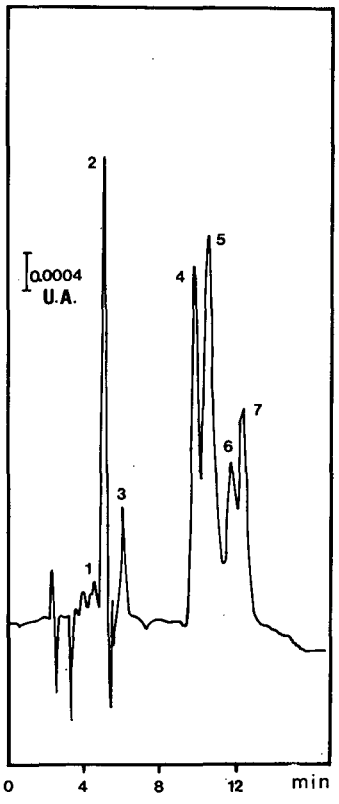

Fig. 7. Chromatogram showing the separation NO_3^-–Fe(III)–Cu(II)–Cr(VI)–Ni(II)–Co(II). Mobile phase: methanol–water (10:90), $1 \cdot 10^{-2}$ *M* DCTA, $1 \cdot 10^{-2}$ *M* TBA, $1 \cdot 10^{-3}$ *M* phosphate buffer (pH 4.15). 1 and 3 = NO_3^-; 2 = Fe(III); 4 = Cu(II); 5 = Cr(VI); 6 = Ni(II); and 7 = Co(II).

detection limits and these phases differ only with respect to the counterion used: TPA was used for Hg(II) to improve the peak shape at pH 5.8. The concentration of TPA was $1 \cdot 10^{-2}$ *M*.

Table I shows that the sensitivity of the method is similar for all the metal ions studied and that detection of these species at the nanogram level is possible. The height of the chromatographic peak varied with the amount of metal ion injected in a linear manner over at least two or three orders of magnitude.

TABLE I

DETECTION LIMITS FOR SOME METAL IONS

Injection volume 20 μl.

Metal ion	Mass (ng)	Concentration (ng/ml)
Cu(II)[a]	4.91	245.6
Pb(II)[a]	1.85	92.57
Cr(VI)[a]	3.23	161.39
Hg(II)[b]	3.87	193.76

[a] Mobile phase: methanol–water (10:90), $1 \cdot 10^{-2}$ *M* DCTA, $1 \cdot 10^{-2}$ *M* TBA, $1 \cdot 10^{-3}$ *M phosphate buffer (pH 5.8).*

[b] Mobile phase: methanol–water (10:90), $1 \cdot 10^{-2}$ *M* DCTA, $1 \cdot 10^{-2}$ *M* TPA, $1 \cdot 10^{-3}$ *M* phosphate buffer (pH 5.8).

CONCLUSIONS

The following conclusions can be drawn from the results presented. DCTA is a suitable complexing agent for the separation of metal ion mixtures by RP-HPLC. The introduction of DCTA into the mobile phase eliminates the need for preparatory metal complexation steps. The modification of the methanol content and pH of the mobile phase makes it possible to obtain a good peak shape and adequate selectivity for the separation of mixtures. A concentration of $1 \cdot 10^{-2}$ *M* in DCTA, $1 \cdot 10^{-2}$ *M* in TBA, $1 \cdot 10^{-3}$ *M* in phosphate buffer, a methanol content ranging from 0 to 20% and a pH value between 4.15 and 6.2 provide adequate separation conditions. As a positively charged counter ion is used to separate anionic complexes, the separation of inorganic anions from metal ions is also possible. Good sensitivity is obtained and it is possible to detect the metal ions at the nanogram level.

REFERENCES

1 M. L. Marina, J. C. Díez-Masa and M. V. Dabrio, *J. Liq. Chromatogr.*, 12 (1989) 1973.
2 H. Veening and B. R. Willeford, *Rev. Inorg. Chem.*, 1 (1979) 281.
3 B. R. Willeford and H. Veening, *J. Chromatogr.*, 251 (1982) 61.
4 H. Veening and B. R. Willeford, *Adv. Chromatogr.*, 22 (1983) 117.
5 R. M. Smith, *Anal. Proc.*, 21 (1984) 73.
6 J. W. O'Laughlin, *J. Liq. Chromatogr.*, 7 (1984) 127.
7 B. Steinbrech, *J. Liq. Chromatogr.*, 10 (1987) 1.
8 S. Kotrly and L. Sucha, *Handbook of Chemical Equilibria in Analytical Chemistry*, Wiley, Chichester, 1985.
9 M. L. Marina, J. C. Díez-Masa and M. V. Dabrio, *J. High Resolut. Chromatogr. Chromatogr. Commun.*, 9 (1986) 300.
10 W. Buchberger, P. R. Haddad and P. W. Alexander, *J. Chromatogr.*, 558 (1991) 181.
11 G. Sacchero, O. Abollino, V. Porta, C. Sarzanini and E. Mentasti, *Chromatographia*, 31 (1991) 539.
12 Cs. Horváth (Editor), *High Performance Liquid Chromatography. Advances and Perspectives*, Vol. 2, Academic Press, New York, 1980.

Journal of Chromatography, 607 (1992) 215–219
Elsevier Science Publishers B.V., Amsterdam

CHROM. 24 104

High-performance liquid chromatography–diode-array detection of photosynthetic pigments

Luis Almela*, José A. Fernández-López and José M. López-Roca

Department of Agricultural Chemistry, University of Murcia, Campus of Espinardo, E-30100 Murcia (Spain)

ABSTRACT

High-performance liquid chromatography and photodiode-array detection were applied simultaneously for the separation and identification of the photosynthetic pigments of a plant extract. Using a photodiode-array detector permitted simultaneous recording of the chromatographic analysis at different wavelengths, the contour plots of the chromatograms and the spectra of the pigments separated by high-performance liquid chromatography. Employing these techniques, and on the basis of their spectroscopic characteristics, the following compounds were identified: β-carotene, lutein, taraxanthin, violaxanthin, neoxanthin and chlorophylls *a* and *b* and their respective epimers, chlorophylls *a'* and *b'*. The rapidity, specificity, sensitivity and reproducibility of this technique make it particularly suitable for plant pigment analysis.

INTRODUCTION

High-performance liquid chromatographic (HPLC) methods are extensively used nowadays in the analysis of photosynthetic pigments [1–5]. This technique combines the ability to separate the pigments with the spectroscopic features of sensitive, selective identification through peak scanning and quantification. The identification of the peaks in a chromatogram is easy when known standards are available, but in the case of plant pigments only chlorophylls and some carotenes can be obtained commercially. Most pigments must be prepared by means of semipreparative chromatographic techniques, but this procedure is rather tedious and is not exempt from possible alterations [3].

At present, detectors based on photodiode-array spectroscopy permit the immediate identification of the components of a mixture by using their spectral characteristics. Moreover, photodiode-array detection (PAD) provides the spectrum, the absorbance ratio and the criteria for assessing the purity of the peaks.

In this paper we describe the separation and spectrophotometric identification of foliar photosynthetic pigments, using normal-phase HPLC with PAD.

EXPERIMENTAL

Apparatus

HPLC separation was carried out using as Shimadzu liquid chromatographic system (Shimadzu, Kyoto, Japan) equipped with two LC-6A pumps, an SCL-6A controller and an SPD-M6A photodiode-array detector. The data were stored and processed by a 386 SX personal computer (Olivetti, Ivrea, Italy) provided with chromatographic software (Shimadzu).

The absorption spectra of isolated pigments were recorded on a Hitachi U-3200 spectrophotometer (Hitachi, Tokyo, Japan), with double monochromator and wavelength(λ) accuracy of 0.3 nm. The spectrophotometric software provided,among other things, the automatic detection of λ-maxima.

Columns

Analytical separation was performed on a stainless-steel column (25 cm × 4.6 mm I.D.) of Spherisorb (Phase Separations, Norwalk, CT, USA)

0021-9673/92/$05.00

(5-μm spherical particles). Semipreparative separation was carried out on a stainless-steel column (30 cm × 7.8 mm I.D.) of μPorasil (Waters, Milford, MA, USA) (10-μm irregular particles).

Pigment extraction

A uniform sample of *Citrus limon* leaves was chopped into small pieces, and 10-g subsamples were extracted with 100% acetone in a Sorvall omni-mixer (Sorvall, Norwalk, CT, USA) at low temperature. The homogenate was filtered through a sintered-glass funnel and the residue was re-extracted until it was colourless. The filtrates were combined and made up to 250 ml with the same solvent. For HPCL analysis a 5-ml aliquot was dried in a nitrogen stream and the residue was dissolved in 500 μl of methanol and passed through a 0.45-μm nylon filter (Lida, Kenosha, WI, USA) prior to injection. The extract (20 or 200 μl for analytical or semipreparative separation, respectively) was injected into the chromatograph. The reagents employed were HPLC quality (Romil Chemicals, Loughborough, UK).

Chromatography

The pigments were eluted using an initial solvent mixture of light petroleum (LP) (b.p. 40–60°C) and ethanol (97:3, v/v). After 7 min, a gradient was initiated, changing the LP concentration linearly to 85% in 3 min. This composition was maintained until the pigments were completely eluted. The flow-rate for the analytical separation was 1 ml/min. Semipreparative separation was performed with the same gradient with the flow-rate increased to 4 ml/min.

Identification of pigments

Isolated pigments were identified according to their visible absorption characteristics compared with those in the literature [5–14]. The presence of epoxide groups was shown by their hypsochromic shift after treatment with hydrochloric acid [3].

RESULTS AND DISCUSSION

Fig. 1 shows a typical chromatogram of a methanol extract obtained from *Citrus limon* leaves. Complete separation of all pigments was obtained in less than 12 min, showing that the stepwise gradient elution minimizes elution time without loss of resolution. Thus, with this chromatographic programme in normal-phase, we achieved a much sorter separation time than is usual with reversed-phase chromatography. The quality of the separation was evaluated by means of separation selectivity and resolution of the peaks was calculated according to Kirkland [15] (Table I).

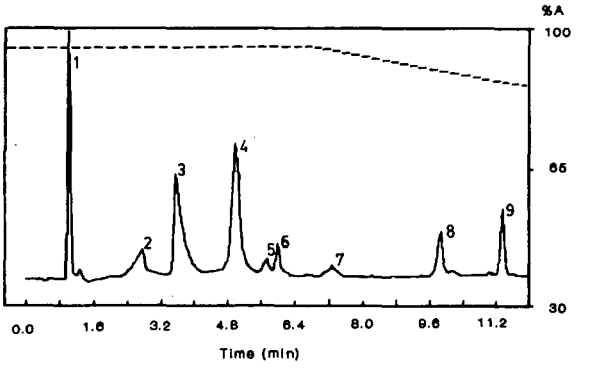

Fig. 1. Chromatogram of a foliar extract recorded at 430 nm. The linear gradient of light petroleum (A)–ethanol (B) is indicated by the dotted line. Analytical conditions are described in the text.

PAD is a powerful tool for the identification of different pigments present in a leaf extract; it permits a spectral analysis in real time without stopping the flow. The post-analysis treatment of data

TABLE I

CHROMATOGRAPHIC PARAMETERS CORRESPONDING TO THE CHROMATOGRAM SHOWN IN FIG. 1

Symbols: t' = reduced retention time ($t' = t_R - t_0$); t_0 (dead time) = 0.80 min; ω = band width (min); α = separation factor; R_s = resolution.

Peak No.	t'	ω	α	R_s
1	0.28	0.09	–	–
2	1.97	0.47	7.03	6.04
3	2.77	0.19	1.41	2.42
4	4.21	0.19	1.52	7.58
5	4.95	0.09	1.18	5.29
6	5.20	0.14	1.05	2.17
7	6.49	0.19	1.25	7.82
8	9.07	0.09	1.40	18.43
9	10.57	0.09	1.17	16.66

employing chromatographic software provides spectra, contour plots, three-dimensional representations, maxima detection and peak purity. The spectra obtained can be overlaid on a standard stored in a computer-aided library to help subsequent identification.

Table II summarizes the identification of the chromatographic peaks according to spectral data provided by PAD and data obtained from pure pigments isolated by semipreparative chromatography, subsequently purified in an analytical column and characterized in a typical solvent. These last data agreed with those referred to previously by us [5]. Data were compared with those presented in the references.

The chromatographic system made possible the identification of nine pigments. Five of them were carotenoids: β-carotene, lutein, taraxanthin, violaxanthin and neoxanthin. The others were chlorophylls and derivatives. We wish to emphasize the resolution of the epimers chlorophyll *a'* and chlorophyll *b'* in relation to chlorophylls *a* and *b*, respectively.

The contour plot, which is a pseudo-tridimensional representation of the absorbance, wavelength and time data (isogram), has proved to be very useful for the identification of plant pigments. The isograms summarize the chromatographic information and can aid in the selection of an optimal detection wavelength; they also give information on the spec-

TABLE II

IDENTITIES, RETENTION TIMES (t_R), PURITY AND SPECTRAL DATA FOR PIGMENTS SHOWN IN FIG. 1

Peak No.	t_R (min)	Pigment	Spectra maxima of the PAD (nm)			Purity	Solvent	Published maxima (nm)			Ref.
1	1.08	β-carotene	421	446	472	0.999	Eluent				
							Hexane	425	449	476	5
							Hexane	427	450	476	6
							Hexane	425	450	477	7
2	2.77	Chlorophyll *a'*	429	614	663	0.999	Eluent				
							Diethyl ether	428	614	663	8
3	3.57	Chlorophyl *a*	429	616	663	0.999	Eluent				
							Diethyl ether	430	615	661	5
							Diethyl ether	430	614	662	9
							Diethyl ether	430	615	662	10
4	5.01	Lutein	420	446	472	0.999	Eluent				
							Hexane	420	447	472	5
							Hexane	420	445	474	11
							Hexane	420	445	475	7
5	5.75	Chlorophyll *b'*	456	643		0.999	Eluent				
6	6.00	Chlorophyll *b*	456	645		0.999	Eluent				
							Diethyl ether	452	642		5
							Diethyl ether	453	643		9
							Diethyl ether	455	644		10
7	7.29	Taraxanthin	421	446	472	0.996	Eluent				
							Hexane	420	444	470	5
							Hexane	419	442	470	12
							Hexane	420	445	470	7
8	9.87	Violaxanthin	419	442	470	0.999	Eluent				
							Hexane	420	444	473	5
							Hexane	416	441	471	13
							Hexane	414	436	468	14
9	11.37	Neoxanthin	415	437	466	0.997	Eluent				
							Hexane	412	435	465	5
							Hexane	412	436	465	12
							Hexane	408	432	462	14

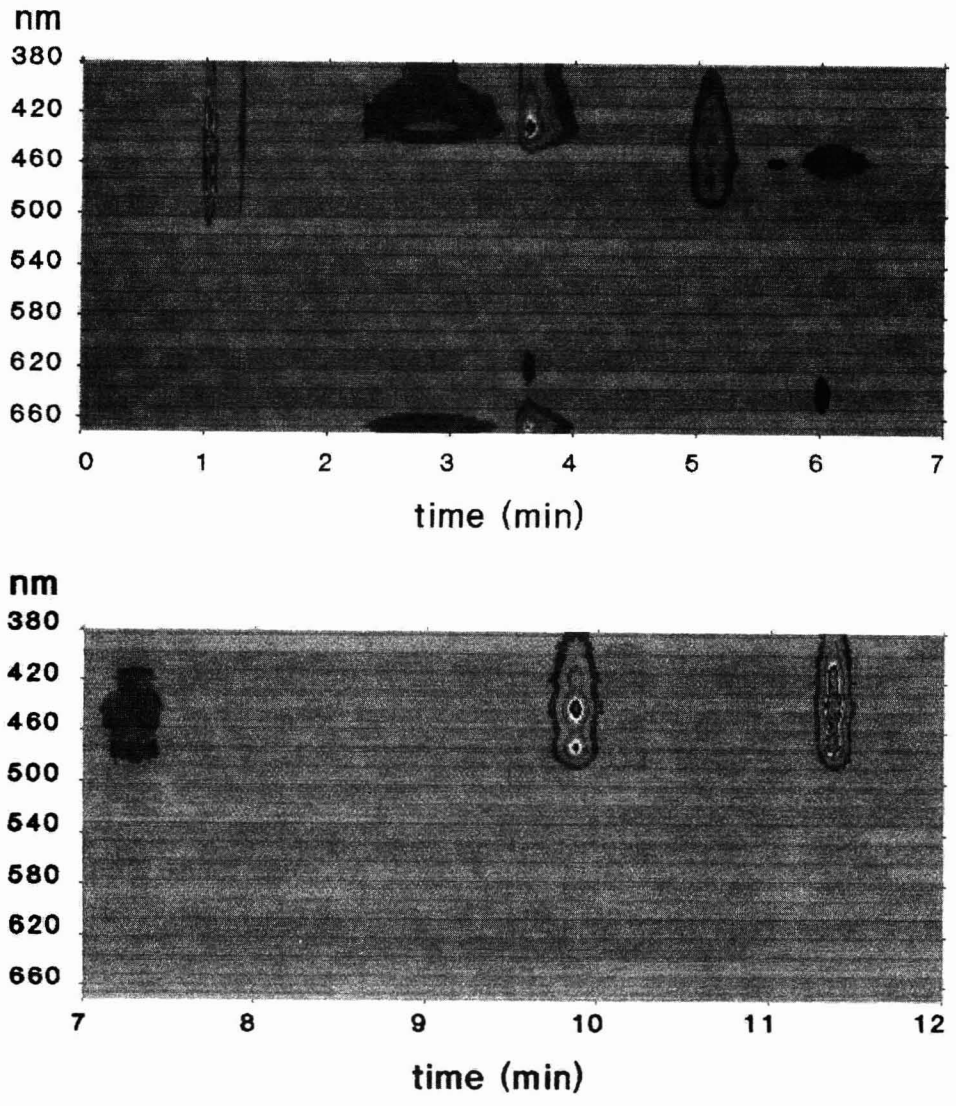

Fig. 2. Isogram of the chromatographic separation shown in Fig. 1.

tral maxima of the peaks. Fig. 2 shows the isogram of the chromatographic separation displayed in Fig. 1.

While the contour plots of the carotenoids show a high degree of symmetry, those of the chlorophylls present signs of tailing (poor chromatographic symmetry); nevertheless, their purity is proved by the symmetry in the wavelength dimension.

In addition, the isogram permits the detection of co-eluting peaks, particularly when their absorption maxima are sufficiently separated. Fig. 3 shows an isogram corresponding to a chromatogram where lutein and chlorophyll *b* co-eluted at the same time (*ca.* 3 min) in a seemingly symmetric peak. Nevertheless, the isogram shows a distortion between 2.7 and 3.3 min and, also, a contour plot is displayed around 645 nm; both effects are the result of the presence of chlorophyll *b*. When this chromatogram is run at 446 and 645 nm simultaneously, a

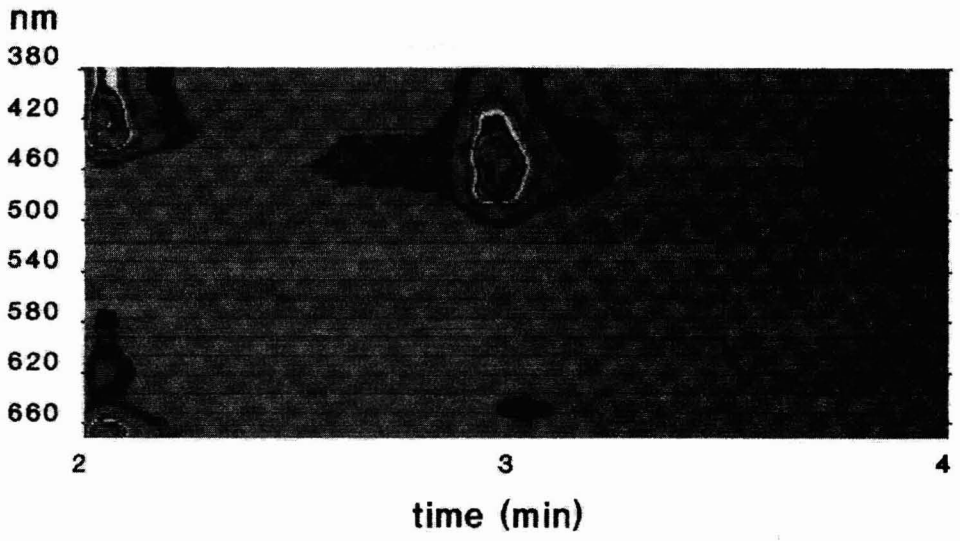

Fig. 3. Isogram of a poor chromatographic separation in which lutein and chlorophyll *b* co-eluted at the same time.

slight displacement in the retention time of the peaks eluted around 3 min can be observed. It is attributed to the fact that in each case a different pigment is detected. Thus, isograms may prove useful in setting up the conditions to optimize the elution programme and to obtain a rapid overview of the quality of the separation.

In conclusion, the joint use of HPLC and PAD is very useful in separating and identifying plant pigments as absorption spectra are obtained within fractions of a second. PAD also permits simultaneous chromatographic analyses at different wavelengths. In this way, each pigment can be detected at its maximum absorption wavelength, which provides a higher sensitivity. Even in the case of co-eluting peaks, the use of factor analysis and peak suppression techniques permits the mathematical resolution of overlapping peaks.

REFERENCES

1 H. G. Daood, B. Czinkotai, A. Hoschke and P. Biacs, *J. Chromatogr.*, 472 (1989) 296.
2 N. Suzuki, K. Saitoh and K. Adachi, *J. Chromatogr.*, 408 (1987) 181.
3 L. Almela, J. M. López-Roca, M. D. Alcázar and M. E. Candela, *J. Chromatogr.*, 502 (1990) 95.
4 M. Rise and E. E. Goldsmidt, *Plant Sci.*, 71 (1990) 147.
5 J. A. Fernández-López, L. Almela and J. M. López-Roca, *Photosynthetica*, 25 (1991) 81.
6 T. Philip and F. J. Francis, *J. Food Sci.*, 36 (1971) 823.
7 B. H. Davies, in T. W. Goodwin (Editor), *Chemistry and Biochemistry of Plant Pigments*, Vol. 2, Academic press, London, 1976, p. 38.
8 P. H. Hynninen, *Acta Chem. Scand.*, 27 (1973) 1487.
9 O. T. G. Jones, in L. P. Miller (Editor), *Phytochemistry*, Vol. 1, Van Nostrand-Reinhold, London, 1973, p. 75.
10 J. H. C. Smith and A. Benítez, in K. Peach and M. V. Tradey (Editors), *Modern Methods of Plant Analysis*, Springer, Berlin, 1955, p. 142.
11 D. J. Chapman, *Arch. Mikrobiol.*, 55 (1966) 17.
12 J. Val, J. Abadía, L. Heras and E. Monge, *J. Micronutr. Anal.*, 2 (1986) 305.
13 B. Camara and B. Moneger, *Phytochemistry*, 17 (1978) 91.
14 S. W. Wright and J. D. Shearer, *J. Chromatogr.*, 294 (1984) 281.
15 J. J. Kirkland (Editor), *Modern Practice of Liquid Chromatography*, Wiley, New Yok, 1971.

Journal of Chromatography, 607 (1992) 221–225
Elsevier Science Publishers B.V., Amsterdam

CHROM. 24 127

Gas chromatographic retention of carbohydrate trimethylsilyl ethers

IV. Disaccharides

A. García-Raso

Departament de Química Orgánica, Facultat de Ciències, Universitat de les Illes Balears, 07071 Palma de Mallorca (Spain)

M. I. Páez, I. Martínez-Castro* and J. Sanz

Instituto de Química Orgánica General (CSIC), Juan de la Cierva 3, 28006 Madrid (Spain)

M. M. Calvo

Instituto de Fermentaciones Industriales (CSIC), Juan de la Cierva 3, 28006 Madrid (Spain)

ABSTRACT

Trimethylsilyl ethers of seventeen disaccharides were injected on two stationary phases and their retention indices were calculated. Multiple linear regression was used to discuss relationships between retention indices and structural features of disaccharides.

INTRODUCTION

In spite of the large number of papers dealing with the gas chromatographic (GC) analysis of disaccharides as their trimethylsilyl (TMS) derivatives [1,2], most of them are restricted to only a few compounds (sucrose, lactose and maltose being the most representative). Sweeley *et al.* [3] gave the first retention data for eight disaccharides. The most complete reports are those of Haverkamp *et al.* [4] and Nikolov and Reilly [5]. The former lists relative retentions (with respect to sucrose at 228°C) for 23 dissacharides on three stationary phases, and the latter gives retention times relative to sucrose at 240°C for seventeen disaccharides on SE-54. In both instances the elution orders were related to some structural characteristics of the constituent monosaccharides, but the comparisons were restricted to components differing in one structural aspect only. Percival [6] measured relative retentions of fifteen unusual disaccharides on Apiezon and SE-30.

Unfortunately, it is impossible to collect a complete series of disaccharides, *i.e.*, those having the same rings and glycosidic linkages in all possible positions (twelve isomers) or those differing only in the monosaccharide having a free reducting group (eight possible isomers). Most such compounds have not yet been described, and others are very difficult to prepare.

We have previously studied the chromatographic behaviour of pentoses [7], aldohexoses [8] and ketohexoses [9] as TMS ethers. Some general features were found: an unusual retention when they were compared with other ethers, a decrease in their retention indices with increasing temperature and sta-

0021-9673/92/$05.00

tionary phase polarity and several relationships between some structural descriptors and retention.

In this work we determined the retention indices of seventeen disaccharides on two stationary phases, SE-54 and OV-17. The quantitative relationships between the retention of disaccharides and those of their constituent monosaccharides were evaluated.

EXPERIMENTAL

Samples

Lactose (4-O-β-D-galactopyranosyl-D-glucose) and sucrose (2-O-α-D-glucopyranosyl-β-D-fructofuranoside) were purchased from Ferosa (Spain); lactulose (4-O-β-D-galactopyranosyl-D-fructose), melibiose (6-O-α-D-galactopyranosyl-D-glucose), palatinose (6-O-α-D-glucopyranosyl-D-fructofuranose) and turanose (3-O-α-D-glucopyranosyl-D-fructose) were from Fluka (Buchs, Switzerland); cellobiose (4-O-β-D-glucopyranosyl-D-glucose) and gentiobiose (6-O-β-D-glucopyranosyl-D-glucose) from Merck (Darmstadt, Germany); maltose (4-O-α-D-glucopyranosyl-D-glucose) from Difco; and isomaltose (6-O-α-D-glucopyranosyl-D-glucose), galactobiose (6-O-α-D-galactopyranosyl-D-galactose), laminaribiose (3-O-β-D-glucopyranosyl-D-glucose), nigerose (3-O-α-D-glucopyranosyl-D-glucose), α,α-trehalose (1-O-α-D-glucopyranosyl-α-D-glucopyranoside) from Sigma (Eisenhofen, Germany). Epilactose (4-O-β-D-galactopyranosyl-D-mannose), neolactose (4-O-β-D-galactopyranosyl-D-altrose) and maltulose (4-O-α-D-glucopyranosyl-D-fructose) were prepared by Professor A. Olano (Instituto de Fermentaciones Industriales, CSIC, Madrid, Spain).

Samples were dissolved in pyridine or water and left to stand until equilibrated. Aliquots containing about 1 mg of carbohydrate were silylated with trimethylsilylimidazole [7].

Gas chromatographic analysis

GC analyses were carried out on two columns of different polarity. Their characteristics and operating conditions are summarized in Table I. Nitrogen was used as the carrier gas.

Kováts retention indices were calculated from the retention times of disaccharide TMS ethers and those of suitable *n*-alkanes. The dead time was determined by linear regression [10].

Assignments of peaks were made according to previous references [3–5]. In some instances, peaks were assigned by comparison with NMR equilibrium data.

Calculations

Calculations of retention indices and multiple linear regressions were carried out on a personal microcomputer using a multiple linear regression program written in QuickBasic.

RESULTS AND DISCUSSION

Retention indices on SE-54 and OV-17 of the examined disaccharides are given in Table II and their structures are depicted in the Fig. 1.

Separation and identification

Although the studied disaccharides covered a wide range of retention (367 index units on SE-54 and 431 index units on OV-17), the separation of anomeric forms was worse than that found previously for monosaccharides [7–9], which covered a narrower range (192 and 244 i.u., respectively, for aldohexoses). Most of disaccharides gave only one or two peaks. As expected, sucrose and trehalose showed only one component. All the examined disaccharides having a 1,4-glycosidic bond showed a maximum of two peaks, although in one of them (neolactose) the free monosaccharide corresponding to the reducing unit (altrose) had noticeable

TABLE I

CHARACTERISTICS AND OPERATING CONDITIONS OF THE CAPILLARY COLUMNS USED FOR THE GC ANALYSIS OF DISACCHARIDE TMS ETHERS

Column	Stationary phase	Origin	Temperature (°C)
Pyrex glass (40 m × 0.18 mm I.D.)	SE-54	Laboratory-made	280
Fused silica (25 m × 0.20 mm I.D.)	OV-17	Chrompack	240

TABLE II

RETENTION INDICES OF DISACCHARIDE OTMS ETHERS

Compound	Retention index	
	SE-54	OV-17
α,α-Trehalose	2820	2697
Sucrose	2710	2596
α-Laminaribiose	2844	2757
β-Laminaribiose	2876	2783
α-Nigerose	2780	2678
β-Nigerosa	2806	2714
Turanose	2783	2670
α-Cellobiose	2754	2666
β-Cellobiose	2861	2771
α-Maltose	2744	2652
β-Maltose	2785	2658
α-Lactose	2707	2626
β-Lactose	2833	2738
α-Epilactose	2627	2498
β-Epilactose	2723	2577
α-Neolactose	2671	2544
β-Neolactose	2650	2519
Maltulose-1[a]	2773	2659
Maltulose-2[a]	2774	2667
Lactulose-1[a]	2684	2558
Lactulose-2[a]	2695	2578
α-Melibiose	2924	2848
β-Melibiose	2947	2869
α-Palatinose	2828	2682
β-Palatinose	2828	2726
α-Isomaltose	2946	2879
β-Isomaltose	2994	2929
α-Galactobiose	2831	2741
β-Galactobiose	2901	2814
α-Gentiobiose	2971	2912
β-Gentiobiose	2978	2921

[a] Peaks 1 and 2 from maltulose and lactulose were assigned as β-furanose and β-pyranose, respectively.

proportions of furanose forms [8,11]. It seems that the bulky substituent at C-4 avoids the formation of furanose forms in such compounds.

Furanose forms are possible in 1,6-glycosyl aldohexoses; in fact, galactobiose showed four components. The two main peaks were assigned to α- and β-pyranoses, these being the most abundant forms in the disaccharide [12] and also in the free galactose [13].

Three disaccharides containing fructose as the reducing end (palatinose, turanose and lactulose) showed a main peak with a tail or two partially overlapping peaks on SE-54; the resolution was improved on OV-17. Similar results have been reported by other workers [3–5]. A more detailed study of lactulose revealed that up to three tautomeric forms (β-furanose, β-pyranose and α-furanose) could be separated on a more polar column (SP-3240, with retention indices I_x of 2668, 2700 and 2733) [14]. It is reasonable to suppose a similar overlapping of peaks in turanose, which has the same tautomers as shown by NMR [15]. Palatinose only has furanose forms [16], which could be separated on OV-17. We found four peaks for maltulose, and two of them were assigned as β-furanose and β-pyranose, which have been included in Table II.

The change in column polarity increased the overall resolution, and decreased slightly the I_x values, but it did not produce noticeable changes in the elution order of α- and β-anomers, as was previously observed [4].

Structure–retention relationships

In previous studies of quantitative structure–retention relationships [7–9] we calculated the contributions to the retention index of several structural descriptors of monosaccharides. As the large number of parameters necessary to describe the structure of disaccharides avoids the use of this approach, we have tried a simpler retention model:

$$I_{xp} = a1_p I_{x1p} + a2_p I_{x2p} + c_{ip} + b_0 \quad (1)$$

which assumes that the retention index of a disaccharide x in a stationary phase p depends on the retention indices of the two constituent monosaccharides in the same phase (I_{x1p} and I_{x2p}) and on the type of glycosidic bond i. The intercept b_0 and the coefficients $a1_p$, $a2_p$ and c_{ip} are calculated by multiple linear regression.

The quality of fit obtained using this model is lower than that with monosaccharides because the data/variables ratio is higher. The low fit limits the use of the model in the prediction of retention indices of other disaccharides; however, the values found for a_1, a_2 and c_i can be used to assess quantitatively the influence of the related structural features on the chromatographic retention. These values, the intercept and the regression coefficient are listed in Table III.

When we consider a group of disaccharides dif-

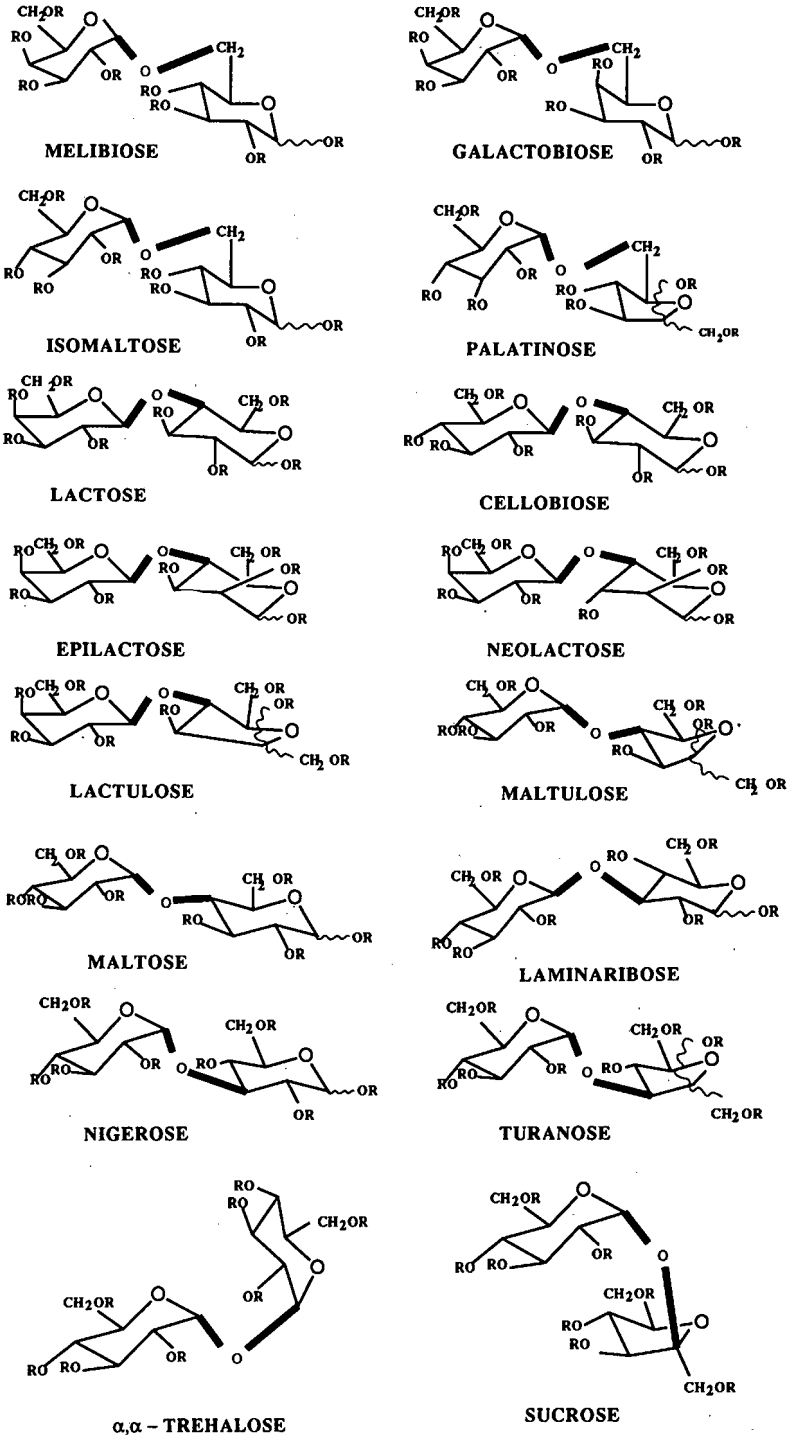

Fig. 1. Structural formulae of the disaccharides investigated.

TABLE III

VALUES OF COEFFICIENTS $a1$, $a2$, c_{ip} AND b_0 CALCULATED BY LINEAR REGRESSION

Phase	$a1$	$a2$	$c_{1,2}$	$c_{1,3}$	$c_{1,4}$	$c_{1,6}$	b_0	r
OV-17	0.455	0.694	10.3	44.4	0	181.2	497.9	0.95
SE-54	0.330	0.375	30.4	60.1	0	168.3	1384.7	0.91

fering in the reducing unit (*e.g.*, 4-O-β-galactosyl derivatives of fructose, altrose, mannose and glucose), their elution order is very similar to that of corresponding monosaccharides.For this reason, the retention model in eqn. 1 includes the experimental retention index of the monosaccharide constituents taken from ref. 8; however the coefficients depend on the position of the monosaccharide unit in the molecule. We have called the monosaccharide with the glycosidic linkage A and the monosaccharide with the free reducing end B.

The contributions associated with the monosaccharide retentions ($a1$ for unit A and $a2$ for unit B) have significant positive values, higher for the OV-17 phase and for unit B. Similar results are found when the relative retentions listed in ref. 4 are converted into retention indices using the experimental data available; the contributions for units A and B are always positive, the latter being higher.

The data of Haverkamp *et al.* [4] show also that glucosyl glucoses were eluted forming three groups: first those with a 1,4-link, second those with 1,1-, 1,2- and 1,3-links and finally those with 1,5- and 1,6-links. Similarly, the 1,4-galactosyl glucoses were eluted before their 1,6-isomers. The contributions c_{ip} calculated for these structural features are similar to those found from our retention indices which appear in Table I. Glycosidic bond contributions seem to be related with the overall molecular shape of the disaccharide. The higher retention of the 1,6-disaccharides can be attributed to the three atoms linking the two rings, which afford a greater flexibility of conformation. Previous data on monosaccharides indicate that the more planar forms present the highest I_x values.

The quality of fit improves when other variables are added to the model in eqn. 1. For instance, when the α- or β-character of A and B monosaccharide units is also considered, the correlation coefficient is 0.96 for OV-17 and 0.94 for SE-54. The contribution of an α-link is positive for the A unit and negative for the B unit; however, the significance of the values is low.

ACKNOWLEDGEMENTS

The authors thanks M. I. Jiménez for technical assistance. This work was supported by DGICYT (Project No. PB88-0034).

REFERENCES

1 K. Robards and M. Whitelow, *J. Chromatogr.*, 373 (1986) 81.
2 M. F. Laker, *J. Chromatogr.*, 163 (1979) 9.
3 C. C. Sweeley, R. Bentley, M. Makita and W. W. Wells, *J. Am. Chem. Soc.*, 85 (1963) 2497.
4 J. Haverkamp, J. P. Kamerling and J. F. G. Vliegentart, *J. Chromatogr.*, 59 (1971) 281.
5 Z. L. Nikolov and P. J. Reilly, *J. Chromatogr.*, 254 (1983) 157.
6 E. Percival, *Carbohydr. Res.*, 4 (1967) 441.
7 A. García-Raso, I. Martínez-Castro, M. I. Páez, J. Sanz, J. García-Raso and F. Saura-Calixto, *J. Chromatogr.*, 398 (1987) 9.
8 I. Martínez-Castro, M. I. Páez, J. Sanz and A. García-Raso, *J. Chromatogr.*, 462 (1989) 49.
9 A. García-Raso, M. Fernández-Díaz, M. I. Páez, J. Sanz and I. Martínez-Castro, *J. Chromatogr.*, 471 (1989) 205.
10 R. J. Smith, J. K. Haken and M. S. Wainwright, *J. Chromatogr.*, 334 (1985) 95.
11 S. J. Angyal, *Adv. Carbohydr. Chem. Biochem.*, 42 (1984) 15.
12 J. H. Pazur, F. J. Hiskiel and B. Liu, *Anal. Biochem.*, 174 (1988) 46.
13 T. E. Acree, R. S. Shallenberger and L. R. Mattick, *Carbohydr. Res.*, 6 (1968) 498.
14 I. Martínez-Castro, M. M. Calvo and A. Olano, *Chromatographia*, 23 (1987) 132.
15 P. E. Pfeffer and K. B. Hicks, *Carbohydr. Res.*, 102 (1982) 11.
16 J. Reuben, *J. Am. Chem. Soc.*, 107 (1985) 1747.

Journal of Chromatography, 607 (1992) 227–237
Elsevier Science Publishers B.V., Amsterdam

CHROM. 24 400

Inverse gas chromatography in the characterization of polymeric materials

Agustín Etxeberría, Jokin Alfageme, Cristina Uriarte and Juan J. Iruin*

Departamento de Ciencia y Tecnología de Polímeros, Universidad del País Vasco, Apartado de Correos 1072, San Sebastián (Spain)

ABSTRACT

Different experimental results are presented for the use of inverse gas chromatography in the determination of the physico-chemical properties of pure polymers, polymer solutions and polymer blends. Using poly(hydroxy ether of bisphenol-A) (Phenoxy), its solutions and its blends with other polymers, thermal transitions, polymer solubility parameters, polymer–solvent and polymer–polymer interaction parameters and diffusion coefficients of small molecules in pure Phenoxy have been measured by inverse gas chromatography.

INTRODUCTION

Gas chromatography (GC) is based on the distribution of a compound between two phases. In gas–solid chromatography (GSC) the phases are gas and solid. The injected compound is carried by the gas through a column filled with solid phase, and partitioning occurs via the sorption–desorption of the compound (probe) as it travels past the solid. Separation of two or more components injected simultaneously occurs as a result of differing affinities for the stationary phase. In gas–liquid chromatography (GLC), the stationary phase is a liquid coated on a solid support.

In inverse GC [1], the species of interest is the stationary phase, which usually consist of a polymer-coated support of finely ground polymer mixed with an inert support. This is in contrast to conventional analytical GC, where the stationary phase is of interest only as far as its ability to separate the injected compounds is concerned. Also, in inverse GC, usually only one pure compound (standard solvent or probe) at a time is injected.

The knowledge of the retention volume due to the dissolution of a substance makes it possible to calculate relevant thermodynamic characteristics of the solution process, namely the partition coefficient, the activity coefficient and the change in the excess partial molar thermodynamic functions of the solute in the given stationary phase [2–7].

This technique has also been used in determining other polymer properties such as glass transition temperatures, as reported by Smidrød and Guillet [8,9], melting temperatures [10] and the degree of crystallinity of the polymer [11,12]. On the other hand, GLC has received general recognition as an effective and simple technique for the rapid measurement of polymer-solubility parameters [13,14] (by applying the Hildebrand–Scatchard theory) and polymer–solvent interactions in molten homopolymers [15,16]. Further, Galin and Maslinko [17] have showed that inverse GC can be used for studying polymer–solvent pairs which can be considered as model compounds of polymer–polymer systems. From this type of measurement, predictions about polymer–polymer miscibility can be made.

The study of the interactions between a homopolymer and a volatile probe by means of inverse GC was extended to the investigation of polymer blends. The miscibility of blends such as poly(vinyl chloride) (PVC)–polycaprolactone (PCL) [18], polystyrene (PS)–poly(vinyl methyl ether) (PVME) [19–21], PS–polydimethylsiloxane (PDMS) [22], PS–poly(butyl methacrylate) (PBMA) [23] and poly(methyl acrylate) (PMA)–poly(epichlorohydrin) (PECH) [24] has been studied by analysing the

0021-9673/92/$05.00

interaction between the volatile probe (1) and each of the two non-volatile components (2 and 3), and then with a mixture of components 2 and 3. In general, the classical Flory–Huggins theory [25] can be used to interpret the results and to determine the polymer–polymer interaction parameter χ'_{23}, which is a measure of the thermodynamic miscibility of the two polymers.

On the other hand, some workers [26] have determined the temperature of the phase separation of mixed systems by observing their corresponding chromatographic retention diagrams.

Finally, the shapes of eluted peaks in GC on polymeric substrates are governed by several factors, one of the most important being the slow diffusion in the polymer phase. By a suitable choice of conditions, the simple Van Deemter equation [27] enables diffusion coefficients to be calculated from the variation of the chromatographic peak width with carrier gas flow-rate [28].

The objective of this paper is to present different experimental results concerning the use of inverse GC in the determination of the above-mentioned physico-chemical magnitudes using poly(hydroxy ether of bisphenol-A) (Phenoxy; PH), poly(vinyl-methyl ether) (PVME), poly(ethylene oxide) (PEO) and their blends, PVME–PH and PEO–PH.

EXPERIMENTAL

Apparatus and procedures

The columns were prepared in the usual manner [29]. The pure polymers and the polymer blends were coated from a solvent solution on to the packing support. After drying in a vacuum oven for *ca.* 48 h at 323 K, the coated support was packed into a ¼-in. O.D. stainless-steel column by applying vacuum to the end. Glass-wool was used to block the ends of the columns. The relative concentration of the polymer in the blends was assumed to be identical with that in the original solution prior to the deposition on the inert support. A description of the columns is given in Table I.

Measurements were made on a modified Perkin-Elmer (Norwalk, CT, USA) Sigma 300 gas chromatograph equipped with a flame ionization detector. Nitrogen was used as the carrier gas. Methane was used as a non-interacting marker to correct the dead volume in the column and the retention time was measured directly with the aid of an Olivetti M-24 microcomputer, equipped with a CHROM+ card and appropriate software. A minimum of four measurements were taken for every molecular probe and for each temperature in all columns. Pressures at the inlet and outlet of the column, read from a

TABLE I

DESCRIPTION OF THE GAS CHROMATOGRAPHIC COLUMNS

Column No.	Length (m)	Packing support	Mass of packing in column (g)	Polymer coating	Mass of coating in column (g)
1	0.1	80–100-mesh Chromosorb W AW DMCS	4.4071	PVME	0.4415
2	0.1	80–100-mesh Chromosorb W AW DMCS	4.9757	PEO	0.4966
3	0.1	80–100-mesh Chromosorb W AW DMCS	4.9978	Phenoxy resin	0.5028
4	0.1	80–100-mesh Chromosorb W AW DMCS	4.9196	Phenoxy–PVME (60:40)	0.4941
5	0.1	80–100-mesh Chromosorb W AW DMCS	4.9919	Phenoxy–PEO (50:50)	0.4926
6	0.1	60–80-mesh glass beads	34.1981	Phenoxy resin	0.3549

mercury manometer, were used to calculate corrected retention volumes by the usual procedures. Flow-rates were measured at the end of the column with a soap bubble flow meter.

Columns were conditioned at temperatures above the glass transition temperature (T_g) for *ca.* 48 h prior to use, while nitrogen was flushed through the column in order to achieve equilibrium. The oven temperature was measured within ± 0.1 K over the whole temperature range. The molecular probes, including a small amount of methane marker (<0.01 μl in total), were injected manually with a 10-μl Hamilton syringe.

Materials

Phenoxy was obtained from Quimidroga (Barcelona, Spain) and corresponds to the PKHH product of Union Carbide. The commercial sample, after being purified by dissolution in dioxane and precipitation in methanol, had an average molecular mass, measured by gel permeation chromatography (GPC) (Waters 150-C ALC/GPC system, Waters–Millipore, Milford, MA, USA) in tetrahydrofuran (THF) at 303 K of $\bar{M}_n = 18\,000$ ($\bar{M}_w/\bar{M}_n = 2.8$) [30] (where $\bar{M}_n$ is the average number-average molecular mass and $\bar{M}_w$ is the average mass-average molecular mass).

Poly(vinyl methyl ether) (PVME) ($T_g = 245$ K) was obtained from Polysciences (catalogue no. 3032) and purified in a benzene–isooctane mixture. Its molecular mass, measured by GPC in THF at 303 K, was $\bar{M}_n = 29\,000$ ($\bar{M}_w/\bar{M}_n = 2.1$) [31].

Polyethylene oxide (PEO) was obtained from Union Carbide and corresponds to the WSR-35 product. It was purified in a benzene–*n*-heptane mixture and its molecular mass was $M_v = 365\,000$, measured by viscometry in benzene [32].

All the solutes (probes) were of chromatographic or analytical-reagent grade and were used without further purification.

Computations

Specific retention volumes were calculated using

$$V_g^0 = \Delta t \cdot \frac{F}{w_L} \cdot \frac{273.16}{T_r} \cdot \frac{3}{2} \cdot \frac{(P_i/P_o)^2 - 1}{(P_i/P_o)^3 - 1} \qquad (1)$$

where $\Delta t = t_p - t_m$ is the difference between the retention times of the probe and the marker, F is the flow-rate of the carrier gas at room temperature (T_r), w_L is the mass of the stationary phase (weight of the coated polymer in the column) and P_i and P_o are the inlet and outlet pressures, respectively.

RESULTS AND DISCUSSION

The graph of the logarithm of retention volume *versus* reciprocal of the temperature (retention diagram) is a straight line when the polymer is in a fixed state (solid, liquid), the slope being related to the solution enthalpy in GLC or to the adsorption process in GSC:

$$\frac{\partial \ln V_g}{\partial (1/T)} = -\frac{\Delta H}{R} \qquad (2)$$

where ΔH is the enthalpy of the process and R is the gas constant. As a result of a phase transition, the original polymeric stationary phase changes into a different state which must have, in general, different physico-chemical properties. This change is reflected in the retention diagram.

Smidrød and Guillet [9] were the first to use the inverse GC technique to investigate the glass transition in a polymeric material [poly-(N-isopropylacrylamide)]. The retention diagram, which would normally give a straight line, gave curves with a minimum, and this was interpreted as being due to a glass transition which was confirmed by using differential scanning calorimetry. Lavie and Guillet [33] extended this study to the glass transitions of other polymers such as poly(methyl methacrylate) (PMMA), PS and PVC.

The shape of the diagram was explained by postulating that at temperatures below T_g, the probe interacts only with the surface because the rate of diffusion of the probe through the polymer is too slow to permit significant bulk interaction. Several degrees above T_g, the retention volume is a measure of the interaction of the probe with the bulk polymer. Close to T_g both factors contribute to retention. As the temperature rises, the increasing penetrability outweights the effects of increasing vapour pressure, so that retention volumes increase with increasing temperature in this region. This is the intermediate region where diffusion of probe molecules into the polymer matrix is too slow to permit complete equilibrium to be reached within the chromatographic time scale.

The retention diagram of the Phenoxy resin with

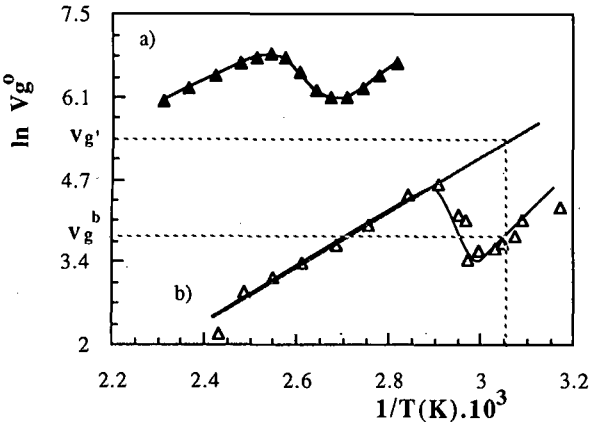

Fig. 1. (a) Retention diagram of Phenoxy resin with *n*-decane in the temperature range 353–433 K including the glass transition temperature (T_g). (b) Retention diagram of PEO with benzene in the temperature range 313–413 K including the melting temperature (T_m).

n-decane (Fig. 1a) shows a deviation of the straight line due to the glass transition. When the polymer begin to flow, that is, in the glass transition, the retention volume of the probe increases until a maximum when the whole stationary phase has changed its state. Then, as temperature increases, the probe volatility increases and the retention volume is smaller.

A similar phenomenon occurs in the phase transformation of semicrystalline polymers. Fig. 1b shows the retention diagram of PEO with benzene in a temperature range including the melting temperature (T_m). In this case, below T_m the crystalline regions are impenetrable and the retention volume is due to the amorphous portion of the polymer. Then the polymer melts and one observes the characteristic maximum, after which the whole polymer mass takes part in the dissolution of the sample molecules.

An important contribution to the development of inverse GC for the study of phase transitions in polymeric materials was made by Guillet and coworkers [9,12]. They proposed a method for determining the crystallinity of polymers from retention diagrams.

The determination of crystallinity of polymeric stationary phases is based on the different solubilities of the probe in the crystalline and amorphous regions. In fact, as it is assumed that in the range below T_m the crystalline regions do not participate in the retention of the molecules of the probe, it is possible to estimate the degree of crystallinity of the sample. Indeed, the extrapolation of the line above T_m into the temperature range below the melting point makes it possible to estimate the retention volume that would correspond to the hypothetical amorphous state of the entire polymer in this temperature range. If we do this on the PEO retention diagram, we can calculate the percentage of crystallinity (PC) by means of the equation

$$PC = 100\left(1 - \frac{V_g^b}{V_g'}\right) \tag{3}$$

where V_g' and V_g^b are the extrapolated and measured values of the unit retention volume at a given temperature, respectively (see Fig. 1).

Fig. 2 shows the average crystallinity of PEO at different temperatures from data for different probes. A crystalline fraction value of 0.85 for PEO below T_m is in accord with values quoted by Bergman [34] (0.8 and 0.9 for PEO samples of molecular masses 8000 and 300 000, respectively) derived from NMR and X-ray methods.

As is well known, a knowledge of the retention volume due to the dissolution of a substance makes it possible to calculate important thermodynamic characteristics of the solution process, namely the partition coefficient, the activity coefficient and excess partial molar thermodynamic functions of the solute in the given stationary phase.

Partial molar activity coefficients at infinite dilution can be calculated using

$$\ln(a_1/w_1)^\infty = \ln\left(\frac{273.16R}{P_1^0 V_g^0 M_1}\right) - P_1^0(B_{11} - V_1)/RT \tag{4}$$

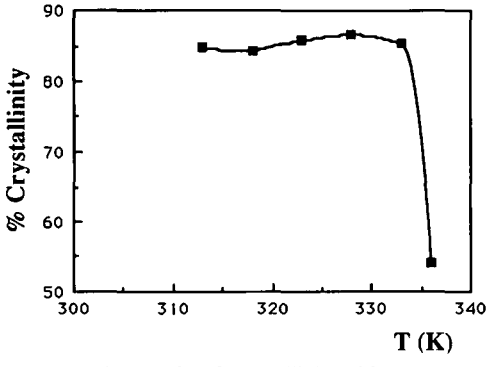

Fig. 2. Evolution of PEO crystallinity with temperature from IGC data.

The application of GC in studying the thermodynamics of the interaction of volatile substances with a polymer phase was specially considered by Smidrød and Guillet [9]. They used excess thermodynamic functions of mixing at temperatures above the flow-point of the polymer:

$$\overline{\Delta G_1^\infty} = RT \ln (a_1/w_1)^\infty \quad (5)$$

$$\overline{\Delta H_1^\infty} = R \cdot \frac{\partial \ln (a_1/w_1)^\infty}{\partial (1/T)} \quad (6)$$

$$\overline{\Delta S_1^\infty} = \frac{(\Delta H_1^\infty - \Delta G_1^\infty)}{T} \quad (7)$$

where $\overline{\Delta G_1^\infty}$, $\overline{\Delta H_1^\infty}$ and $\overline{\Delta S_1^\infty}$ are the solvent partial molar free energy, enthalpy and entropy of mixing, respectively, at infinite dilution (see Table II).

From the pioneering work of Freeman and Rowlinson [35], it has been recognized that polymer solutions can exhibit two critical temperatures, the upper critical solution temperature (UCST) and lower critical solution temperature (LCST). The critical conditions can be elucidated by means of the well known Flory–Huggins interaction parameter, χ, whose physical meaning has been conveniently redefined by modern polymer solution theories. In these new theories, the interaction parameter χ can be understood as an excess partial molar free energy parameter which exhibits a parabolic dependence on the temperature. The two critical temperatures correspond to the points where χ reaches the $\chi_{crit.}$ value. Between these two points, χ passes through a minimum which gives the maximum of polymer solubility in the solvent.

Inverse GC provides valuable information of the dependence of χ on temperature. Starting with the specific retention volume V_g^0, calculable [25,36] from the retention time of a solvent in a column packed with the polymer, it is possible [25,36] to calculate the interaction parameter χ as

$$\chi = \ln (273.16 R v_{sp,2}/P_1^0 V_g^0 V_1) - 1 - [(B_{11} - V_1)/RT]P_1^0 \quad (8)$$

where V_1 is the molar volume of the solvent and $v_{sp,2}$ the specific volume of the polymer.

As we have mentioned before, the inverse GC literature recommends that the inverse GC measurements of thermodynamic properties should be made at a temperature at least 50°C higher than T_g, or a temperature higher than T_m if the polymer is semicrystalline. This precaution allows us to avoid problems related to slow attainment of the equilibrium in the column, and to render possible the proper comparison of experimental results. In the case of PVME, it exhibits a T_g below room temperature, and therefore retention diagrams were obtained in the temperature range 363–423 K. Linear variations of ln V_g^0 *vs.* $1/T$ were observed within the temperature range.

Fig. 3 summarizes the χ–T behaviour of different

TABLE II

EXCESS THERMODYNAMIC FUNCTIONS OF MIXING OF THE PHENOXY RESIN WITH VARIOUS PROBES AT 393 K

Solvent	$\overline{\Delta G_1^\infty}$ (J/mol)	$\overline{\Delta S_1^\infty}$ (J/mol · K)
Acetonitrile	7 689.76	−18.251
1,2-Dichloroethane	4 998.11	−7.235
Benzene	6 751.87	−3.458
n-Butanone	6 436.84	−11.313
Chlorobenzene	5 479.36	−6.151
n-Decane	12 842.41	16.007
DEGDEE[a]	3 755.11	−25.273
Dioxane	3 973.55	−10.903
Dimethylformamide	2 628.68	−29.891
Ethyl acetate	6 430.77	−18.017
n-Propanol	7 967.40	−13.252
n-Tetradecane	13 531.55	5.393
Toluene	5 479.36	−1.612

[a] DEGDEE = Diethyleneglycol diethyl ether.

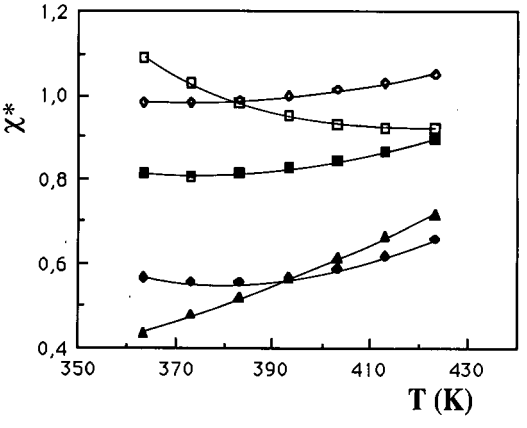

Fig. 3. Interaction parameter *vs.* temperature for the PVME with various probes: ■ = *n*-decane; ◆ = *n*-propanol; □ = *n*-tetradecane; ◇ = acetonitrile; ▲ = *n*-butanone.

PVME–solvent pairs studied by inverse GC in the range 363–423 K. The curves can be interpreted in all instances as parts of the general parabolic behavior mentioned before. It is important to realize that in inverse GC systems we are in a range of concentrations of $\phi_{solvent} \rightarrow 0$, in precisely the opposite range to that in which the critical conditions are satisfied. However, two important aspects can be inferred from these diagrams.

First, the value of the χ parameter: high values such as those of *n*-decane correspond to very poor solvents for PVME. In contrast, low values, as for *n*-butanone, reflect the good solubility capacities of such solvents for the polymer. The second important aspect is the χ–T behavior. Solvents for which χ decreases with increasing T correspond to systems leaving the UCS temperature, as with *n*-tetradecane in the range 363–423 K. *n*-Propanol seems to be at the minimum of its parabolic dependence, showing its maximum solubility in this range. Other solvents, such as *n*-butanone, leave the maximum of solubility towards their LCST.

The high χ values for *n*-propanol can be explained by the existence of hydrogen bonds in the pure liquid. In the case of acetonitrile its value has been ascribed to the difference in dipolar interactions between pure and diluted acetonitrile.

Of course, this analysis is restriced by the χ value and by the fact that we are in the other extreme of the critical conditions. However, qualitative conclusions similar to those explained above can give a first insight into the quality of different solvents for PVME.

For practical purposes, the so-called solubility parameter has been used as a tool for characterizing polymer solubility in organic liquid, such as those used in coatings. DiPaola-Baranyi and Guillet [13] have shown that inverse GC can be a simple and convenient method for calculating solubility parameters for polymeric stationary phases. The method is based on the fact that the Flory–Huggins χ parameter can be related to solubility parameters by means of a combination of the Hildebrand–Scatchard and Flory theories [25] as follows:

$$\chi = (V_1/RT)(\delta_1 - \delta_2)^2 \qquad (9)$$

where δ_1 is the solubility parameter of the probe and δ_2 is that of the polymer.

TABLE III

SOLUBILITY PARAMETERS OF PHENOXY RESIN AT SEVERAL TEMPERATURES

δ_2 [$(J/m^3)^{1/2} \cdot 10^3$]	T (K)
37.56	373
37.01	383
36.26	393
35.25	403
34.75	413

Following the method developed by DiPaola-Baranyi and Guillet [13], eqn. 9 can be rewritten as

$$(\delta_1^2/RT - \chi/V_1) = (2\delta_2/RT)\delta_1 - \delta_2^2/RT \qquad (10)$$

Therefore, a plot of $(\delta_1^2/RT - \chi/V_1)$ *vs.* δ_1 of the probes will give a straight line with a slope of $2\delta_2/RT$ and an intercept of $-\delta_2^2/RT$. Slopes and intercepts were obtained from a linear least-squares analysis. Derived values of δ_2 for the Phenoxy resin at several temperatures are listed in Table III.

From the extrapolation to 298 K of the data in Table III, we obtain a δ_2 value of $21.10 \cdot 10^{-3}$ $(J/m^3)^{1/2}$. This extrapolatad value is in good agreement with the value derived from a method recently proposed by Coleman *et al.* [37], $\delta_2 = 20.93 \cdot 10^{-3}$ $(J/m^3)^{1/2}$.

Galin and Maslinko [17] showed that inverse GC can be used for predicting polymer–polymer miscibility. They demonstrated that the specific retention volume, V_g^0, and its related magnitude, the partial molar enthalpy of mixing at infinite dilution (ΔH_1^∞), can be used for predicting polymer 1–polymer 2 miscibility [17,30], using systems where the solvent is a model compound for polymer 2.

The average value of ΔH_1^∞ for each solvent can be determined by least-squares analysis of the ln $(a_1/w_1)^\infty$ *vs.* $1/T$ plots. Table IV summarizes experimental ΔH_1^∞ values for the different solvents investigated. It illustrates the capacity of this type of analysis. ΔH_1^∞ becomes negative in solvents such as ethers and esters, reflecting, in a qualitative way, the preference of the Phenoxy resin for this type of interaction. A similar analysis has been carried out by Galin and Maslinko [17] with poly(vinylidene fluoride) (PVDF).

This qualitative analysis can be extended to any

TABLE IV

POLARIZABILITY, P, DIPOLE MOMENT, μ, AND HYDROGEN BOND ACCEPTING POWER, β, OF PURE SOLVENTS AND PARTIAL MOLAR HEATS OF MIXING, ΔH_1^∞, OF THE VARIOUS SOLUTE–PHENOXY SYSTEMS

Solvent	$(\overline{\Delta H_1^\infty})_{exp}$ (kJ/mol)	$P \cdot 10^{30}$ (m^3)	μ (D)	β
Chlorobenzene	3.14	12.34	1.71	0.07
Acetonitrile	0.79	4.44	3.94	0
1,2-Dichloroethane	2.22	8.34	1.40	0
n-Propanol	3.52	6.90	3.09	0.95
Benzene	5.48	10.40	0	0.10
n-Decane	19.34	19.1	0	0
Toluene	4.90	12.34	0.37	0.11
Dioxane	−0.54	8.56	0.42	0.37
Dimethylformamide	−9.04	7.85	3.86	0.69
DEGDEE[a]	−6.11	13.8	1.97	0.55
Tetradecane	15.951	26.0	0	0
Ethyl acetate	−1.30	8.83	1.78	0.45
n-Butanone	2.26	8.24	2.70	0.48

[a] See Table II.

kind of solvent. Experimental values of ΔH_1^∞ can be correlated with probe polarizabilities P, dipole moments μ and Taft's β empirical parameter, which measures the probe hydrogen bond accepting power through the general equation

$$\overline{\Delta H_1^\infty}\ (\text{kJ/mol}) = aP + b\mu + d\beta \qquad (11)$$

Data for P, μ and β for the different solvents employed are also given in Table IV [17,38–40].

Fig. 4 shows ΔH_1^∞ experimental values compared with calculated values for the different Phenoxy–solvent systems, according to the best fit:

$$\overline{\Delta H_1^\infty}\ (\text{kJ/mol}) = 0.145P\ (\text{m}^3 \cdot 10^{-30}) - 0.25\ \mu\ (\text{D}) - 1.63\beta \qquad (12)$$

The data summarized in Fig. 4 may be characterized as a random scatter. The correlation coefficient is worse than that obtained by Galin and Maslinko [17] in a similar analysis of PVDF. Whether or not the correlation is correct obviouly depends on the accuracy of the ΔH_1^∞ measurements and on the reliability of the literature data for β. In spite of these shortcomings at the experimental level, this correlation has allowed the PVF_2 miscibility with a variety

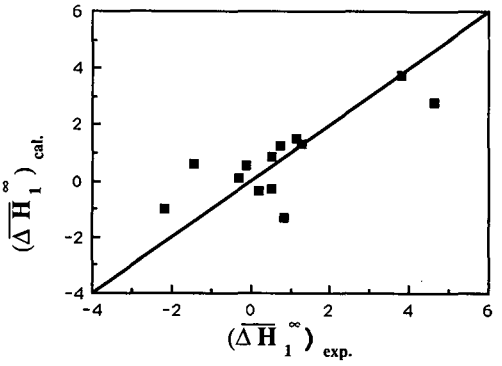

Fig. 4. Experimental *vs.* calculated ΔH_1^∞ values for the various Phenoxy–probe mixtures according to the multiparametric correlation (eqn. 12).

of polyesters to be rationalized and, as may be seen later, it can be used, in a qualitative way, to illustrate the miscibility of Phenoxy with other different polymers. For instance, in the case of N-methylpyrrolidone [model solvent of poly(N-vinylpyrrolidone)], $P = 10.56 \cdot 10^{-30}$ m^3, $\mu = 4.09$ D and $\beta = 0.72$ [31], $(\Delta H_1^\infty)_{cal} = -2.763$ kJ/mol, in good agreement with the well established miscibility of Phenoxy with poly(N-vinylpyrrolidone). In a similar way $(\Delta H_1^\infty)_{cal} = -1.172$ kJ/mol for the system Phenoxy–tetramethylene sulphone. Given the negative values of Phenoxy with ethers and sulphones, the reported miscibility of our resin with a poly(ether sulphone) [40] is not surprising.

The study of the thermodynamics of interaction between a homopolymer and a volatile probe [41] by GLC has been extended to the investigation of ternary systems containing a probe and blends of two polymer components [15].

If the stationary phase is the polymer blend, we can relate the chromatographic data with the interaction parameter between polymers, if the weight fractions of the each homopolymer in the column and the homopolymer–solvent interaction parameter of each component of the blend are known.

Starting with the classical Flory–Huggins expression applied to three-component systems, a method of analysis of inverse GC measurements on polymer blends may be proposed which gives us the polymer–polymer interaction coefficient. In inverse GC, this interaction coefficient is expressed as

$$\chi'_{23} = \frac{\chi_{23}}{x_2} = \frac{\chi_{23} V_1}{V_2} \qquad (13)$$

where x_2 is the number of segments in the polymer molecule, V_1 is the molar volume of the solvent injected into the column, V_2 is the molar volume of polymer 2 and χ_{23} and χ'_{23} refer to the interaction between polymer 2 and polymer 3.

Deshpande *et al.* [42] proposed a relationship to obtain such an interaction parameter if we previously know the binary polymer–solvent interaction parameter of each polymer:

$$\left[\left(\frac{\chi_{12}}{V_1}\right)\phi_2 + \left(\frac{\chi_{13}}{V_1}\right)\phi_3 - \left(\frac{\chi_{23}}{V_2}\right)\phi_2\phi_3\right]V_1 = \ln\left[\frac{273.16R(w_2v_{sp,2} + w_3v_{sp,3})}{P_1^0V_g^0V_1}\right] - \left(1 - \frac{V_1}{V_2}\right)\phi_2 - \left(1 - \frac{V_1}{V_3}\right)\phi_3 - \frac{P_1^0}{RT}(B_{11} - V_1) \quad (14)$$

where ϕ_i is the volume fraction of component i and 2 and 3 are the homopolymers.

However, it is easily derivable [24] that the interaction parameter χ'_{23} can be calculated without auxiliary parameters (P_i^0, B_{11}, etc.) by means of

$$\chi'_{23} = \ln\left(\frac{V_{g_{blend}}}{w_2v_{sp,2} + w_3v_{sp,3}}\right) - \left[\phi_2\ln\left(\frac{V_{g_2}}{v_{sp,2}}\right) - \phi_3\ln\left(\frac{V_{g_3}}{v_{sp,3}}\right)\right](\phi_2\phi_3)^{-1} \quad (15)$$

Table V summarizes the binary interaction parameter for several probes and the polymer–polymer interaction parameters for the system PEO–Phenoxy obtained from eqn. 15.

As noted in other chromatographic investigations on polymer–polymer miscibility [31], probe to probe variations are observed. This probe dependence can be explained if we take into account the thermodynamic aspects of a ternary system. χ_{12} and χ_{13} should be obtained in its own ternary system instead of being calculated in the homopolymer–probe binary system. Therefore, the measured χ'_{23} parameter is an apparent parameter which takes into account the real polymer–polymer interaction and other ternary effect not reflected in χ_{12} and χ_{13}.

Galin and Maslinko [43] recently studied the dependence of the PVDF–poly(ethyl methacrylate) (PEMA) interaction parameter on the probe. They observed that a preferential solubility of the probe with respect to one of the components of the blend leads to an artificial increase in the χ'_{23} interaction parameter. Similar results have been obtained for PS–PVME with chlorinated probes [19] and for PVC–PCL with chloroform [18].

TABLE V

POLYMER–SOLVENT BINARY INTERACTION PARAMETERS AND POLYMER–POLYMER INTERACTION PARAMETERS FOR THE SYSTEM PEO–PHENOXY RESIN AND DIFFERENT PROBES OBTAINED FROM EQN. 15 AT 413 K

Solvent	χ_{12}	χ_{13}	χ'_{23}
Toluene	0.652	0.276	0.147
Benzene	0.601	0.124	0.093
Chlorobenzene	0.505	0.045	0.303
1,2-Dichloroethane	0.466	−0.148	0.108
n-Decane	2.101	1.676	0.079
n-Tetradecane	2.435	2.128	0.330
DEGDEE[a]	−0.074	0.086	−0.266
Dioxane	0.015	0.127	−0.289
n-Butanone	0.463	0.391	−0.314
Ethyl acetate	0.579	0.363	−0.272
n-Propanol	0.925	0.458	0.009
Acetonitrile	0.830	0.407	−0.035
Dimethylformamide	−0.335	0.304	−0.176

[a] See Table II.

The use of a poor solvent of both polymers, such as *n*-decane and *n*-tetradecane, which give high values for χ_{12} and χ_{13}, induces the appearance of diffusion phenomena which yield bad results.

Fig. 5 shows that χ'_{23} interaction parameter at 393 K is an increasing function of $|\Delta\chi| = |\chi_{12} - \chi_{13}|$, but there is no theoretical argument to explain this

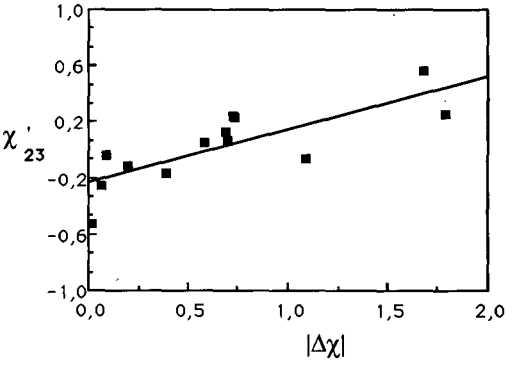

Fig. 5. Variation of χ'_{23} interaction parameter with $|\Delta\chi| = |\chi_{12} - \chi_{13}|$ at 293 K for the PVME–Phenoxy resin system.

dependence. Galin and co-workers [43] observed a similar dependence. Qualitatively, the variation of χ'_{23} with $|\Delta\chi|$ is not surprising. In fact, the preferential interaction of the probe with one of the components of the blend leads to a decrease in $\chi_{1,23}$ in relation with its ideal randomly interaction value. Then there is an artificial increase in χ'_{23}.

Prolongo *et al.* [44] proposed a method for calculating the real polymer–polymer interaction parameter from measurements performed on ternary systems composed of the polymer pairs plus a probe. They obtained an equation, simplified for the IGC data:

$$(\chi_{23})_{app.} = (\chi_{23})_{true} \cdot \frac{s_1}{s_3} + \\ + (\chi_{12} - \chi_{13}) \cdot \frac{(s_3 - s_2) V_2^*}{(\psi_2 s_2 + \psi_3 s_3) V_1^*} \quad (16)$$

where V_i^* is the characteristic molar volume, ψ_i the segment fraction and s_i the number of contact sites per segment of component i.

This equation explains why the interaction parameters determined by IGC are dependent on the probe: they depend on the difference in solvent quality of the probe with regard to the two polymers in the blend, $\chi_{12} - \chi_{13}$, and on the number of contact sites per segment of the solvent s_i.

In order to obtain the $(\chi_{23})_{true}$ value, we rewrite this eqn. 16 as

$$\frac{(\chi_{23})_{app.}}{V_2^* s_1} = \frac{(\chi_{23})_{true}}{V_2^* s_3} + \\ + \frac{(\chi_{12} - \chi_{13})}{V_1^* s_1} \cdot \frac{(s_3 - s_2)}{(\psi_2 s_2 + \psi_3 s_3)} \quad (17)$$

The plot of $(\chi_{23})_{app.}/V_2^* s_1$ *versus* $\Delta\chi/V_1^* s_1$ should be linear with an intercept $(\chi_{23})_{true}/V_2^* s_3$. Such a type of plot is shown in Fig. 6. The s_1 values needed were calculated according to Bondi [45]. Then the $(\chi_{23})_{true}$ for the PVME–Phenoxy system at 393 K is -0.15.

Phase separation processes can be observed for homopolymer blends using inverse GC. From the chromatographic point of view, the location of the phase separation temperatures can be studied by means of the molecular probe retention volumes in the blend compared with the mean values of the retention volumes of the same molecular probes in the homopolymers. Several workers [23,46–48] have shown that the retention volumes of inmiscible

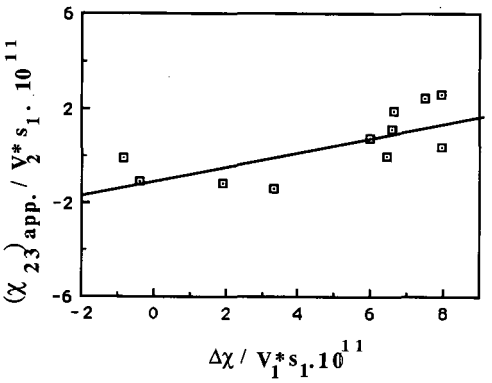

Fig. 6. Representation of $(\chi_{23})_{app.}/V_2^* s_1$ *vs.* $\Delta\chi/V_1^* s_1$ for the PVME–Phenoxy resin system with several probes at 393 K.

blends are a linear combination of the retention volumes of each component:

$$V_g = V_{gl,2} w_2 + V_{gl,3} w_3 \quad (18)$$

Miscible polymer blends have a retention volume lower than the arithmetic average volume of the homopolymers at the corresponding composition because the probe must compete with one of the components for the sites of possible interaction with the other, thus giving a shorter time or volume of elution. In contrast, retention volumes of a phase-separated blend are equal to the linear combination of the retention volumes of the pure constituents.

Retention diagrams of a PVME–Phenoxy blend (40:60) with several molecular probes were determined in the temperature range 384–480 K far from the glass transition temperature of the blend [31]. In all instances, as can be seen in Fig. 7 for *n*-tetra-

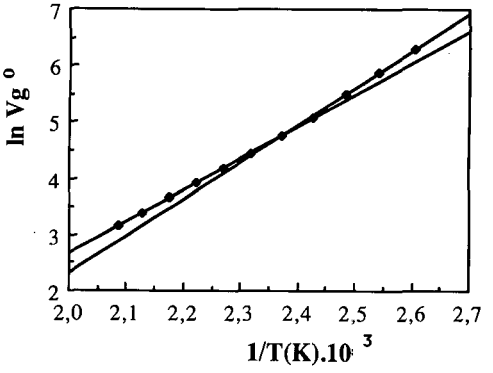

Fig. 7. Retention diagram of PVME–Phenoxy blend (40:60) with *n*-tetradecane in the temperature range 384–480 K including the phase separation temperature.

decane, the diagram showed a deviation from strict linearity between 425 and 445 K. This change in the slope may be identified with the location of the phase separation in the column, and has been confirmed by thermo-optical analysis.

The shapes of eluted peaks in GC on polymeric substrates may have a significant effect on the validity of the data derived from peak retention measurements, and in addition may be related to the thermodynamics and kinetics of the polymer–probe interaction.

One of the most important factors that govern peak shape is slow diffusion in the polymer phase. The method for determining the approximate values of diffusion constants was first reported by Gray and Guillet [28] and utilizes the peak broadening of a probe molecule injected on to a GLC column containing a polymeric stationary phase. Recently, the technique has been extended to coated capillary columns [49].

Van Deemter *et al.* [27] related peak broadening to column properties through the equation

$$H = A + B/u + Cu \tag{19}$$

where H is the plate height, u is the linear velocity of the carrier gas and A, B and C are constants independent of u. A and B are related to instrument performance and gas-phase spreading and C is given by

$$C = (8/\pi^2)(d^2/D_1)\left[\frac{k}{(1+k)^2}\right] \tag{20}$$

where d is the thickness of the stationary phase, D_1 is the diffusion coefficient of the solute in the stationary phase and k is the partition ratio.

From the resulting plot, the slope C of the linear portion obtained at high velocity ($B/u \rightarrow 0$) is determined and D_1 is calculated through eqn. 20, d and k being known.

The average thickness of the stationary phase d was found from the known volume of polymer on the column and the geometric surface area of the beads, which were assumed to be spherical. If this sample bead is coated with a weight w of polymer having a density ρ,

$$d = (w/\rho)/(3\,V/r) \tag{21}$$

where r is an average radius and V is the volume of the sample bead.

The plate height H was determined from the eluted peaks:

$$H = (l/5.54)(w_{1/2}/t_r)^2 \tag{22}$$

where l is the column length, $w_{1/2}$ is the width of the peak at half-height and t_r is the retention time from the injection to the peak maximum.

The flow-rate was measured at the column outlet in the usual manner. The measured volume flow-rate, F, was converted into linear velocity in the column, u, by the relationship

$$u = (jF/a)(T_c/T_f) \tag{23}$$

where T_c and T_f are column and flow meter temperatures, a is the volume of gas per unit length of column and j is the James–Martin correction factor of gas compressibility.

The results of a series of experiments to measure the amount of peak spreading as a function of flow-rate for the Phenoxy resin with *n*-octadecane, a non-polar solvent, are shown in Fig. 8.

At higher flow-rates, H increases linearly with u and C can be determined from the slope. The resulting value of D_1 calculated from the Van Deemter equation is $2.20 \cdot 10^{-6}$ m^2 s^{-1} at 418 K.

The GC measurement of diffusion rates appears to complement the usual sorption and permeation methods, as can be seen in the data obtained by Gray and Guillet [28] for benzene in low-density polyethylene with a resulting value of D_1 of $0.82 \cdot 10^{-4}$ m^2 s^{-1} compared with the value of $1.2 \cdot 10^{-4}$ m^2 s^{-1} obtained by McCall and Slichter [50] using both desorption and time lag measurements.

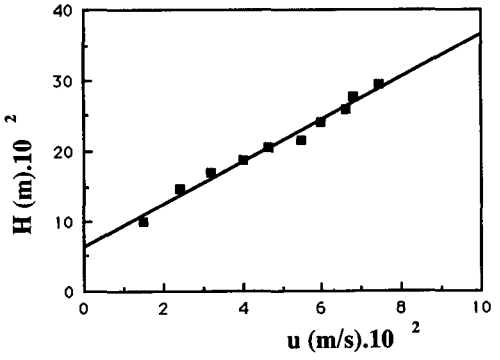

Fig. 8. Representation of the plate height H determined from the Van Deemter equation *vs.* the linear flow-rate u for a column of Phenoxy on glass beads at 418 K with *n*-octadecane.

However, use of the simple Van Deemter equation to interpret the GC data may only be valid for relatively non-polar penetrants and polymers at temperatures well above the glass transition temperature of the polymer.

ACKNOWLEDGEMENTS

The authors gratefully acknowledge the Basque Government (Project number PGV 9017) and the Diputación Foral de Guipuzcoa for financial support.

REFERENCES

1 A. V. Kiselev, *Adv. Chromatogr.*, 3(1967) 177.
2 J. M. Braun and J. E. Guillet, *Adv. Polym. Sci.*, 21 (1976) 108.
3 D. G. Gray, *Proc. Polym. Sci.*, 5 (1977) 1.
4 R. J. Laub and R. L. Pecsok, *Physicochemical Applications of Gas Chromatography*, Wiley, New York, 1978.
5 J. R. Conder and C. L. Young, *Physicochemical Measurements by Gas Chromatography*, Wiley, New York, 1979.
6 J. E. G. Lipson and J. E. Guillet, in J. V. Dawkins (Editor), *Developments in Polymer Characterization*, Applied Science Publ., London, 1982, Vol. 3, Ch. 2.
7 G. J. Price, J. E. Guillet and J. H. Purnell, *J. Chromatogr.*, 369 (1986) 273.
8 J. E. Guillet, in J. H. Purnell (Editor), *New Developments in Gas Chromatography*, Wiley, New York, 1973, p. 187.
9 O. Smidrød and J. E. Guillet, *Macromolecules*, 2 (1969) 272.
10 G. J. Courval and D. G. Gray, *Macromolecules*, 8 (1975) 326.
11 J. M. Braun and J. E. Guillet, *Macromolecules*, 10 (1977) 101.
12 J. E. Guillet and A. N. Stein, *Macromolecules*, 3 (1979) 102.
13 G. DiPaola-Baranyi and J. E. Guillet, *Macromolecules*, 11 (1978) 228.
14 K. Ito and J. E. Guillet, *Macromolecules*, 12 (1979) 1163.
15 D. G. Gray, *Prog. Polym. Sci.*, 5 (1977) 1.
16 J. M. Braun and J. E. Guillet, *Adv. Polym. Sci.*, 21 (1976) 107.
17 M. Galin and L. Maslinko, *Macromolecules*, 18 (1985) 2192.
18 O. Olabisi, *Macromolecules*, 8 (1975) 316.
19 C. S. Su and D. Patterson, *Macromolecules*, 10 (1977) 708.
20 S. Klotz, R. H. Schuster and H.-J. Cantow, *Makromol. Chem.*, 187 (1986) 1491.
21 J. M. Elorza, M. J. Fdz.-Berridi, J. J. Iruin and C. Uriarte, *Makromol. Chem.*, 189 (1988) 1855.
22 M. Galin and M. C. Rupprecht, *Macromolecules*, 12 (1979) 506.
23 G. DiPaola-Baranyi and P. Degree, *Macromolecules*, 14 (1981) 1456.
24 Z. Y. Al-Saigh and P. Munk, *Macromolecules*, 17 (1984) 803.
25 P. J. Flory, *Principles of Polymer Chemistry*, Cornell University Press, Ithaca, NY, 1953.
26 C. P. Doubé and D. J. Walsh, *Eur. Polym. J.*, 17 (1981) 63.
27 J. J. Van Deemter, F. J. Zuiderweg and A. Klinkenberg, *Chem. Eng. Sci.*, 5 (1966) 271.
28 D. G. Gray and J. E. Guillet, *Macromolecules*, 6 (1973) 223.
29 M. J. Fernández-Berridi, T. F. Otero, G. M. Guzmán and J. M. Elorza, *Polymer*, 23 (1982) 1361.
30 J. I. Iribarren, M. Iriarte, C. Uriarte and J. J. Iruin, *J. Appl. Polym. Sci.*, 37 (1989) 3459.
31 C. Uriarte, J. J. Iruin, M. J. Fernández-Berridi and J. M. Elorza, *Polymer*, 30 (1989) 1155.
32 M. Iriarte, E. Espi, A. Etxeberría, M. Valero, M. J. Fernández-Berridi and J. J. Iruin, *Macromolecules*, 24 (1991) 5546.
33 A. Lavie and J. E. Guillet, *Macromolecules*, 2 (1969) 443.
34 K. Bergman, *Kolloid-Z. Z. Polym.*, 251 (1973) 962.
35 P. I. Freeman and J. S. Rowlinson, *Polymer*, 10 (1960) 2.
36 D. Patterson, Y. B. Tewari, H. P. Schreiber and J. E. Guillet, *Macromolecules*, 4 (1971) 356.
37 M. M. Coleman, C. J. Serman, D. E. Bhagwagar and P. C. Painter, *Polymer*, 31 (1990) 1187.
38 K. A. Karim and D. C. Bonner, *J. Appl. Polym. Sci.*, 22 (1978) 1277.
39 M. J. Kamlet, J. L. M. Abboud, M. H. Abraham and R. W. Taft, *J. Org. Chem.*, 48 (1983) 2877.
40 A. L. McClellan, *Tables of Experimental Dipole Moments*, Rahava Enterprises, El Cerrito, CA, 1974, Vol. 2.
41 V. B. Singh and D. J. Walsh, *J. Macromol. Sci. Phys.*, B25 (1987) 65.
42 D. D. Deshpande, D. Patterson, H. P. Schreiber and C. S. Su, *Macromolecules*, 7 (1974) 565.
43 M. Galin and L. Maslinko, *Eur. Polym. J.*, 23 (1987) 923.
44 M. G. Prolongo, R. M. Masegosa and A. Horta, *Macromolecules*, 22 (1989) 4346.
45 A. Bondi, *J. Phys. Chem.*, 64 (1964) 441.
46 C. Zhikuan and D. J. Walsh, *Eur. Polym. J.*, 19 (1983) 519.
47 J. Klein, H. Widdecke and G. Walte, *J. Polym. Sci. Polym. Symp.*, 68 (1980) 221.
48 J. M. Braun and J. E. Guillet, *Macromolecules*, 9 (1976) 341.
49 D. Arnould and R. L. Laurence, in D. R. Lloyd, H. P. Schreiber and T. C. Ward (Editors), *Inverse Gas Chromatography (ACS Symposium Series*, No. 391), American Chemical Society, Washington, DC, 1989, Ch. 8, p. 87.
50 D. W. McCall and W. P. Slichter, *J. Am. Chem. Soc.*, 80 (1958) 1861.

Journal of Chromatography, 607 (1992) 239–243
Elsevier Science Publishers B.V., Amsterdam

CHROM. 24 382

Solid-phase extraction of prostanoids using an automatic sample preparation system

Georgina Hotter, Gloria Gómez, Isabel Ramis, Gloria Bioque, Joan Roselló-Catafau and Emilio Gelpí*

Department of Neurochemistry, Eicosanoid Branch, Centro de Investigación y Desarrollo, CSIC, Jordi Girona 18–26, 08034-Barcelona (Spain)

ABSTRACT

A commercial automated solid-phase extraction system for cyclooxygenase arachidonic acid metabolites in urine samples has been evaluated. Comparison of manual and automatic batch (36 samples) extraction procedures for tritium labelled prostanoids added as tracers to urine samples has shown equivalent results with recoveries greater than 90% for prostaglandins E_2, $F_{2\alpha}$ and 6-keto prostaglandin $F_{1\alpha}$ as well as thromboxane B_2. Analyte stability is not affected by the automated procedure, which uses less solvents and has a faster overall processing time than the manual method. The automated system has been applied to the extraction of prostanoids in urine samples from workers exposed to dichloroethane.

INTRODUCTION

Prostaglandins (PGs), prostacyclin (PGI_2) and thromboxane A_2 (TXA_2) are cyclooxygenase metabolites of arachidonic acid (AA), collectively known by the generic term prostanoids. Current evidence supports the potential pathophysiological role played by prostanoids in many diseases [1]. The prostanoid pathway can be studied *in vivo* by determining its metabolites in biological fluids [2]. Thus determination of the AA metabolites 6-keto-$PGF_{1\alpha}$ (from PGI_2), TXB_2 (from TXA_2), $PGF_{2\alpha}$ and PGE_2 in urine has been shown to be a powerful way to estimate changes in the total body production of prostanoids [3–5].

One of the problems encountered in the determination of these compounds is to quantify them at their occasionally extremely low physiological concentrations. Suitable analytical procedures for prostanoids include solid reversed-phase extraction, purification by high-performance liquid chromatography (HPLC) and determination of selected HPLC fractions by radioimmunoassay (RIA) [6]. Reversed solid-phase extraction has an important limitation, namely it requires several time-consuming steps [7].

Commercial systems that completely automate solid-phase extraction have become available. One of these systems, ASPEC (automatic sample preparation with extraction columns), has been evaluated in this laboratory as a possible automated extraction method for determining cyclooxygenase AA metabolites in urine. For this purpose the extraction recoveries obtained from urine samples supplemented with tritiated standards of 6-keto-$PGF_{1\alpha}$, TXB_2, $PGF_{2\alpha}$ and PGE_2 have been determined using both the manual and ASPEC extraction protocols. To establish the chemical stability of these prostanoids during extraction HPLC radiochromatographic profiles of urine samples extracted by ASPEC and those extracted manually have been compared [8]. This method provides excellent recoveries for cyclooxygenase AA metabolites with low intra-assay variation and the same radiochromatographic profiles as those obtained manually. Finally, using this method prostanoids were determined in urine samples from workers exposed to dichloroethane and in control subjects.

0021-9673/92/$05.00

EXPERIMENTAL

Apparatus

The ASPEC from Gilson (Villiers-le-Bel, France) consisted of three modules: a sample processor and injector module with a 143 mm stroke vertical arm and a 10-ml syringe for the dilutor, one Model 401 dilutor in slave configuration with its specific standard accessories (dilutor pipetting valve) and an automatically controlled module of various kinds of sample racks.

Air pressure was used to force the samples and eluents through the extraction columns. The HPLC system consists of two ABI 400 pumps from Applied Biosystems (Ramsey, NJ, USA), a high-pressure dynamic mixer, a 100 S diode array detector from Applied Biosystems to control both pumps and a radioactivity detector (Ramona) from Issomes (Straubenhardt, Germany) or a 2211 Superrack collector (LKB, Bromma, Sweden).

Cartridges and HPLC columns

Extractions were carried out on C_{18} cartridges (Amprep C_{18}) (400 mg adsorbent, 40 μm mean particle size) purchased from Amersham International (Buckinghamshire, UK) and on Amprep C_{18} minicolumns (100 mg adsorbent, 40 μm mean particle size). Reversed-phase HPLC was carried out on a Spherisorb ODS-2 column (25 cm × 4.6 mm I.D.; particle size 10 μm) from Phase Separations (Deesire, UK).

Chemicals

Tritiated 6-keto-$PGF_{1\alpha}$ (180 Ci/mmol), TXB_2 (120 Ci/mmol), $PGF_{2\alpha}$ (180 Ci/mmol) and PGE_2 (160 Ci/mmol) were from Amersham International. Methanol, acetonitrile and isopropanol were from Merck (Darmstadt, Germany). Petroleum ether and methyl formate were from Fluka (Buchs, Switzerland). TXB_2 and PGE_2 antisera were provided by the Institute Pasteur (Marnes la Coquette, France).

Samples

Urine samples from workers exposed to dichloroethane and from corresponding matched control subjects were stored at −40°C until required.

Manual procedure

Urine samples (5 ml) were spiked with [^{3}H]6-keto-$PGF_{1\alpha}$, [^{3}H]TXB_2, [^{3}H]$PGF_{2\alpha}$ and [^{3}H]PGE_2 (90 000 dpm/ml of each tritiated prostanoid). Spiked samples were acidified at pH 3.15 with 1 *M* HCl and centrifuged at 1500 *g* for 10 min at 4°C. Aliquots of the supernatants were then processed through C_{18} Amprep columns previously activated with methanol and acidified water (pH 3.15). After passing the urine samples through the columns they were washed with acidified water and petroleum ether. Finally the prostanoids were eluted with methyl formate, which was vacuum-evaporated in a concentrator-evaporator from Savant Instruments (Hicksville, NY, USA) [9] (see Table I).

ASPEC procedure

Aliquots of prostanoid-spiked urine samples, centrifuged and acidified as described above were automatically extracted on the ASPEC system. Briefly, 1 ml of urine was processed through C_{18} Amprep cartridges (100 mg adsorbent) previously activated with 2 ml of methanol and 2 ml of acidified water (pH 3.15). After washing the column with 2 ml of water and 2 ml of light petroleum (b.p. 40–60°C) prostanoids were eluted with 3 ml of methyl formate which was then vacuum-evaporated (see Table I).

TABLE I

COMPARISON BETWEEN MANUAL AND AUTOMATED (ASPEC) EXTRACTION OF PROSTANOIDS IN URINE SAMPLES

	Extraction method		
	Manual		ASPEC
Adsorbant (mg)			
C_{18}	400	100	100
Activation (ml)			
Methanol	10	2	2
Water	10	2	2
Sample volume (ml)			
Urine	5	1	1
Washing solvent (ml)			
Water	10	2	2
Light petroleum ether	20	2	2
Elution (ml)			
Methyl formate	8	3	3

HPLC procedure

The dry residue was redisolved in the mobile phase [40 m*M* formic acid, pH 3.15, with triethylamine–acetonitrile (65:35, v/v) at flow-rate of 1.5 ml/min] and processed through the HPLC system [10]. The HPLC system was connected either to a radioactivity detector or to a fraction collector. The later was used to obtain purified fractions for subsequent RIA determination as described in detail elsewhere [6].

RESULTS AND DISCUSSION

The analytical procedures used in the manual and the automated solid-phase extraction determinations of urinary prostanoids are summarized in Table I. As the volumetric characteristics of the system do not allow the use of eluent volumes greater than 3 ml, the routine manual extraction procedure was scaled down to make the adsorbent bed (100 mg) and solvent eluent volumes directly comparable with those used in the ASPEC system. This resulted in an overall reduction in the analysis time as well as lower solvent consumption in the automated batch processing mode for a total of 36 samples.

Table II shows the recoveries obtained in the manual and automated extraction procedures. The samples used were human urine samples spiked with radioactively-labelled prostanoid standards. The recoveries are equivalent for all practical purposes and are greater than 90% when the smaller (100 mg) cartridges are used in the ASPEC system. The intra-assay variation of the ASPEC procedure equivalent or better than that of the manual procedure.

The data in Table III show the results obtained after extraction and HPLC separation of human urine samples spiked with tritium-labelled prostanoids. In this instance each of the dry extract residues was injected into the HPLC system and elution was monitored by an on-line radioactive HPLC detector. The values shown correspond to the detector response (in counts/s) for each prostanoid; there was no significant difference between the manual and automated ASPEC extraction systems. The relative standard deviations (R.S.D.) are at least equivalent or better than those obtained by manual processing.

A possible limitation of automated batch sequential processing of 36 samples could be the degradation of the analytes to be extracted and analysed. In the ASPEC system this is carried out in batch mode using the same steps as in the manual mode, namely individual sample loading into each extraction column, column washing and finally elution of the retained prostanoids. This implies that in the approximately 2 h that the whole process takes, the samples could undergo degradation and autoxidation, thus affecting the determination. In contrast, in the manual processing, the analytes once loaded do not have to wait for other samples to be loaded and washed and thus spend the minimum possible time

TABLE II

COMPARISON BETWEEN AUTOMATED (ASPEC) AND MANUAL EXTRACTION RECOVERIES OF PROSTANOIDS (6-KETO-PFG$_{1\alpha}$, TXB$_2$, PGF$_{2\alpha}$, PGE$_2$ y PGD$_2$) IN URINE

Results expressed as mean ± standard deviation (intra-assay R.S.D.); n = 10.

	Recovery (%)		
	Manual extraction, 400 mg absorbent	Manual extraction, 100 mg absorbent	ASPEC extraction, 100 mg absorbent
6-keto-PGF$_{1\alpha}$	93.0 ± 2.0 (2.1%)	89.6 ± 1.1 (1.2%)	92.6 ± 1.2 (1.2%)
TXB$_2$	95.7 ± 4.1 (4.2%)	85.9 ± 5.7 (6.6%)	92.3 ± 2.0 (2.1)
PGE$_2$	93.7 ± 3.2 (3.4%)	95.1 ± 1.8 (1.9%)	91.6 ± 1.1 (1.2%)
PGF$_{2\alpha}$	94.0 ± 3.0 (4.3%)	93.6 ± 2.1 (2.1%)	90.2 ± 2.9 (3.2%)

TABLE III

COMPARISON OF ABSOLUTE RESPONSES OF THE RADIOACTIVITY HPLC DETECTOR FOR EACH OF THE FIVE TRITIUM-LABELLED PROSTANOIDS ADDED TO HUMAN URINE SAMPLES

Values under the manual or ASPEC headings represent the results obtained after manual processing of the urine samples *versus* ASPEC extraction of aliquots of the same samples.

Compound	Response (counts/s)	
	Manual	ASPEC
$PGF_{2\alpha}$	1467	1489
	1139	1143
	1548	1588
	1537	1545
	1505	1523
	946	855
	2056	1539
Mean	1457	1383
S.D.	350	277
R.S.D. (%)	24	20
PGE_2	1386	1440
	1296	1198
	1523	1380
	1451	1442
	1581	1530
	1071	924
	1922	1584
Mean	1461	1357
S.D.	263	222
R.S.D. (%)	18	16.3
6-Keto-$PGF_{1\alpha}$	868	787
	681	675
	816	897
	814	890
	1213	1200
	523	456
	1068	1175
Mean	855	868
S.D.	230	264
R.S.D. (%)	26.9	30.4
TXB_2	702	553
	533	470
	496	607
	565	632
	596	594
	395	396
	863	667
Mean	593	560
S.D.	151	96
R.S.D. (%)	25.4	17.1

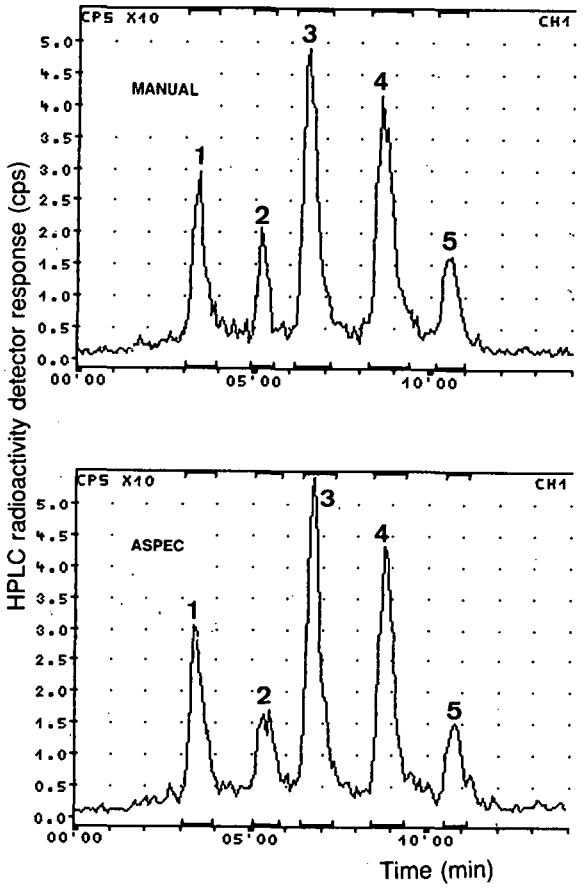

Fig. 1. Representative radiochromatograms of tritiated prostanoid standards in urine samples previously extracted by the manual (top) or ASPEC procedure (bottom).The HPLC mobile phase was a mixture of 40 m*M* formic acid (pH 3.15) with triethylamine–acetonitrile (65:35, v/v) at a flow-rate of 1 ml/min. Peaks: 1 = 6-keto-$PGF_{1\alpha}$; 2 = TXB_2; 3 = $PGF_{2\alpha}$; 4 = PGE_2; and peak 5 = PGD_2.

TABLE IV

URINARY CONCENTRATIONS (pg/ml) OF TXB_2 AND PGE_2 IN WORKERS EXPOSED TO DICHLOROETHANE (n = 12) COMPARED WITH UNEXPOSED CONTROLS (n = 12)

Urine samples were extracted with the ASPEC system and were analysed by HPLC–RIA. Results are expressed as mean ± S.E.M.; Student's t-test was used; ns = not significant.

	Worker exposed to dichloroethane	Control subject
TXB_2	148.1 ± 17.6	93.7 ± 13.2 (ns)
PGE_2	74.9 ± 49.7	94.9 ± 53.3 (ns)

in the extraction column before finally being eluted into the methyl formate fraction. However, the almost identical radiochromatograms obtained for the manual and automated sample extraction modes (Fig. 1) show that the automatic system does not affect the stability of these analytes.

The automated ASPEC technique has been used in conjunction with an HPLC–RIA procedure [6] to determine TXB_2 and PGE_2 in urine from workers exposed to dichloroethane.

Prostanoids could be used as an early marker of environmentally induced nephrotoxicity. Although a detailed account of this work showing that prostanoid urinary excretion is altered in workers exposed to heavy metal pollution will be published elsewhere, for dichloroethane no significant differences were found relative to healthy control subjects (Table IV).

In conclusion, the automated extraction of prostanoids from urine samples has been shown to be feasible using a commercially available ASPEC system. Compared with manual extraction methods reported previously the method uses less organic solvents and has a shorter processing time while maintaining equivalent or lower inter- and intra-assay variation coefficients.

ACKNOWLEDGEMENTS

This work was supported by FIS grant 89/386. We are grateful to Carmen Sarmiento, who is a recipient of a CIRIT grant, for her technical assistance. We thank the firm PACISA S.A., Barcelona, Spain, for their generous provision of the ASPEC system and L. M. Garcia Gros for his expert technical support.

REFERENCES

1 V. S. von Euler and O. Vesterquist, in P. B. Curtis-Prior (Editor), *Prostaglandins: Biology and Chemistry of Prostaglandins and Related Eicosanoids*, Churchill Livingstone, Edinburgh, 1988, p. 1.
2 M. Yamaguchi and N. Mori, *Prostaglandins, Leukotrienes Essent. Fatty Acids*, 39 (1990) 43.
3 K. Green and O. Vesterquist, in U. Zor, Z. Naor and F. Kohen (Editors), *Advances in Prostaglandin, Thromboxane and Leuktriene Research*, Vol. 16, Raven Press, New York, 1986, p. 309.
4 G. Hotter, J. R. Catafau, M. Artigot, O. Bulbena, F. Pi, A. Sáenz, L. F. Cruz and E. Gelpí, *Prostaglandins*, 41 (1991) 529.
5 S. Katayama, M. Inabe, Y. Mamuno, A. Omoto, S. Kawazy, J. Ishii and S. Sawade, *Prostaglandins, Leukotrienes Essent. Fatty Acids*, 39 (1990) 47.
6 E. Gelpí, I. Ramis, G. Hotter, G. Bioque, O. Bulbena and J. Roselló, *J. Chromatogr.*, 492 (1989) 223.
7 I. Ramis, J. Roselló-Catafau, M. Artigot, O. Bulbena, C. Picado and E. Gelpí, *J. Chromatogr.*, 532 (1990) 217.
8 M. W. F. Nielen, A. J. Valk, R. W. Frei, U. A. Th. Brinkman, Ph. Mussche, R. de Nijs, B. Ooms and W. Smink, *J. Chromatogr.*, 393 (1987) 69.
9 W. S. Powell, *Prostaglandins*, 20 (1980) 947.
10 D. M. Desiderio, M. D. Cunningham and J. A. Trimble, *J. Liq. Chromatogr.*, 4 (1981) 1261.

Journal of Chromatography, 607 (1992) 245–251
Elsevier Science Publishers B.V., Amsterdam

CHROM. 24 239

High-performance liquid chromatographic determination of acridine orange in nucleic acids isolated from dye-treated *Himantormia lugubris* thalli

M. Estrella Legaz*, Mercedes M. Pedrosa, J. L. Mateos, Silvia V. Caffaro and C. Vicente

Department of Plant Physiology, The Lichen Team, Faculty of Biology, Complutense University, 28040 Madrid (Spain)

ABSTRACT

The natural fluorescence of acridine orange was used for detecting and determining this dye in extracts of lichen thalli floated on acridine solutions after reversed-phase chromatography on Nucleosil 5 C_8; acetonitrile–water (80:20) was used for elution at a flow-rate of 1.2 ml min^{-1}. Fluorescence emission was monitored at 460 nm using an Mn^{2+}–atranorin chelate as internal standard. The response was linear over the range 0.01–0.4 μg of injected dye. This method is superior to those published previously in terms of sensitivity (from 60 to 300 times higher) and rapidity. This method was applied to measure the amount of acridine orange that binds to polynucleotides in lichen samples and to establish that cyclic AMP is able to impede the binding of the dye to lichen DNA. The method could be applied to intercalating action studies on DNA and dye detection in biological samples.

INTRODUCTION

Acridine dyes act as intercalating agents in bacterial episomes, impeding both replication and transcription [1]. This action, in a similar way to catabolite repression effected by glucose [2], is reversed by cyclic AMP by protecting the formation of the transcription initiation complex [3]. In addition to those described for bacteria, several catabolite-sensitive promotors have been found in eukaryota. In these organisms, the catalytic subunit of A kinase is sufficient to induce expression of cyclic AMP-sensitive genes [4]. Many promoters in eukaryota are also sensitive to acridine dyes and, to our knowledge, to nalidixic acid, like many prokaryota operons [5,6]. Production of some enzymes involved in the synthesis of lichen phenolics is regulated by catabolite-sensitive promoters, also inhibited by acridine orange, in *Evernia prunastri* [7], *Pseudevernia furfuracea* [8] and *Himantormia lugubris* [9]. This inhibition is always reversed by cyclic AMP.

Acridines, usually acridine isothiocyanate [10], are often used as derivatizing agents, but the excess of dye is not easily destroyed and this excess produces, according to the technique, a corresponding spot or peak that must be identified. The most usual chromatographic procedures applied to acridine dyes are paper [11,12] and silica gel [13,14] and cellulose [15] thin-layer methods using chloroform or dimethylformamide–water (35:65, v/v), respectively, as mobile phase. Detection procedures include chromogenic reactions [11,12] and fluorescence under UV radiation. The determination of acridines after their elution from thin layers by using a conventional spectrofluorimeter is linear over the range 3–25 μg [15–17], but it is probable that even lower amounts of the dye could be intercalated in the polynucleotide sequence. Gas–liquid chromatography (GLC) using 5% (w/w) Triton X-305 on acid-washed Chromosorb G (70–80 mesh) [18] gives retention times longer than 40 min for acridine derivatives. However, mixtures of bound acridine with free nucleotides or extraction agents could produce many artifactual interferences during derivatization

0021-9673/92/$05.00

and during a prolonged separation. Hence an accurate, easy, rapid and sensitive method for determining acridine dyes is required to relate the amount of the intercalating agent in DNA and the degree of inhibition of the sensitive promoter. In addition, the method must be equally applicable to other biological samples in which traces of acridine accidentally occur.

In this paper, we report the determination of acridine orange by high-performance liquid chromatography (HPLC) either in standard solutions or in nucleic acid fractions isolated from *H. lugubris* thalli. As the amount of isolated nucleic acid from lichen thalli was always very small and contained very low amounts of bound acridine, the method needed to be sufficiently sensitive to determine the dye. The use of protamine to precipitate DNA introduces an additional problem because of the fluorescence of the peptide, but the very good resolution of the chromatographic separation avoids any errors.

EXPERIMENTAL

Plant material

Himantormia lugubris (Hue) Lamb, growing on soil in King George Island (Antarctica), was used. Thalli were air-dried and stored in the dark at 5°C until required.

Sample preparation from incubated thalli

Samples of 0.5 g of air-dried thalli were floated on 12 ml of 0.1 *M* sodium acetate–acetic acid buffer (pH 6.8) for 3 h at 26°C in the dark. When indicated, 0.1 m*M* acridine orange and 0.5 m*M* cyclic AMP were added to the buffer. After incubation, thallus samples were washed with distilled water, gently dried with filter-paper and macerated in a mortar with 25 ml of chloroform for 15 min at room temperature to extract lichen phenolics [9]. Homogenates were filtered through Whatman No. 3 filter-paper and solid residues were air dried and stored at −34°C. Filtrates were dried in an air flow and residues were redissolved in 1.0 ml of acetonitrile (HPLC grade) and filtered through Millipore GS filters (0.22 μm pore diameter). These filtrates are called chloroformic extracts.

Thalline powders were macerated with 4.0 ml of distilled water and centrifuged at 38 000 *g* for 30 min at 2°C. The supernatants were adjusted to 5% (w/v) protamine sulphate and stored for 20 min in ice. Then, they were spun at 43 000 *g* for 30 min at 0°C. The pellets were washed with 2.0 ml of dilute protamine sulphate solution (0.05%, w/v), extracted with 2.0 ml of acetonitrile (HPLC grade) and filtered through Millipore GS filter as above. These filtrates are called nucleic acid fractions.

Reagents

Acridine orange, atranorin, cyclic AMP and protamine sulphate were obtained from Sigma (St. Louis, MO, USA). Acetonitrile (HPLC grade) (Carlo Erba, Milan, Italy) was used as received and doubly distilled water (Carlo Erba) was filtered through Millipore GS filters (0.22 μm pore diameter) before use. A Nucleosil 5 C_8 column (Varian, Palo Alto, CA, USA) was kept in acetonitrile until required.

HPLC separation of acridine orange

HPLC was performed on a Varian Model 5060 liquid chromatograph equipped with a Varichrom TM VUV 10 V detector and a Fluorichrom TM detector (Varian) in series and a Vista CDS 401 computer. The chromatographic conditions were as follows: column, Nucleosil 5 C_8 (125 mm × 4 mm I.D.); sample loading, 10 μl; mobile phase, acetonitrile–water (80:20, v/v), isocratic; flow-rate, 1.2 ml min^{-1}, as deduced from the Van Deemter equation; temperature, 20°C; detectors, UV (254 nm for atranorin), VIS (440 nm for Mn^{2+}–atranorin chelate complex and 490 nm for acridine orange) and fluorescence (excitation wavelengths from 340 to 380 nm using filters No. 7-54 and 7-60 from Varian, and emission wavelength 460 nm using filters No. 3-71 and 4-76 from Varian); 0.002 a.u.f.s.; attenuation, 64; internal standard, 1.0 mg ml^{-1} atranorin as Mn^{2+} chelate.

Chelate preparation

To 2.0 ml of 3.0 m*M* atranorin solution in acetonitrile, 1.0 ml of an aqueous solution of $MgCl_2$ or $MnCl_2$ (50 m*M*) was added [19]. The mixtures were incubated for 1 h at 30°C and atranorin was extracted with 6.0 ml of diethyl ether after vigorous shaking for 2 h to separate the phenolic derivative from the excess of inorganic ions [20]. The organic phases were dried *in vacuo* and used as internal standards.

Absorbance and fluorescence emission spectra were obtained by using a Varian DMS 90 spectrophotometer and a Kontron (Milan, Italy), SFM 25 spectrofluorimeter, respectively.

RESULTS AND DISCUSSION

Choice of detector and internal standard

As 0.1 m*M* acridine orange in acetonitrile showed a natural, pale green fluorescence, a fluorimetric detector (Fluorichrom TM, cell volume 12.5 μl) was used. Atranorin was chosen as an internal standard for several reasons. It is the main component of the phenolic fraction of many lichen species [21], including *H. lugubris* [9], it produces natural fluorescence [22] and it does not change substantially the pH of acridine solutions (water-dissolved acridine orange has a pH of 5.46).

Spectra of the fluorescence emission of atranorin and its chelates are shown in Fig. 1. However, atranorin in acetonitrile produced a quantitative response in the absorbance detector at 254 nm (Fig. 2A), with a retention time of 3.01 min, but no significant fluorescence response was found (Fig. 2B). Atranorin in lichen thalli occurs as a salt or chelate with inorganic cations [22,23]. Hence both magnesium and manganese chelates were prepared and chromatographed under the same conditions. The retention time of the absorbance peak at 440 nm for the Mn^{2+}–atranorin complex (Fig. 2C) coincided with the fluorescence peak, but decreased to 1.34 min from that for free atranorin (Fig. 2D).

By using this chelate as an internal standard, the retention time of which slightly increased to 1.41 min, acridine orange separated as a well resolved peak with a retention time of 10.54 min. The fluorescence response was 2.5 times higher than that obtained in the absorbance detector at 490 nm (Fig. 2E and F). A very small peak at 9.37 min seemed to be due to a contaminant of the standard dye. As the retention time in GLC for acridine varied from 40 to 50 min on Triton X-307–Chromosob G [17]. The HPLC separation described here was 4–5 times more rapid than GLC.

Baseline correction was always applied. This was constructed from the start of the first peak (internal standard) to the lowest valley point at the end of the same peak and, in this way, after a baseline segment was constructed, the area of the peak was corrected. The result was stored in a time and area file and then the next baseline segment was calculated for the included peak. Each successive baseline segment started at the end of the preceding one, to include all the peaks [24].

Linearity of response

Once the detector conditions had been chosen, the flow-rate was changed from 0.2 to 2.0 ml min^{-1}

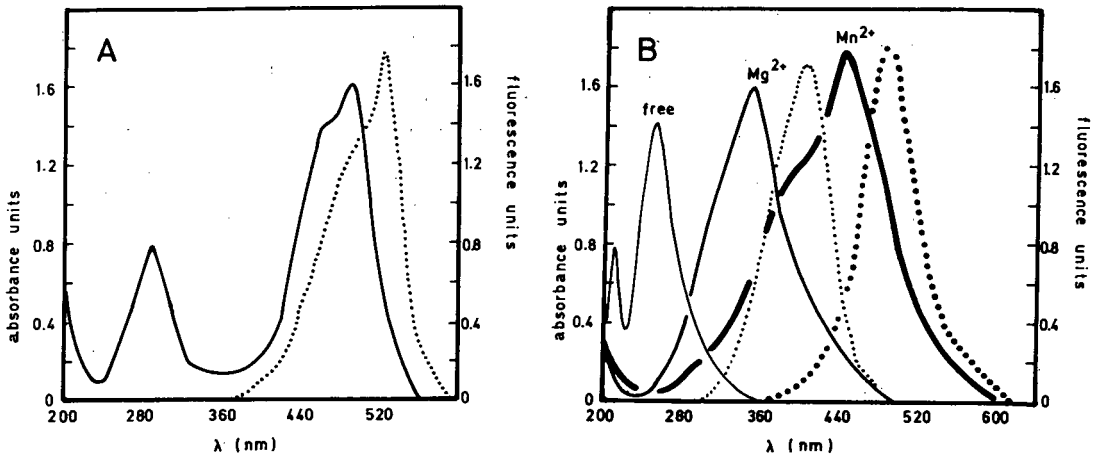

Fig. 1. Absorbance (continuous lines) and fluorescence emission (dotted lines) of (A) acridine orange and (B) atranorin as free or chelate compound.

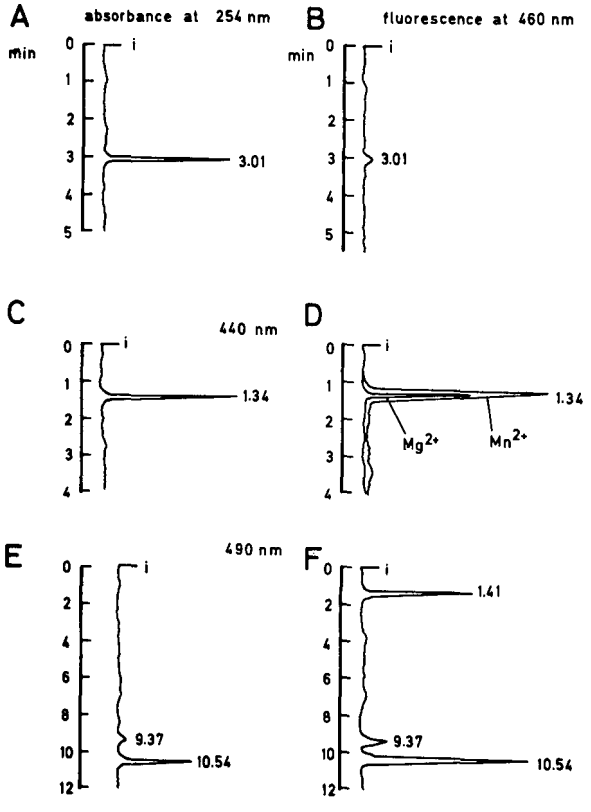

Fig. 2. HPLC traces of free atranorin monitored by (A) its absorbance at 254 nm or (B) fluorescence emission at 460 nm, Mg^{2+} and Mn^{2+} chelates of atranorin monitored by (C) their absorbance at 440 nm, where both peaks are exactly superimposed, or (D) fluorescence emission at 460 nm, and acridine orange monitored by (E) its absorbance at 490 nm or (F) fluorescence emission at 460 nm using Mn^{2+}–atranorin chelate as internal standard. The numbers on the peaks indicate retention times (min) and i indicates injection.

and the number of effective theoretical plates was calculated. The maximum number of theoretical plates (750 mm^{-1}) was obtained for a flow-rate of 1.2 ml min^{-1}. This flow-rate was then adapted throughout. The response of the detector was virtually linear in the range 0.01–0.4 μg injected (Fig. 3). The error inherent in direct calibration was estimated as the standard error for six repeated injections for each concentration of standard solutions. The equation for the calibration straight line was obtained by linear regression, the r^2 value of which measured the goodness of fit.

Determination of acridine orange in chloroformic extracts of H. lugubris

Samples of 0.5 g of *H. lugubris* thalli were floated on 0.1 m*M* acridine orange in 0.1 *M* acetate buffer (pH 6.8) for 2 h in the dark at 26°C or, alternatively, on 0.1 *M* acetate alone, using the latter as a culture control. Chloroformic extracts of both samples were dried *in vacuo* and residues were redissolved in 2.0 ml of pure acetonitrile. The chromatographic traces indicated that only atranorin gave a fluorescence peak at 1.41 min, as barbatolic acid, the other phenolic contained in this extract, did not show natural fluorescence (Fig. 4A). When extracts from samples floated on acridine orange were chromatographed in the same way, a sharp, well resolved peak appeared with a retention time of about 10.6 min (Fig. 4B). This peak increased when 1.0 μg acridine orange was added to the extracts dissolved in acetonitrile (Fig. 4C).

Determination of acridine orange in the nucleic acid fraction from H. lugubris

The precipitate of total nucleic acids, obtained by treatment with 5% (w/v) protamine sulphate, was either dialysed against distilled water or filtered through a column of Sephadex G-75 (10 cm × 1 cm I.D.), using distilled water as the mobile phase. In both instances, acridine orange was lost during these processes. Even during filtration through Sephadex G-75, visible fluorescence was retained in the column whereas nucleic acids were eluted in the void volume. Either acridine orange was removed from nucleic acids by physical strength or was exchanged from DNA to protamine, it did not seem convenient to remove protamine sulphate from the precipitate. Therefore, the complete pellet was washed with dilute protamine sulphate solution (0.05%, w/v) and extracted with 2.0 ml of pure acetonitrile prior to chromatography. Extraction of the dye from nucleic acids was required in order to avoid the irreversible quenching of acridine fluorescence by guanine–cytosine pairs after binding of the dye to polynucleotides [25]. When acridine-untreated thalli were used as a control to precipitate nucleic acids, protamine gave a strong fluorescence peak with a retention time of 2.03 min (Fig. 5A) that did not completely overlap that of atranorin, used as an internal standard (1.41 min), and that increased after loading the sample with protamine

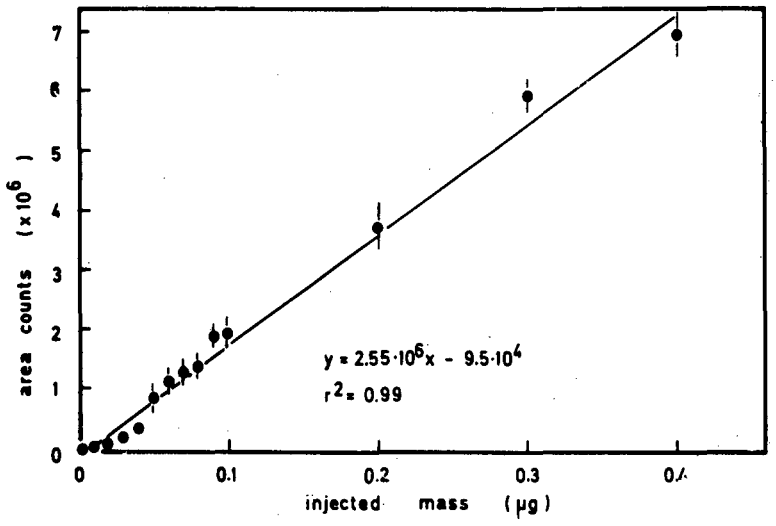

Fig. 3. Direct calibration for acridine orange where area counts recorded for fluorescence emission behave as a linear function of the mass injected. Values are the means of six replicates. Vertical bars give standard errors where larger than the symbols.

itself (Fig. 5B). A short but well resolved peak with a retention time of about 10.6 min (Fig. 5C), which increased on adding 1.0 μg of acridine orange to the sample (Fig. 5D), revealed the appearance of the dye extracted from the pellet of nucleic acids.

Application of the method to determine the role of cyclic AMP on the intercalation process

This HPLC method was applied to determine the time course of acridine orange intercalation in nucleic acids, mainly DNA [1,2], and the role of cyclic

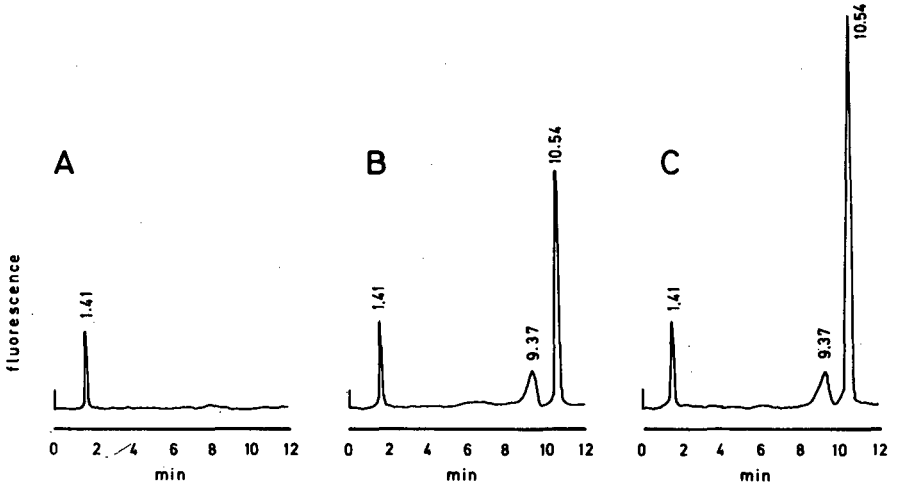

Fig. 4. HPLC identification of acridine orange extracted with chloroform from thalli of *H. lugubris* floated for 3 h on 0.1 m*M* acridine orange in 0.1 *M* acetate buffer (pH 6.8). (A) Control extract obtained from untreated thalli; (B) extract from thalli incubated on the dye; (C) extract used in (B) loaded with 1.0 μg of acridine orange in the injection volume.

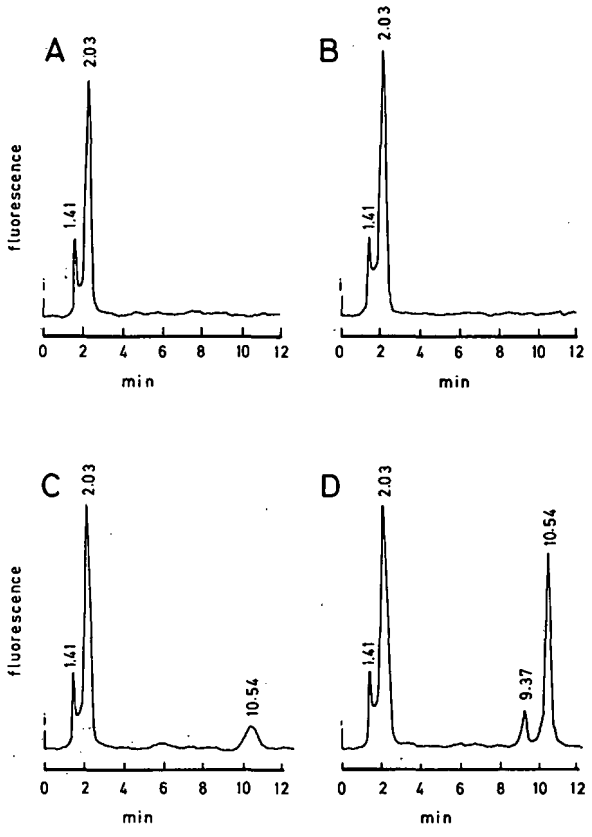

Fig. 5. HPLC of acridine orange bound to nucleic acids after precipitation with protamine sulphate. (A) Dye-untreated thalli used as control; (B) the same extract loaded with pure protamine sulphate; (C) extract prepared from thalli floated for 3 h on 0.1 m*M* acridine orange; (D) the same extract loaded with the dye.

AMP in this process. Samples were floated for 3 h in the dark on 0.1 *M* acetate containing 0.1 m*M* acridine orange or 0.1 m*M* acridine orange and 0.5 m*M* cyclic AMP. Both chloroformic extracts and protamine precipitates were prepared as indicated and redissolved in 2.0 ml of acetonitrile prior to chromatography. Fig. 6A shows the time course of acridine orange in chloroformic extracts. The amount of the dye increased continuously with the time of thalli incubation. When cyclic AMP was included in the incubation medium, the amounts of the dye recovered in the extracts were always higher than those found in the absence of the nucleotide, although the maximum value was obtained at 1 h of thalli incubation. When both dye and cyclic AMP were included in the incubation medium, the amount of acridine orange bound to the nucleic acid fraction was always lower than that extracted from thalli floated on the dye alone (Fig. 6B). These results, which were found to be highly reproducible, are in agreement with those obtained for binding of acridine to isolated DNA by using conventional spectrofluorimetric methods [26].

As cyclic AMP impedes the binding of acridine orange to the polynucleotide fraction (the excess of acridine, which remained as free dye after thalli incubation on the cyclic nucleotide, was recovered in the chloroformic extract), this action would be in agreement with that proposed by Ullmann [27] for the function of catabolite-sensitive operons during

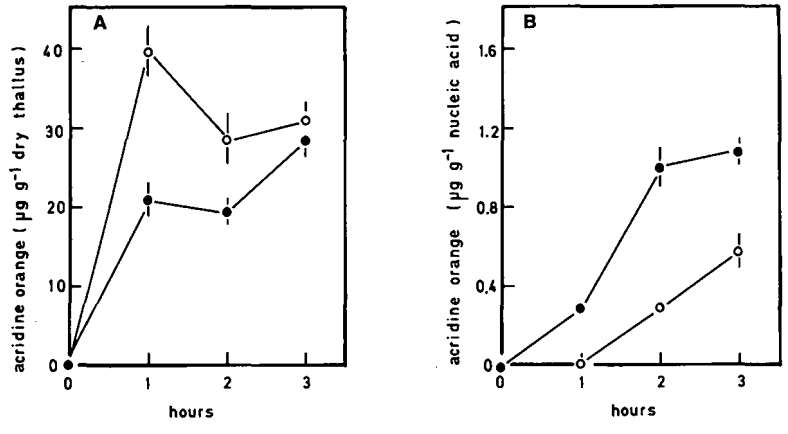

Fig. 6. (A) Time course of acridine orange accumulation by thalli of *H. lugubris* floated on (●) 0.1 m*M* dye or (○) 0.1 m*M* dye and 0.5 m*M* cyclic AMP. (B) Time course of the binding of acridine orange to nucleic acids from *H. lugubris* thalli floated on (●) 0.1 m*M* dye or (○) 0.1 m*M* dye and 0.5 m*M* cyclic AMP. Values are the means of four replicates. Vertical bars give standard errors where larger than the symbols.

experimental inhibition, even for cells in which cyclic AMP was not really produced.

ACKNOWLEDGEMENT

This work was supported by a grant from the Comunidad Autónoma de Madrid (Spain), No. C 243/91.

REFERENCES

1 P. P. Slonimski, G. Perrodin and J. J. Croft, *Biochem. Biophys. Res. Commun.*, 30 (1968) 232.
2 L. Sankaran and B. M. Pogell, *Nature New Biol.*, 245 (1973) 257.
3 G. Zubay, D. Schwartz and J. Beckwith, *Proc. Natl. Acad. Sci. U.S.A.*, 66 (1970) 104.
4 K. T. Riabowol, J. S. Fink, M. Z. Gilman, D. A. Walsh, R. H. Goodman and J. R. Feramisco, *Nature (London)*, 336 (1988) 83.
5 A. Puga and I. Tessman, *J. Mol. Biol.*, 75 (1974) 99.
6 H. Shuman and M. Schwartz, *Biochem. Biophys. Res. Commun.*, 64 (1975) 204.
7 P. Herrero, M. M. Pedrosa, J. Norato and C. Vicente, *J. Plant Physiol.*, 135 (1989) 170.
8 E. Garcia-Junceda, A. González and C. Vicente, *Biochem. System. Ecol.*, 15 (1987) 289.
9 J. L. Mateos, E. Conde, T. Miranda and C. Vicente, *Plant Sci.*, 77 (1991) 1.
10 N. Seiler and L. Demisch, in K. Blau and G. S. King (Editors), *Handbook of Derivatives for Chromatography*, Heyden, London, 1978, p. 346.
11 L. Reio, *J. Chromatogr.*, 13 (1964) 475.
12 L. Reio, *J. Chromatogr.*, 47 (1970) 60.
13 H. J. Petrowitz, G. Patuska and S. Wagner, *Chem. Ztg.*, 89 (1965) 7.
14 J. Janack, *J. Chromatogr.*, 15 (1964) 15.
15 E. Sawicki, H. Johnson and K. Kosinski, *Microchem. J.*, 10 (1966) 78.
16 J. E. Sinsheimer, D. D. Hong, J. T. Stewart, M. L. Fink and J. H. Burckhalter, *J. Pharm. Sci.*, 60 (1971) 141.
17 A. DeLeenheer, J. E. Sinsheimer and J. H. Burckhalter, *J. Pharm. Sci.*, 62 (1973) 1370.
18 R. E. Poulson, *J. Chromatogr. Sci.*, 7 (1969) 152.
19 A. Schatz, *J. Agric. Food Chem.*, 11 (1963) 112.
20 M. E. Legaz, M. M. Pedrosa, P. Martinez and V. Planelles, *Endocyt. Cell Res.*, 7 (1990) 85.
21 C. Culberson, W. L. Culberson and A. Johnson, *Second Supplement to Chemical and Botanical Guide to Lichen Products*, American Society for Bryology and Lichenology, St. Louis, MO, 1977, p. 19.
22 J. Redon, *Liquenes Antárticos*, Instituto Antártico Chileno, Santiago de Chile, 1985, p. 171.
23 P. W. Rundel, *Biochem. System. Ecol.*, 6 (1978) 157.
24 C. Vicente, J. L. Mateos, M. M. Pedrosa and M. E. Legaz, *J. Chromatogr.*, 553 (1991) 271.
25 L. M. Chan and Q. Van Winkle, *J. Mol. Biol.*, 40 (1969) 491.
26 A. Blake and A. R. Peacocke, *Biopolymers*, 6 (1968) 1225.
27 U. Ullmann, *Biochem. Biophys. Res. Commun.*, 57 (1974) 348.

Journal of Chromatography, 607 (1992) 253–259
Elsevier Science Publishers B.V., Amsterdam

CHROM. 24 206

Gas chromatographic determination of isoprenoid alkylglycerol diethers in archaebacterial cultures and environmental samples

Pilar Teixidor

LIFS, Department of Geochemistry, Faculty of Geology, University of Barcelona, 08071-Barcelona, Catalonia (Spain)

Joan O. Grimalt*

Department of Environmental Chemistry (CID-CSIC), Jordi Girona 18, 08034-Barcelona, Catalonia (Spain)

ABSTRACT

A method has been developed for the determination of dialkylglycerol ethers in sedimentary samples using gas chromatography (GC) and GC–mass spectrometry (GS–MS). The method includes a fractionation procedure based on solvent Soxhlet extraction, acidic hydrolysis and column chromatography clean-up in which the dialkylglycerol ethers are separated in an alcohol fraction. GC or GC–MS analysis of these fractions after trimethylsilyl ether derivatization has shown no coelutions of the dialkylglycerols and other polar products present in the extracts, allowing their determination even in samples where they are only minor constituents of the total lipid mixtures. Examples of application to the determination of halophiles, methanogens and sedimentary environments containing residues of these archaebacteria are given.

INTRODUCTION

Archaebacteria represent a well defined third line of evolutionary descent different from other prokaryotes and eukaryotes. These phenotypically diverse prokaryotes show characteristics such as cell walls containing ether-linked isoprenoid lipids [1] instead of the ester-linked phospholipid fatty acids found in eubacteria. Some archaebacteria, *e.g.* the methanogens, are ubiquitous in most anoxic environments and are responsible for the generation of methane, the end-product of about 50% of anaerobically degraded organic carbon [2,3]. Other archaebacteria, *e.g.* the halophiles and the thermoacidophiles, occur in restricted environments such as extreme hypersaline habitats [4] or acyclic hot springs [5].

The isolation of these organisms in pure cultures has given a considerable understanding of their morphological and metabolic characteristics but knowledge of their biogeochemical roles depends on the feasibility of biomass measurements in recent and ancient sedimentary environments. The specific membrane composition of archaebacteria points to the use of isoprenoid dialkylglycerol ethers, namely di-O-phytanylglycerol, as biomass estimators.

Diverse methods based on high-performance liquid chromatography (HPLC) have been proposed for the determination of these dialkylglycerol ethers [6–8]. The low molar ultraviolet absorptivity of these compounds is avoided by using Fourier transform infrared spectroscopy [6,7] or by derivatization to *p*-nitrobenzoates [8]. These methods have been tested with lipid extracts from pure cultures [6,7] but only one has effectively been used for the analysis of environmental samples [8].

Unfortunately, the application of these HPLC methods to environmental samples is limited by several detection-related problems. First, neither ultraviolet nor infrared detectors are specific for dialkyl-

0021-9673/92/$05.00

glycerol ethers. Second, the procedures for the formation of ultraviolet chromophore ester derivatives are general for most hydroxy-substituted molecules which may give rise to serious interference problems. The lack of simple methods for the structural determination of the HPLC-eluted peaks is a major disadvantage in these analyses.

These difficulties have led to the use of gas chromatography (GC) for the determination of these compounds, and especially GC coupled to mass spectrometry (GC–MS). GC methods have usually been applied after cleavage of the ether linkages using boron trichloride [9] or hydroiodic acid [10,11]. Subsequent analysis of the resulting moieties, either as halogenated hydrocarbons or after the formation of other derivatives, allows the identification of the original structures from the molar proportion of the cleaved products. These procedures, developed as a consequence of the low volatility of many polyalkylglycerol ethers, have been successfully applied to the analysis of thin-layer chromatography fractionated mixtures obtained from pure cultures. Obviously, these cleavage methods are not useful for the direct analysis of complex mixtures such as the extracts resulting from environmental samples.

This paper reports the development of a GC method for the determination of entire dialkylglycerol ethers, namely di-O-phytanylglycerol and O-sesterpanyl-O-phytanylglycerol, in sedimentary environments. This method uses a clean-up procedure, essentially hydrolysis and separation by column chromatography, for the isolation of the neutral hydroxy-substituted lipid fraction. These alcohols are subsequently analysed using high-temperature capillary columns. The method is applicable to the identification of methanogenic and halophilic archaebacterial inputs in sediments. Examples illustrating the suitability of the method for the determination of these dialkylglycerol ethers in representative environments containing these two types of microorganisms are given.

EXPERIMENTAL

Materials

Pestipur grade *n*-hexane and methanol were purchased from SDS (Peypin, France). Resi-analyzed grade dichloromethane and chloroform were from Baker (Phillipsburg, NJ, USA). Analytical-reagent grade acetone was from Carlo Erba (Milan, Italy). Analytical-reagent grade hydrochloric acid (25%), neutral silica gel (Kieselgel 40, 70–230 mesh) and alumina (aluminum oxide 90 active, 70–230 mesh) were from Merck (Darmstadt, Germany). Potassium hydroxide was purchased from Fluka Chemie (Buchs, Switzerland). Soxhlet thimbles were from Schleicher and Schuel (Dassel, Germany).

The potassium hydroxide was cleaned by sonication in dichloromethane. Silica gel, alumina and the Soxhlet thimbles were extracted with dichloromethane–methanol (2:1, v/v) in a Soxhlet apparatus for 24 h. After solvent evaporation, silica and alumina were heated for 12 h at 120 and 350°C, respectively. A total of 5% (w/w) of Milli-Q grade water was then added to the chromatographic adsorbents for deactivation.

The purity of the solvents was checked by concentrating 100 ml of solvent to 10 μl under vacuum for GC analysis. Blank requirements were as follows: splitless injection of 2.5 μl should result in chromatograms with no unresolved GC envelope and only very few peaks, representing up to 1 ng in terms of their flame ionization detector response. This threshold, under the above dilution factor, is equivalent to 0.08 ng/g when referred to 30 g of sediment.

Extraction of archaebacterial cultures

The cultures of halobacteria and methanogens were extracted in a Soxhlet apparatus with 150 ml of dichloromethane–methanol (2:1) for 18 h. The extract was evaporated under vacuum to 0.5 ml and hydrolysed by reflux with chloroform–methanol–concentrated hydrochloric acid (10:1:0.5); 2 ml of Milli-Q grade water were added to the mixture after 1 h of reflux. The alkylglycerols were recovered by extraction with chloroform (3 × 2 ml). The combined extracts were evaporated under vacuum almost to dryness and derivatized with N,O-bis(trimethylsilyl)trifluoroacetamide (BSFTA; 100 μl, 20 min, 200°C) before instrumental analysis.

Extraction and fractionation of sedimentary environmental samples

Before extraction the halite samples were grinded in a ring mill and the mud samples were freeze-dried. The lipids were Soxhlet-extracted with chloroform for 36 h. The extract was vacuum evaporat-

ed to about 1 ml and hydrolysed with 15 ml of 6% methanolic KOH for 12 h at room temperature. After digestion 15 ml of Milli-Q grade water were added and the solution was extracted with *n*-hexane (3 × 10 ml). The combined extracts were vacuum evaporated to about 0.5 ml and fractionated by column chromatography according to previously established methods [12]. A column filled with 0.8 g each of 5% water–deactivated alumina (top) and silica (bottom) was used. The alkylglycerols were collected in a third fraction of 6 ml of dichloromethane–methanol (4:1) after elution with 3 ml of *n*-hexane and 6 ml of *n*-hexane–dichloromethane (4:1). This alcohol fraction was evaporated under vacuum to a small volume and derivatized with BSTFA as described in the previous section.

Instrumental analysis

The samples were analysed by GC with a Hewlett-Packard Model 5890 Series II chromatograph equipped with a flame ionization detector and a splitless injector. Two fused-silica columns were used for separation: (1) 30 m × 0.32 mm I.D. SPB-5 (film thickness 0.25 μm) (Supelco, Bellefonte, PA, USA) and (2) 10 m × 0.25 I.D. OV-1 (film thickness 0.15 μm) high-temperature column (Rescom, Kortrijk, Belgium). The carrier gas was helium. The oven temperatures were (1) from 60 to 310°C at 6°C/min and (2) from 60 to 250°C at 10°C/min and from 250 to 350°C at 4°C/min. The injector and detector were maintained at 300 and 350°C, respectively. The injection was in the splitless mode (solvent, iso-octane, hot-needle technique) keeping the split valve closed for 40 s. Nitrogen was used as the make-up gas (flow-rate 30 ml/min). Detector gas flow-rates were: hydrogen 30 ml/min and air 300 ml/min.

Selected samples were analysed by GC–MS using a HP 5890 Series II gas chromatograph coupled to a HP 5970 mass-selective detector equipped with an HP 300 data system. Spectra were obtained in the electron-impact mode (70 eV), scanning between 50 and 600 mass units at 1.5 scans/s. The transfer line temperature was 320°C. The chromatographic conditions were the same as described earlier.

RESULTS AND DISCUSSION

The mass spectrum of the trimethylsilyl derivative of bis-O-phytanylglycerol, the target compound for methanogen biomass estimation [8], is shown in Fig. 1. The structures corresponding to the mass ions are given in Table I. The structural assignments have been performed by comparison with the mass spectra of a synthetic standard, bis-O-hexadecyl-*rac*-glycerol (Sigma, St. Louis, MO, USA), that has also been run as trimethylsilyl ether under the same instrumental conditions.

In both compounds the molecular ion and other related mass fragments such as $M - CH_3$, $M - CH_2OSi(CH_3)_3$ (see Table I) are very minor, and are of limited use for structural identification. The most prominent and informative ions correspond to the loss of C_nH_{2n+1}, namely $m/z = M - C_nH_{2n+1}OH$ and $m/z = M - C_nH_{2n+1}OCH_3$, and to the combination between alcoxy and trimethylsilyl groups, namely $m/z = C_nH_{2n+1}O + Si(CH_3)_3 - H$. These are the mass fragments of choice for the identification of the compounds contained in the samples. Accordingly, the selection of wide mass scan ranges for the inclusion of the molecular ions are of limited use and may involve important losses in sensitivity.

The mass spectrum of bis-O-hexadecyltrimethylsilylglycerol shown in Fig. 1 is similar to that previously reported [13], which was obtained by packed-column GC–MS, although the intensity of the mass fragments >300 is higher in the mass spectrum of this study. Another difference between the two mass spectra concerns the *m/z* 130/133 ratio; *m/z* 130 predominates in Fig. 1 but *m/z* 133 was the base peak in the previous study. As a result of this, the *m/z* 133 ion was proposed instead of *m/z* 130 for dialkyltrimethylsilylglycerol monitoring [13] because *m/z* 130 is also the base peak of the 1-alkyl-2-acyltrimethylsilylglycerols [14]. Nevertheless, the mass spectra shown in Fig. 1 indicate that *m/z* 130 have also to be considered as bis-O-phytanyltrimethylsilylglycerol does not show a significant *m/z* 133 peak.

Bis-O-phytanylglycerol is the dominant compound in the alcohol fraction resulting from the application of the described experimental procedure to solvent extracts of halobacteria (Fig. 2A and B). Some of these halobacteria also contain O-sesterpanyl-O-phytanylglycerol that elutes in the same fraction (Fig. 2B). The analysis of this latter glycerol as the trimethylsilyl derivative requires the use of short capillary columns (about 10 m, column 2 in the experimental procedure). Bis-O-phytanylglycerol is

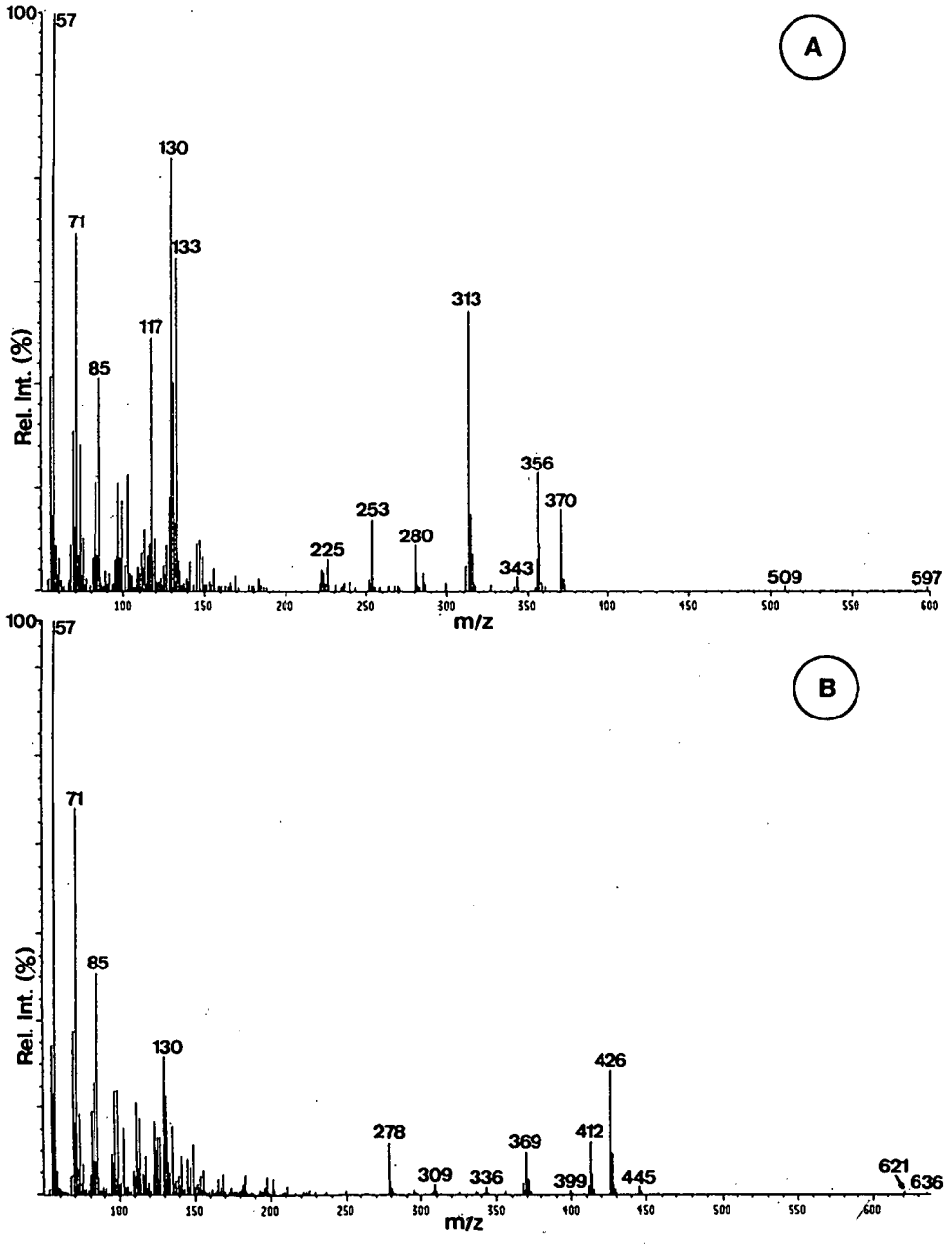

Fig. 1. Mass spectra of (A) bis-O-hexadecyltrimethylsilylglycerol and (B) bis-O-phytanyltrimethylsilylglycerol. Ion structure assignments in Table I.

also the major compound in the alcohol fraction of halite deposits (Fig. 2C) where it occurs together with other alcohols and O-sesterpanyl-O-phytanylglycerol.

Bis-O-phytanylglycerol is also the dominant compound in the equivalent alcohol fraction of methanogens such as *Methanosarcina* sp. (Fig. 3A). Conversely, this glycerol may be a minor lipid con-

TABLE I

MAJOR MASS FRAGMENTS OF THE MASS SPECTRA OF FIG. 1 CORRESPONDING TO THE TRIMETHYLSILYL (TMS) DERIVATIVES OF BIS-O-HEXADECYLGLYCEROL (16/16) AND BIS-O-PHYTANYLGLYCEROL (20/20)

Mass fragment		Ion structure
16/16 ($n=16$)	20/20 ($n=20$)	
Molecular groups		
612	724	M
597	709	M − CH_3
524[a]	636	M − $OSi(CH_3)_3$ + H
509	621	M − $CH_2OSi(CH_3)_3$
Loss of C_nH_{2n+1} groups		
389[a]	445	M − C_nH_{2n-1}
370	426	M − $C_nH_{2n+1}OH$
356	412	M − $C_nH_{2n+1}OCH_3$
C_nH_{2n+1} groups		
343	399	$H_{2n+1}C_nOCH_2O$ + $Si(CH_3)_3$ − H
313	369	$C_nH_{2n+1}O$ + $Si(CH_3)_3$ − H
280	336	$CH_2CHCH_2OC_nH_{2n+1}$ − 2H
253	309	$CH_2OC_nH_{2n+1}$ − 2H
225	281	C_nH_{2n+1}
223	279	C_nH_{2n-1}
222	278	C_nH_{2n-2}
TMS-glycerol groups		
133	133	$HOCHCH_2OSi(CH_3)_3$
130	130	$CH_2CHCH_2OSi(CH_3)_3$
117	117	$CH_2CH_2OSi(CH_3)_3$
Alkyl groups		
85	85	C_6H_{13}
71	71	C_5H_{11}
57	57	C_4H_9

[a] Not detected.

stituent in anoxic sediments in which methanogens are active, with the corresponding alcohol fraction being dominated by other products such as *n*-alkan-1-ols, *n*-alkandiols, sterols, hopanols, tetrahymanol and other triterpanols (Fig. 3B). Nevertheless, even in these instances no coelution between bis-O-phytanylglycerol and these other polar compounds has been observed in the GC traces, which allows an easy determination for biomass measurement.

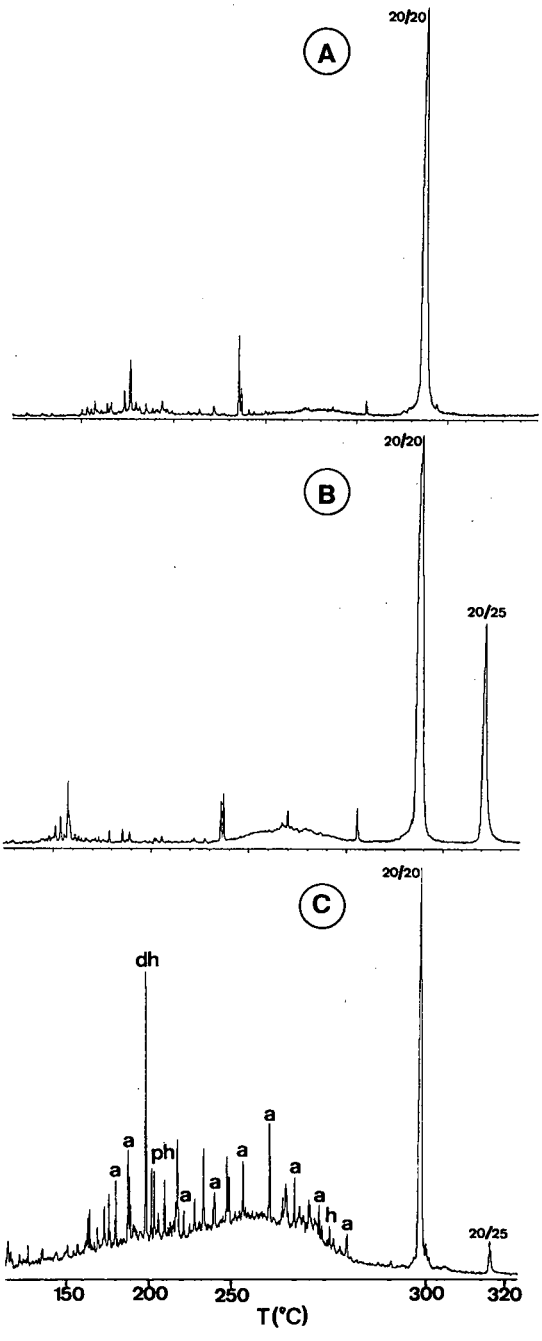

Fig. 2. Gas chromatograms of the trimethylsilyl-derivatized alcohol fraction of two halophile bacteria (A) Ma 2.38 [15] and (B) Ma 2.20 [15], and a halite deposit (C) Bonmatí, Santa Pola, Comunitat Valenciana, Spain. The instrumental conditions correspond to column 2 described under Experimental. 20/20 and 20/25 refer to bis-O-phytanylglycerol and O-sesterpanyl-O-phytanylglycerol, respectively. a = *n*-Alkan-1-ols; dh = dihydrophytol; ph = phytol; h = hopanols.

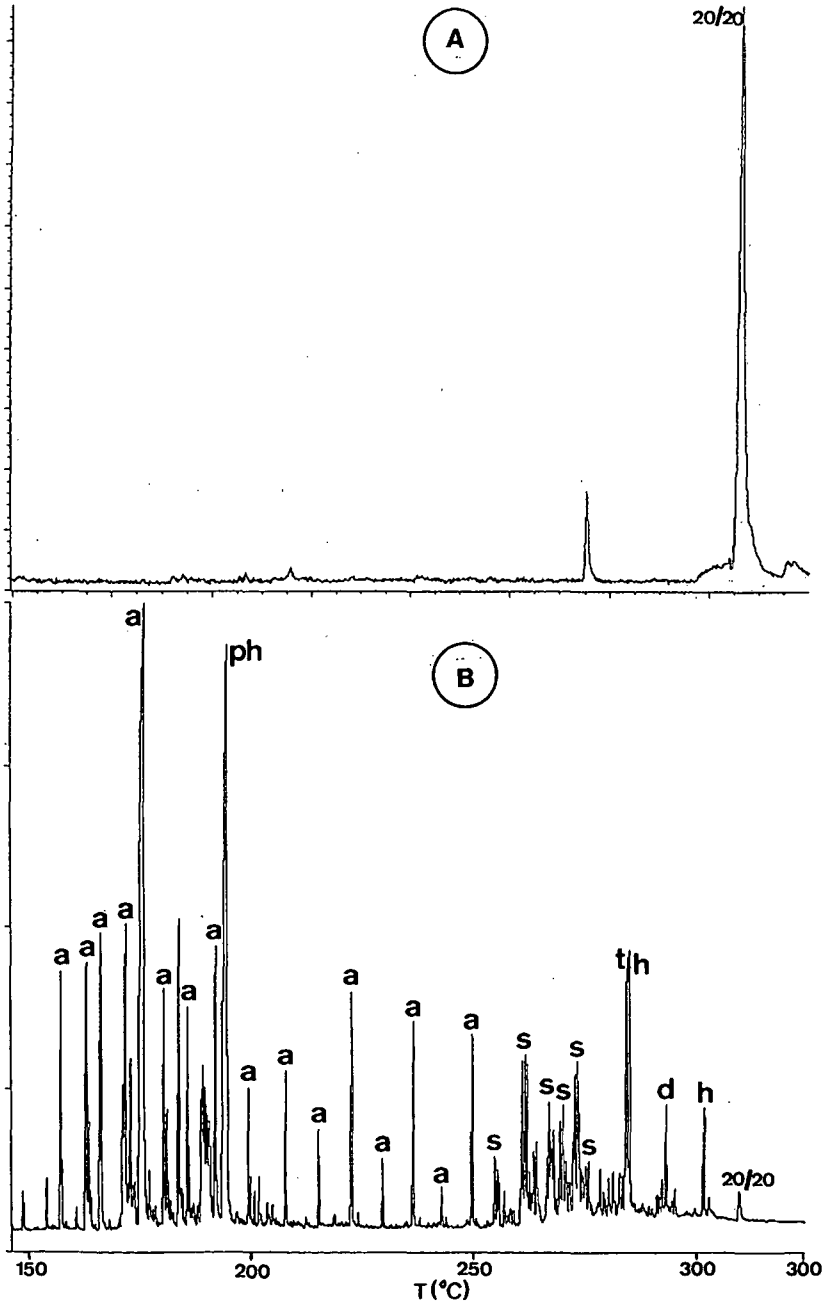

Fig. 3. Gas chromatograms of the alcohol fraction of (A) *Methanosarcina* sp. and (B) an anoxic sediment from Santa Olalla lagoon (Southwest Spain). The instrumental conditions correspond to column 1 described under Experimental. 20/20 refers to bis-O-phytanylglycerol. a = *n*-Alkan-1-ols; ph = phytol; d = *n*-alkandiols; s = sterols; h = hopanols; t = tetrahymanol.

CONCLUSIONS

Dialkylglycerols, namely di-O-phytanylglycerol, can be used for biomass estimation of halophilic and methanogenic archaebacteria. The method proposed here allows the GC or the GC–MS determination of these compounds in sedimentary samples even when they are only present as minor constituents in the total lipid mixtures. No coelutions between the sedimentary dialkylglycerols and other polar products have been detected after isolation of these compounds by the column chromatography clean-up procedure described in the method.

ACKNOWLEDGEMENTS

We thank Professor Francisco Rodriquez-Valera for the cultures of halophile bacteria. We also thank Dr. Rutger de Wit for a culture of *Methanosarcina* sp. Financial support from the EEC (SCIENCE Project No. SC1-CT91-0736) is acknowledged.

REFERENCES

1 M. Kates, *Chem. Fats Other Lipids*, 15 (1978) 301.
2 I. J. Higgins, D. J. Best, R. C. Hammond and D. Scott, *Microbiol Rev.*, 45 (1981) 556.
3 J. G. Zeikus, *Bacteriol. Rev.*, 41 (1977) 514.
4 F. Rodriguez-Valera, *FEMS Microbiol. Rev.*, 39 (1986) 17.
5 T. D. Brock, in M. P. Starr, H. Stolp, H. G. Truper, A. Belows and H. G. Schegel (Editors), *The Prokaryotes*, Springer, New York, pp. 978–984.
6 C. A. Mancuso, P. D. Nichols and D. C. White, *J. Lipid Res.*, 27 (1986) 49.
7 C. A. Mancuso, P. D. Nichols and D. C. White, *FEMS Microbiol. Lett.*, 35 (1986) 115.
8 R. F. Martz, D. I. Sebacher and D. C. White, *J. Microbiol. Methods*, 1 (1983) 53.
9 M. Kates, L. S. Yengoyan and P. S. Sastry, *Biochim. Biophys. Acta*, 98 (1965) 252.
10 M. De Rosa, A. Gambacorta and J. D. Bu'Lock, *Phytochemistry*, 15 (1976) 143.
11 M. De Rosa, S. De Rosa and A. Gambacorta, *Phytochemistry*, 16 (1977) 1909.
12 J. Albaigés, J. Algaba and J. O. Grimalt, *Org. Geochem.*, 6 (1984) 223.
13 K. Satouchi, K. Saito and M. Kates, *Biomed. Mass Spectrom.*, 5 (1978) 87.
14 K. Satouchi and K. Saito, *Biomed. Mass Spectrom.*, 3 (1976) 122.
15 M. Torreblanca, F. Rodriguez-Valera, G. Juez, A. Ventosa, M. Kamekura and M. Kates, *Syst. Appl. Microbiol.*, 8 (1986) 89.

Journal of Chromatography, 607 (1992) 261–270
Elsevier Science Publishers B.V., Amsterdam

CHROM. 24 409

Gas chromatographic screening of organic compounds in urban aerosols

Selectivity effects in semi-polar columns

Merce Aceves

Environmental Control Service, Entitat Metropolitana de Barcelona, Carrer 62, 420 Edifici A Zona Franca, 08004 Barcelona, Catalonia (Spain)

Joan O. Grimalt*

Department of Environmental Chemistry (CID–CSIC), Jordi Girona 18, 08034 Barcelona, Catalonia (Spain)

ABSTRACT

A gas chromatographic–mass spectrometric study of aerosols collected in Barcelona allowed the identification of the major sources of airborne organic matter in an urban environment. The extracts were separated by column chromatography into three fractions encompassing aliphatic hydrocarbons, aromatic hydrocarbons plus semi-polar compounds and polar products. The overall procedure allowed the identification of 108 molecular species that were grouped according to their precursors. The study also allowed the characterization of significant changes in the elution order of linear and polycyclic molecules of similar retention using different semi-polar capillary columns such as DB-5, SE-52, CP-Sil 8 CB, SE-54 and HP-5.

INTRODUCTION

The emission of pollutants to the atmosphere often involves the direct, uncontrolled exposure of large populations to toxic substances, representing the environmental process of highest potential hazard to human health. This is especially relevant in urban areas where the proximity between humans and pollutant sources is closest. In this respect, the aerosol composition of *n*-alkanes and polycyclic aromatic hydrocarbons (PAHs) has sometimes been described [1–3], but the more polar products should also be considered because they may have significant health implications [4].

Since 1985 we have regularly monitored the composition of solvent extractable compounds in the aerosol of Barcelona (Spain) using methods based on gas chromatography (GC) and GC coupled with mass spectrometry (GC–MS). This regular sampling and analysis has afforded a detailed knowledge of the major lipid atmospheric particulates of the city. In this study, standard GC traces corresponding to the central area of Barcelona, the most densely populated area, are reported and their composition is interpreted in terms of predominant input sources. These GC distributions provide reference patterns for comparison with those obtained in other cities.

However, the use of different capillary columns involves significant changes in the relative retentions of several major compounds. These selectivity changes are produced even among semi-polar stationary phase columns (5% phenyl–95% methyl type) which are reported to be equivalent in commercial catalogues. The study included, therefore, a comparison of five semi-polar columns (Table I)

0021-9673/92/$05.00

TABLE I

SEMI-POLAR CAPILLARY COLUMNS COMPARED IN THIS STUDY

Column	Stationary phase[a]	Dimensions (m × mm I.D.)	Film thickness (μm)	Manufacturer
DB-5	5% Phenyl–95% methyl	30 × 0.25	0.2	J & W Scientific, Folsom, CA, USA
SE-52 (cross-bond)	5% Diphenyl–95% dimethyl	25 × 0.32	0.1–0.15	Carlo Erba, Milan, Italy
CP-Sil 8 CB	5% Phenyl–95% dimethyl	25 × 0.25	0.13	Chrompack, Middelburg, Netherlands
SE-54 (cross-bond)	1% Vinyl–5% diphenyl–94% dimethyl	25 × 0.32	0.1–0.15	Carlo Erba
HP-5 (Ultra-2)	5% Diphenyl–95% dimethyl	25 × 0.2	0.11	Hewlett-Packard, Palo Alto, CA, USA

[a] As defined by the manufacturer.

with regard to the differences in their relative retention of dominant aerosol components.

EXPERIMENTAL

Materials

Pestipur-grade dichloromethane was purchased from Mallinckrodt (Paris, KY, USA). Chromatography quality *n*-hexane, methanol, isooctane, neutral silica gel (Kieselgel 40, 70–230 mesh) and alumina (aluminium oxide 90 active, 70–230 mesh) were from Merck (Darmstadt, Germany). The Soxhlet cartridges were from Schleicher and Schüll (Dassel, Germany). The glass microfibre filters were purchased from Whatman (Maidstone, UK).

The silica gel, the alumina and the Soxhlet cartridges were extracted with dichloromethane–methanol (2:1, v/v) in a Soxhlet apparatus for 24 h. After solvent evaporation, the silica and the alumina were heated for 12 h at 120 and 350°C, respectively. A total of 5% (w/w) of Milli-Q-grade water was then added to the chromatographic adsorbents for deactivation. The glass-fibre filters were kiln-fired for 12 h at 400°C and weighed prior to sampling.

The purity of the solvents was checked by concentrating under vacuum 100 ml of solvent to 10 μl for GC analysis. Blank requirements were as follows: splitless injection of 2 μl should result in chromatograms with no unresolved GC envelope and only a few peaks, representing up to 1 ng in terms of their flame ionization detector response. This threshold, under the above dilution factor, is equivalent to less than 0.02 ng/m^3 when referred to 100 ml of solvent used for the extraction of one third of a filter that corresponds to 1000 m^3 of air.

Sampling, extraction and fractionation

The air samples (1200 m^3 and 50 m^3/h) were taken with a High-Vol pumping system (CAV-P; MCV, Collbato, Spain) equipped with 20.3 × 25.4 cm glass microfibre filters (Whatman). After sampling the filters were frozen at −20°C until analysis in the laboratory. One third of each filter was Soxhlet extracted with 100 ml of dichloromethane for 24 h. The extract was vacuum and nitrogen evaporated until almost dryness and diluted to 0.5 ml with *n*-hexane, then fractionated by column chromatography according to previously established methods [5]. A column filled with 1 g each of 5% water-deactivated alumina (top) and silica (bottom) was used. The aliphatic hydrocarbons were obtained in the first fraction (4 ml of *n*-hexane), the aromatic hydrocarbons were collected in the second fraction (4 ml of 20% dichloromethane in *n*-hexane) and the polar compounds eluted in the third fraction (4 ml of 20% methanol in dichloromethane). These frac-

tions were vacuum and nitrogen concentrated almost to dryness and the residue was dissolved in isooctane.

Instrumental analysis

The samples were analysed by GC and GC–MS. These analyses were performed with a Carlo-Erba Model 5300 gas chromatograph equipped with a flame-ionization detector and with a Hewlett-Packard Model 5970 mass spectrometer provided with an HP-5994A data adquisition system. The GC analyses were performed with the capillary columns described in Table I. The oven temperature was programmed from 60 to 300°C at 6°C/min, and the injector and detector temperatures were set at 280 and 330°C, respectively. Hydrogen was used as carrier gas at 50 cm/s. The oven temperature programme for the GC–MS analyses was from 60 to 280°C at 6°C/min, the injector and tranfer line temperatures were 280 and 300°C, respectively, and helium was used as the carrier gas at 50 cm/s. Data were acquired in the electron impact mode (70 eV), scanning from 40 to 600 mass units at 1 s per decade. In both instances the injector was in the splitless mode (1 μl; hot needle technique), the split valve being closed for 35 s.

Identification and quantification

Compound identification was based on the GC–MS data and on co-injection with authentic standards. Quantification was performed from the GC profiles using the external standard method. Samples and standards were repeatedly injected until less than 5% dispersion in the area measurements was observed. An external standard containing *n*-eicosane, *n*-tricosane, *n*-octacosane, *n*-dotriacontane and *n*-hexatriacontane was used for the alkane fraction and the aromatic hydrocarbons were determined with a standard containing phenanthrene, fluoranthene, pyrene, benzo[*ghi*]fluoranthene, benz[*a*]anthracene, chrysene, benzo[*e*]pyrene, dibenz[*a*,*h*]anthracene, benzo[*ghi*]perylene and coronene. These two standards were also used as test mixtures for the assessment of undesired column adsorption effects or sample discrimination in the injector. The polar compounds were determined with a standard containing coprostanol and *n*-octacosan-1-ol.

RESULTS AND DISCUSSION

The sampling site was located in Barcelona city centre, in a square (Plaça Molina) with heavy traffic. The High-Vol pump was situated 3 m above ground level and 100 m away from any vertical obstacle. The sampling periods were performed under conditions of atmospheric stability, in the absence of precipitation and with a wind speed of less than 4 m/s at 25 m above ground level.

Hydrocarbons and semi-polar lipids

The GC profile of the first column chromatographic fractions (Fig. 1 and Table II) is dominated

TABLE II

ALIPHATIC HYDROCARBONS IDENTIFIED IN THE PARTICULATE FRACTIONS OF THE AEROSOL SAMPLES COLLECTED IN BARCELONA CITY

No.	Compound	Diagnostic ions (*m/z*)	Average concentration (ng/m^3)
1	*n*-Pentadecane	212	
2	*n*-Hexadecane	226	
3	*n*-Heptadecane	240	1.3
4	Pristane	268	
5	*n*-Octadecane	254	2.0
6	Phytane	282	
7	*n*-Nonadecane	268	3.3
8	*n*-Eicosane	282	5.7
9	*n*-Heneicosane	296	8.9
10	*n*-Docosane	310	16
11	*n*-Tricosane	324	16
12	*n*-Tetracosane	338	16
13	*n*-Pentacosane	352	16
14	*n*-Hexacosane	366	16
15	*n*-Heptacosane	380	15
16	*n*-Octacosane	394	4.5
17	*n*-Nonacosane	408	10
18	*n*-Triacontane	422	3.5
19	17α(H),21β(H)-30-Norhopane	191	
20	*n*-Hentriacontene	434	
21	*n*-Hentriacontane	436	12
22	17α(H),21β(H)-Hopane	191	
23	*n*-Dotriacontene	448	
24	*n*-Dotriacontane	450	3.2
25	*n*-Tritriacontane	464	4.2
26	*n*-Tetratriacontane	478	0.97
27	*n*-Pentatriacontane	492	0.98
Total *n*-alkanes			160
Unresolved complex mixture			2400

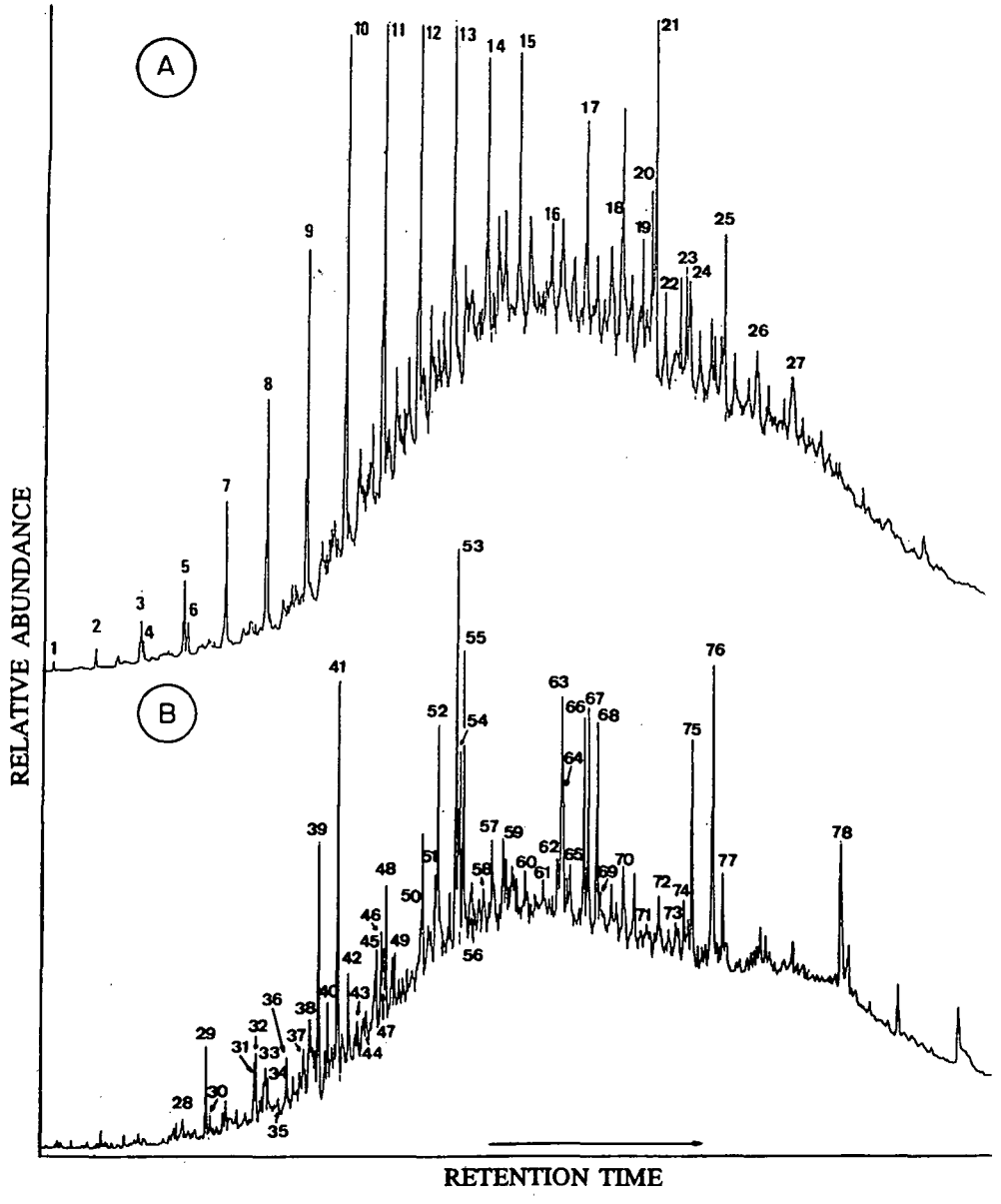

Fig. 1. GC profiles of the aliphatic and aromatic hydrocarbons present in the aerosols collected in Barcelona during winter. Column: CP-Sil 8 CB (See Table I). The numbered peaks refer to Tables II and III.

by *n*-alkane distributions ranging between C_{16} and C_{35} without odd–even carbon number predominance. Other characteristic resolved peaks in this GC trace encompass regular isoprenoids, pristane (4) and phytane (6), and olefins, *n*-hentriacontene (20) and *n*-dotriacontene (23). These compounds overlay an unresolved complex mixture (UCM) of hydrocarbons eluting over all the temperature range of the chromatogram. The *n*-alkanes without odd–even carbon number predominance occurring together with pristane and phytane, and an unresolved mixture of aliphatic hydrocarbons are char-

acteristic of petroleum residues and vehicular exhausts [6,7]. Similarly, the olefins are likely pyrolysis products in the vehicular combustion processes. Thus, pyrolysis naphtha produced by thermal cracking of naphtha contains large amounts of olefins and aromatics [8]. The presence of 17α(H), 21β (H)-hopanes is consistent with the petroleum-related origin of these hydrocarbon mixtures [6,9].

The GC traces of the aromatic hydrocarbon fractions (Fig. 1 and Table III) are dominated by parent PAHs, namely fluoranthene (39), pyrene (41), benzo[*ghi*]fluoranthene (52), 4(H)-cyclopenta[*cd*]pyrene (53), benz[*a*]anthracene (54), chrysene/triphenylene (55), benzofluoranthenes (63–65), benzopyrenes (66,67), indeno[1,2,3-*cd*]pyrene (74), benzo[*ghi*]perylene (76) and coronene (78). The abundance of catacondensed structures and the predominance of parent hydrocarbons over alkylated homologues indicate that these distributions of resolved compounds are of pyrolytic origin [10,11].

Further assessment of processes determining the composition of these hydrocarbons can be obtained from the consideration of some concentration ratios. Thus, the fluoranthene/(fluoranthene + pyrene) ratio, 0.40, approaches that reported for exhausts of gasoline-fuelled vehicles [12]. The indeno[1,2,3-*cd*]pyrene/(indeno[1,2,3-*cd*]pyrene + benzo[*ghi*]perylene) ratio, 0.45, corresponds to coal combustion emissions [13,14]. The benzo[*e*]pyrene/(benzo[*e*]pyrene + benzo[*a*]pyrene) ratio, 0.47, also reflects pyrolytic emissions related to coal use.

An important UCM is found in addition to these resolved compounds. This mixture is related to petrogenic sources such as that observed in the aliphatic hydrocarbon chromatograms. In fact, the "baseline humps" from the GC traces in Figs. 1 and 3 merely reflect the fractionation of the same UCM by the column chromatographic method selected for this study. These petrogenic inputs are also represented by some minor resolved compounds such as the alkylated phenanthrenes and chrysenes/triphenylenes.

The occurrence of some aromatic hydrocarbons such as retene (47), a compound characteristic of coniferous vegetation [15], is related to higher plant inputs. Squalene (68) is another biogenic product that is usually representative of microorganism contributions [16].

Squalene, often a major peak in the chromatograms of the semi-polar fraction, is a compound exhibiting a high column dependence of its retention indices. This is illustrated in Table IV, where the relative retention indices of this unsaturated hydrocarbon and those of benzo[*a*]pyrene and benzo[*e*]pyrene are shown. These indices were calculated according to the PAH series of naphthalene, phenanthrene, chrysene and picene for better reproducibility [17]. Squalene elutes before benzo[*e*]pyrene in the DB-5 column. In the SE-52 column it elutes between the two benzopyrenes and may co-elute with benzo[*a*]pyrene in columns of this type with lower efficiency. Finally, squalene elutes after benzo[*a*]pyrene in the CP-Sil 8 CB, SE-54 and HP-5 columns. GC traces corresponding to the elution time windows of the benzofluoranthene, benzopyrene and squalene peaks are illustrated in Fig. 2.

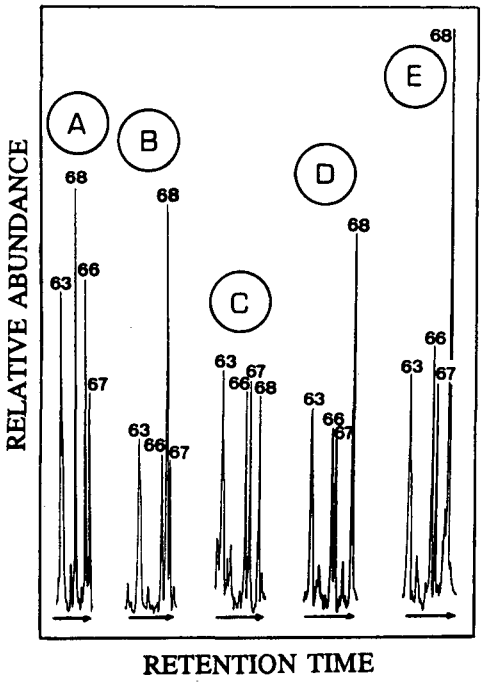

Fig. 2. GC profiles showing the elution order of benzofluoranthenes, squalene and benzopyrenes in the semi-polar capillary columns described in Table I: (A) DB-5; (B) SE-52; (C) CP-Sil 8 CB; (D) SE-54; (E) HP-5. Peak numbers refer to Table III.

Polar compounds

The major compounds in the GC profiles of the polar fractions are phthalates, fatty acids and alco-

TABLE III

AROMATIC HYDROCARBONS AND SEMI-POLAR COMPOUNDS IDENTIFIED IN THE PARTICULATE FRACTIONS OF THE AEROSOL SAMPLES COLLECTED IN BARCELONA

No.	Compound	Diagnostic ions (*m/z*)	Average concentration (ng/m^3)
28	Dibenzothiophene	184	
29	Phenanthrene	178	2.6
30	Anthracene	178	0.96
31	3-Methylphenanthrene	192	
32	2-Methylphenanthrene	192	
33	4/9-Methylphenanthrene	192	
34	1-Methylphenanthrene	192	
35	Methyl hexadecanoate	270	
36	4H-Methylcyclopenta[*def*]phenanthrene	204	
37	Dimethyl-178	206	
38	Dimethyl-178	206	
39	Fluoranthene	202	10
40	Acephenanthrylene	202	
41	Pyrene	202	15
42	Methyl octadecanoate	298	
43	Trimethyl-178	220	
44	Trimethyl-178	220	
45	8/7-Methylpyrene	216	
46	Benzo[*a*]fluorene	216	
47	Retene	234	
48	Benzo[*b*]fluorene	216	
49	1-Methylpyrene	216	
50	Dimethyl-202	230	
51	Benzo[*b*]naphtho[2,1-*d*]thiophene	234	
52	Benzo[*ghi*]fluoranthene	226	12
53	4(H)-Cyclopenta[*cd*]pyrene	226	23
54	Benz[*a*]anthracene	228	8.8
55	Chrysene/triphenylene	228	16
56	Methyl-234	248	
57	Methyl-234	248	
58	*n*-Octyl hexadecanoate	112	
59	Methylchrysene	242	
60	Methyl-226	240	
61	Binaphthyl	254	
62	*n*-Octyl octadecanoate	112	
63	Benzo[*b/j*]fluoranthene	252	27
64	Benzo[*k*]fluoranthene	252	
65	Benzo[a]fluoranthene	252	
66	Benzo[*e*]pyrene	252	19
67	Benzo[*a*]pyrene	252	22
68	Squalene	410	
69	Perylene	252	
70	Quaterphenyl	306	
71	Methyl-252	266	
72	Methylene-252	264	
73	Dibenzonaphthothiophene	284	
74	Indeno[7,1,2,3-*cdef*]chrysene	276	
75	Indeno[1,2,3-*cd*]pyrene	276	24
76	Benzo[*ghi*]perylene	276	29
77	Anthantrene	276	
78	Coronene	300	10
Total HAP			220
Unresolved aromatic hydrocarbons			1800

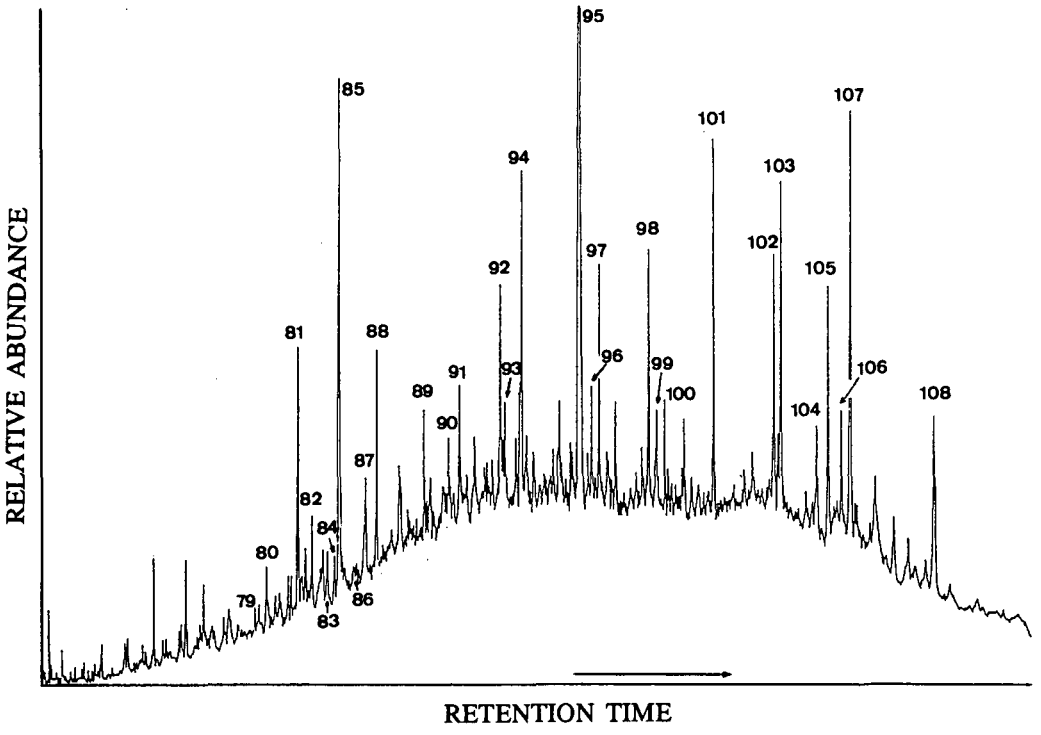

Fig. 3. Representative GC profile of the TMS-derivatized polar compounds present in the winter aerosols of Barcelona. Column: DB-5 (see Table I). The numbered peaks refer to Table V.

hols (Fig. 3 and Table V). Phthalates are in fact the predominant constituents in all instances. These compounds are found world-wide in soils [18] and waters [19], reflecting the widespread use of plastiziers. Di-*n*-octyl phthalate (95) is the major homologue; its presence is concurrent with other *n*-octyl esters identified in these samples such as di-*n*-octyl hexanedioate (94), a major compound in fraction 3, and *n*-octyl hexadecanoate (58) and octadecanoate (62), in fraction 2.

TABLE IV

RETENTION INDICES OF BENZO[*e*]PYRENE, BENZO[*a*] PYRENE AND SQUALENE IN THE SEMI-POLAR COLUMNS LISTED IN TABLE I

Retention indices relative to the PAH scale [17].

Column	Benzo[*e*]pyrene	Benzo[*a*]pyrene	Squalene
DB-5	451.1	452.3	446.9
SE-52	452.7	456.4	454.9
CP-Sil 8 CB	449.4	451.0	454.3
SE-54	453.1	454.3	462.4
HP-5	452.4	454.5	459.4

n-Akan-1-ols and sterols constitute the second major group of polar compounds. The *n*-alkan-1-ols encompass a distribution of even-carbon-numbered homologues ranging between C_{16} and C_{32} in which the C_{28}–C_{32} mode is predominant. This type of distrubution is characteristic of contributions from higher plant waxes [20]. The sterols constitute a mixture of C_{27}–C_{29} compounds dominated by 24-ethylcholest-5-en-3β-ol (107) in which cholest-5-en-3β-ol (103), 24-methylcholest-5-en-3β-ol (104) and 24-ethylcholest-5,22-dien-3β-ol (105) are other major species. This composition is also representative of inputs from higher plant materials [21,22] which in some cases may be introduced anthropogenically [4].

TABLE V

POLAR COMPOUNDS IDENTIFIED IN THE PARTICULATE FRACTIONS OF THE AEROSOL SAMPLES COLLECTED IN BARCELONA

No.	Compound	Diagnostic ions (*m/z*)	Average concentration (ng/m^3)
79	9H-Fluoren-9-one	180	
80	*n*-Tetradecanoic acid[a]	285	
81	Diisobutyl phthalate	149	
82	1H-Phenalen-1-one	180	
83	*n*-Pentadecanoic acid	299	
84	*n*-Hexadecan-1-ol[a]	299	
85	Di-*n*-butyl phthalate	149	
86	9,10-Anthracenedione	180	
87	*n*-Hexadecenoic acid	311	3.8
88	*n*-Hexadecanoic acid	313	7.1
89	*n*-Octadecan-1-ol	327	
90	*n*-Octadecenoic acid	339	3.8
91	*n*-Octadecanoic acid	341	4.7
92	Benzyl butyl phthalate	149	
93	Methyl dehydroabietate	239	
94	Dioctyl hexanedioate	370	
95	Di-*n*-octyl phthalate	149	
96	1-*n*-Hexadecenoylglycerol[a]	369	
97	1-*n*-Hexadecanoylglycerol	371	
98	*n*-Tetracosan-1-ol	412	9.5
99	1-*n*-Octadecenoylglycerol	397	
100	1-*n*-Octadecanoylglycerol	399	
101	*n*-Hexacosan-1-ol	440	12
102	*n*-Octacosan-1-ol	468	9.5
103	Cholest-5-en-3β-ol	129	16
104	24-Methylcholest-5-en-3β-ol	129	4.0
105	24-Ethylcholesta-5,22-dien-3β-ol	484	11
106	*n*-Triacontan-1-ol	496	5.0
107	24-Ethylcholest-5-en-3β-ol	129	19
108	*n*-Dotriacontan-1-ol	524	9.8

[a] Acids and alcohols analysed as trimethylsilyl ether derivatives.

The fatty acids constitute another major group of solvent-extractable compounds present in these aerosol fractions. They constitute distributions of even-carbon-numbered C_{14}–C_{18} saturated straight-chain homologues occurring together with *n*-hexadecenoic (87) and *n*-octadecenoic (90) acids. The presence of these fatty acid mixtures in atmospheric samples is generally attributed to inputs from microorganisms [23]. These fatty acids are present in unbound form. However, the saturated and unsaturated C_{16} and C_{18} *n*-alkanoic homologues, the major free fatty acids, show a similar composition to that of the monoacylglycerols. This parallelism is in agreement with their presumed microorganism origin and suggest that the free fatty acids may have originated from hydrolysis of these monoglycerides. However, inputs related to decomposition of di- or triglycerides cannot be excluded because the analytical methods used in this study were not aimed at their identification.

In contrast with these distributions, the occurrence of methyl dehydroabietate (93) is representative of contributions from coniferous vegetation. This compound can be transformed into retene by

TABLE VI

RETENTION INDICES OF THE MAJOR *n*-ALKAN-1-OLS AND STEROLS IN THE SEMI-POLAR COLUMNS LISTED IN TABLE I

Retention indices relative to *n*-alkan-1-ols.

Column	*n*-Octacosan-1-ol	Cholest-5-en-3β-ol	*n*-Tridecan-1-ol	β-Sitosterol
DB-5	2800.0	2819.7	3000.0	3020.3
SE-52	2800.0	2803.6	3000.0	2998.2
CP Sil 8 CB	2800.0	2776.9	3000.0	2974.1
SE-54	2800.0	2782.5	3000.0	2985.3
HP-5	2800.0	2774.4	3000.0	2969.1

photochemical oxidation in the atmosphere [15], a hydrocarbon that has also been identified (47 in Table III).

Important changes in relative retention are again observed when analysing the polar fraction with different capillary columns. These changes again concern the elution order of linear and polycyclic molecules, namely the *n*-alkan-1-ols and the sterols (see Table VI and Fig. 4). Thus, in the DB-5 column, the trimethylsilyl (TMS) ethers of *n*-octacosan-1-ol and *n*-triacontan-1-ol elute before than the TMS ethers of cholest-5-en-3β-ol and β-sitosterol, respectively, whereas in the CP-Sil 8 CB, SE-54 and HP-5 columns the elution order is the reverse. The TMS ethers of these *n*-alkan-1-ols and sterols co-elute in the SE-52 column. These selectivity effects parallel, in fact, the elution order changes observed in fraction 2 and define three groups of columns, corresponding to early (DB-5), intermediate (SE-52) or late (CP-Sil 8 CB, SE-54, HP-5) elution of the linear compounds in relation to the polycyclic molecules.

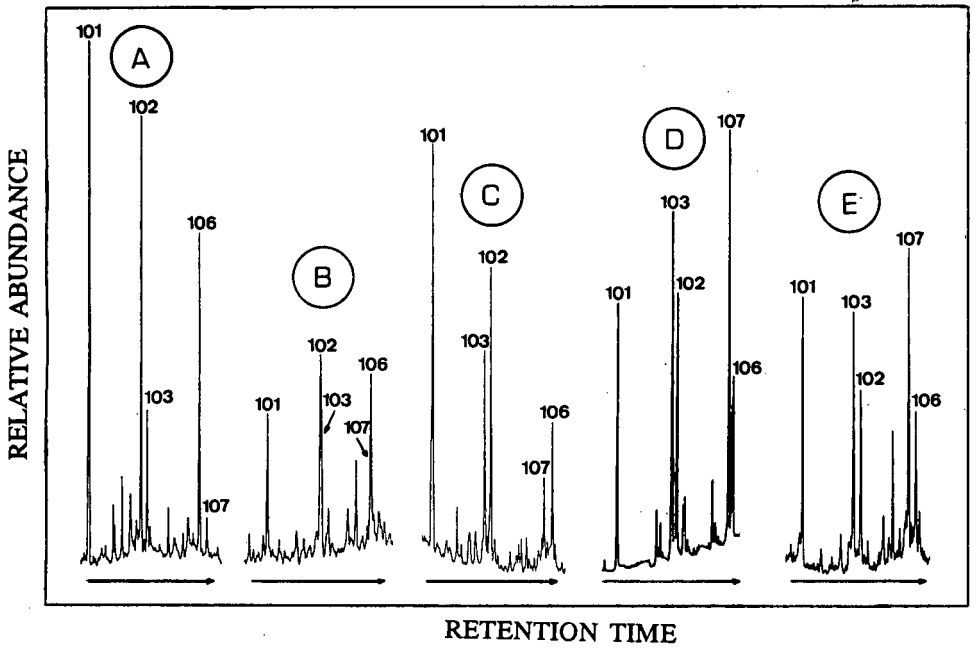

Fig. 4. GC profiles showing the elution order of the TMS ether derivatives of *n*-alkan-1-ols and Δ^5-sterols in the semi-polar columns described in Table I. (A)–(E) as in Fig. 2. Peak numbers refer to Table V.

CONCLUSIONS

Petrogenic hydrocarbons are the dominant products in the GC profiles of the solvent-extractable organic fractions from large and small airborne particles collected in urban areas. They are essentially represented by an UCM of hydrocarbons, *n*-alkanes with no odd–even carbon number predominance, 17α(H),21β(H)-hopanes, and parent and alkylated phenanthrenes and chrysenes/triphenylenes. Pyrolytic products, namely parent PAHs eluting between fluorene and coronene, constitute the second major quantitative group of molecules that can be recognized in these chromatographic traces. The third major group of anthropogenic compounds is related to the plastiziers, being constituted by phthalates and related esters.

The largest group of biogenic products corresponds to higher plant lipids and constitute distributions of straight-chain and polycyclic molecules, including even-carbon-numbered *n*-alkan-1-ols, 24-ethylcholent-5-en-3β-ol, retene and methyl dehydroabietate. Other biogenic sources leaving a fingerprint in these chromatograms are related to microbial contributions. They can be recognized by the distributions of predominant fatty acids and 1-*n*-alkanoyl and 1-*n*-alkenoyl glycerols.

Important changes in relative retention are observed on analysis of these organic compounds with different semi-polar columns. These changes essentially concern the elution order of linear *vs.* polycyclic molecules of similar retention and define three groups of columns. The first group, DB-5, corresponds to the elution of linear (squalene, C_{28}/C_{30} *n*-alkan-1-ol TMS ethers) before polycyclic compounds (benzopyrenes, cholest-5-en-3β-ol and β-sitosterol TMS ethers). The second (SE-52) represents an intermediate situation in which squalene elutes between benzo[*e*]pyrene and benzo[*a*]pyrene and the TMS ethers of the C_{28}/C_{30} linear alcohols co-elute with those of the C_{27}/C_{29} Δ^5-sterols. Finally, the third group (CP-Sil 8 CB, SE-54, HP-5) exhibits a reverse elution order.

REFERENCES

1 R. C. Pierce and M. Katz, *Environ. Sci. Technol.*, 19 (1975) 347.
2 L. Van Vaeck and K. Van Cauwenberghe, *Atmos. Environ.*, 12 (1978) 2229.
3 P. Pistikopoulos, H. M. Wortham, L. Gomes, S. Masclet-Beyne, E. Bon Nguyen, P. A. Masclet and G. Mouvier, *Atmos. Environ.*, 24A (1990) 2573.
4 M. Aceves, J. O. Grimalt, J. Sunyer, J. M. Anto and Ch. E. Reed, *J. Allergy Clin. Immunol.*, 88 (1991) 124.
5 M. Aceves, J. O. Grimalt, J. Albaiges, F. Broto, L. Comellas and M. Gassiot, *J. Chromatogr.*, 436 (1988) 503.
6 B. R. T. Simoneit, *Atmos. Environ.*, 18 (1984) 51.
7 C. V. Hampton, W. R. Pierson, D. Schuetzle and T. M. Harvey, *Environ. Sci. Technol.*, 17 (1983) 699.
8 J. Albaiges and X. Guardino, *Chromatographia*, 13 (1980) 755.
9 J. W. Farrington and P. A. Meyers, in G. Eglinton (Editor), *Environmental Chemistry*, Vol. 1, Chemical Society, London, 1975, p. 109.
10 R. E. LaFlamme and R. A. Hites, *Geochim. Cosmochim. Acta*, 42 (1978) 289.
11 B. R. T. Simoneit, *Int. J. Environ. Anal. Chem.*, 29 (1985) 203.
12 G. Grimmer and A. Hildebrandt, *Zentralbl. Bakteriol. Parasitenkd. Infektionskr. Hyg. Abt. 1: Orig. Reihe B*, 161 (1975) 104.
13 G. Grimmer, J. Jacob, K.-W. Naujack and G. Dettbarn, *Anal. Chem.*, 55 (1983) 892.
14 E.-A. Ratajczak, E. Ahland, G. Grimmer and G. Dettbarn, *Staub-Reinhalt. Luft*, 44 (1984) 505.
15 B. R. T. Simoneit and M. Mazurek, *Atmos. Environ.*, 16 (1982) 2139.
16 C. W. Bird and J. M. Lynch, *Chem. Soc. Rev.*, 3 (1971) 309.
17 M. L. Lee, D. L. Vassilaros, C. M. White and M. Novotny, *Anal. Chem.*, 51 (1979) 768.
18 D. J. Russel and B. McDuffie, *Int. J. Environ. Anal. Chem.*, 15 (1983) 165.
19 R. Ritsema, W. P. Cofino, P. C. M. Frintrop and U. A. Th. Brinkman, *Chemosphere*, 18 (1989) 2161.
20 G. Eglinton and R. Hamilton, *Science*, 156 (1967) 1322.
21 B. A. Knights, *Phytochemistry*, 7 (1968) 1707.
22 E. Kvanta, *Acta Chem. Scand.*, 22 (1968) 2161.
23 B. R. T. Simoneit, R. E. Cox and L. J. Standley, *Atmos. Environ.*, 22 (1988) 983.

Journal of Chromatography, 607 (1992) 271–278
Elsevier Science Publishers B.V., Amsterdam

CHROM. 24 317

Simplex optimization of the analysis of polychlorinated biphenyls

Application to the resolution of a complex mixture of congeners of interest on a single gas chromatographic column

B. Jiménez*

Instituto de Química Orgánica General, CSIC, Juan de la Cierva 3, 28006 Madrid (Spain)

J. Tabera

Instituto de Fermentaciones Industriales, CSIC, Juan de la Cierva 3, 28006 Madrid (Spain)

L. M. Hernández and M. J. González

Instituto de Química Orgánica General, CSIC, Juan de la Cierva 3, 28006 Madrid (Spain)

ABSTRACT

The modified sequential simplex method was applied to optimize the oven temperature programming of a single-column gas chromatographic procedure developed to determine polychlorinated biphenyl congeners in a mixture of technical Aroclors. Both the overall resolution of fourteen congeners of interest and the time of analysis were taken into account in the optimization. Successful separations of some clusters usually unresolved with a single column have been obtained.

INTRODUCTION

Polychlorinated biphenyls (PCBs) are ubiquitous environmental contaminants. They appear as complex mixtures of theoretically 209 congeners which exhibit wide differences in their toxic and biological effects.

Several studies have indicated that the toxic nature of technical PCB mixtures may be associated with the presence of trace levels of particular toxic PCB congeners having four or more chlorine atoms at both *para* and *meta* positions in the biphenyl rings but no chlorine atoms in *ortho* positions [1]. Among the twenty possible coplanar PCB congeners, 77, 126 and 169 (numbers from Ballsmiter and Zell [2]) were found to be the most toxic [1,3–5]. Recent quantitative structure–activity relationship (QSAR) studies indicated that not only non-*ortho*-chlorine-substituted PCBs but also a few mono- and di-*ortho* analogues of coplanar PCBs possess comparable toxic potential [6,7].

The complex composition of PCB mixtures in environmental samples is characterized by a large number of peaks detected by electron-capture detection (ECD) after elution from a capillary gas chromatographic (GC) column. The evaluation of

0021-9673/92/$05.00

their constituents is not yet possible for all peaks [8]. For accurate data, each congener to be determined should appear as a single peak, well resolved from other compounds.

Our objective was the development of a chromatographic method with a single BP-5 column that will resolve as completely as possible the set of fourteen selected congeners (Table I) from different complex matrices. The total resolution of these isomers is very difficult and involves a great experimental effort. In that situation, it is of great importance to apply a suitable optimization procedure for the simultaneous handling of experimental variables. The sequential simplex method [9] has been broadly recognized as a very efficient empirical optimization procedure [10,11] which can attain an optimum in a reduced number of experimental runs. This method has been successfully used in chromatographic research [12,13].

As a first step to attain our objective, in this work we optimized the chromatographic separation of the fourteen above-mentioned PCB congeners in a mixture of Aroclors of different chlorination grade by means of the modified sequential simplex method [14].

TABLE I

SET OF PCB CONGENERS SELECTED FOR ANALYSIS

Congener number[a]	Structure	Closely eluting congeners[b]
101	2,2',4,5,5'	90 (5)
77	3,3',4,4'	101 (5)
151	2,2',3,5,5',6	82 (5)
118	2,3',4,4',5	123 (5), 149 (6)
153	2,2',4,4',5,5'	105 (5), 132 (6)
105	2,3,3',4,4'	153 (5), 132 (6)
138	2,2',3,4,4',5'	160 (6), 158 (6)
126	3,3',4,4',5	129 (6), 178 (7)
167	2,3',4,4',5,5'	— — —
156	2,3,3',4,4',5	202 (8), 171 (7)
180	2,2',3,4,4',5,5'	— — —
169	3,3',4,4',5,5'	— — —
170	2,2',3,3',4,4',5	190 (7)
194	2,2',3,3',4,4',5,5'	— — —

[a] According to ref. 2.

[b] Chlorine numbers are given in parentheses.

EXPERIMENTAL

PCB samples

The PCB congeners for this study were selected on the bases of toxicity and/or abundance in environmental samples. A 1:1:1:1 (v/v) mixture of Aroclor 1242, 1248, 1254 and 1260 was chosen because their great similarity to environmental samples. In this mixture we identified all the congeners shown in Table I except 126 and 169 which were added in an equal but different mass than the others. All fourteen congeners were identified by comparison of their retention times with those of standards.

Capillary gas chromatography

All measurements were carried out on a Perkin-Elmer Model 8600 gas chromatograph equipped with a nickel-63 electron-capture detector. A fused-silica column (50 m × 0.22 mm I.D.) with a 0.25-μm film thickness of the chemically bonded phase BP-5 (5% phenyl–95% polymethylsiloxane) (SGE, Victoria, Australia) was used. The carrier gas (nitrogen) flow-rate was 40 ml/min. The oven temperature programme was subjected to optimization. The detector temperature was 300°C and the injector temperature (splitless mode) was 280°C.

Selection of variables

The temperature programming consisted of three stages. Based on previous experience, we considered the first, second and third oven temperatures and the second temperature gradient as the four variables to work with. In order to select the most influential of them to include in the optimization study, a fractional factorial 2^{4-1} experimental design [15] was performed as explained under Results and Discussion. Estimates of the main effect of each variable were calculated according to the equation

$$E(i) = \frac{1}{4}\sum_{j} X_{ij} Y_j \qquad (1)$$

where X_{ij} is the coded level (-1 for the low level and 1 for the high level) of the variable i in run j, and Y_j is the response value of run j.

The response function

The effect of modifying the experimental condi-

tions on the overall performance of the analytical method was evaluated in terms of the differences between the retention times of each chromatographic peak achievable in each analytical run. The time spent in the analysis was also taken into account. The response function was designed as a summation of inverse differences in retention times in order to magnify the influence of low values of those differences and so penalize bad resolutions. The inverse of analysis time is affected by a negative sign, so a longer analysis time leads to higher response values. The optimization of the chromatographic method is then equivalent to the minimization of the response function.

Several chromatographic response functions (CRFs) developed to assign a numerical value to the quality of each chromatogram, as is needed in empirical optimization studies, have been reported [16–18]. Most of them are based on criteria such as the peak-to-valley ratio, fractional peak overlap, separation factor or resolution, which require high-performance data treatment. When a sufficiently complex mixture is analysed, this data elaboration cannot be performed manually. Although we considered some of these CRFs, the complexity of our PCB mixture and the limitations of our GC equipment led us to formulate the response function (eqn. 2) in terms of retention time, a characteristic well measured in our chromatograms.

As we were interested in the fourteen PCB congeners shown in Table I, the summation of the response function was extended to fourteen terms. Each of these terms corresponds to the chromatographic peak of a selected PCB congener, and is the sum of two differences in retention time: that with the preceding peak and that with the following peak in the chromatogram. Some separations were more desirable than others owing to known special difficulties in achieving them or to special significance of the congener involved (toxicity, abundance, etc.), therefore the influence of each difference in retention time over the response function was modulated by means of weighing factors. Another weighting factor was applied to the term accounting for analysis time in order to equilibrate the reward for high resolutions with the penalty for long analysis time. Our scope was to consider more valuable the attainment of new peaks or better resolutions than shortening of the analysis time. Therefore, the weighing factor of the term accounting for the time of analysis was fixed in order to affect only the ranking between chromatograms with not very different resolution performances. The response function designed for this study is

$$FR = \sum_{i=1}^{14} \left(\frac{p_{i1}}{t_{r_i} - t_{r_{i-1}}} + \frac{p_{i2}}{t_{r_{i+1}} - t_{r_i}} \right) - \frac{q}{t_f} \qquad (2)$$

where t_{r_i}, $t_{r_{i-1}}$ and $t_{r_{i+1}}$ are the corrected retention times of the ith selected peak, its preceding peak and its following peak, respectively, t_f is the final analysis time, p_{i1} (p_{i2}) are the weighing factors assigned to the differences in retention time between each selected peak and the preceding (following) peak, respectively, and q is the weighing factor assigned to the final analysis time. The value of q was fixed at 6000, as will be explained later. The weighing factors p_{i1}, p_{i2} used in this work are shown in Table II.

Evolution of the response function

Throughout the optimization process, new peaks appeared in some chromatograms. When these peaks were contiguous with the fourteen selected ones, they could emanate from the PCBs of interest and we considered them as previously co-eluting with these PCBs. Once such a peak had appeared it could no longer be ignored, and any other chromatogram without this peak must be evaluated as not properly resolving the selected congener. The values $t_{r_{i-1}}$ and/or $t_{r_{i+1}}$ in eqn. 2 corresponded to the new peak/peaks and, if these do not exist, the differences in retention time, $t_{r_i} - t_{r_{i-1}}$ and/or $t_{r_{i+1}} - t_{r_i}$, would be equal to zero[a]. Therefore, the occurrence of new peaks contiguous with any of those of the PCB congeners of interest forced the recalculation of the response value of old chromatograms in order to make good comparisons. Therefore even though the expression for the response function did not vary, the terms included in it did vary. As far as we know, no simplex optimizations with such an evolutionary response function have been reported previously. This adaptation of the

[a] In these cases, to avoid "division by zero error" when running the calculation program, a very small value of 0.01 was assigned to these differences.

TABLE II

WEIGHING FACTORS ASSIGNED TO THE PEAKS CONTIGUOUS WITH THE SELECTED PCB CONGENERS

PCB congener	p_{i1}	p_{i2}
101	1	1
77	3	1
151	1	1
118	1	4
153	1	2
105	2	1
138	1	3
126	1	3
167	2	1
156	4	1
180	3	3
169	1	1
170	1	2
194	1	1

response function to new knowledge obtained from experimentation could be valuable for other workers.

Simplex optimization

The sequential simplex method [9] begins with a patterned set of experiments in all the variables of interest. The pattern is an equilateral triangle in two variables, a regular tetrahedron in three variables or a simplex (*i.e.*, a regular multi-dimensional figure) in four or more variables. The effects on the performance of the process of changes in operating variables are measured according to a previously defined criterion or response function; from the results, the directions in which further changes should be made to obtain an improvement in process performance are inferred. The resulting new values of the variables are then tested and the procedure is repeated until no further improvement can be achieved.

The initial experimental design was established according to Spendley *et al.* [19]. Physical values of factors were calculated from their mathematical co-ordinates by using

$$x_{phys} = x_0 + x_{math} \cdot SOC \quad (3)$$

where x_{phys} is the physical value of the variable x, x_{math} the corresponding mathematical coordinate, x_0 its base level (starting physical value) and SOC the step of change of each variable.

The initial and successive simplex were moved in the directions given by the rules of movement of the modified simplex method [14] and the corresponding responses were subsequently evaluated. In all instances, two replicates of each analysis were carried out. The coordinates of each new vertex were calculated according to the expression

$$V_i^* = C + \alpha(C - V_i) \quad (4)$$

where V_i^* is the new vertex, C the centroid of the retained vertices in the movement, V_i the rejected vertex and α a factor with different values depending on whether a reflection ($\alpha = 1$), an expansion ($\alpha > 1$) or a contraction ($\alpha < 1$) was performed.

It should be pointed out that the self-directing nature of this optimization method makes possible a boundary violation (*i.e.*, a movement outside the feasible experimental conditions); then, the corresponding vertex must be rejected without experimentation and so the simplex is subsequently forced to move back inside the boundaries by applying an $\alpha = -0.5$ factor [20].

RESULTS AND DISCUSSION

Table III summarizes the experiments carried out and the results obtained in the fractional factorial 2^{4-1} experimental design. The experimental runs

TABLE III

EXPERIMENTAL RUNS, RESULTS AND ESTIMATES OF MAIN EFFECTS FOR THE 2^{4-1} FRACTIONAL FACTORIAL DESIGN

Run	*T*1 (°C)	*T*2 (°C)	*R*2 (°C/min)	*T*3 (°C)	Response
1	80	160	1	230	28.00
2	120	160	1	270	23.00
3	80	200	1	270	30.10
4	120	200	1	230	33.00
5	80	160	3	270	735.60
6	120	160	3	230	36.10
7	80	200	3	230	320.80
8	120	200	3	270	1007.30

Main effects:
$E(T1) = -4$; $E(T2) = 142$; $E(R2) = 497$; $E(T3) = 345$

TABLE IV

VARIABLES INCLUDED IN THE SIMPLEX OPTIMIZATION

Variable	Base level	Step of change
2nd oven temperature, *T*2 (°C)	160	5
2nd temperature gradient, *R*2 (°C/min)	1	1
3rd oven temperature, *T*3 (°C)	270	5

were carried out in randomized order. Each response value was the average of two replicates. Because the 2^{4-1} design is of resolution IV, its confounding structure leads to estimation of first-order (main) effects together with third-order (3rd interactions) effects. Hence the estimation of main effects is of high precision by assuming, as is usually done, that the effects of interactions of order higher than 2 are negligible. The response function used was eqn. 2, which was tested against these first experimental results. The value of weighing factor q was varied in the testing, and finally adjusted to 6000 in order to obtain a ranking of response values as

TABLE V

EXPERIMENTAL RUNS AND RESULTS FOR THE SIMPLEX OPTIMIZATION

Vertex No.	Simplex No.	Retained vertices	Experimental variables levels			Response[a]			
			*T*2 (°C)	*R*2 (°C/min)	*T*3 (°C)	Y_1	Y_2	Y_3	Y_4
1	1	–	160	1.0	270	26.50	622	721	1117
2	1	–	165	1.2	271	34.25	629	728	1123
3	1	–	161	1.9	271	63.49	655	754	1145
4	1	–	161	1.2	275	33.51	628	727	1122
5	2	1,2,4	163	0.4	273		20	119	518[b]
6[c]	2	1,2,4	163	−0.4[d]	273		–	–	–
7	3	1,4,5	158	0.5	274		320	420	818[b]
8[e]	4	1,5,7	159	0.01	270			–	–
9	4	1,5,7	161	0.9	273			621	1017
10	5	5,7,9	161	0.2	277				304[b]
11[c]	5	5,7,9	161	−0.2[d]	280				–
12[e]	6	5,7,10	160	−0.2	275				–
13	6	5,7,10	161	0.6	274				
14[e]	7	5,7,10	160	0.07	275				–
15	7	5,7,10	161	0.5	274				611
16	8	5,10,15	165	0.2	275				305[b]
17[e]	9	5,10,16	165	0.02	276				–
18	9	5,10,16	162	0.4	275				413
19	10	10,16,18	162	0.2	278				305
20[e]	11	10,16,19	163	0.004	279				–
21	11	10,16,19	162	0.30	276				105[b]
22	12	10,16,21	163	0.30	273				110
23	13	10,21,22	159	0.30	275				109
24	14	21,22,23	162	0.40	273				411
25[f]	14	21,22,23	161	0.30	276				109

[a] Successive responses originating from the appearance of new peaks contiguous with the selected ones in vertices Nos. 5, 9 and 10.
[b] Value checked in the $(k + 1)$th simplex from the first occurrence of the vertex.
[c] Obtained from expansion $\alpha = 2$.
[d] Vertex not better than preceding $\alpha = 1$ vertex. Rule of expansion failure rather than rule of boundary violation applied. Vertex excluded from the new simplex.
[e] Boundary violation. Impossible to apply temperature gradients below 0.1°C/min. Next vertex obtained with $\alpha = -0.5$.
[f] Obtained from contraction $\alpha = -0.5$.

coincident as possible with that obtained from a careful inspection of chromatograms. The estimated main effects are also included in Table III. From their values, the variables $T2$, $R2$ and $T3$ were selected to be simplex optimized. Base levels and steps of change of these variables are shown in Table IV. The first oven temperature, $T1$, was set at 120°C. Previously, the first temperature gradient, $R1$, was set to 20°C/min.

Table V summarizes the sets of experimental values tested throughout the optimization procedure. The starting point (vertex No. 1) is that of the best results in the factorial design. Values obtained for the response function (eqn. 2) are included in the response columns of Table V. As explained previously, these response values were recalculated each time a new peak contiguous with the fourteen selected peaks appeared. The decisions concerning the simplex movements were based, at any time, on the actual values of response; however, no discrepancies have been detected with the movements that would be performed if definitive response (Y_4) were available from the starting point. This agreement in ranking has made easy the optimization progress with evolutionary response function. If a change in the response used would cause a change in the order of desirability of vertices involved in already performed movements, some unfavourable situations could occur. The optimum could be attained, but some erratic movements would be carried out with the older response functions and a less economical search would be made.

The optimization study was initiated by performing the first four experiments defined in Table V, which constitute the initial simplex. The assessment of the values obtained for the response function in each analysis allows the worst vertex (No. 3) to be rejected. Then, a new simplex was formed with the retained vertices and a new one (No. 5) resulting from the mirror image ($\alpha = 1$) of the rejected vertex. As the response at vertex 5 is better than the best of the preceding simplex (vertex No. 1), an expansion is indicated ($\alpha = 2$), and the new simplex is formed with the recently obtained vertex No. 6 instead of No. 5. In vertex No. 8 a boundaryviolation occurred in $R2$ (no values lower than 0.1°C/min can be used); then the response at vertex No. 8 was considered as the worst one without experimentation, and a negative contraction ($\alpha = -0.5$) was carried out to obtain vertex No. 9. The procedure must be repeated to move from one simplex to another by rejecting the worst observation and by selecting an adequate α value.

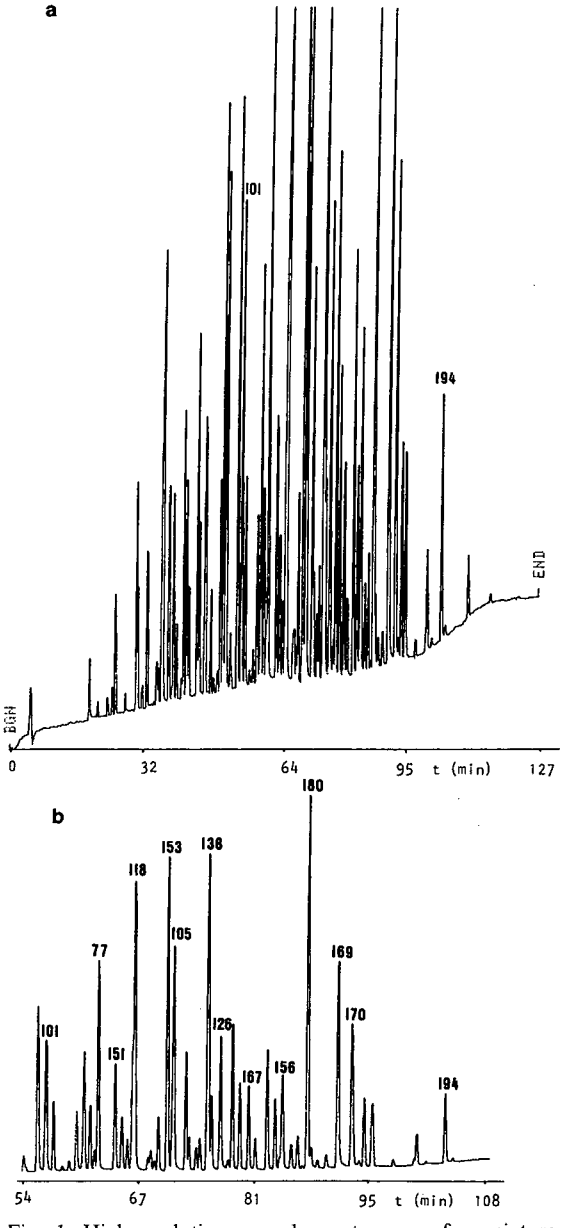

Fig. 1. High-resolution gas chromatogram of a mixture of Aroclors with PCBs 126 and 169 added. Analysis conditions of the simplex starting point (vertex No. 1). (a) Whole chromatogram. (b) Detail of the 101–194 zone.

Searching was stopped after vertex 25 because the responses in all the vertices of the last simplex (21, 22, 23 and 25) and their experimental conditions were very similar, thus indicating that a stable region had been reached and no further improvement could be expected. The calculation of a tentative new movement leads to a set of experimental values very close to that of the above mentioned vertices, which confirms the assumption of reaching a stable region. Hence, we can accept that an optimum has been attained at vertex No. 21. The value of the temperature gradient for this optimum was 0.3°C/min, which gave an analysis time of 240 min.

As far as the resolution of the PCB congeners is concerned, the results can be summarized as follows:

(a) Isomers where the peak elutes as a single peak (180, 169 and 194). Congener 180 appears in the chromatogram (Fig. 2) as a peak well resolved from the adjacent ones. This peak can be unequivocally identified in complex chromatograms because it is a characteristic large peak in commercial mixtures and environmental samples [8]. Peak 169 provides useful information on the chromatographic determination of corresponding congeners. It should be noted that this isomer was added to the mixture of Aroclors because of their toxicological interest. Despite its low ECD response, isomer 194 has been determined without ambiguity problems.

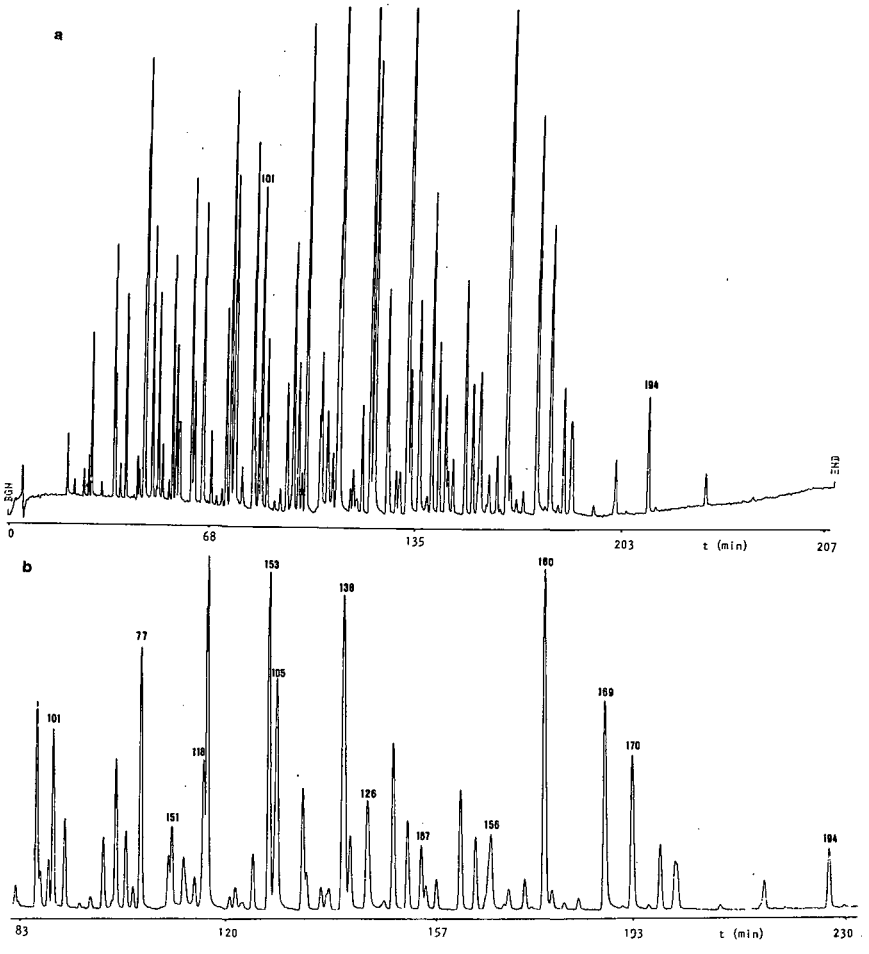

Fig. 2. High-resolution gas chromatogram of a mixture of Aroclors with PCBs 126 and 169 added. Analysis conditions of the simplex optimum (vertex No. 21). (a) Whole chromatogram. (b) Detail of the 101–194 zone.

(b) Isomers co-eluting that were resolved in this work as a single peak (see Figs. 1b and 2b). The peak corresponding to congener 101 that co-elutes with 90 [8] was split into two peaks after the optimization of the chromatographic conditions. The same splitting for the peak preceding 101 can be observed. On the left of the peak corresponding to congener 151 a new peak has appeared. On the basis that 151 is known as a congener co-eluting with isomer 82, the new peak could be tentatively identified as the congener 82. However, conclusions on the compositions of two new peaks mentioned above require the availability of Nos. 90 and 82 as reference compounds. Very good resolution was attained for the cluster 153/105 that usually appear in the literature as a set unresolved with columns similar to BP-5. The isomer 77, with four chlorine atoms, co-elutes with the pentachlorobiphenyl 110. This problem has been successfully resolved using GC–mass spectrometry (GC–MS) in the selected ion monitoring. MS allows an unambiguous identification of the two isomers.

(c) Isomers with very closely eluting congeners. Peak 118, known to co-elute with 123 and 149, is only split into two peaks (Figs. 1b and 2b). The situation is similar for the peak corresponding to congener 138, which co-elutes with 160 and 158, and for which we have obtained only two peaks. From Fig. 2b it could be observed that congener 156 has a marked trend to split into two peaks, but at present the situation remains unresolved for the cluster 156/202/171 [21]. Fortunately, this situation could be easily resolved by GC–MS, as we have observed for isomer 77, because the congeners have different chlorine numbers. In spite of the fact that isomer 126 co-elutes with 129 and 178, the peak in this work consists of 126 only, because this was added individually to the mixture. A similar situation occurs with congener 169. Hence, from this work, information could be obtained on the behaviour of two toxic coplanar congeners, 126 and 169, when analysing complex samples. The peak corresponding to congener 170, which co-elutes with 190, could be considered as mainly due to 170 because of its larger proportion in commercial Aroclors.

Finally, an interesting observation can be derived for congener 167 from this work. From Fig. 2b, it can be seen that the peak that appeared as a single one in the initial chromatogram (Fig. 1b) has been split into two peaks after the optimization of the chromatographic conditions. We have not found in the literature any references to co-elution for this congener. Hence confirmation by MS and using another column with different polarity is required for this new peak, in order to obtain a deeper knowledge of the behaviour of this toxic coplanar congener.

REFERENCES

1 S. Safe, *CRC Crit. Rev. Toxicol.*, 13 (1984) 319.
2 K. Ballsmiter and M. Zell, *Fresenius' Anal. Chem.*, 302 (1980) 20.
3 H. Yoshimura, I. Wada, N. Koga, K. Nagata, Y. Yamauchi, S. Yoshihara and O. Kamata, *Fukuoka Acta Med.*, 72 (1981) 149.
4 N. Kannan, S. Tanabe, M. Ono and R. Tatsukawa, *Arch. Environ. Contam. Toxicol.*, 18 (1989) 850.
5 S. Tanabe, N. Kannan, T. Wakimoto and R. Tatsukawa, *Int. J. Environ. Anal. Chem.*, 29 (1987) 199.
6 A. Parkinson, S. Safe, L. W. Robertson, P. E. Thomas, D. E. Ryan, L. M. Reik and W. Levin, *J. Biol. Chem.*, 258 (1983) 5967.
7 S. Safe, S. Bandiera, T. Sawyer, L. Robertson, L. Safe, A. Parkinson, P. E. Thomas, D. E. Ryan, L. M. Reik, W. Levin, M. Denomme and T. Fujita, *Environ. Health Perspect.*, 60 (1985) 47.
8 J. C. Duinker, D. E. Schultz and G. Petrick, *Mar. Pollut. Bull.*, 19 (1988) 19.
9 C. Hendrix, *CHEMTECH*, August (1980) 488.
10 J. C. Berridge, *Anal. Chim. Acta*, 191 (1986) 243.
11 R. J. Fisher, *Food Technol.*, 43 (1989) 90.
12 J. Tabera, G. Reglero, M. Herraiz and G. P. Blanch, *J. High Resolut. Chromatogr.*, 14 (1991) 392.
13 J. Tabera, B. Jiménez, L. M. Hernández and M. J. González, *J. Chromatogr.*, 557 (1991) 481.
14 J. A. Nelder and R. Mead, *Comput. J.*, 7 (1965) 308.
15 G. E. P. Box and N. R. Draper, *Empirical Model-Building and Response Surfaces*, Wiley, New York, 1987, pp. 143–167.
16 H. J. G. Debets, B. L. Bajema and D. A. Doornbos, *Anal. Chim. Acta*, 151 (1983) 131.
17 P. T. Schoenmakers, *Optimization of Chromatographic Selectivity*, Elsevier, Amsterdam, 1986, pp. 119–169.
18 J. A. Crow and J. P. Foley, *Anal. Chem.*, 62 (1990) 378.
19 W. Spendley, G. R. Hext and F. R. Himsworth, *Technometrics*, 4 (1962) 441.
20 S. L. Morgan and S. N. Deming, *Anal. Chem.*, 46 (1974) 1170.
21 D. E. Schultz, G. Petrick and J. C. Duinker, *Environ. Sci. Technol.*, 23 (1989) 852.

Journal of Chromatography, 607 (1992) 279–286
Elsevier Science Publishers B.V., Amsterdam

CHROM. 24 037

Gas chromatographic–mass spectrometric characterization of polycyclic aromatic hydrocarbon mixtures in polluted coastal sediments

Lourdes Canton

Department of Applied Chemistry, College of Chemistry, University of the Basque Country, P.O. Box 1072, 20080-Donostia (Spain)

Joan O. Grimalt*

Department of Environmental Chemistry (CID–CSIC), Jordi Girona 18, 08034-Barcelona (Spain)

ABSTRACT

A gas chromatographic–mass spectrometric (GC–MS) study of the polycyclic aromatic hydrocarbon (PAH) composition of a series of 72 marine sediments collected from the Guipuzcoan Coast (Bay of Biscay, Spain) showed three end-member distributions, one related to pyrolytic soot contributions (type A), another to combined paper mill effluents and soot inputs (type B) and the third to petrogenic residues (type C). The detailed composition of each of these end-member mixtures is given. Further examination of the PAH extracts by GC–negative ion chemical ionization MS illustrated several previously unreported selectivity effects such as enhancement of the parent PAHs eluting with longer retention times and the increased response factor of the alkyl homologues corresponding to the *m/z* 252, 276 and 302 hydrocarbons.

INTRODUCTION

Many polycyclic aromatic hydrocarbons (PAHs) are carcinogenic, mutagenic and/or co-carcinogenic [1,2]. These features and the fact that these toxic species are spread extensively in the environment have led to PAH monitoring being a priority task in many health risk assessment studies.

Among other environments, PAHs commonly occur in polluted coastal areas [3–7] as a result of intentional or accidental oil spillages, combustion of fossil fuels, waste discharges, automobile exhausts, forest fires, etc. The evaluation of the impact of these pollutants on marine life requires the assessment of concentrations and the recognition of their sources. In this respect, sediments are particularly useful for the identification of the predominant contributions because they act as pollutant sinks and provide an integrated picture of the events taking place in the water column. Thus, the analysis of these sedimentary mixtures of PAHs allows the characterization of the chronic inputs into the areas of concern and their corresponding sources.

Many techniques have been used for the analysis of environmental samples for PAHs, but no reported method separates and resolves adequately the entire PAH fraction on a microgram scale from samples that contain a very large excess of non-hydrocarbons. Gas chromatography (GC) coupled with mass spectrometry (GC–MS) is the technique that has provided the most conclusive and detailed data, and has been applied to the study of the composition of standard PAH mixtures such as coal extracts [8–10] and atmospheric particulates [11–15]. PAHs in sediments have been comparatively less studied and less information is available on the PAH mixtures defining the input sources in this environmental compartment.

We have performed an extensive study of the hy-

0021-9673/92/$05.00

drocarbon pollutants along the Guipuzcoan Coast (Bay of Biscay, Spain). Among other aspects, this study encompassed the determination of PAH distributions corresponding to sediments collected in front of the discharge sites of six rivers (Bidasoa, Oria, Oyarzun, Urumea, Urola and Deba) along radials encompassing three water depths (10, 20 and 50 m) and four replicates (July 1986, November 1986, February 1987 and May 1987). The resulting PAH sedimentary mixtures were analysed by GC using different detectors and by GC–MS, which allowed the characterization of diverse end members corresponding to very dominant single pollutant inputs. The detailed composition of these sedimentary end members is described is this paper.

In addition to the usual electron impact mode (EI), GC–MS analyses of selected samples were performed using negative-ion chemical ionization (NICI), which provided several interesting selectivity effects. The usefulness of NICI for the description of sedimentary PAHs is also considered.

EXPERIMENTAL

Materials

Pestipur-grade *n*-hexane and methanol were purchased from SDS (Peypin, France), Resi-analyzed grade dichloromethane from Baker (Phillipsburg, NJ, USA), analytical-reagent grade acetone from Carlo Erba (Milan, Italy), analytical-reagent grade hydrochloric acid (25%), neutral silica gel (Kieselgel 40, 70–230 mesh), alumina (aluminium oxide 90 active, 70–230 mesh) and copper from Merck (Darmstadt,Germany), potassium hydroxide from Fluka (Buchs, Switzerland) and Soxhlet thimbles from Schleicher and Schüll (Dassel, Germany).

Potassium hydroxide was cleaned by sonication in dichloromethane Silica gel, alumina and the Soxhlet thimbles were extracted with dichloromethane–methanol (2:1, v/v) in a Soxhlet apparatus for 24 h. After solvent evaporation, the silica and alumina were heated for 12 h at 120 and 350°C, respectively. A total of 5% (w/w) of Milli-Q-grade water was then added to the chromatographic adsorbents for deactivation. Copper was activated with two rinses with 10% (w/w) hydrochloric acid (5 min each) and prepared for sample desulphurization by a series of successive rinses using Milli-Q-grade water, acetone and *n*-hexane (two rinses with each).

All organic solvents were distilled on a 1-m packed column (Raschig) equivalent to twelve theoretical plates, with a reflux ratio of 12:1. The purity of the solvents was checked by concentrating under vacuum 100 ml of solvent to 10 μl for GC analysis. Blank requirements were as follows: splitless injection of 2.5 μl should result in chromatograms with no unresolved GC envelope and only very few peaks, representing up to 1 ng in terms of their flame ionization detector response. This threshold, under the above dilution factor, is equivalent to 0.08 ng/g when referred to 30 g of sediment.

Sampling, extraction and fractionation

Surface sediments were taken by gravity coring from the R/V Elorrio and stored at −20°C in the dark. The upper 3 cm were cut prior to analysis and Soxhlet extracted with 150 ml of dichloromethane–methanol (2:1) for 36 h. The extract was vacuum evaporated to 2 ml and hydrolysed overnight with 35 ml of 6% potassium hydroxide–methanol. The neutral fraction was recovered with *n*-hexane (3 × 30 ml) and desulphurized with activated copper. The volume of this fraction was again vacuum evaporated to 0.5 ml and fractionated by column chromatography according to previously established methods [16]. A column filled with 8 g each of 5% water-deactivated alumina (top) and silica (bottom) was used. The PAHs were collected in a third fraction of 40 ml of dichloromethane–*n*-hexane (20:80) after elution with 20 ml of *n*-hexane (first fraction) and dichloromethane in *n*-hexane (10:90) (second fraction). These PAH fractions were vacuum and nitrogen concentrated almost to dryness and the residues were dissolved in *n*-hexane.

Instrumental analysis

All samples were analysed by GC with a Perkin-Elmer Model 8310 instrument equipped with a split–splitless injector and with flame ionization detection (FID). The separation was carried out on a 30 m × 0.32 mm I.D. SPB-5 (film thickness 0.25 μm) fused-silica capillary column (Supelco, Bellefonte, PA, USA). Injections were made in the splitless mode (split valve closed for 48 s; hot needle technique) with the column held at 60°, then heated to 300°C at 6°C/min. The carrier gas was hydrogen (0.5 m/s linear velocity). The injector and detector were maintained at 300 and 330°C, respectively. Ni-

trogen was used as make-up gas (30 ml/min). The detector gas flows were hydrogen 30 ml/min and air 300 ml/min.

Selected samples were analysed by GC with a Hewlett-Packard Model 5890A chromatograph equipped with a split–splitless injector and with electron-capture detection (ECD). The chromatographic conditions were the same as described above except that helium was used as the carrier gas.

Selected samples were also analysed by GC–MS using a Hewlett-Packard Model 5995 instrument coupled with an HP-300 data system. The mass spectrometer temperatures were as follows: transfer line, 300°C; ion source, 200°C; and analyser, 230°C. Data were acquired in the electron impact (EI) mode (70 eV), scanning from 50 to 650 mass units at 1 s per decade. Helium was used as the carrier gas and the other chromatographic conditions were the same as described above.

Alternatively, some samples were analyzed by GC–MS using a Hewlett-Packard Model 5998A instrument coupled with an HP-300 data system. Negative ions were recorded in the chemical ionization mode (NICI) [reagent gas methane, 1.5 Torr (199.98 Pa)]. The mass spectrometer temperatures were as follows: transfer line, 300°C; ion source 150°C; and analyser 130°C. The scan mode and chromatographic conditions were the same as described for GC–EI-MS.

Quantification

Compound identification was based on the GC–MS data and on co-injection with authentic standards. The predominant hydrocarbons were measured from the GC profiles using an external standard containing phenanthrene, anthracene, fluoranthene, benz[*a*]anthracene, retene, benzo[*a*]pyrene, perylene, indeno[1,2,3-*cd*]pyrene, benzo[*ghi*]-perylene, dibenzo[*a,h*]anthracene and coronene. The unresolved complex mixture (UCM) of PAHs was integrated with a digital planimeter connected to a Hewlett-Packard Model 86 microprocessor and quantified according to the average response factor of phenanthrene, fluoranthene, benzo[*a*]pyrene and benzo[*ghi*]perylene. Samples and standards were repeatedly injected until less than 3–5% dispersion in the area measurements was obtained.

RESULTS AND DISCUSSION

Identification of PAH sources

Three main end-member PAH distributions were found in the sediments corresponding to the 72 samples considered in this study. Their composition is represented in Fig. 1 by the corresponding GC–MS total ion current traces. Table I gives the list of the peaks indentified in these samples and Table II shows the concentrations of the predominant PAHs.

Sample A is a sediment collected in May 1987 at a water depth of 10 m in the Deba transect. Its PAH distribution is that most abundantly found on the Guipuzcoan coast. Phenanthrene, fluoranthene, py-

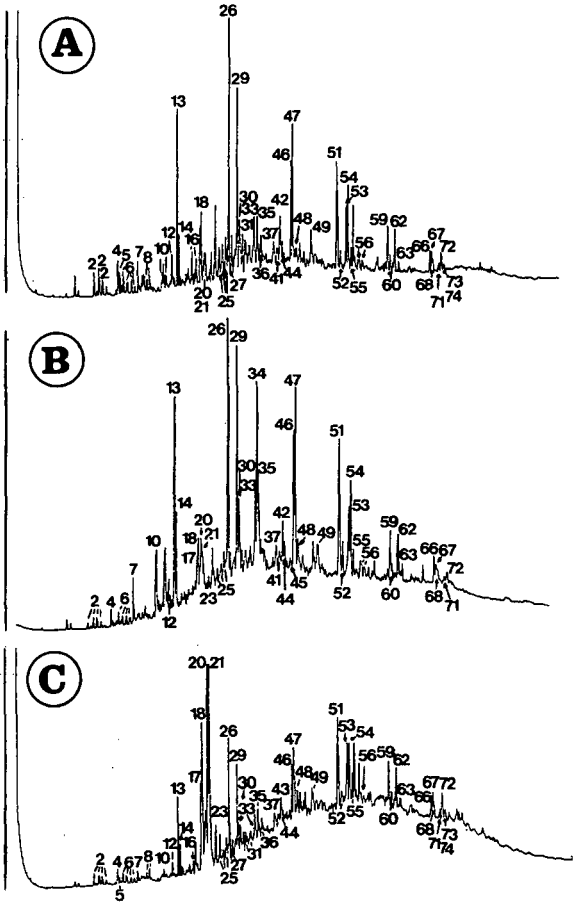

Fig. 1. Total ion current GC–EI-MS traces of the three end-member PAH mixtures identified in the sediments from the Guipuzcoan coast. The numbered peaks are identified in Table I.

TABLE I

POLYCYCLIC AROMATIC HYDROCARBONS IDENTIFIED IN THE SEDIMENTS COLLECTED FROM THE GUIPUZCOAN COAST

No.	Compound	No.	Compound
1	Ionene	41	Benzo[*b*]naphtho[2,1-*d*]thiophene
2	Dimethylnaphthalene	42	Benzo[*ghi*]fluoranthene
3	Acenaphthylene	43	Benzo[*c*]phenanthrene
4	Acenaphthene	44	Benzo[*b*]naphtho[1,2-*d*]thiophene
5	Dibenzofuran	45	Benzo[*b*]naphtho[2,3-*d*]thiophene
6	Trimethylnaphthalene	46	Benz[*a*]anthracene
7	Fluorene	47	Chrysene/triphenylene
8	Methyldibenzofuran	48	Benzo[*a*]carbazole
9	Tetramethylnaphthalene	49	Methyl-228
10	Methylfluorene	50	Dimethyl-228
11	Dimethyldibenzofuran	51	Benzo[b/*j*/*k*]fluoranthene
12	Dibenzothiophene	52	Benzo[*a*]fluoranthene
13	Phenanthrene	53	Benzo[*e*]pyrene
14	Anthracene	54	Benzo[*a*]pyrene
15	Dimethylfluorene	55	Perylene
16	Methyldibenzothiophene	56	Methyl-252
17	3-Methylphenanthrene	57	Dibenz[*a,j*]anthracene
18	2-Methylphenanthrene	58	Dimethyl-252
19	4*H*-Cyclopenta[*def*]phenanthrene	59	Indeno[1,2,3-*cd*]pyrene
20	4/9-Methylphenanthrene	60	Dibenz[*a,h*]anthracene/pentaphene
21	1-Methylphenanthrene	61	Benzo[*b*]chrysene
22	Dimethyldibenzothiophene	62	Benzo[*ghi*]perylene
23	4,5-Dihydropyrene	63	Anthanthrene
24	Ethylphenanthrene	64	Methyl-276
25	Dimethylphenanthrene	65	Dimethyl-276
26	Fluoranthene	66	Dibenzo[*e,l*]pyrene
27	Trimethyldibenzothiophene	67	Naphtho[1,2-*a*]pyrene
28	Benzoxanthene	68	Naphtho[2,3-*a*]pyrene
29	Pyrene	69	Coronene
30	Benzo[*b*]naphtho[2,3-*d*]furan	70	Naphtho[1,2-*e*]pyrene
31	Trimethylphenanthrene	71	Dibenzo[*a,e*]fluoranthene
32	Methyl-202	72	Dibenzo[*a,f*]fluoranthene
33	Benzo[*a*]fluorene	73	Dibenzo[*a,j*]fluoranthene
34	Retene	74	Dibenzo[*a,k*]fluoranthene
35	Benzo[*b*]fluorene	75	Dibenzo[*a,l*]fluoranthene
36	Ethylmethyl-4*H*-cyclopenta[*def*]phenanthrene	76	Dibenzo[*b,e*]fluoranthene
37	Dimethyl-202	77	Methyl-302
38	11*H*-Benzo[*a*]fluoren-11-one	78	Dimethyl-302
39	7*H*-Benzo[c]fluoren-7-one	79	*m/z* 326
40	11*H*-Benzo[*b*]-fluoren-11-one	80	*m/z* 328

rene, benz[*a*]anthracene, chrysene + triphenylene, benzofluoranthenes, benzo[*a*]pyrene, benzo[*e*]pyrene, indeno[1,2,3-*cd*]pyrene and benzo[*ghi*]perylene constitute the predominant compounds. The abundance of catacondensed structures and the predominance of parent hydrocarbons over alkylated homologues indicate a pyrolytic origin [17,18]. In principle, this origin may include a wide range of sources such as soots from car emissions, power plants, wood and coal combustion products and coal tars. The assignment of a few of these specific sources to the composition of type A sediments requires a more detailed comparison of the PAH distributions.

The PAH mixtures from car emissions and urban aerosols exhibit a high proportion of cyclopenta-

TABLE II

CONCENTRATIONS OF THE PREDOMINANT POLYCYCLIC AROMATIC HYDROCARBONS IN THE MODEL SEDIMENTARY ENVIRONMENTS CORRESPONDING TO FIG. 1

No.	Compound	Concentration (ng/g)		
		Sample type[a]		
		A	B	C
13	Phenanthrene	57	71	20
14	Anthracene	17	24	6
17	3-Methylphenanthrene	17	8	22
18	2-Methylphenanthrene	25	13	40
20	4/9-Methylphenanthrene	5	13	100
21	1-Methylphenanthrene	5	11	100
26	Fluoranthene	93	100	30
29	Pyrene	67	87	25
30	Benzo[*b*]naphtho[2,3-*d*]furan	17	22	4
33	Benzo[*a*]fluorene	16	27	6
34	Retene	1	76	1
35	Benzo[*b*]fluorene	16	33	7
46	Benz[*a*]anthracene	28	54	15
47	Chrysene + triphenylene	50	65	19
51	Benzo[*b*/*j*/*k*]fluoranthene	39	87	33
52	Benzo[*a*]fluoranthene	6	16	1.5
53	Benzo[*e*]pyrene	22	41	18
54	Benzo[*a*]pyrene	30	60	19
55	Perylene	6	14	8
59	Indeno[1,2,3-*cd*]pyrene	18	38	16
62	Benzo[*ghi*]perylene	18	35	17
	Unresolved complex mixture of PAH	1000	2700	10 000

[a] See text.

[*cd*]pyrene and a high benzo[*a*]pyrene to benzo[*e*]pyrene ratio [19,20], two features that are not observed in sample A. However, these differences have a limited assignment value because benzo[*a*]pyrene and, particularly, cyclopenta[*cd*]pyrene are unstable in the environment [21,22]. Other more stable features of the PAHs produced by traffic activities involve the predominance of pyrene *vs.* fluoranthene and benzo[*ghi*]perylene *vs.* indeno[1,2,3-*cd*]pyrene. type A sediments exhibit an inverse relationship between these *m/z* 202 PAHs and almost the same amount of benzo[*ghi*]perylene and indeno[1,2,3-*cd*]pyrene, which establishes a significant difference between the PAH distributions of these sediments and possible crude oil combustion or traffic sources.

The fluoranthene to pyrene and the indeno[1,2,3-*cd*]pyrene to benzo[*ghi*]perylene ratios of sample A are similar to those found in the PAH mixtures of coal tars and coal soots [9,23–26]. A close look at the *m/z* 226 and 228 homologues allows a more precise source characterization. Thus, benz[*a*]anthracene predominates over chrysene + triphenylene in coal tars whereas, as observed in sample A, chrysene + triphenylene is more abundant in coal soots. The predominant *m/z* 226 PAH in this sample is benzo[*ghi*]fluoranthene, which is also in agreement with the coal soot distributions. Conversely, the major *m/z* 226 aromatic hydrocarbon in the coal tars is cyclopenta[*cd*]pyrene, a compound that is below the detection limit in type A sediments.

Sample B corresponds to a sediment collected in July 1986 at a water depth of 50 m in the Oyarzun transect. The PAH distributions of samples A and B are similar but the high proportion of retene in the latter represents a very distinct feature. Retene is usually a transformation product of diterpenoids

with an abietane skeleton, particularly dehydroabietic acid. In aquatic environments, the presence of large amounts of retene and dehydroabietic acid may be indicative of effluents from kraft paper milling processes [27,28]. This applies to the Oyarzun River, which contains several paper industries near the mouth. The PAH distributions of the sediments located in front of this river are therefore indicative of paper mill effluents and soot contributions.

Sample C corresponds to a sediment collected in February 1987 at a water depth of 20 m in the Oria transect. Its PAH distribution strongly contrasts with those of samples A and B by the predominance of methylphenanthrenes and the high UCM. These two features are indicative of petrogenic inputs [29,30]. In this respect, the vehicular emissions are characterized by alkylphenanthrene distributions maximized at the C_1 homologues [18]. The predominance of 4/9- and 1- methylpenanthrenes over the 3- and 2-methyl isomers is probably indicative of partial biodegradation of these crude oil residues [31]. In addition to these petrogenic hydrocarbons, the pyrolytic PAH pattern described in sample A also occurs as a minor contribution in type C sediments.

Electron impact vs. GC–MS negative-ion chemical ionization

The PAH composition of the predominant type A sediments has been investigated in more detail using GC–NICI-MS. Fig. 2 displays the gas chromatographic profiles obtained by FID, ECD and MS in the EI and NICI modes from the PAH fraction of a sediment sample collected in July 1986 at a water depth of 20 m in the Bidasoa transect. As expected, the strongest contrast is observed between the FID and ECD traces. In fact, the ECD profile corresponds to a series of brominated compounds that also elute with the PAH in the column fractionation procedure of the sample extracts. These brominated compounds are also detected in the NICI trace.

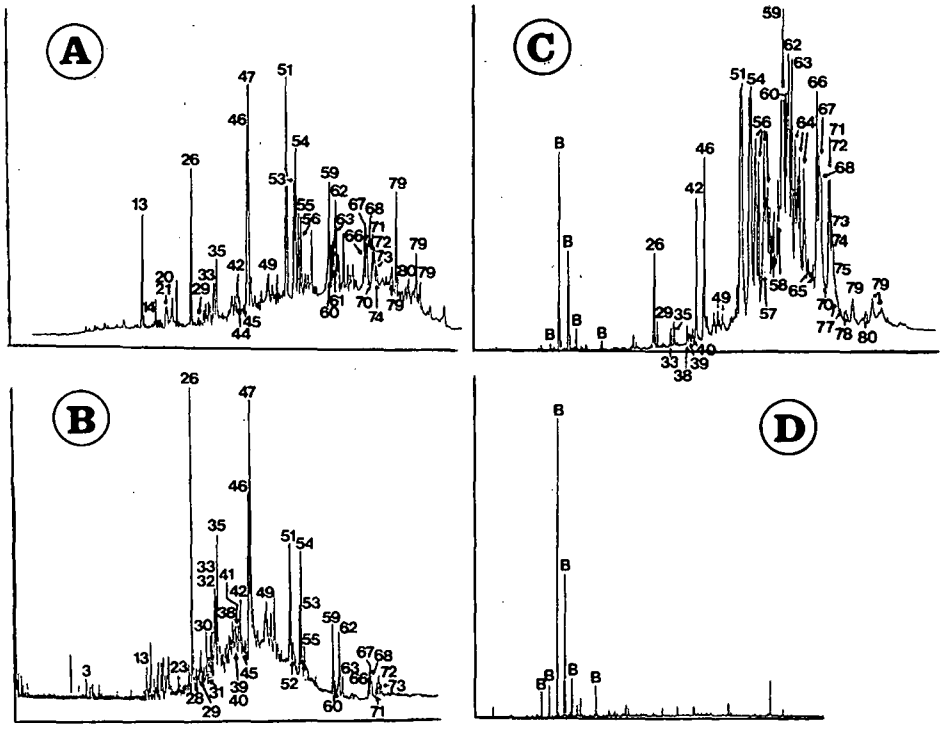

Fig. 2. GC profiles of a type A PAH sedimentary mixture recorded with (A) flame ionization detection, (B) electron impact and (C) negative-ion chemical ionization mass spectrometry and (D) electron-capture detection. The numbered peaks are identified in Table I. B refers to a series of brominated compounds.

The PAH composition is represented by the FID, EI and NICI traces. The FID and EI profiles show the closest similarity and NICI selectivity enhances the compounds eluting at higher retention times. These NICI-selective effects are also important at the level of isomeric mixtures. As described previously [32,33], Fig. 2 shows a strong enhancement of benzo[*a*]pyrene *vs.* benzo[*e*]pyrene and of benz[*a*]anthracene *vs.* chrysene + triphenylene and a high sensitivity for benzo[*ghi*]fluoranthene. NICI is also very sensitive to many nitrogen-containing PAHs [34,35]. The absence of these heteroatomic hydrocarbons in the GC–MS profile displayed in Fig. 2 indicates that these compounds are not very significant in the PAH fractions isolated from these pyrolytic type A sediments.

In addition to these previously described selectivity features, further high-molecular-weight enhancement effects have been observed in this study. Thus, the *m/z* 302 compounds appear as one of the most prominent group of peaks in the NICI trace whereas these compounds are usually detected as minor peaks in the FID and GC–EI-MS traces of the PAH extracts [10]. These effects also allow the determination of the GC–MS profiles of isomeric mixtures of high molecular weight, such as the *m/z* 326 and 328 PAHs. To date, the identification of these hydrocarbons in environmental samples has been performed by direct probe introduction MS in the EI mode [11,36].

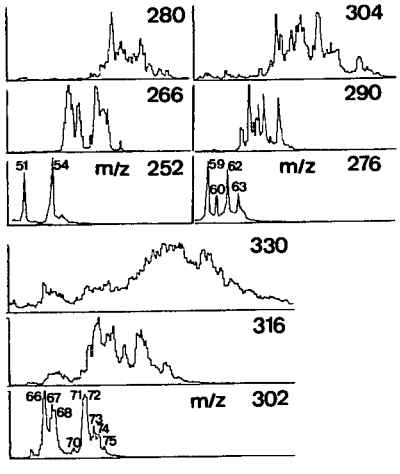

Fig. 3. Representative negative-ion chemical ionization mass fragmentograms of a type A PAH sedimentary distribution. The numbered peaks are identified in Table I.

The higher NICI response factor for high-molecular-weight PAHs also includes the alkylated homologues. This effect is illustrated in Fig. 3 by means of the mass fragment ions corresponding to the *m/z* 252, 276 and 302 series. The study of the alkylated series of these PAHs is difficult because they are essentially produced in combustion processes which, at the same time, give rise to distributions with a strong predominance of parent *vs.* alkylated homologues. As shown in Fig. 3, sensitive and selective methods such as GC–NICI-MS appear to be the most suitable techniques for their structural elucidation.

CONCLUSIONS

Three main end-member PAH distributions have been identified by GC–EI-MS analysis of the sediments of the Guipuzcoan coast. The type A mixtures correspond to pyrolytic soot contributions and are characterized by the predominance of phenanthrene, fluoranthene, pyrene, benz[*a*]anthracene, chrysene + triphenylene, benzofluoranthenes, benzo[*a*]pyrene, benzo[*e*]pyrene, indeno[1,2,3-*cd*]pyrene and benzo[*ghi*]perylene. The type B sediments exhibit distributions with a high proportion of retene in addition to the above-described pyrolytic PAHs. Finally, the type C mixtures are predominated by methylphenanthrenes and contain a high UCM that is found together with a minor proportion of pyrolytic PAHs. The analysis by GC–NICI-MS of some type A samples revealed selectivity effects not reported in previous studies. These include the enhancement of the parent PAHs eluting with longer retention times, such as the *m/z* 302, 326 and 328 isomers, and an increased response factor of the alkylated PAHs corresponding to *m/z* 252, 276 and 302.

ACKNOWLEDGEMENTS

We are grateful to Professor J. Albaigés for his useful comments. We thank the Servicio de Investigaciones Oceanográficas for technical assistance during ship sampling. Financial support from the Excma. Diputación Foral de Guipuzcoa is acknowledged.

REFERENCES

1 M. J. Suess, *Sci. Total Environ.*, 6 (1976) 239.
2 L. Van Vaeck and A. Van Cauwenberghe, *Environ. Sci. Technol.*, 19 (1985) 707.
3 R. J. Law, *Mar. Pollut. Bull.*, 12 (1981) 153.
4 J. D. Smith and W. A. Maher, *Aust. J. Mar. Freshwater Res.*, 35 (1984) 119.
5 A. Saliot, C. Andrie, R. Ho and J. C. Marty, *Int. J. Environ. Anal. Chem.*, 22 (1985) 25.
6 P. D. Dunn and H. F. Stich, *J. Fish. Res. Board Can.*, 33 (1976) 2040.
7 I. Ramos, M. Fuentes, R. Mederos, J. O. Grimalt and J. Albaigés, *Mar. Pollut. Bull.*, 20 (1989) 262.
8 W. J. Simonsick, Jr., and R. A. Hites, *Anal. Chem.*, 56 (1984) 2749.
9 S. A. Wise, B. A. Benner, G. D. Byrd, S. N. Chesler, R. E. Rebbert and M. M. Schantz, *Anal. Chem.*, 60 (1988) 887.
10 S. A. Wise, B. A. Benner, H. Liu, G. D. Byrd and A. Colmsjo, *Anal. Chem.*, 60 (1988) 630.
11 T. Romanowski, W. Funcke, J. Konig and E. Balfanz, *J. High Resolut. Chromatogr. Chromatogr. Commun.*, 4 (1981) 209.
12 U. R. Stenberg and T. E. Alsberg, *Anal.Chem.*, 53 (1981) 2067.
13 T. Ramdahl, G. Becher and A. Bjorseth, *Environ. Sci. Technol.*, 16 (1982) 861.
14 M. Oehme, *Anal. Chem.*, 55 (1983) 2290.
15 H. Stray, A. Mikalsen, B. Sonsterud and M. Oehme, *J. Chromatogr.*, 349 (1985) 331.
16 M. Aceves, J. O. Grimalt, J. Albaigés, F. Broto, L. Comellas and M. Gassiot, *J. Chromatogr.*, 436 (1988) 503.
17 R. E. LaFlamme and R. A. Hites, *Geochim. Cosmochim. Acta*, 42 (1978) 289.
18 B. R. T. Simoneit, *Int. J. Environ. Anal. Chem.*, 22 (1985) 203.
19 A. Rosell, J. O. Grimalt, M. G. Rosell, X. Guardino and J. Albaigés, *Fresenius' J. Anal. Chem.*, 339 (1991) 689.
20 G. Grimmer, J. Jacob, K-W. Naujack and G. Dettbarn, *Fresenius' Z. Anal. Chem.*, 309 (1981) 13.
21 R. M. Kamens, Z. Guo, J. N. Fulcher and D. A. Bell, *Environ. Sci. Technol.*, 22 (1988) 103.
22 T. Nielsen, *Atmos. Environ.*, 22 (1988) 2249.
23 G. Grimmer, J. Jacob, K.-W. Naujack and G. Dettbarn, *Anal. Chem.*, 55 (1983) 892.
24 G. Grimmer, J. Jacob, G. Dettbarn and K.-W. Naujack, *Fresenius' Z. Anal. Chem.*, 322 (1985) 595.
25 R. C. Lao, R. S. Thomas and J. L. Monkman, *J. Chromatogr.*, 112 (1975) 681.
26 E.-A. Ratajczak, E. Ahland, G. Grimmer and G. Dettbarn, *Staub Reinhalt. Luft*, 44 (1984) 505.
27 M. E. Fox, in L. H. Keith (Editor), *Identification and Analysis of Organic Pollutants in Water*, Ann Arbor Sci. Publ., Ann Arbor, MI, 1976, p. 641.
28 L. H. Keith, in L. H. Keith (Editor), *Identification and Analysis of Organic Pollutants in Water*, Ann Arbor Sci. Publ., Ann Arbor, MI, 1976, p. 671.
29 W. W. Youngblood and M. Blumer, *Geochim. Cosmochim. Acta*, 39 (1975) 1303.
30 J. W. Farrington and B. W. Tripp, *Geochim. Cosmochim. Acta*, 41 (1977) 1627.
31 J. M. Bayona, J. Albaigés, A. M. Solanas, R. Parés, P. Garrigues and M. Ewald, *Int. J. Environ. Anal. Chem.*, 23 (1986) 289.
32 L. R. Hilpert, G. D. Byrd and C. R. Vogt, *Anal. Chem.*, 56 (1984) 1842.
33 M. Oehme, *Anal. Chem.*, 55 (1983) 2290.
34 M. Oehme, *Chemospere*, 14 (1985) 1285.
35 J. M. Bayona, D. Barceló and J. Albaigés, *Biomed. Environ. Mass Spectrom.*, 16 (1988) 461.
36 W. Giger and M. Blumer, *Anal. Chem.*, 46 (1974) 1663.

Journal of Chromatography, 607 (1992) 287–294
Elsevier Science Publishers B.V., Amsterdam

CHROM. 24 105

Effect of solvent polarity on the determination of oxo- and nitro-polycyclic aromatic hydrocarbons using capillary gas chromatography with splitless injection

M. T. Galceran* and E. Moyano

Department of Analytical Chemistry, University of Barcelona, Diagonal 647, 08028 Barcelona (Spain)

ABSTRACT

The importance of solvent polarity in the injection conditions for the determination of oxo- and nitro-polyclic aromatic hydrocarbons in capillary gas chromatography was investigated. When standard solutions of these compounds were analysed by high-resolution gas chromatography using splitless injection, peak splitting with two or more maxima was obtained when methanol and acetonitrile were used, in the preceding steps no peak splitting was observed with dichloromethane or acetone. This splitting can be eliminated using a retention gap or by increasing the initial column temperature. Response factors for all these compounds at different initial temperatures and different solvents were studied. The best results were obtained using acetonitrile, an initial temperature of 60°C and a retention gap. Reproducibility gave a relative standard deviation from 1.8 to 6.7 when measured by peak area; detection limits (signal-to-noise ratio of 2:1) using a flame ionization detector ranged from 129 pg for 2-methyl-1-nitronaphthalene to 1.5 ng for 9,10-phenanthroquinone.

INTRODUCTION

Increasing attention is being devoted to the determination of polycyclic aromatic hydrocarbons (PAHs) containing heteroatoms or polar functional groups in the molecule (PAH derivatives) in environmental samples, mainly of atmospheric aerosols and diesel exhausts [1–3], as it has been shown that these species act as direct mutagens in the Ames test [4]. General concern about the possible health effects of PAH derivatives, particularly those containing nitro, hydroxy and carbonyl groups, has led to a need for the specific determinations of these compounds.

Owing to the extremely complex composition, dilution and variability of the soluble organic fraction (SOF) extracted from particles, the extract must be subjected to an efficient clean-up and enrichment procedure to provide samples suitable for gas chromatography (GC), gas chromatography–mass spectrometry (GC–MS) or high-performance liquid chromatography (HPLC). The published fractionation methods, some of which are designed for specific samples, are usually carried out using low- and high-resolution liquid chromatography and solvents of various polarities. The polar fractions which contain the PAH derivatives are eluted with solvents such as dichloromethane, acetone, methanol or acetonitrile [5–7]; direct injection of these fractions in high-resolution gas chromatography (HRGC) without changing the solvent may be useful. Moreover, on-line coupling of HPLC and GC using polar solvents might be advisable as about 80% of HPLC analyses are performed by a reversed-phase mechanism; the use of polar solvents and water in coupling has been studied [8–10].

The solvent is one of the most important factors in improving sensitivity in HRGC. The solvent effect was first described by Grob and Grob [11,12] for the determination of hydrocarbons by splitless injection; it is now considered to be an important mechanism for some of the most frequently used injection modes, such as splitless and on-column injection. Cold-trapping and the solvent effect are two

0021-9673/92/$05.00

factors that lead to a recondensation of the sample components at the top of the chromatographic column [12–14]. The solvent effect requires conditions which recondense a large portion of the solvent in the first part of the column. Grob and Grob [15] have emphasized that this is controlled by four independent factors: initial column temperature, volatility of the solvent, amount of solvent and injection time. By selecting these variables correctly, the effect can be optimized for any combination of sample and column.

Although the solvent effect in splitless and on-column injection in capillary gas chromatography has been discussed, showing that band broadening or splitting appear to be the result of increasing solvent polarity [16,17], few quantitative results on the response factors caused by solvents of different polarities have been published. Lee *et al.* [18] and Brindle and Li [19] have studied the effect of the solvent in the analysis of PAHs by HRGC. These workers indicate that different solvents can drastically change the response of the analyte under the same chromatographic conditions, and that the best results are obtained using non-polar solvents such as isooctane or xylenes.

For more polar compounds few data have been published, but, generally, these compounds and polar solvents lead to band broadening and splitting [20,21]. In this work we studied the effect of the solvent in the determination of oxo- and nitro-PAHs by capillary GC. The relationship between the optimum initial temperature of the column and the boiling point of the solvent, the use of retention gaps and other factors that might effect the performance in the GC system are reported.

EXPERIMENTAL

Working conditions

A DANI (Milan, Italy) Model 3800 HRGC gas chromatograph equipped with a flame ionization detector was used for all determinations. DB-5 (J&W Scientific, Rancho Cordova, CA, USA) 30 m × 0.25 mm I.D. (film thickness 0.25 μm) fused-silica capillary columns with a retention gap 2.5 m × 0.25 mm I.D., deactivated) were used with splitless injection. The operating temperatures were: injection port, 250°C; detector, 300°C; and temperature programme as shown in Table I. Flow-rates were as follows: hydrogen, 30 ml min^{-1}; air, 280 ml min^{-1}; detector makeup gas (nitrogen), 30 ml min^{-1}. The linear velocity of the carrier gas (helium) was 30 cm s^{-1} at 60°C. The splitless valve was on for 45 s; 1 μl of each sample was injected onto the column by hot needle injection. A Merck–Hitachi (Tokyo, Japan) Model D-2000 integrator was used to measure peak areas and heigths for the subsequent calculation of response factors.

Materials

The compounds studied are listed in Table II and were provided by Carlo Erba (Milan, Italy), EGA Chemie (Steinheim, Germany), Fluka (Buchs, Switzerland), Jessen-Chimica (Geel, Belgium) or Merck (Darmstadt, Germany). Acetone and dichloromethane (Panreac, Barcelona, Spain) were distilled and acetonitrile and methanol were of HPLC grade (Merck).

A stock solution of the compounds studied was prepared containing 1 mg ml^{-1} of each in acetonitrile. The 20 μg ml^{-1} solutions in the various sol-

TABLE I

TEMPERATURE PROGRAMME

Program No.	Initial temperature (°C)	Initial time (min)	Rate of increase (°C/min)	Final temperature (°C)	Final time (min)
1	40	2	6	260	15
2	60	2	5	260	15
3	80	4	4	260	15
4	100	4	4	260	15

TABLE II

RETENTION TEMPERATURES OF OXO- AND NITRO-PAHs IN ACETONITRILE USING PROGRAMME NO. 2

Peak No.	Compound	Symbol	Retention temperature (°C)
1	1,4-Naphthoquinone	1,4-NQ	145
2	5-Nitroindan	5-NI	160
3	2-Methyl-1-nitronaphthalene	2-M-1-NN	173
4	2-Nitronaphthalene	2-NN	174
5	9-Fluorenone	9-Fl	185
6	Acenaphthenequinone	ACQ	199
7	9-Nitroanthracene	9-NA	226
8	9,10-Phenanthroquinone	9,10-PQ	229
9	Benzanthrone	BZ	257
10	1-Nitropyrene	1-NP	268

vents were prepared by dilution of appropriate volumes of this stock solution. Pyrene was used as an internal standard.

RESULTS AND DISCUSSION

Effect of solvent and temperature

The solvents studied were dichloromethane, acetone, methanol and acetonitrile, which all have different boiling points and polarities and are generally used in the clean-up of the medium and high polar fractions of aerosol samples in which the PAH derivatives are found.

Peak splitting was observed when methanol and acetonitrile were used as sample solvents. Figs. 1 and 2 show the sample gas chromatograms for these two solvents obtained with the DB-5 column at different initial column temperatures. For the two sol-

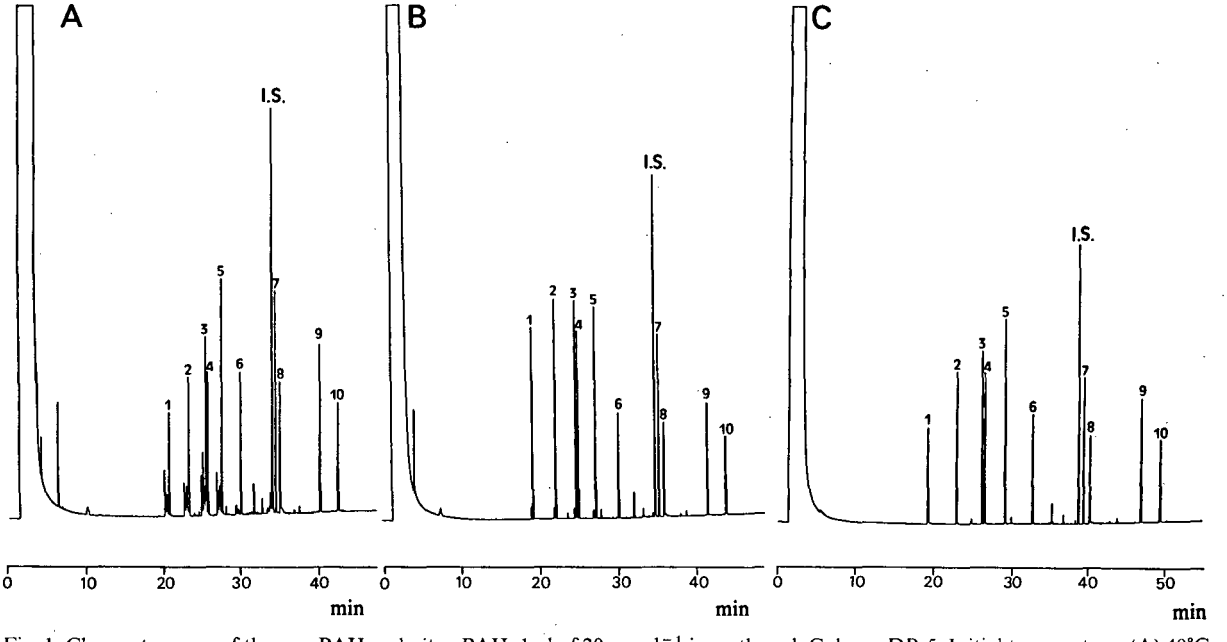

Fig. 1. Chromatograms of the oxo-PAH and nitro-PAH, 1 μl of 20 μg ml^{-1} in methanol. Column DB-5. Initial temperature: (A) 40°C, (B) 60°C and (C) 80°C. For peak identification, see Table II.

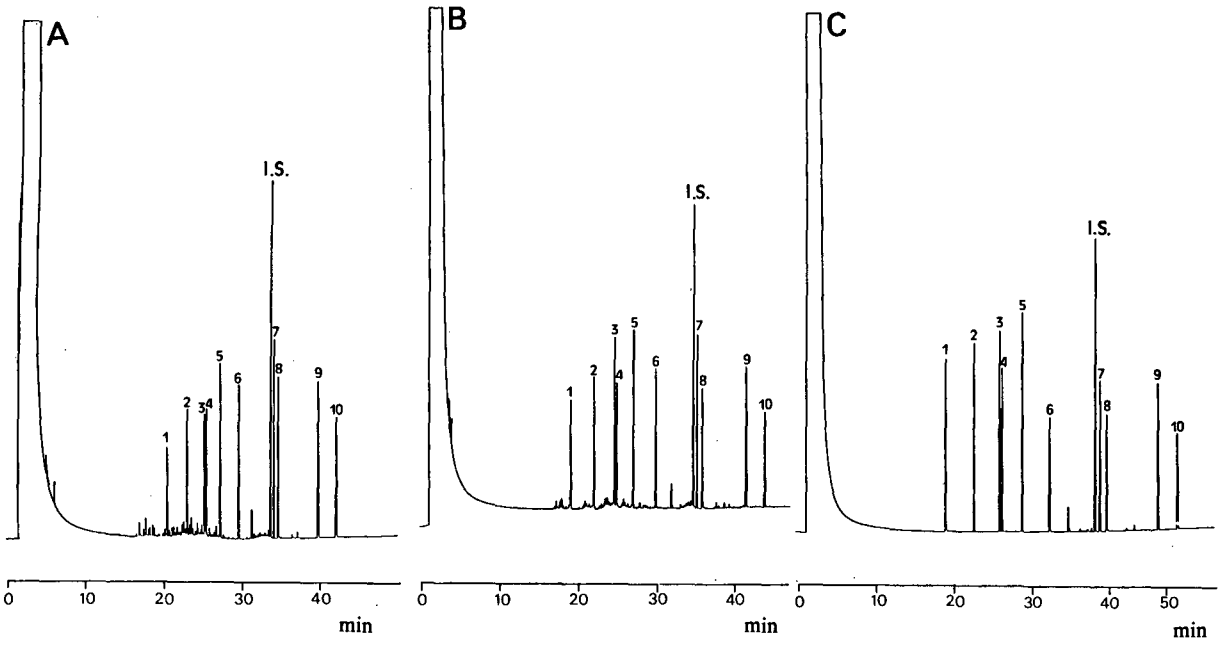

Fig. 2. Chromatograms of the oxo-PAH and nitro-PAH, 1 μl of 20 μg ml^{-1} in acetonitrile. Column DB-5. Initial temperature: (A) 40°C, (B) 60°C and (C) 80°C. For peak identification, see Table II.

vents, splitting was observed at two temperatures (60 and 40°C). An explanation for peak splitting observed in splitless and on-column injection has been provided in detail by Grob [16,22]. Grob points out than when two maxima are observed in a split peak, these correspond to an uneven distribution of the liquid sample injected into the flooded section of the column. Increasing the temperature tends to keep the solutes within the rear portion of the flooded zone, and at a high enough temperature, this focusing effect essentially eliminates peak splitting. These phenomena are illustrated in Figs. 1 and 2. When the initial column temperature is raised, the length of the flooding zone is reduced, providing additional focusing, and the splitting disappears. In this instance several maxima are observed in a split peak for both solvents, probably due to the difference between the polarity of the solvent and the stationary phase. The polar solvent did not wet the non-polar stationary phase and the sample was sprayed into the column in the form of micro-droplets. This leads to a pattern of multiple peak distortion, which can be eliminated if the column inlet has a much lower retention power than the coated column. In practice this means that an uncoated inlet section, a "retention gap" [17,23] should be used. Fig. 3 shows the chromatograms obtained for the two solvents at 40°C using a "retention gap", in which no splitting is observed.

Column temperature and temperature programming are two factors affecting the resolution and sensitivity. In our study the temperature programmes were optimized for each initial temperature to obtain a high enough resolution, and were the same for the four solvents studied. To determine the effect of the initial temperature on the peak height and area, the samples were injected at different initial temperatures from 40 to 100°C and the chromatograms were obtained. Peak heights and peak areas were determined and the relative peak height and peak area of each compound were calculated based on the values obtained at 40°C. These relative peak heights for each compound, temperature and solvent are shown in Table III, in which low values are observed for most of the compounds and solvents at high temperatures. The changes in areas are smaller owing to a simultaneous increase in peak width, so a low initial temperature near to or below the boiling point of the solvent seems to give the best results, as has been pointed out by

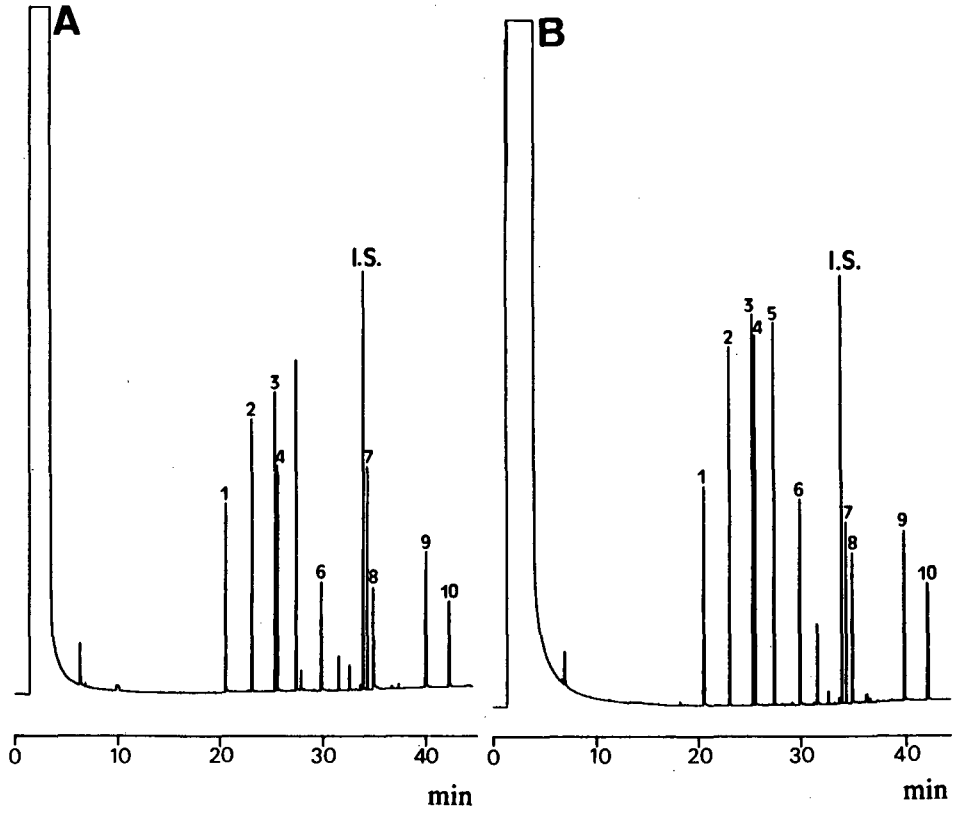

Fig. 3. Chromatograms of the oxo-PAH and nitro-PAH, 1 μl of 20 μg ml^{-1} in (A) methanol and (B) acetonitrile. Column DB-5. Initial column temperature 40°C; retention gap 2.5 m. For peak identification, see Table II.

Grob [16] for *n*-alkane compounds. Indeed, initial temperature also affected the resolution and peak shape, as shown in Fig. 4, in which the peak height-to-peak width ratios for the first two eluted compounds (1,4-naphthoquinone and 5-nitroindan) at different initial temperatures are shown. Decreases in this ratio at high initial column temperatures were observed for the two compounds in all the solvents studied and were related to a decrease in the solvent effect. Decreases at low initial column temperatures were only observed for the first eluted peak (1,4-naphthoquinone) in acetonitrile, and this may be due to the slow evaporation of the solvent. There seems to be a critical inital temperature, above or below which the solvent loses its efficiency; this effect was not observed for the other solvents studied because the working temperatures were not far enough below their boiling points.

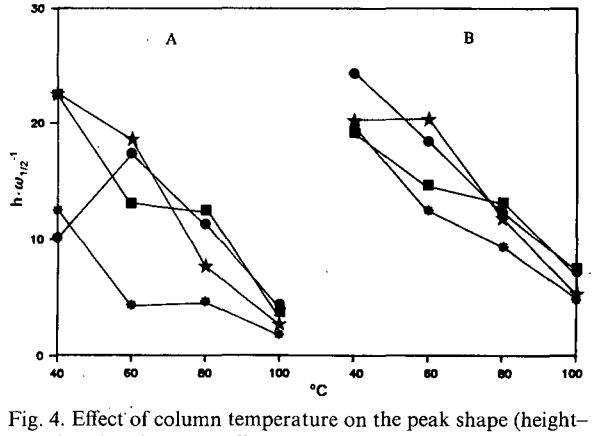

Fig. 4. Effect of column temperature on the peak shape (height–width) ratio of solvent effect. (A) 1,4-naphthoquinone and (B) 5-nitroindan. Key: ■ = dichloromethane; ★ = acetone; * = methanol; ● = acetonitrile.

To optimize the chromatographic conditions, response factors for each oxo- and nitro-PAH in the four solvents studied relative to dichloromethane at 40°C were calculated. These factors are listed in Table IV. From the results obtained for the height response factors, we can conclude that the best condi-

TABLE III

RELATIVE PEAK HEIGHTS IN DIFFERENT SOLVENTS AT INITIAL TEMPERATURES OF 40, 60, 80 AND 100°C

Compound[a]	Relative peak height (%)															
	Dichloromethane (40.0°C)[b]				Acetone (56.0°C)				Methanol (65.0°C)				Acetonitrile (81.6°C)			
	100°C	80°C	60°C	40°C	100°C	80°C	60°C	40°C	100°C	80°C	60°C	40°C	100°C	80°C	60°C	40°C
1,4-NQ	41	76	73	100	36	62	93	100	41	64	58	100	59	95	130	100
5-NI	62	84	84	100	54	82	103	100	52	70	82	100	49	64	88	100
2-M-1-NN	66	79	76	100	65	87	94	100	57	72	90	100	64	63	88	100
2-NN	72	63	70	100	67	83	98	100	71	84	104	100	53	55	83	100
9-Fl	83	75	91	100	68	78	82	100	77	78	89	100	69	69	96	100
ACQ	86	67	86	100	79	61	73	100	138	127	89	100	86	68	88	100
9-NA	86	70	91	100	78	79	76	100	82	80	86	100	101	101	108	100
9,10-PQ	101	72	74	100	78	73	88	100	119	108	77	100	85	95	101	100
BZ	96	134	87	100	101	112	96	100	124	112	112	100	89	104	112	100
1-NP	90	139	68	100	93	99	83	100	124	119	123	100	84	100	103	100

[a] For explanation of solvent abbreviations, see Table II.
[b] Boiling point.

TABLE IV

RELATIVE RESPONSE FACTORS IN DIFFERENT SOLVENTS AT INITIAL TEMPERATURES OF 40, 60, 80 AND 100°C

Compound[a]	Relative response factor															
	Dichloromethane (40.0°C)[b]				Acetone (56.0°C)				Methanol (65.0°C)				Acetonitrile (81.6°C)			
	100°C	80°C	60°C	40°C	100°C	80°C	60°C	40°C	100°C	80°C	60°C	40°C	100°C	80°C	60°C	40°C
1,4-NQ	41	76	73	100	33	57	86	92	25	39	35	61	41	66	91	70
5-NI	62	84	84	100	51	78	97	95	47	63	74	90	58	75	102	117
2-M-1-NN	66	79	76	100	55	74	80	85	47	60	76	84	68	67	93	106
2-NN	72	63	70	100	55	68	80	82	51	60	75	72	60	62	94	113
9-Fl	83	75	91	100	78	89	94	115	76	76	87	98	77	78	107	112
ACQ	86	67	86	100	84	65	78	106	77	70	49	56	89	70	91	103
9-NA	86	70	91	100	85	87	83	109	88	86	93	108	87	87	93	86
9,10-PQ	101	72	74	100	83	78	94	106	94	85	61	79	97	108	115	114
BZ	96	134	87	100	109	121	104	108	138	125	125	112	122	143	154	138
1-NP	90	139	68	100	98	105	87	105	129	123	128	104	116	138	143	138

[a] For explanation of solvent abbreviations, see Table II.
[b] Boiling point.

tions were acetonitrile as solvent at an initial column temperature of 60°C, as there was a marked loss of efficiency in the first peak eluted at 40°C in acetonitrile.

There are other factors that must be optimized. For instance, the injection port temperature affects the amount of sample retained in the capillary section of the column or in the retention gap in the bottom of the injector, and peak splitting can be observed owing to this warm connection. To study this effect, the injection port temperature was increased from 200 to 300°C. No difference was observed in the peak areas or peak heights. An increase in the inlet vent flow, which can be achieved by increasing the split ratio to 1:100, gives solvent peaks with a better shape due to a faster removal of the last traces of vapour from the vaporizing chamber.

As is well known, the peak splitting depends on the solvent, on the solutes and on the stationary phase. In Fig. 5 it can be seen that when a more polar stationary phase (DB-17) was used without a retention gap, peak splitting was obtained using acetonitrile as solvent, but with a different pattern; now two maxima appear rather than multiple maxima as happens when DB-5 is used (Fig. 2A). This lower peak splitting may be due to the different acetonitrile wettability of both stationary phases, giving a less homogeneous flooding zone for the DB-5 stationary phase.

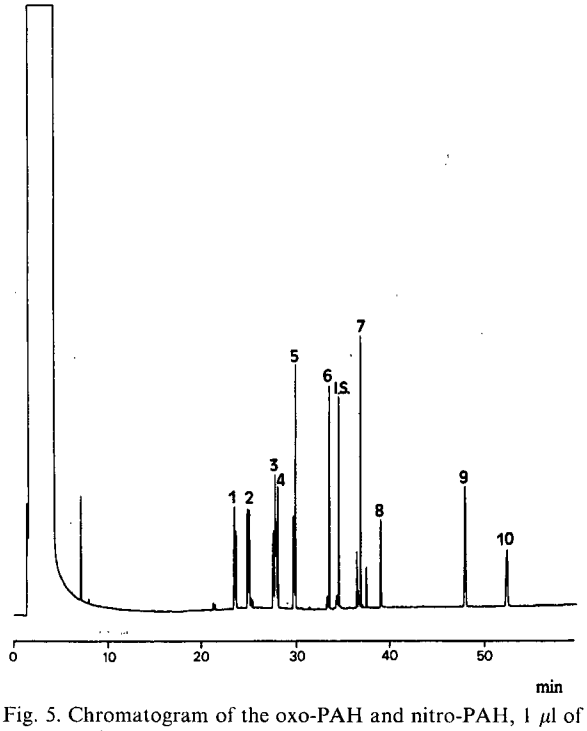

Fig. 5. Chromatogram of the oxo-PAH and nitro-PAH, 1 μl of 20 μg ml^{-1} in acetonitrile. Column DB-17. Initial column temperature 40°C. For peak identification, see Table II.

Quality parameters

Calibrations for oxo- and nitro-PAHs in acetonitrile were carried out under the optimum conditions, with concentrations in the range 2–20 μg ml^{-1}. Peak area was used as the response. The correlation coefficients of calibration graphs in the concentration range 2–20 μg ml^{-1} were better than 0.9990 for all oxo- and nitro-PAHs.

Five replicate determinations of 8 ng (8 μg ml^{-1} solution) of each oxo- and nitro-PAH in acetonitrile were carried out under the optimum conditions to determine the precision in the analysis of PAH derivatives. Relative standard deviations (R.S.D.) in the range 1.8–6.7% based on peak area were obtained.

The detection limits for the determination of oxo- and nitro-PAHs by GC with a flame ionization detector ranged from 129 pg for 2-methyl-1-nitronaphthalene to 1.5 ng for 9,10-phenanthroquinone when determinations were made in acetonitrile (Table V). These values are higher than those obtained

TABLE V

DETECTION LIMITS AND PRECISION OF OXO- AND NITRO-PAHs IN ACETONITRILE

Chromatographic conditions: programme 2.

Compound[a]	Detection limit[b] (pg)	Precision R.S.D. %
1,4-NQ	130	2.5
5-NI	135	2.3
2-M-1-NN	129	2.3
2-NN	132	2.0
9-Fl	133	1.8
ACQ	189	4.1
9-NA	408	1.9
9,10-PQ	1500	2.0
BZ	399	4.6
1-NP	404	6.7

[a] For explanation of solvent abbreviations, see Table II.
[b] As 2 S.D.

for the PAHs with non-polar solvents such as isooctane or toluene [19], showing that the polar solvents are less efficient in transferring the compounds to the column.

CONCLUSIONS

When methanol and acetonitrile were used as solvents of oxo- and nitro-PAHs in HRGC with non-polar phases, peak splitting was observed, showing multiple maxima for acetonitrile, which are related to the poor wetting ability of this solvent. We conclude that the optimum initial column temperature depends on the boiling point of the solvent; the highest response factors were obtained using acetonitrile at an initial temperature of 60°C. These results could be applied to the determination of oxo- and nitro-PAHs in the fractions obtained from the clean-up of environmental samples.

ACKNOWLEDGEMENTS

We thank the DGICYT for financial support (Project PB87-0057) and E. Moyano gratefully acknowledges the support of the CIRIT, Generalitat de Catalunya (Conv. 1989).

REFERENCES

1 H. Stray, A. Mikalsen, B. Sønsterud and M. Oehme, *J. Chromatogr.*, 349 (1985) 97.
2 K. P. Ang, B. T. Tay and H. Gunasingham, *Int. J. Environ. Stud.*, 29 (1987) 163.
3 J.Schilhabel and K. Leusen, *Anal. Chim. Acta*, 136 (1982) 163.
4 M. Moller and I. Alfheim, *Atmos. Environ.*, 14 (1980) 83.
5 A. Liberti, P. Ciccioli, A. Cecinato, E. Brancaleoni and C. Di Palo, *J. High Resolut. Chromatogr. Chromatogr. Commun.*, 7 (1984) 389.
6 P. Ciccioli, E. Brancaleoni, A. Cecinato, C. Di Palo, P. Buttini and A. Liberti, *J. Chromatogr.*, 351 (1986) 451.
7 K. P. Naikwadi, G. M. Charbonneau, F. W. Karasek and R. E. Clement, *J. Chromatogr.*, 398 (1987) 227.
8 A. Pouwelse, D. De Jong and J. H.M. van den Berg, *J. High Resolut. Chromatogr. Chromatogr. Commun.*,11 (1988) 607.
9 E. Dolecka, J. J. Vreuls, G. J. de Jong, U. A. Th. Brinkman and F. A. Maris, *J. High Resolut. Chromatogr. Chromatogr. Commun.*, 13 (1990) 405.
10 K. Grob and A. Artho, *J. High Resolut. Chromatogr. Chromatogr. Commun.*, 14 (1991) 212.
11 K. Grob and K. Grob, Jr., *J. Chromatogr. Sci.*, 7 (1969) 584.
12 K. Grob and K. Grob, Jr., *J. Chromatogr. Sci.*, 94 (1974) 53.
13 G. Schomburg, H. Belan, R. Dielmann, F. Weeke and H. Husmann, *J. Chromatogr.*, 142 (1977) 87.
14 K. Grob and K. Grob, Jr., *J. Chromatogr.*, 151 (1978) 311.
15 K. Grob and K. Grob, Jr., *J. High Resolut. Chromatogr. Chromatogr. Commun.*, 1 (1978) 275.
16 K. Grob, Jr., *J. Chromatogr.*, 213 (1981) 3.
17 K. Grob, Jr., *J. Chromatogr.*, 237 (1982) 15.
18 H. Lee, R. Szawiola and A. S. Y. Chay, *J. Assoc. Off. Anal. Chem.*, 70 (1987) 929.
19 J. D. Brindle and X. Li, *J. Chromatogr.*, 498 (1990) 11.
20 L. Ghaoui, F.-S. Wang, H. Shanfield and A. Zlatkis, *J. High Resolut. Chromatogr. Chromatogr. Commun.*, 6 (1983) 497.
21 P. Sandra, M. van Roelenbosch, M. Verzele and C. Bicchi, *J. Chromatogr.*, 279 (1983) 279.
22 J. Grob, Jr., *J. Chromatogr.*, 279 (1983) 225.
23 K. Grob, Jr. and K. Grob, *J. Chromatogr.*, 270 (1983) 17.

Journal of Chromatography, 607 (1992) 295–302
Elsevier Science Publishers B.V., Amsterdam

CHROM. 24 148

Flame ionization detection relative response factors of some polycyclic aromatic compounds

Determination of the main components of the coal tar pitch volatile fraction

C. G. Blanco, J. S. Canga, A. Domínguez and M. J. Iglesias

Instituto Nacional del Carbón, CSIC, Ap. 73, 33080-Oviedo (Spain)

M. D. Guillén*

Facultad de Farmacia, UPV, Portal de Lasarte s/n, 01007-Vitoria (Spain)

ABSTRACT

The flame ionization detection (FID) relative response factors of some commercially available polycyclic aromatic compounds using split injection were determined and compared with other published FID relative response factors obtained using splitless and cold on-column injection technique. From these data FID relative response factors of some non-available polycyclic aromatic compounds were calculated in an approximate way. These factors were used in a quantitative study of the main components of a coal tar pitch volatile fraction. For this quantification the internal standard method and the absolute calibration with separate standard method were employed. Good reproducibility of the determinations using both methods was found.

INTRODUCTION

Coal tar pitches are very complex mixtures of polycyclic aromatic compounds (PACs). The behaviour and properties of coal tar pitches should be governed by their composition, and in the study of relationships between composition, properties and behaviour of this carbonaceous material, gas chromatography (GC) and combined gas chromatography–mass spectrometry (MS), apart from other techniques, are very useful tools.

The chromatographic retention of several commercially available PACs has been studied on stationary phases of different polarity [1–3]. Likewise, relationships between the chromatographic retention of some polycyclic aromatic hydrocarbons (PAHs) and some of their structural and physicochemical properties have also been studied [1,4,5]. On the other hand, the identification of the components of the volatile fraction of a coal tar pitch on stationary phases of different polarity has been carried out, using PAH retention indices and GC–MS [6,7].

However, the determination of different PACs in a sample is a difficult task. If the sampling being studied is not a very complex mixture and its components are volatile compounds, the cold on-column injection technique is recommended for quantitative purposes [8,9]. However, coal tar pitch extracts form a very complex mixture and are difficult to separate using splitless injection as they contain considerable amounts of non-volatile compounds, which cause problems in the column if the cold on-column injection technique is used.

0021-9673/92/$05.00

For these reasons, in this work the split injection technique was used for the quantitative study of the various components of a coal tar pitch volatile fraction. In order to carry out a more rigorous study, the relative response factors of 47 commercially available PACs were determined using split injection. The relative response factors of non-available PACs were calculated by extrapolation. Owing to the almost complete absence of the relative response factors of PACs in the literature, the values obtained here were compared with others obtained using the splitless and on-column injection techniques. The influence of volatility and carbon content of the different compounds on their relative response factors is discussed. The determination of the components of the sample under study was carried out by making use of the relative response factors determined here.

EXPERIMENTAL

The chromatographic study was carried out using a Hewlett-Packard (Palo Alto, CA, USA) Model 5890 Series II gas chromatograph with flame ionization detection (FID) and using a Hewlett-Packard Vectra ES/12 computer which allows chromatograms to be stored. A fused-silica capillary column coated with OV-1701 stationary phase (Quadrex, New Haven, CT, USA) was used. The operating conditions and column characteristics are given in Table I.

The standard compounds used are listed in Table II and were obtained from Fluka (Buchs, Switzerland), Aldrich (Milwaukee, WI, USA), Merck (Darmstadt, Germany) and Janssen (Beerse, Belgium). Their purities were tested and in most instances were greater than 98%.

The sample of coal tar pitch to be analysed was obtained by extraction using pyridine as solvent and a procedure described elsewhere [10]. All samples to be chromatographed were dissolved in pyridine and kept for a few minutes in an ultrasonic bath in order to effect total dissolution. This is very important because of the large difference in solubility between PACs.

RESULTS AND DISCUSSION

First, careful checks of the purity of the standard compounds used in this study were carried out, in order to make the corresponding corrections. Then, the influence of the concentration of the compounds in the sample injected on their chromatographic responses was tested. The results show that, over the wide concentration range studied (250–4250 ng/μl), the response factor [peak-area counts/amount of compound injected (ng)] does not change with the amount of compound injected. The experimental data fitted the linear equation $y = 2195.61 + 69.55x$ [y = peak area counts and x = amount of compound injected (ng)] with a correlation coefficient of 0.9964.

The next step was the determination of the FID response factors of the available commercially compounds. To this end, mixtures of different groups of PACs with known concentrations were analysed using the previously mentioned operating conditions. Obviously the response factors determined here will be affected not only by the detector and injection technique used, but also by the human factor, technique, operating conditions and characteristics of the gas chromatograph and column used. Table II gives the FID relative response factors (*RRF*) obtained here for various compounds, using as reference compounds fluoranthene and 7,12-dimethylbenz[*a*]anthracene. To the best of our knowledge, the FID *RRF* values for many of the compounds in Table II have not been reported previously. The relative response factor of a compound i in relation to a reference compound r is defined as $RRF_i = A_r, M_i/M_r\, A_i$, where A and M are peak-area counts and weight of the compounds, respectively. From this

TABLE I

CHROMATOGRAPHIC OPERATING CONDITIONS

Stationary phase	OV-1701
Film thickness (μm)	0.18
Column length (m)	25
Column inside diameter (mm)	0.22
Carrier gas (hydrogen) flow-rate (ml min^{-1})	2
Splitting ratio	1:87
Injector temperature (°C)	300
Detector temperature (°C)	350
Temperature programming rate from 50 to 300°C (°C min^{-1})	4
Volume of sample injected (μl)	1
Minimum number of sample injections	5

definition, it is clear that compounds with a response lower (higher) than that of the reference compound shows an *RRF* greater (less) than 1. The small values of the standard deviation, S.D., and of the relative standard deviation R.S.D., obtained in the determination of the *RRF* values are notable. These show the high reproducibility of the chromatographic run obtained under the conditions applied. Other workers have found R.S.D.s from 8 to 45% when they used split injection [11].

Response factors of PACs have not been frequently reported. Lao *et al.* [12] reported FID relative response factors using fluoranthene as a reference compound for 57 PACs (from compounds such as biphenyl with 12 carbon atoms to coronene or dibenzopyrene with 24 carbon atoms), obtained using the split injection technique. Table II also gives FID response factors relative to fluoranthene calculated from data obtained, using splitless (RRF_F') [13] and cold on-column injection techniques (RFF_F'') [14] for a smaller number of compounds (15 and 22, respectively). The carbon contents, defined as *CC* = mass of the total carbon atoms/molecular mass, and the boiling points (b.p.) [15,16] of the different compounds are also given in Table II.

It is generally accepted [17,18] that, if the entire amount of solute injected reaches the flame ionization detector, the response factor will theoretically only be a function of the carbon content of each

TABLE II

RELATIVE RESPONSE FACTORS OF SOME PACs OBTAINED IN THIS STUDY, AND OTHERS CALCULATED FROM THE LITERATURE [13,14], TOGETHER WITH THEIR CARBON CONTENTS AND BOILING POINTS

Compound	RRF_F	S.D.	R.S.D. (%)	RRF_{DMBA}	RRF_F' [13]	RRF_F'' [14]	*CC*	B.p. (°C)
Naphthalene	0.793	0.012	1.5	0.651	0.912	0.964	0.9375	218.00
Quinoline	0.915	0.027	3.0	0.751			0.8372	238.00
2-Methylnaphthalene	0.832	0.016	1.9	0.683	0.991	0.983	0.9296	241.00
8-Methylquinoline	0.996	0.039	3.9	0.818			0.8392	247.00
Diphenyl	0.837	0.024	2.9	0.687	1.037		0.9351	255.90
2-Ethylnaphthalene	0.824	0.005	0.6	0.677			0.9231	257.90
Diphenyl ether	0.956	0.029	3.0	0.785			0.8471	257.90
1,6-Dimethylnaphthalene	0.898	0.026	2.9	0.737			0.9231	264.00
2,6-Dimethylnaphthalene						0.992	0.9231	262.00
2,3-Dimethylnaphthalene						0.992	0.9231	268.00
Diphenylmethane	0.884	0.026	2.9	0.726			0.9286	264.30
Acenaphthylene	0.871	0.030	3.4	0.715			0.9474	265-75
Acenaphthene	0.804	0.007	0.9	0.660		0.954	0.9351	279.00
Dibenzofuran	1.096	0.022	2.0	0.900			0.8571	287.00
2,3,5-Trimethylnaphthalene	0.892	0.034	3.8	0.732			0.9176	
Fluorene	0.883	0.014	1.6	0.725	1.036	0.989	0.9397	293-95
4-Azafluorene	1.006	0.002	0.2	0.826			0.8612	306.00
9,10-Dihydrophenanthrene	0.838	0.019	2.3	0.688			0.9333	
9,10-Dihydroanthracene						0.993	0.9333	305.00
1-Methylfluorene	0.934	0.014	1.5	0.767			0.9333	
2-Methylfluorene					1.135		0.9333	
Dibenzothiophene	1.119	0.009	0.8	0.919			0.7826	332-33
Phenanthrene	0.901	0.023	2.6	0.740	1.107	0.981	0.9438	340.00
Anthracene	0.883	0.015	1.7	0.725		0.975	0.9438	340.00
Benzo[*h*]quinoline	1.130	0.013	1.2	0.928			0.8715	338.00
1-Phenylnaphthalene	0.868	0.006	0.7	0.713			0.9412	334.00
Acridine	1.127	0.012	1.1	0.925			0.8715	346.00
Phenanthridine	1.168	0.013	1.1	0.959			0.8715	349.00
1-Methylphenanthrene					1.041		0.9375	358.60
2-Methylphenanthrene	0.938	0.014	1.5	0.770			0.9375	354.80
2-Methylanthracene	0.956	0.009	0.9	0.785		1.007	0.9375	358.60
9-Methylanthracene						0.946	0.9375	

(Continued on p. 298)

TABLE II *(continued)*

Compound	RRF_F	S.D.	R.S.D. (%)	RRF_{DMBA}	RRF'_F [13]	RRF''_F [14]	*CC*	B.p. (°C)
Carbazole	1.069	0.008	0.7	0.878			0.8623	355.00
1,2,3,6,7,8-Hexahydropyrene	0.980	0.020	2.0	0.805			0.9231	
3,6-Dimethylphenanthrene	0.977	0.032	3.3	0.802			0.9320	363.20
1,2,6,7-Tetrahydropyrene						1.139	0.9320	
Fluoranthene	1.000	0.000	0.0	0.821	1.000	1.000	0.9505	383.00
9-Phenylfluorene	0.995	0.015	1.5	0.817			0.9421	
9,10-Dimethylanthracene	0.982	0.008	0.8	0.806			0.9320	
Pyrene	0.992	0.008	0.8	0.814	1.092	0.985	0.9505	393.00
2-Phenylindole	1.192	0.016	1.3	0.979			0.8705	
Benzo[*a*]fluorene	1.149	0.009	0.8	0.943		1.072	0.9444	407.00
Benzo[*b*]fluorene	1.137	0.027	2.4	0.933	1.158		0.9444	401.00
1,1-Binaphthyl						0.971	0.9449	
Benz[*a*]anthracene	1.177	0.035	3.0	0.966			0.9473	437.50
Chrysene	1.117	0.076	6.8	0.917	1.260	1.049	0.9473	441.00
Triphenylene	1.161	0.012	1.0	0.953		0.959	0.9473	385.00
7,12-Dimethylbenz[*a*]anthracene	1.218	0.019	1.6	1.000		1.051	0.9375	
Benzo[*b*]fluoranthene	1.250	0.020	1.6	1.026			0.9524	
Benzo[*e*]pyrene	1.242	0.022	1.8	1.020	1.216	1.055	0.9524	492.90
Benzo[*a*]pyrene	1.251	0.041	3.3	1.027		0.912	0.9524	495.50
o-Phenylenepyrene					1.539		0.9565	
Perylene	1.253	0.061	4.9	1.029			0.9524	
Dibenz[*a,h*]anthracene	1.256	0.081	6.4	1.031		1.171	0.9496	
Benzo[*ghi*]perylene	1.269	0.036	2.8	1.042			0.9565	500.00
Anthanthrene					1.997		0.9103	
Coronene					2.134		0.9600	525.00

compound. Obviously, of the three above-mentioned injection methods, taking into account the great difference in volatility between the various PACs studied, those closest to and furthest from this ideal case are the cold on-column and split injection methods, respectively.

However, the unsubstituted PAHs, regardless of their carbon content and the injection technique used, show a decreasing response (and for that reason the *RRF* increases) as the boiling point increases. This variation is small in the cold on-column injection method (RRF_F dibenzo[*a,h*]anthracene − RRF_F naphthalene = 0.207) and greater for the other methods (split injection, RRF_F dibenzo[*a,h*]anthracene − RRF_F naphthalene = 0.463). In splitless injection, there is a sharp decrease in the response of the compounds of very high molecular mass (see anthanthrene and coronene in Table II). In Table II it can also be observed with cold on-column injection that the response is not the same for PAH isomers with the same carbon content. The difference in response between isomers increases as the carbon content and boiling point of these PAHs increase. The isomer that elutes later has a higher response (and a smaller *RRF*) than the isomer that elutes first [see Table II; RRF_F''(phenanthrene) − RRF_F''(anthracene) = 0.006, RRF_F''(fluoranthene) − RRF_F''(pyrene) = 0.015, RRF_F''(chrysene) − RRF_F''(triphenylene) = 0.090 and RRF_F''(benzo[*e*]pyrene) − RRF_F''(benzo[*a*]pyrene) = 0.143]. This effect is also observed in split injection but only with some isomers and is smaller than in the cold on-column injection technique. All these results show that even using the cold on-column injection method, the carbon content alone does not determine the response of the compounds in a flame ionization detector.

The alkylated PAHs, regardless of the injection technique, show an FID response lower (and for that reason a higher RRF_F) than the parent PAH compounds. In this group of compounds both the carbon content and the volatility are smaller than those of the corresponding PAHs. However, the hydro-PAH derivatives with split and cold on-column injection show a higher and lower response, respectively, than the parent PAHs. These compounds

show a higher volatility and a smaller carbon content than the parent PAHs. Finally, the hetero-PAH derivatives show in the split injection method a lower response (and a higher RRF_F) than the corresponding parent PAHs. FID response factors of hetero-PAH derivatives obtained using splitless or cold on-column injection techniques are not available in the literature. The carbon content and volatility of all these compounds is lower than those in the parent PAHs.

In general, from the data in Table II it can be concluded that, regardless of the nature of the PAC, the volatility is the factor that has the most influence on their response factors when the split and splitless injection techniques are used. When the cold on-column injection technique is used, the carbon content and volatility of the compound have an effect on their response factors, besides other factors not determined for isomers. However, the relative response factors obtained using the cold on-column injection technique are close to unity for the compounds studied.

The *RRF* values of some compounds not commercially available but present in the volatile fraction of coal tar pitch were calculated in an approximate way by taking the *RRF* values of the standard compounds as a basis. Table III gives these RRF_F and RRF_{DMBA} calculated values. The *RRF* values of compounds 5, 12, 13b, 14, 15, 16, 25, 26, 27, 36, 37 and 39a (peak numbers, see Fig. 1) were calculated by adding to the *RRF* values of the first of their series (namely dibenzofuran, dibenzo[*b*,*d*]thiophene, phenanthrene, benzo[*h*]quinoline, carbazole, fluoranthene, chrysene and benzo[*a*]pyrene) an increase corresponding to four or two carbon atoms, forming a new ring. In the phenanthrene–chrysene isomer interval the increase due to four or two carbon atoms was calculated from the difference in the *RRF* values of the average of the chrysene isomers or pyrene, respectively, and phenanthrene. In the

TABLE III

RELATIVE RESPONSE FACTORS CALCULATED FOR SOME COMPOUNDS

Peak No.[a]	Compound	RRF_F	RRF_{DMBA}
2	4*H*-Cyclopenta[*def*]phenanthrene	0.947	0.777
5	Benzonaphthofuran	1.367	1.122
10	Methylbenzonaphthofuran	1.409	1.157
11	Methylpyrene	1.034	0.849
12	Benzo[*b*]naphtho[2,1-*d*]thiophene	1.389	1.140
13b	Benzo[*c*]phenanthrene	1.172	0.962
14	Benzo[*ghi*]fluoranthene	1.091	0.896
15	Dibenzoquinoline	1.401	1.150
16	Benzo[*a*]naphtho[2,3-*d*]thiophene	1.389	1.140
20	Methylbenz[*a*]anthracene	1.219	1.001
22a	11*H*-Benz[*b*,*c*]aceantrylene	1.223	1.004
23a	4*H*-Cyclopenta[*def*]chrysene	1.223	1.004
24a	4*H*-Cyclopenta[*def*]triphenylene	1.207	0.991
25	11*H*-Benzo[*a*]carbazole	1.339	1.099
26	7*H*-Benzo[*c*]carbazole	1.339	1.099
27	5*H*-Benzo[*b*]carbazole	1.339	1.099
36	Benzo[*b*]chrysene	1.261	1.035
37	Picene	1.261	1.035
39a	Anthanthrene	1.326	1.089

[a] See Fig. 1.

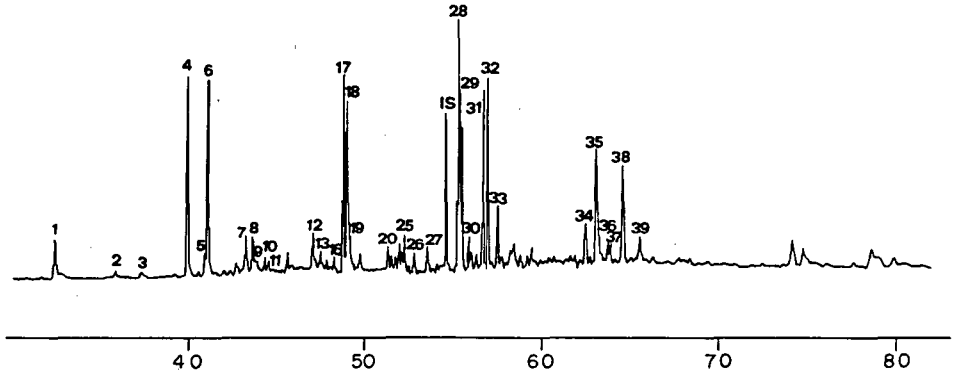

Fig. 1. Capillary gas chromatogram of the volatile fraction of a coal tar pitch on OV-1701 stationary phase. For peak identification, see Table IV. Internal standard (IS) = 7,12-dimethylbenz[*a*]anthracene.

TABLE IV

PAC CONCENTRATION IN THE COAL TAR PITCH EXTRACT, OBTAINED USING THE INTERNAL STANDARD METHOD (1) AND THE SEPARATE STANDARD METHOD (2)

Peak No.[a]	Compound	Method 1				Method 2			
		A_i/A_r[b]	S.D.[c]	R.S.D. (%)	mg/g of extract	A_i[b]	S.D.[c]	R.S.D. (%)	mg/g of extract
1	Phenanthrene	0.2025	0.0110	5.35	4.00	5785.33	203.99	3.53	3.52
2	4*H*-Cyclopenta[*def*]phenanthrene	0.0243	0.0006	2.56	0.50	783.67	20.27	2.59	0.50
3	Carbazole	0.0281	0.0016	5.69	0.65	997.33	39.47	3.95	0.72
4	Fluoranthene	0.5712	0.0160	2.74	12.53	17466.00	848.65	4.89	11.79
5	Benzonaphthofuran	0.0730	0.0022	3.04	2.19	2767.33	65.34	2.36	2.55
6	Pyrene	0.4900	0.0140	2.80	10.66	15783.00	302.08	1.91	10.55
7	Benzo[*a*]fluorene	0.1271	0.0045	3.59	3.20	4100.67	138.45	3.38	3.19
8	Benzo[*b*]fluorene	0.1221	0.0048	3.97	3.07	4291.00	78.79	1.84	3.32
9	Benzo[*c*]fluorene	0.0351	0.0023	6.06	0.89	848.00	4.97	0.59	0.65
10	Methylbenzonaphthofuran	0.0258	0.0017	6.81	0.80	951.00	23.04	2.42	0.90
11	Methylpyrene	0.0203	0.0010	4.94	0.46	825.67	18.45	2.23	0.58
12	Benzo[*b*]naphtho[2,1-*d*]thiophene	0.0981	0.0015	1.59	2.99	3341.33	145.51	4.35	3.13
13a	Tetrahydrochrysene	0.0489	0.0009	1.88	1.26	1401.00	89.71	6.40	1.11
13b	Benzo[*c*]phenanthrene								
14	Benzo[*ghi*]fluoranthene	0.0226	0.0009	4.18	0.54	955.00	58.67	6.14	0.71
15	Dibenzoquinoline	0.0259	0.0009	3.64	0.80	1020.00	59.60	5.84	0.96
16	Benzo[*a*]naphtho[2,3-*d*]thiophene	0.0379	0.0015	4.16	1.15	1114.33	33.31	2.99	1.04
17	Benz[*a*]anthracene	0.3808	0.0050	1.33	9.83	12337.67	387.92	3.14	9.81
18	Chrysene	0.5207	0.0083	1.60	13.45	16687.67	677.80	4.06	13.25
19	Triphenylene	0.1494	0.0054	3.60	3.81	3906.33	51.14	1.32	3.06
20	Methylbenz[*a*]anthracene	0.0676	0.0030	4.46	1.80	2058.67	24.53	1.19	1.69

21	Methylbenz[*a*]anthracene	0.0245	0.0005	0.02	0.65	770.00	55.76	7.24	0.64
22a	11*H*-Benz[*bc*]aceanthrylene	0.0227	0.0009	3.96	0.61	896.67	65.45	7.30	0.75
22b	Binaphthalene								
23a	4*H*-Cyclopenta[*def*]chrysene	0.0499	0.0024	4.84	1.33	1756.00	22.46	1.28	1.45
23b	Binaphthalene								
24a	4*H*-Cyclopenta[*def*]triphenylene	0.0483	0.0026	5.52	1.27	2095.33	43.21	2.06	1.70
24b	Dimethylbenz[*a*]anthracene								
25	11*H*-Benzo[*a*]carbazole	0.0930	0.0012	1.27	2.73	3188.67	84.95	2.66	2.88
26	7*H*-Benzo[*c*]carbazole	0.0578	0.0019	3.26	1.69	1790.33	106.91	5.97	1.62
27	5*H*-Benzo[*b*]carbazole	0.0417	0.0038	9.09	1.22	1743.33	43.41	2.49	1.58
28	Benzo[*j*]fluoranthene	0.5190	0.0032	0.61	14.42	16017.33	211.40	1.32	13.68
29	Benzo[*b*]fluoranthene	0.5068	0.0045	0.90	14.07	14438.00	123.79	0.86	12.34
30	Benzo[*k*]fluoranthene	0.0776	0.0014	1.87	2.16	2298.33	62.78	2.73	1.97
31	Benzo[*e*]pyrene	0.4273	0.0036	0.83	11.73	12730.00	123.81	0.97	10.75
32	Benzo[*a*]pyrene	0.4928	0.0019	0.38	13.53	14627.00	370.58	2.53	12.35
33	Perylene	0.1215	0.0021	1.70	3.34	3909.00	88.23	2.26	3.31
34	Dibenz[*a,j*]anthracene	0.1241	0.0031	2.48	3.42	3670.33	117.01	3.19	3.12
35a	Indenopyrene	0.4335	0.0220	4.96	11.95	12622.33	135.14	1.07	10.69
35b	Dibenz[*a,c*]anthracene								
36	Benzo[*b*]chrysene	0.0723	0.0077	10.68	1.99	1924.67	90.87	4.72	1.63
37	Picene	0.0691	0.0031	4.43	1.91	1911.67	74.84	3.92	1.62
38	Benzo[*ghi*]perylene	0.3404	0.0150	4.39	9.42	10709.67	43.52	0.41	9.11
39a	Anthanthrene	0.0953	0.0028	2.99	2.63	3892.67	435.97	11.20	2.52
39b	Methyl derivative of indenopyrene								

[a] See Fig. 1.
[b] A_i and A_r are peak-area counts of the particular compound i and the reference compound, respectively.
[c] Standard deviation obtained in five determinations.

chrysene–anthanthrene interval, the increase due to four or two carbon atoms was calculated from the difference in the *RRF* values of dibenzo[*a*,*h*]-anthracene or average of benzo[*a*]- and benzo[*e*]pyrene, respectively, and the average of the chrysene isomers. The *RRF* values of methyl derivatives [compounds (peaks) 10, 11 and 20] were calculated by adding to each parent compound (namely benzonaphthofuran, pyrene and benzo[*a*]anthracene) an increase for the methyl group. This increase is an average value obtained from different methyl derivative compounds in Table II. Finally, the RRF values of compounds (peaks) 2, 22a, 23a and 24a were calculated adding to the RRF of phenanthrene, benz[*a*]anthracene, chrysene and triphenylene an increase corresponding to a ring-forming methylene group. This increase was calculated from the difference between the RRF_F values of fluorene and diphenyl.

Taking into account the relative response factors in Tables II and III, the determination of the main components of the coal tar pitch volatile fraction was carried out. Fig. 1 shows the capillary gas chromatogram of the sample to be quantified. For quantification the internal standard method (method 1) was used. The standard compound to be used must satisfy certain requirements [19,20] and for this mixture 7,12-dimethylbenz[*a*]anthracene was selected. The absolute calibration method with a separate standard (method 2) was also used [8,21]. In this instance, fluoranthene was the separate standard compound. Table IV shows the results of quantification with both methods. The reproducibility of the determinations in both methods represented by the S.D. and R.S.D. can be considered to be satisfactory. Only in a small number of cases is the R.S.D. value higher than 5%. The PAC concentrations found in the coal tar pitch extract are also fairly similar using both methods. However, it should be pointed out that from benzo[*j*]fluoranthene to the end, a slightly higher concentration is obtained with the internal standard method. This could be due to the use of fluoranthene as a separate standard, because this compound elutes at the beginning of the chromatogram. In spite of this, either of the two methods can be used to determine the main components of the coal tar pitch volatile fraction.

ACKNOWLEDGEMENTS

This work was supported by the DGICYT, Project No. PB88-0002. M. J. Iglesias thanks the Consejo Superior de Investigaciones Cientificas for a postdoctoral fellowship. We are indebted to E. Peláez and M. Pozo for assistance with this work.

REFERENCES

1 C. G. Blanco, J. Blanco, J. Bermejo and M. D. Guillén, *J. Chromatogr.*, 465 (1989) 378.
2 M. D. Guillén, J. Blanco, J. Bermejo and C. G. Blanco, *J. High Resolut. Chromatogr.*, 12 (1989) 552.
3 M. L. Lee, D. L. Vassilaros, C. M. White and M. Novotny, *Anal. Chem.*, 51 (1979) 768.
4 K. D. Bartle, M. L. Lee and S. A. Wise, *Chromatographia*, 14 (1981) 69.
5 R. H. Rohrbaugh and P. C. Jurs, *Anal. Chem.*, 58 (1986) 1210.
6 C. G. Blanco, J. Blanco, P. Bernard and M. D. Guillén, *J. Chromatogr.*, 539 (1991) 157.
7 M. D. Guillén, M. J. Iglesias, A. Domínguez and C. G. Blanco, *J. Chromatogr.*, 591 (1992) 287.
8 A. Bjorseth (Editor), *Handbook of Polycyclic Aromatic Hydrocarbons*, Marcel Dekker, New York, Basle, 1983.
9 A. Bjorseth and T. Randall (Editors), *Handbook of Polycyclic Aromatic Hydrocarbons*, Vol. 2, Marcel Dekker, New York, Basle, 1985.
10 M. D. Guillén, J. Blanco, J. S. Canga and C. G. Blanco, *Energy Fuels*, 5 (1991) 188.
11 C. K. Huynh, *Trav. Hyg.*, 71 (1980) 532.
12 R. C. Lao, R. S. Thomas, H. Oja and L. Dubois, *Anal. Chem.*, 45 (1973) 908.
13 A. Bjorseth, *Anal. Chim. Acta*, 94 (1977) 21.
14 H. Y. Tong and F. W. Karasek, *Anal. Chem.*, 56 (1984) 2124.
15 R. C. Weast (Editor), *Handbook of Chemistry and Physics*, CRC Press, Boca Raton, FL, 66th ed., 1985–86.
16 K. F. Lang and I. Eigen, *Fortschr. Chem. Forsch.*, 8 (1967) 91.
17 A. D. Jorgensen, K. C. Picel and V. C. Stamoudis, *Anal. Chem.*, 62 (1990) 683.
18 Huang Yieru, Ou Quingyu and Ju Weile, *Anal. Chem.*, 62 (1990) 2063.
19 P. Bocek, J. Novak and J. Janak, *J. Chromatogr.*, 42 (1969) 1.
20 L. S. Ettre and A. Zlatkis (Editors), *The Practice of Gas Chromatography*, Wiley-Interscience, New York, London, Sydney, 1967.
21 D. E. Willis, *Chromatographia*, 5 (1972) 42.

Journal of Chromatography, 607 (1992) 303–309
Elsevier Science Publishers B.V., Amsterdam

CHROM. 24 086

Some observations on clean-up procedures using sulphuric acid and Florisil

J. L. Bernal*, M. J. Del Nozal and J. J. Jiménez

Department of Analytical Chemistry, Faculty of Sciences, University of Valladolid, E-47005 Valladolid (Spain)

ABSTRACT

The stability and recovery of 84 pesticides and 12 polychlorinated biphenyls after treatment with sulphuric acid have been studied. The results of these studies have been applied to the analysis of samples with different fat contents and compared with the results obtained using Florisil. The treatment with acid has a narrower field of application than treatment on a Florisil column.

INTRODUCTION

The determination of pesticides by high-resolution gas chromatography (HRGC) usually requires preliminary purification of the extracts before injection to simplify the process and to protect the instrumentation used. Extracts can be purified by various procedures such as liquid–liquid partitioning [1], treatment with acids [2] and bases [3], adsorption chromatography over Florisil [4], silica gel [5] or alumina [6], or gel permeation chromatography (GPC) [7]. These procedures are used alone or in combination depending on the complexity of the sample matrix. For example, a combination of GPC plus adsorption chromatography over silica gel, has been applied to clean-up more than 400 pesticides and metabolites in foods of animal and vegetable origin [8].

In this work we studied in detail the treatment with sulphuric acid, which is recommended by some workers [9–11] for the purification of organochlorine compounds and, in particular, for the rapid determination of polychlorinated biphenyls (PCBs) because of its economy and effectiveness. The main difficulty in the study was to determine the stability of various compounds to the treatment. In fact, although there are much data available for organochlorine substances, there is little information available on pesticides except for that published by the Royal Society of Chemistry [12] and the British Crop Protection Council [13], which give no precise numerical data but state whether the pesticides are stable or are partly or completely destroyed by sulphuric acid treatment. In this context, there seems to be universal agreement about the stability of products such as chlorinated hexanes (HCHs), chlordane, DDT, hexachlorobenzene (HCB) and PCBs. Also, although dieldrin, tetradifon and heptachlor epoxide are generally accepted to be destroyed, other pesticides, including aldrin, are believed by some workers to remain unaltered and to be partly or fully destroyed on treatment by others [14–22].

It is therefore important to obtain a fairly good idea of the effect that a given acid treatment has on pesticides before it is applied to them. We carried out a comprehensive study of the behaviour of different pesticides and PCBs towards sulphuric acid and determined the amounts remaining after treatment wherever possible. The conclusions drawn from this study were subsequently applied to real samples of different fat contents and the results obtained were compared with those achieved by the most commonly used procedure for this purpose: subfractionation on a Florisil column.

0021-9673/92/$05.00

EXPERIMENTAL

Chromatographic system

The chromatographic system consisted of a Hewlett-Packard 5890 gas chromatograph equipped with a ^{63}Ni electron-capture detector, using argon–methane as the auxiliary gas, and a nitrogen–phosphorus thermionic detector. An HP 7673A automatic injector and DB-5 and DB-17 capillary columns (30 m × 0.25 mm I.D., 0.25 μm film thickness) from J&W Scientific were used with 0.6 ml/min of helium as the carrier gas. The equipment was controlled via an HP 3363 ChemStation. The temperature of the injection port was 200°C, whereas that of the detector was 300°C. The temperature programme used was as follows: initial temperature, 57°C for 1 min; 15°C/min ramp up to 130°C, hold for 1 min; 2.3°C/min ramp; final temperature, 270°C for 20 min.

Standards

Chromatographically pure (97% minimum) pesticide and PCB standards were purchased from Chemservice (West Chester, PA, USA), Riedel de Haën (Seelze, Hannover, Germany), Scharlau (Barcelona, Spain) and Promochem (Wesel, Germany). Certified reference materials of different products were supplied by Promochem: potato (R900070), carrot (R900062), olive oil (R900080), butter (R900010) and lyophilized fish tissue (MAB-30C).

Reagents

Trace-analysis-grade methanol, diethyl ether, *n*-hexane and dichloromethane were purchased from Scharlau and SDS (Pepyn, France). Florisil of 60–100 mesh was supplied by Baker (Deventer, Netherlands). Pro-analysis anhydrous sodium sulphate (99% minimum purity) and concentrated 95–97% sulphuric acid were purchased from Scharlau. Ultrapure water obtained with a Nanopure II apparatus from Barnstead (Newton, MA, USA) was used throughout.

Extraction of certified samples

Organochlorine compounds were extracted from the reference materials using a Soxhlet battery and *n*-hexane as the solvent. A 1.5-g amount of each sample was mixed homogeneously with anhydrous sodium sulphate in a 1:3 (w/w) ratio and was subjected to extraction for 3.5 h. The resulting extract was concentrated at 40°C in a rotary evaporator Büchi (Plawil, Switzerland) evacuated to a final volume of 1 ml.

Acid clean-up

Certified reference materials. A 1-ml volume of each *n*-hexane extract was treated with 1 ml of concentrated sulphuric acid in screw-cap septum vials and immersed in an ultrasonic bath (Selecta, Barcelona, Spain) for 10 min. After separation, the organic phase was collected and the acid phase was washed with 2 ml of *n*-hexane. Each organic portion was added to the previous organic portion and then washed with 5 ml of ultrapure water. The organic portion was dried with anhydrous sodium sulphate that had previously been washed with *n*-hexane, and was concentrated at low temperature in the rotary evaporator under vacuum (1 ml); the sample was then ready for analysis by HRGC.

Individual pesticides. Pesticides and PCBs were dissolved in *n*-hexane with the exception of the more polar substances, which were dissolved in *n*-hexane–dichloromethane (1:1, v/v). The working concentration used was 0.1 mg/l. A 1-ml volume of the organic phase was treated with 1 ml of concentrated sulphuric acid in screw-cap septum vials and immersed in an ultrasonic bath for 10 min. After the phases were separated, the acid was washed with 2 ml of *n*-hexane, and the organic phases were combined and concentrated to 1 ml in the rotary evaporator.

Clean-up with Florisil

The organochlorine compounds in the certified reference materials were cleaned up using a glass column packed with 5 g of Florisil that was previously activated by heating. Subfractionation was started by elution first with 11.5 ml of *n*-hexane and then with 15 ml of *n*-hexane–dichloromethane (1:1, v/v). All PCBs were determined in the first fraction and most pesticides were determined in the second. The recovery from individual standards (at a concentration of 0.1 mg/l) was studied and then the same procedure was applied to extracts from the certified samples.

In every instance, the volume eluted in each fraction was evaporated to dryness under vacuum in the rotary evaporator and then dissolved in 1 ml of *n*-hexane.

Quantitation of the compounds

The compounds assayed were quantified by HRGC with an electron-capture detector or a nitrogen–phosphorus thermionic detector. Chlorpyrifos, a chlorinated organophosphorus pesticide, was used as a reference standard to correct instrumental fluctuations. An injected volume of 1 μl was used in all assays, which were performed in quintuplicate.

RESULTS AND DISCUSSION

Treatment of individual compounds with sulphuric acid

Tables I and II list the results obtained in the stability assays performed on the organochlorine compounds and other pesticides, respectively.

A recovery of 95% is considered to be acceptable for the organochlorine compounds (Table I). As expected, compounds such as HCB, HCHs, DDT, dichlorodiphenyldichloroethylene (DDE), tetrachlorodiphenylethane (TDE), dicofol, pentachloronitrobenzene (PCNB) and heptachlor are not affected by the acid. However, compounds such as chlorbenside, chlortal dimethil, endrin aldehyde, endosulfan A and B, endrin and dieldrin are vulnerable to the acid treatment, the last two as reported elsewhere [15,16,19,22]. Aldrin seems to withstand the acid treatment to some extent as only 34% of the initial content is lost, although other workers [19] have found that it is recovered almost completely. Heptachlor epoxide (recovery 52.5%) is not destroyed fully, contrary to previous reports [14]. Tetradifon (recovery 9.9%) and chlorfenson (recovery 22.5%) are only poorly recovered, consistent with earlier findings [15], as are silvex (13.2%) and methoxychlor (15.0%).

With respect to the PCBs, the less chlorinated compounds (*i.e.* those containing one to five chlorine atoms) are recovered in lower proportions (less than 98%) than the others.

It is worth noting the diverse recoveries of the phenols, which in theory should not have been destroyed. Although the recovery of pentachlorophenol can be regarded as normal, those of dichlorophenol and trichlorophenol are not. These anomalies can be attributed to the higher volatility of these two compounds, which implies a greater loss in the clean-up process. In addition, they can be dehydrated by sulphuric acid.

TABLE I

RECOVERY (MEAN AND STANDARD DEVIATION) OF ORGANOCHLORINE COMPOUNDS AFTER PURIFICATION WITH SULPHURIC ACID

Samples were analysed in quintuplicate.

Compound	Recovery (%)	
	Mean	σ_{n-1}
2,4-Dichlorophenol	38.3	7.2
2,4,5-Trichlorophenol	15.7	3.6
Pentachlorophenol	92.0	4.8
α-HCH	91.4	3.8
β-HCH	96.6	4.1
Lindane	97.8	4.6
δ-HCH	97.0	3.5
Aldrin	66.0	4.3
Endrin	N.D.[a]	–
Endrin aldehyde	N.D.	–
Dieldrin	N.D.	–
4,4′-DDT	98.4	3.2
4,4′-DDE	96.3	3.5
4,4′-TDE	97.2	4.3
Methoxychlor	15.0	4.6
Dicofol	95.1	2.6
Heptachlor epoxide	52.5	8.6
Heptachlor	99.4	4.1
PCNB	97.5	8.0
HCB	97.4	4.4
Chlorthal dimethil	N.D.	–
Chlorfenson	22.5	4.6
Chlorbenside	N.D.	–
Tetradifon	9.9	1.7
Endosulfan A	N.D.	–
Endosulfan B	N.D.	–
Fenoprop	13.2	2.1
PCB 2	95.4	4.7
PCB 7	96.8	5.0
PCB 28	97.3	3.7
PCB 47	97.8	4.6
PCB 52	97.6	4.6
PCB 101	97.9	3.5
PCB 138	98.9	3.7
PCB 153	99.5	3.2
PCB 180	98.9	4.0
PCB 194	99.8	2.6
PCB 206	99.4	4.7
PCB 209	99.3	5.0

[a] Not detected.

Most of the members of the other pesticide families (Table II) react to a greater or lesser extent with the acid. This clean-up procedure cannot be applied to compounds such as organophosphates, pyreth-

TABLE II

RECOVERY OF OTHER PESTICIDES AFTER TREATMENT WITH SULPHURIC ACID

Pesticide	Recovery (%)	Pesticide	Recovery (%)
Organophosphates		*Oxazolidine*	
TEPP	N.D.[a]	Vinclozolin	N.D.
Chlorpyrifos	N.D.	*Triazapentadiene*	
Tetrachlorvinphos	1	Amitraz	N.D.
Ethion	N.D.	*Phthalimides*	
Malathion	N.D.	Captan	N.D.
Phorat	N.D.	Captafol	N.D.
Phosalone	1	Dialifos	N.D.
Demeton-s-methyl	N.D.	*Pyrethroids*	
Triazophos	N.D.	Permethrin	32
Phosdrin mevinphos	N.D.	Cypermethrin	10
Azinphos methyl	N.D.	*Acetamides*	
Acephat	N.D.	Alachlor	N.D.
Fenitrothion	18	Propachlor	N.D.
Parathion ethyl	23	Propanil	N.D.
Dichlorvos	3	*Nitro compounds*	
Naled	7	Dinoseb	76
Pirimiphos ethyl	N.D.	Dinobuton	N.D.
Pirimiphos methyl	N.D.	*Ureas*	
Pyrazophos	N.D.	Chlorsulfuron	N.D.
Diazinon	N.D.	Chlortoluron	N.D
Carbamates		Chlorbromuron	N.D.
Triallate	N.D.	Diuron	N.D.
Aldicarb sulphoxide	N.D.	*Amides*	
Pirimicarb	N.D.	Napropamide	N.D.
Sulfallate	N.D.	Dichlofluanid	N.D.
Propham	29	*Imidazols*	
Carbaryl	25	Imazalil	N.D.
Triazines		Prochloraz	N.D.
Atrazine	N.D.	*Nitroanilines*	
Simazine	N.D.	Trifluralin	78
Terbutryn	N.D.	Dicloran	70
Metamitron	16		
Prometryne	10		
Uracil			
Bromacil	N.D.		
Nitriles			
Bromoxynil octano	N.D.		
Chlorothalonil	66		
Dichlobenil	68		

[a] Not detected.

roids, triazines, carbamates, phthalimides and amides. Only a few of the pesticides assayed, such as dinoseb (76%), dicloram (70%), trifluralin (78%), dichlobenil (68%) and chlorothalonil (66%) appear to withstand the acid treatment to some extent. It should be noted that our experimental results diverge from previous reports. Thus acephate and fenitrothion, which are stable against the acid according to some workers [17], were destroyed in this study, [the former completely and the latter almost fully (recovery 18%)]. Also, trifluralin and dicloran, which have been reported as unstable [15], were recovered at rates of 78 and 79%, respectively; in addition our results show that pirimiphos methyl is

completely destroyed on acid treatment and malathion is not recovered. This contrasts with previous reports [20].

The full destruction of compounds such as fenoprop, tetradifon, chlorfenson, methoxychlor and heptachlor epoxide, and the low recoveries obtained for others such as dinoseb, dicloran, trifluralin, dichlobenil and chlorothalonil, make it advisable to conduct preliminary assays to determine their recoveries before any real analyses are undertaken.

Fractionation of organochlorine compounds on a Florisil column

Table III lists the results obtained for the organochlorine compounds and the PCBs. The first fraction contained the PCBs, which were recovered quantitatively, plus some compounds that could not be fully resolved, *e.g.* 2,4-dichlorophenol, 2,4,5-trichlorophenol, pentachlorophenol, aldrin, *p,p'*-DDE, heptachlor and HCB. All these, with the exception of the three chlorophenols, were eluted by 60–70% in the first fraction.

The reproducibility achieved in these assays was fairly good for those compounds that were fully eluted in the first or second fraction (small standard deviations, σ_{n-1}), and poorer for those compounds that divided between two fractions.

Comparison of the treatments with sulphuric acid or Florisil as applied to certified reference materials

To check the results obtained in the individual assays the organochlorine compounds were also extracted from samples of certified composition, aliquots of which were subjected to acid treatment or subfractionation on a Florisil column. The results obtained are summarized in Tables IV–VII for olive oil, butter, lyophilized fish tissue and potato and carrot, respectively. Some interesting conclusions were drawn.

As can be seen in the tables, the clean-up on a Florisil column is as efficient as that obtained with sulphuric acid for a given sample matrix; therefore the recovery is higher than 95% except for the pesticides altered by the acid. The reproducibility (expressed as the relative standard deviation) of the Florisil clean-up procedure (3–4.5%) is higher than that of the sulphuric acid treatment (4.5–5.5%). The chromatograms obtained differed markedly from matrix to matrix. The extracts treated with Florisil (Fig. 1) were noiseless, with a well defined baseline reaching as far as 45 min, after which a large number of tall and well defined peaks appear. The baseline is restored after 65 min.

TABLE III

RECOVERIES (MEAN AND STANDARD DEVIATION) OF ORGANOCHLORINE COMPOUNDS IN THE FIRST AND SECOND FRACTION OBTAINED AFTER TREATMENT WITH A FLORISIL COLUMN

See Experimental for the details of fractionation. Samples were analysed in quintuplicate.

Compound	Recovery (%)		
	First fraction	Second fraction	
		Mean	σ_{n-1}
2,4-Dichlorophenol	5.3	94.7	2.5
2,4,5-Trichlorophenol	6.7	93.3	2.6
Pentachlorofenol	7.6	92.4	3.8
Endosulfan A	–	98.0	0.6
Endosulfan B	–	96.9	0.5
α-HCH	–	97.4	0.4
β-HCH	–	98.6	0.5
Lindane	–	99.5	0.3
δ-HCH	–	98.4	0.4
Endrin	–	98.2	0.4
Dieldrin	–	98.2	0.2
Aldrin	89.4	10.6	7.1
4,4'-DDT	–	99.0	0.5
4,4'-DDE	61.6	38.4	3.2
4,4'-TDE	–	94.3	0.6
Methoxychlor	–	98.0	0.4
Heptachlor epoxide	–	98.4	0.5
Heptachlor	69.6	30.4	7.8
PCNB	–	97.4	0.3
HCB	67.2	32.8	3.3
Chlorthal dimethyl	–	97.8	0.4
Tetradifon	–	96.0	0.6
Chlorfenson	–	98.4	0.2
Fenoprop	–	97.2	1.6
Chlorbenside	–	98.3	1.6
PCB 2	97.8	–	0.2
PCB 7	98.7	–	0.2
PCB 28	99.0	–	0.3
PCB 47	99.4	–	0.2
PCB 52	99.1	–	0.2
PCB 101	99.3	–	0.2
PCB 138	99.5	–	0.2
PCB 153	99.5	–	0.1
PCB 180	99.4	–	0.1
PCB 194	99.8	–	0.2
PCB 206	99.5	–	0.3
PCB 209	99.6	–	0.2

TABLE IV

RECOVERIES (MEAN AND STANDARD DEVIATION) OBTAINED AFTER ACID OR FLORISIL TREATMENT OF CERTIFIED REFERENCE MATERIAL OLIVE OIL

Samples were analysed in quintuplicate.

Compound	Certified amount (μg/g)	Recovery (%)			
		Florisil		H_2SO_4	
		Mean	σ_{n-1}	Mean	σ_{n-1}
Lindane	0.20	95.0	4.6	95.0	5.8
HCB	0.15	96.7	4.2	95.8	4.4
α-HCH	0.20	96.0	4.4	95.4	6.5
β-HCH	0.10	95.4	4.5	96.3	4.7
4,4'-TDE	0.10	94.9	3.6	95.5	5.0
4,4'-DDT	0.30	97.8	3.0	96.4	4.6
Dieldrin	0.25	95.6	3.9	N.D.[a]	N.D.
PCB 52	0.10	98.6	4.1	98.5	5.3
PCB 101	0.20	98.5	4.0	98.9	4.0
PCB 153	0.15	98.5	3.8	98.4	4.7

[a] Not detected.

TABLE V

RECOVERIES (MEAN AND STANDARD DEVIATION) OBTAINED AFTER ACID OR FLORISIL TREATMENT OF CERTIFIED REFERENCE MATERIAL BUTTERFAT

Samples were analysed in quintuplicate.

Compound	Certified amount (μg/g)	Recovery (%)			
		Florisil		H_2SO_4	
		Mean	σ_{n-1}	Mean	σ_{n-1}
Endosulfan A	0.35	98.6	3.1	N.D.[a]	N.D.
Endosulfan B	0.25	97.5	4.7	N.D.	N.D.
α-HCH	0.25	96.9	2.7	97.4	5.3
Lindane	0.30	98.6	3.6	98.0	6.0
Methoxychlor	0.15	96.3	3.8	N.D.	N.D.
HCB	0.20	98.4	3.8	99.0	5.3
PCB 28	0.20	98.4	2.9	98.7	5.0
PCB 52	0.25	98.6	3.1	98.6	4.8
PCB 101	0.30	98.4	3.4	98.7	5.2
PCB 138	0.30	98.5	3.7	98.3	4.7
PCB 153	0.25	98.0	2.8	98.5	5.5
PCB 180	0.20	98.7	3.6	98.4	4.3

[a] Not detected.

TABLE VI

RECOVERIES (MEAN AND STANDARD DEVIATION) OBTAINED AFTER ACID OR FLORISIL TREATMENT OF CERTIFIED REFERENCE MATERIAL LYOPHILIZED FISH

Samples were analysed in quintuplicate.

Compound	Certified amount (ng/g)	Recovery (%)			
		Florisil		H_2SO_4	
		Mean	σ_{n-1}	Mean	σ_{n-1}
Lindane	3.4	99.9	8.7	99.8	9.1
HCB	1.5	99.8	6.8	100.7	10.0
α-HCH	10	100.0	6.9	99.4	8.0
4,4'-DDE	160	98.3	5.3	98.0	6.0
4,4'-DDT	65	99.5	5.0	99.4	7.6
4,4'-TDE	46	99.8	5.5	99.7	7.4
Aldrin	1.8	99.7	7.4	N.D.[a]	N.D.
Dieldrin	5.3	101.0	6.6	N.D.	N.D.
PCB 101	61	99.8	5.2	99.9	8.1
PCB 138	170	98.5	4.2	98.4	5.5
PCB 153	120	98.3	4.3	98.9	5.3
PCB 180	35	99.9	5.1	99.7	6.5

[a] Not detected.

TABLE VII

RECOVERIES (MEAN AND STANDARD DEVIATION) OBTAINED AFTER ACID OR FLORISIL TREATMENT OF CERTIFIED REFERENCE MATERIALS POTATO AND CARROT (NO FATTY SAMPLES)

Samples were analysed in quintuplicate.

Compound	Certified amount (μg/g)	Recovery (%)			
		Florisil		H_2SO_4	
		Mean	σ_{n-1}	Mean	σ_{n-1}
Potato					
Endosulfan A	0.70	97.5	2.8	N.D.[a]	N.D.
Endosulfan B	0.30	97.9	4.1	N.D.	N.D.
Lindane	0.20	99.0	3.4	98.4	5.1
Methoxychlor	0.90	98.4	3.0	N.D.	N.D.
HCB	0.20	99.1	4.0	97.9	4.3
4,4'-DDT	0.50	98.2	3.6	98.5	6.5
PCB 52	0.25	98.5	4.2	97.9	4.5
PCB 101	0.30	98.6	3.6	99.0	5.1
PCB 180	0.50	98.3	3.5	98.5	4.2
PCB 209	0.50	98.5	3.5	98.1	4.4
Carrot					
Pentachlorophenol	1.00	98.5	4.2	95.0	5.2

[a] Not detected.

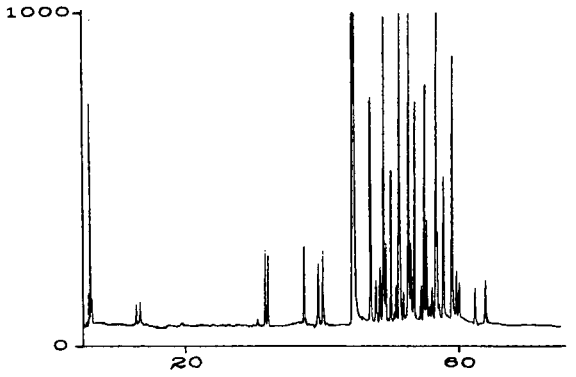

Fig. 1. Chromatogram of a butterfat extract obtained after treatment on a Florisil column. x-Axis in min; y-axis in counts.

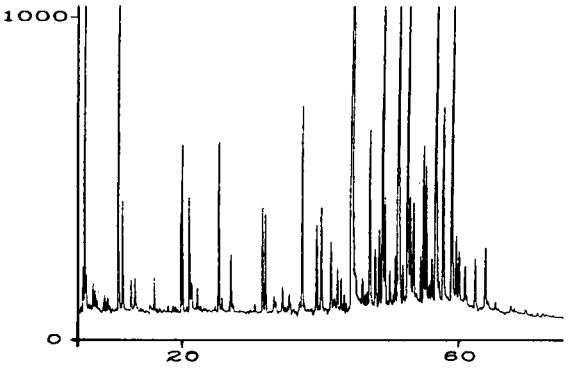

Fig. 2. Chromatogram of a butterfat extract obtained after treatment with sulphuric acid. x- and y-axes as in Fig. 1.

The chromatograms obtained with the acid-treated extracts (Fig. 2) have a noisy baseline, generally after 25 min but occasionally from the beginning. There are low-intensity peaks that can be assigned to the decomposition products.

CONCLUSIONS

Although the acid treatment offers major advantages in terms of simplicity, economy, rapidity and efficiency, it should be applied cautiously as it completely or partly destroys many compounds, which may in turn give rise to spurious results. Thus, although it does not affect the determination of PCBs, HCHs, DDT, DDE, TDE, dicofol, HCB, PCNB or heptachlor, it does decompose organochlorine compounds such as endosulfan A and B, chlorbenside, chlortal dimethil, endrin, endrin aldehyde and dieldrin, and most organophosphorus compounds, pyrethroids, triazines, carbamates, phthalimides and amides. This requires the extent of decomposition to be determined before any analyses are performed or an alternative treatment applied. If the behaviour of the compounds towards the acid is known, then complex samples can be analysed with similar results in terms of recoveries to those provided by Florisil subfractionation, even though the scope of application is more limited.

REFERENCES

1 P. A. Mills, *J. Assoc. Off. Anal. Chem.*, 42 (1959) 734.
2 P. G. Murphy, *J. Assoc. Off. Anal. Chem.*, 55 (1972) 1360.
3 S. J. V. Young and J. A. Burke, *Bull. Environ. Contam. Toxicol.*, 7 (1972) 160.
4 P. A. Mills, J. H. Onley and R. A. Gather, *J. Assoc. Off. Anal. Chem.*, 46 (1963) 186.
5 A. V. Holden and K. Marsden, *J. Chromatogr.*, 44 (1969) 481.
6 N. J. Kueseth and E. M. Brevik, *Bull. Environ. Contam. Toxicol.*, 21 (1979) 213.
7 K. E. McLeod, R. C. Honish and R. G. Lewis, *J. Anal. Toxicol.*, 6 (1982) 38.
8 W. Specht and M. Tillkes, *Fresenius Z. Anal. Chem.*, 322 (1985) 443.
9 R. Amarowicz, B. Olender and L. Pawlicki, *Rocz. Panstw. Zakl. Hig.*, 39 (1988) 297.
10 A. Pastor, F. Hernández and J. Medina, *Mar. Pollut. Bull.*, 19 (1988) 235.
11 S. M. Waliszewski and G. A. Szymczynski, *J. Assoc. Off. Anal. Chem.*, 65 (1982) 677.
12 D. Hartley and H. Kidd (Editors), *The Agrochemicals Handbook*, Royal Society of Chemistry, Nottingham, 2nd ed., 1988.
13 C. R. Worthing (Editor), *The Pesticide Manual*, British Crop Protection Council, Thornton Heath, 8th ed., 1987.
14 Y. Mizushima and M. Hiroyuki, *Niigata Ken Kogai Kenkyusho Kenkya Hokoku*, 6 (1982) 110.
15 F. Hernández, F. J. López Benet and J. Medina, *J. Assoc. Off. Anal. Chem.*, 70 (1987) 727.
16 P. P. Singh and R. P. Chawla, *J. Chromatogr.*, 457 (1988) 387.
17 P. Rodríguez, J. Permanyer, J. M. Grases and C. Gonzalez, *J. Chromatogr.*, 562 (1991) 547.
18 M. Camps, J. Planas and J. Gómez-Catalán, *Bull. Environ. Contam. Toxicol*, 42 (1989) 195.
19 A. DiMuccio, A. Santilio, R. Dommarco, M. Rizzica, L. Gambetti, A. Ausili and F. Vergori, *J. Chromatogr.*, 513 (1990) 33.
20 H. Wan, *J. Chromatogr.*, 516 (1990) 446.
21 A. L. Smrek and L. L. Needham, *Bull Environ. Contam. Toxicol.*, 28 (1982) 718.
22 D. Veierov and N. Aharonson, *J. Assoc. Off. Anal. Chem.*, 61 (1978) 253.

Journal of Chromatography, 607 (1992) 311–318
Elsevier Science Publishers B.V., Amsterdam

CHROM. 24 137

Identification by gas chromatography–electron-capture detection and gas chromatography–mass spectrometry of the ozonation products in wastewater from dicofol and tetradifon manufacturing

M. P. Ormad Melero*, J. Sarasa Alonso, A. Puig Infante, M. C. Martínez Navascués and N. Cebrián Guajardo

Departamento de Ingeniería Química y Tecnología del Medio Ambiente, Facultad de Ciencias, Universidad de Zaragoza, Pza San Francisco s/n, 50009 Zaragoza (Spain)

M. S. Mutuberría Cortabitarte

Confederación Hidrográfica del Ebro, Laboratorio, Paseo de Sagasta 26–28, 50006 Zaragoza (Spain)

J. L. Ovelleiro Narvión

Departamento de Ingeniería Química y Tecnología del Medio Ambiente, Facultad de Ciencias, Universidad de Zaragoza, Pza San Francisco s/n, 50009 Zaragoza (Spain)

ABSTRACT

In this work, a first step has been made in the characterization of the organic pollutants found in the residual water from the production of dicofol and tetradifon pesticides. Two techniques of sample concentration, liquid–liquid and solid–liquid extraction, for nineteen organochlorine compounds are compared. The extracts obtained were analysed using gas chromatography with electron-capture detection and gas chromatography with mass spectrometry; a total of 58 organic compounds were identified. The behaviour of the effluent was also studied using degradation techniques (treatment with ozone in a basic medium), whereby a large number of substances were removed. In all cases, the chemical structures of the molecules involved in the ozonation were determined.

INTRODUCTION

The production of pesticides [1,2] generates effluents of wastewater which contain residues of raw materials, intermediary products of reactions and the final products themselves. Their effects on the receptor medium, when they are known, can limit the uses of the water [3].

The application of corrective means which eliminate or minimize this type of pollution requires first the characterization of the effluent. In addition to the pollution global indicator parameters [total organic carbon (TOC) and chemical oxygen demand (COD)], the various chemical species responsible for the toxic nature of the effluents [4,5] are determined. Thus, the 76/464/EEC Directive [6] contains a list of substances or groups of substances which are to be subjected to regulation in forthcoming Directives, limiting the maximum quantity of effluent and the quality objectives for surface water.

The techniques normally used for the analysis of wastewater are based on prior treatment of the sample for the extraction and concentration of the organic pollutants [7] and subsequent separation by

0021-9673/92/$05.00

gas chromatography (GC) with identification of the various components by mass spectrometry (MS) [8].

The application of degradation treatments of a physical–chemical nature (chloration and ozonation) for the purification of this type of wastewater may generate new chemical substances which modify the toxic nature of effluents, leading to induced pollution [9,10].

This report presents the results obtained in the characterization of the wastewater effluents from the production of dicofol and tetradifon from a plant located in the Ebro Valley. Various sample concentration techniques were tested (liquid–liquid and solid–liquid extraction), and the reliability of the final method chosen was examined. The substances were identified by GC–MS.

Ozonation treatment in basic medium is also applied to the effluents, the chemical structures of the compounds which are completely oxidized are established, and the new chemical species generated are determined [11].

EXPERIMENTAL

Reagents

The complete series of chlorobenzenes, dicofol, tetradifon, DDTs and their metabolites supplied by Cromlab (Barcelona, Spain) were used; the solvents used were hexane, 2,2,4-trimethylpentane, acetone, ethyl acetate and dichloromethane of Mallinckrodt (Paris, KY, USA); Florisil and anhydrous sodium sulphate reagent were supplied by Merck (Darmstadt, Germany); the cartridges used were Sep-Pak C_{18} cartridges from Waters Millipore (Milford, MA, USA); N-55 nitrogen and N-50 helium were supplied by S.E.O. (Zaragoza, Spain).

The organic solvents used were of special grade for pesticide analysis.

Sample

The wastewater used in this study came from an industry situated in Aragon, Spain, which produces the organochlorine pesticides dicofol and tetradifon.

Instrumentation

An HP5890 gas chromatograph equipped with an electron-capture detector and a splitless injector was used in this work. The column was an HP-5 5% diphenyl and 95% dimethylpolysiloxane column of 25 m length supplied by Hewlett Packard (Avondale, PA, USA); a Varian 3300 gas chromatograph supplied by Varian (Walnut Creek, CA, USA) and connected to an ITD Finnigan Mat 800 mass spectrometer supplied by Finnigan MAT (San Jose, CA, USA) was used; the computer data system was an Acer 915T from Acer Computer (Dusseldorf, Germany); the rotating evaporator was a Heildoph VV2011 supplied by Heildoph-Elektro (Kelheim, Germany); a Fischer Model 501 ozonizer supplied by Labor- und Verfahrenstechnic (Germany) was employed; the TOC–total carbon (TC) analyser was an Astro 1850 from Astro (Houston, TX, USA).

Liquid–liquid extraction [12]

A 1-l volume of wastewater, pH 10 (6 *M* sodium hydroxide), was extracted with 3 × 60 ml of methylene chloride and the extracts were collected in a flask. They were concentrated in a rotating evaporator at 40°C until a final volume of approximately 3 ml was achieved. The extract was passed through a Pasteur column packed with Florisil and anhydrous sodium sulphate in the upper part. Previously, sodium sulphate and Florisil had been conditioned for 17 h at 150°C. The column was activated with 5 ml of isooctane (2,2,4-trimethylpentane) and a single fraction containing 10 ml of isooctane was collected. The extract was analysed using GC with electron-capture detection (ECD) and GC–MS. For a complete analysis of the series of chlorobenzenes, the solvent was replaced by hexane through drying with nitrogen.

Solid–liquid extraction [12]

Extraction columns were small cartridges packed with octadecylsilane (C_{18}). The solid phase was first conditioned with 5 ml of methanol, 10 ml of ultrapure water and 5 ml of methanol. A 1-l volume of residual water, pH 10 (6 *M* sodium hydroxide), was passed through the cartridge by continuous vacuum pump suction. A continuous nitrogen stream was passed through to dry the cartridge for 10 min. The final extracts were obtained through two separated fractions of hexane and then combined. In order to analyse dicofol, tetradifon, DDTs and their metabolites, the solvent was changed to isooctane; the hexane was dried with a nitrogen stream. The extract was analysed by GC–ECD and by GC–MS.

GC–ECD conditions

Injection: 2 μl; splitless: 0.8 s. Injection temperature: 250°C. Detection temperature: 350°C. Temperature programmes: chlorobenzenes, 60°C (1 min) up to 280°C at 4°C/min; dicofol, tetradifon, DDTs and their metabolites, 90°C (1 min) up to 170°C at 30°C/min, from 170°C up to 280°C at 2.5°C/min. Carrier gas: helium 30 cm^3/s.

GC–MS conditions

Injection: 2 μl; splitless: 0.8 s. Injection temperature: 250°C. Detection temperature: 350°C. Temperature programmes: chlorobenzenes, 60°C (1 min) up to 280°C at 5°C/min (0); dicofol, tetradifon, DDTs and their metabolites, 90°C (1 min) up to 150°C at 25°C/min, from 150°C up to 280°C at 3°C/min. Carrier gas: helium, 30 cm^3/s. The identification of the compounds was carried out by National Bureau of Standards Library searching and the main substances were verified by comparison with reference standards.

Calibration solutions

Three calibration solutions of 0.1, 0.01 and 0.001 mg/l in hexane were prepared for the complete series of chlorobenzenes and in isooctane for dicofol, tetradifon and DDTs and their metabolites. Table I shows the mathematical expressions of the calibration curves using GC–ECD for the nineteen organochlorine compounds: *op'*-dicofol; *pp'*-dicofol; *o*-tetradifon; *p*-tetradifon; *o,p'*-1,1-dichloro-2,2-bis(4-chlorophenyl)ethylene (*op'*-DDE); *pp'*-DDE; *o,p'*-1,1-dichloro-2,2-bis(*p*-chlorophenyl)ethane) (*op'*-DDD); *pp'*-DDD; *op'*-DDT; *pp'*-DDT; 1,2-dichlorobenzene (1,2-DCB); 1,3-dichlorobenzene (1,3-DCB); 1,4-dichlorobenzene (1,4-DCB); 1,2,3-trichlorobenzene (1,2,3-TCB); 1,2,4-trichlorobenzene (1,2,4-TCB); 1,3,5-trichlorobenzene (1,3,5-TCB); tetrachlorobenzene (TetraCB); pentachlorobenzene (PCB); hexachlorobenzene (HCB).

TABLE I

MATHEMATICAL EXPRESSIONS OF THE CALIBRATION CURVES FOR DDTs, DICOFOL, TETRADIFON AND CHLOROBENZENES

Compound	Mathematic expressions[a]	*r*
op'-Dicofol	Area = 14733330.3*C* + 46659.8	0.999
pp'-Dicofol	Area = 8709932.0*C* + 89763.2	0.999
op'-DDE	Area = 48181442.2*C* − 28242.6	0.999
pp'-DDE	Area = 62275402.4*C* − 89143.9	0.999
op'-DDD	Area = 33769491.8*C* − 18921.6	0.999
pp'-DDD	Area = 36734977.5*C* − 19994.9	0.999
op'-DDT	Area = 12703593.9*C* − 24375.5	0.999
pp'-DDT	Area = 11256519.5*C* − 33764.9	0.999
o-Tetradifon	Area = 29116585.7*C* + 27735.9	0.999
p-Tetradifon	Area = 34870035.1*C* + 2322.6	0.999
1,3-DCB	Area = 6054631.1*C* + 18691.1	0.997
1,4-DCB	Area = 3134420.0*C* + 12291.8	0.994
1,2-DCB	Area = 5063608.6*C* + 9335.3	0.998
1,3,5-TCB	Area = 33837.4*C* + 78706.8	0.999
1,2,4-TCB	Area = 26428556.7*C* + 76516.7	0.999
1,2,3-TCB	Area = 37098350.1*C* + 96530.6	0.999
TetraCB	Area = 82147023.0*C* + 364742.8	0.999
PCB	Area = 68789759.8*C* + 55349.8	0.999
HCB	Area = 66630337.8*C* + 464278.8	0.995

[a] *C* = concentration in mg/l.

Ozonation conditions

The ozone used for the treatment of the water was produced with a silent electrical discharge of dry prefiltered oxygen. Ozonation was carried out using a closed reactor to which 1 l of residual water, pH 10 (6 *M* sodium hydroxide) was added [13]. The current of the apparatus was adjusted to 0.5 A. The excess ozone was retained by two bubblers containing 250 ml of a solution of 2% potassium iodide. The contact time was 50 min during which 78.3 l of oxygen generated 3.33 g of ozone which passed through the sample. By titration of the solutions from the bubblers with sodium thiosulphate and starch as an indicator, the dosage used in the ozonation of the water was calculated as 1.16 g/l.

RESULTS AND DISCUSSION

Total recoveries by the proposed methods

The nineteen organochlorine compounds were added to ultrapure water, adjusted to pH 10 with 6 *M* sodium hydroxide, in 30 μg/l concentration in order to study the percentage recoveries achieved with the extraction techniques previously described and their later analysis by GC–ECD. Figs. 1 and 2 compare the percentage recoveries for the liquid–liquid and solid–liquid extraction techniques.

Neither of the techniques gave good results for the complete series of chlorobenzenes. A result is considered acceptable at around 80%. The best results were obtained with the DDTs and their metabolites with liquid–liquid extraction, these being in the range 89–129%.

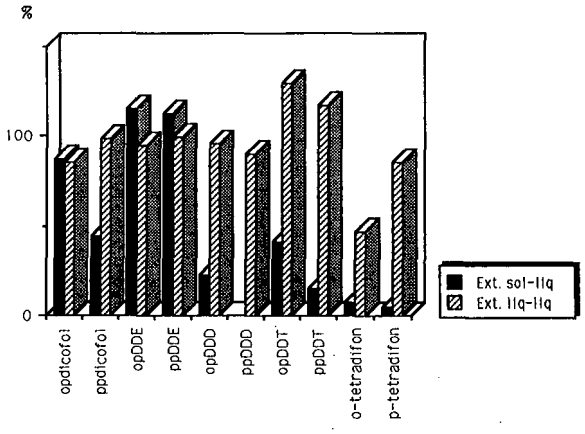

Fig. 1. Total recoveries of DDTs, dicofol and tetradifon.

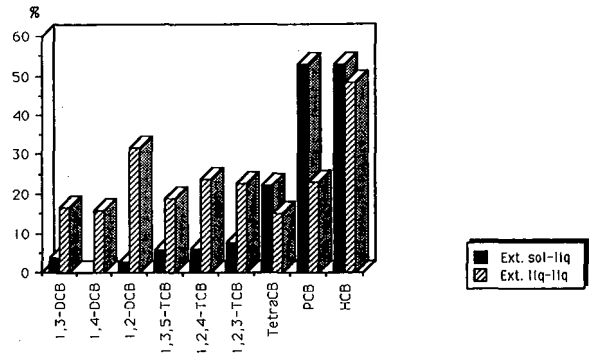

Fig. 2. Total recoveries of chlorobenzenes.

Wastewater ozonation

The wastewater was examined before and after ozonation. The TOC and COD of ozonized and non-ozonized samples were analysed and were reduced by 95 and 99%, respectively. Two 1-l portions of ozonized and non-ozonized water were extracted with C_{18} cartridges and analysed using GC–ECD and GC–MS.

GC–ECD analysis

Figs. 3 and 4 show chromatograms of non-treated and treated water extracts, respectively, indicating clearly the positive effect of the ozone treatment. The reduction of the nineteen organochlorine compounds determined by the previous methods is presented in Figs. 5 and 6.

GC–MS analysis

A total of 58 organic compounds were identified in the wastewater using GC–MS; 17 of these appear

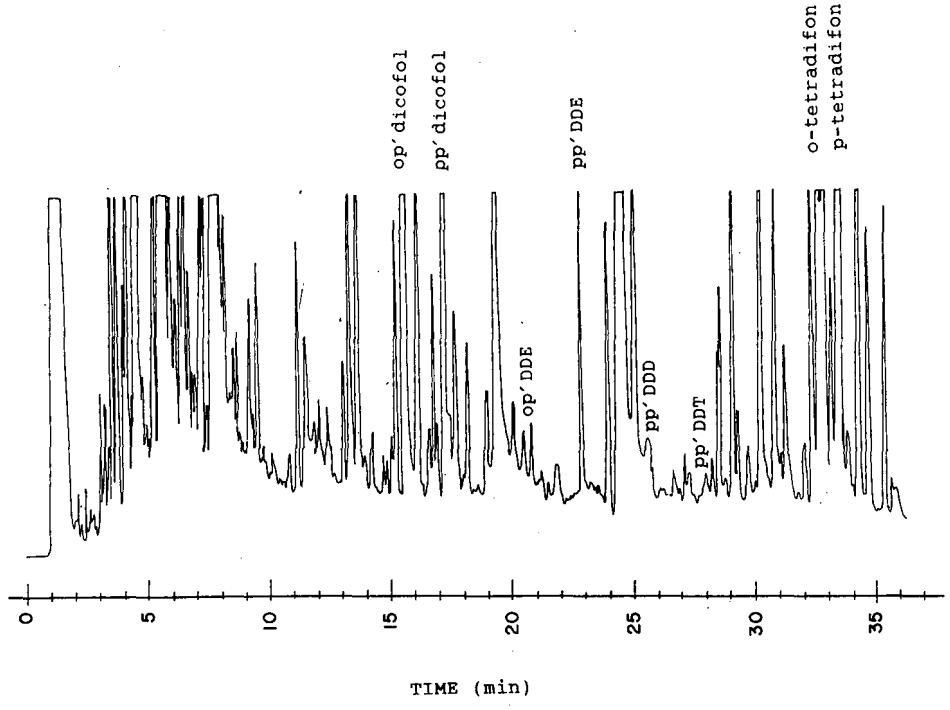

Fig. 3. ECD gas chromatogram for non-ozonated effluent.

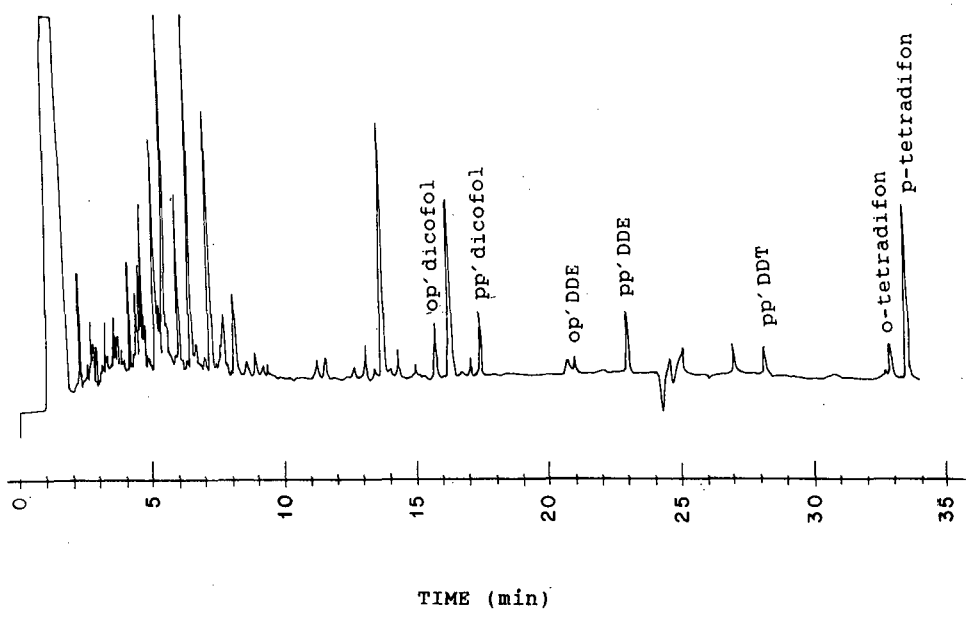

Fig. 4. ECD gas chromatogram for ozonated effluent.

in the group of substances susceptible to the figure in list I of the 74/464/EEC Directive. After ozonation, 46 organic compounds were identified, 8 of which appear in the above-mentioned group. In the ozonation process, 35 substances were removed (Fig. 7), 23 new products were formed (Fig. 8) and 23 others remained unchanged (Fig. 9), *i.e.* they were already present in the polluted water and not derived from ozonation or other degradation steps.

Only the least reactive compounds resist treatment. Ozonation leads to a significant decrease in aromatic compounds together with a slight increase in polar compounds.

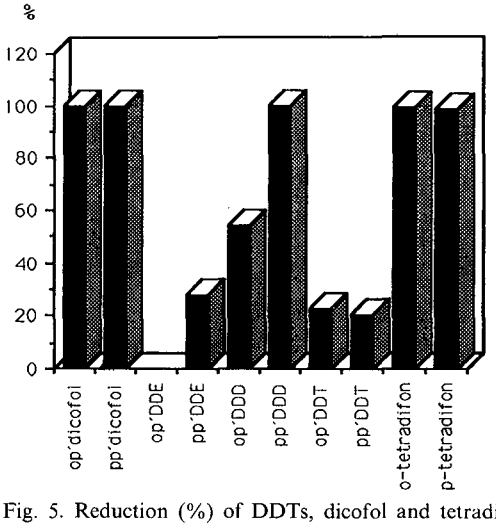

Fig. 5. Reduction (%) of DDTs, dicofol and tetradifon after ozonation treatment.

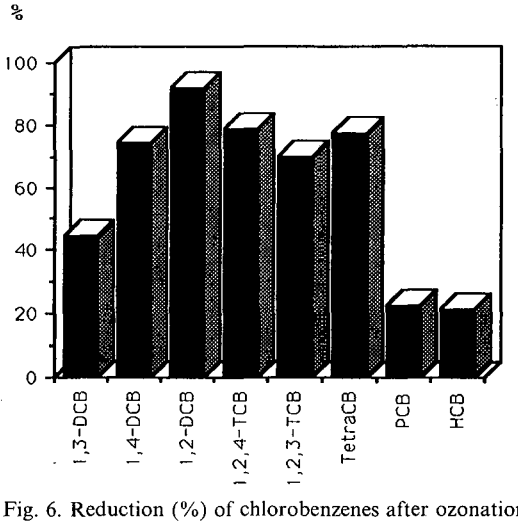

Fig. 6. Reduction (%) of chlorobenzenes after ozonation treatment.

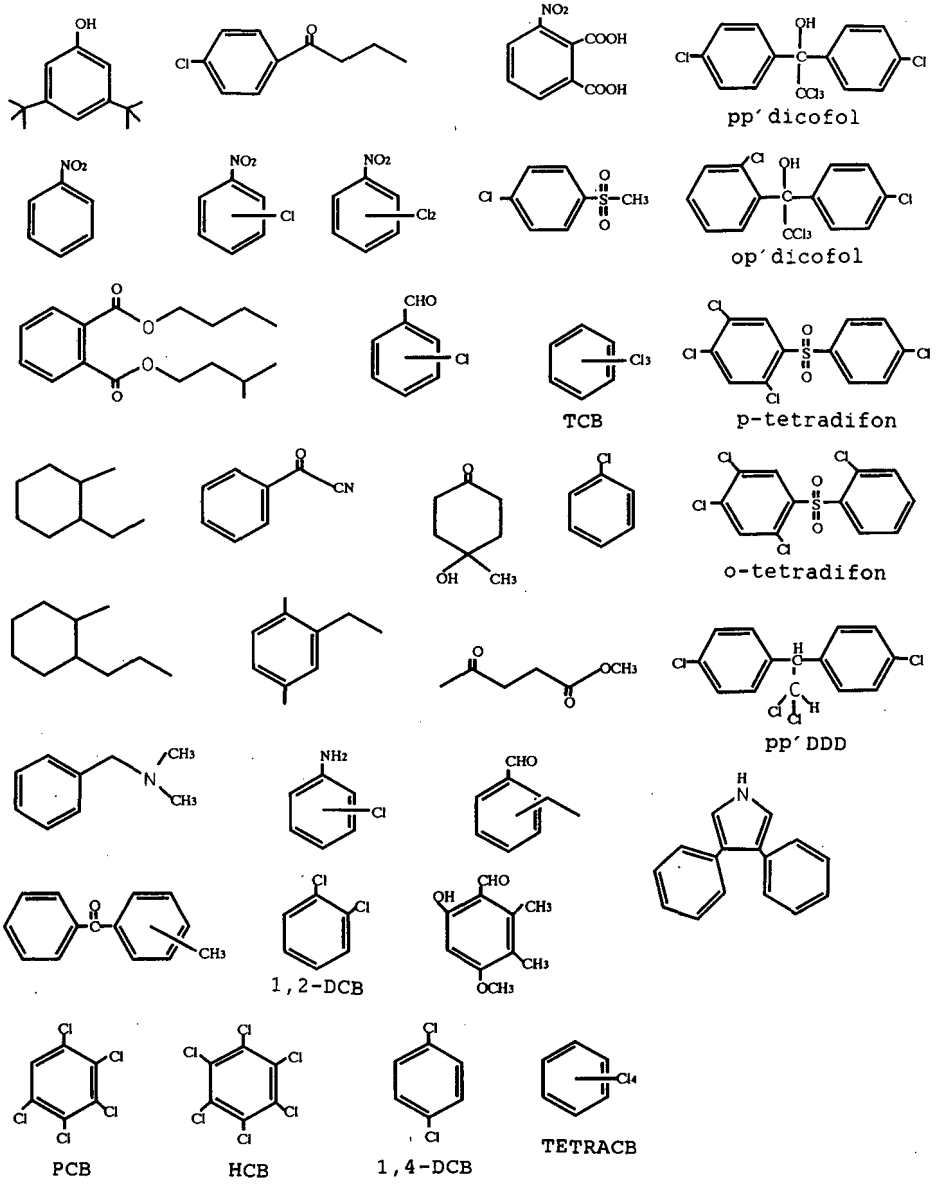

Fig. 7. Removed compounds after ozonation treatment.

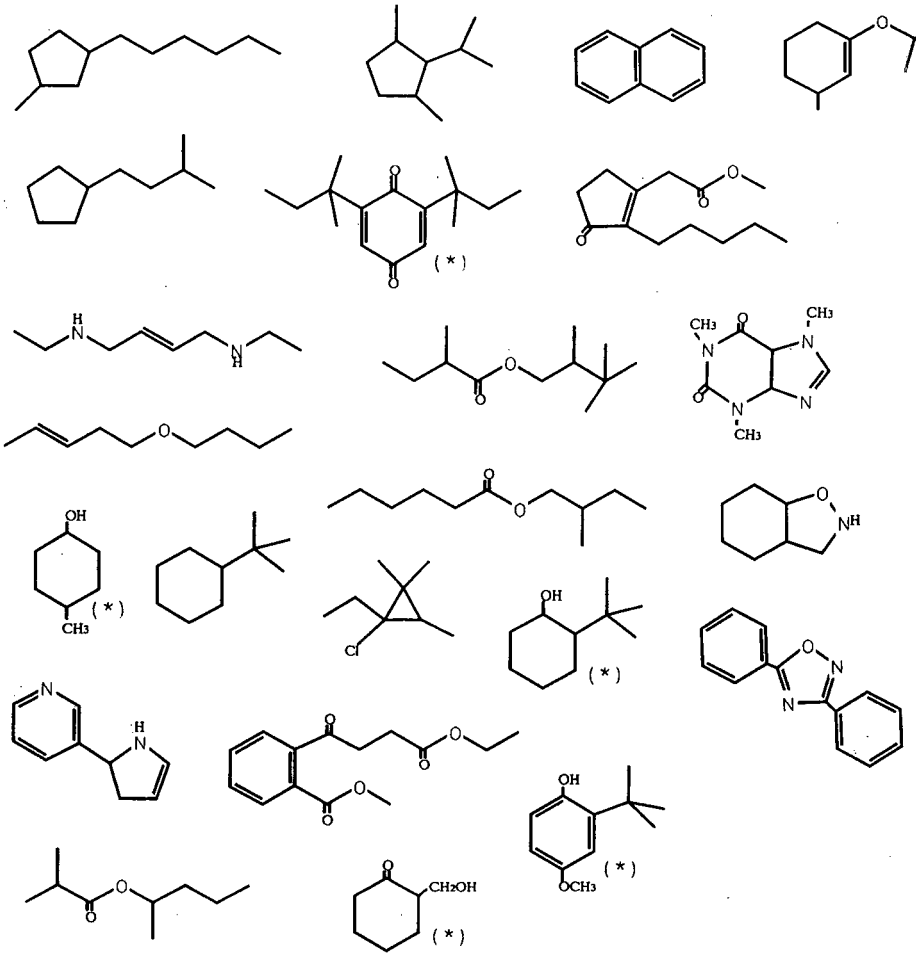

(*): Polar compounds

Fig. 8. New products appearing after ozonation treatment.

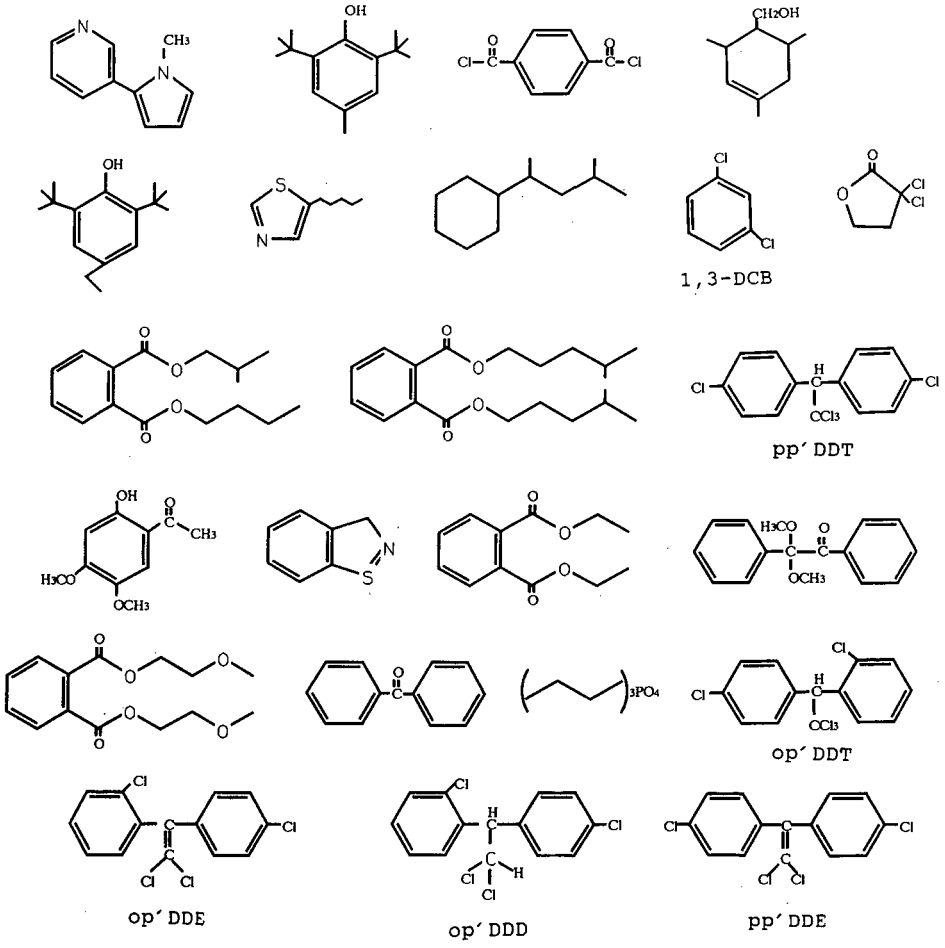

Fig. 9. Unchanged compounds after ozonation treatment.

REFERENCES

1 C. R. Worthing (Editor), *The Pesticide Manual*, British Crop Protection Council, Farnham, 9th ed., 1991.
2 S. Budevari (Editor), *The Merck Index*, Merck, Rahway, NJ, 11th ed., 1989.
3 H. Miller, P. Cramer, A. Drinkwine, A. Shan, G. Trischan and J. Going, *Adv. Identif. Anal. Org. Pollut. Water*, 1 (1981) 115.
4 N. Irving Sax, *Dangerous Properties of Industrial Materials*, Van Nostrand-Reinhold, New York, 6th ed., 1984.
5 M. Sittig, *Handbook of Toxic and Hazardous Chemicals*, Noyes, Park Ridge, NJ, 1981.
6 *76/464/EEC: Council Directive of 4 May 1976 on Pollution Caused by Certain Dangerous Substances Discharged into the Aquatic Environment of the Community*, Official Journal No. L 129, 18/05/76, p. 0023, Greek Special Edition, Chapter 15, Volume 01, Brussels, 1976, p. 138.
7 M. Valls, J. M. Bayona and J. Albaiges, *Int. J. Anal. Chem.*, 39 (1990) 329.
8 T. R. Crompton, *Determination of Organic Substances in Water*, Vol. 2, Wiley, New York, 1985, p. 448.
9 J. F. J. Van Rensburg, A. Hassett, S. Theron and S. G. Wiechers, *Water Sci. Technol.*, 13 No. 1 (1981) 537.
10 P. M. Huck *et al.*, *Proceedings of the 8th Ozone World Congres, Zurich, Sept. 1987*, International Ozone Association, Zurich, 1987, Vol. 1, Ch. 29.
11 R. Andreozzi, A. Insola, V. Caprio and M. G. D'Amore, *Water Res.*, 25 (1991) 655.
12 L. S. Clesceri, A. E. Greenberg and R. R. Trussell (Editors), *Standard Methods for the Examination of Water and Wastewater*, American Public Health Association, Washington, DC, 17th ed., 1989.
13 W. D. Bellamy, G. T. Hickman and P. A. Mueller, *Res. J. WPCF*, 63 (2) (1990) 120.

Journal of Chromatography, 607 (1992) 319–327
Elsevier Science Publishers B.V., Amsterdam

CHROM. 24 140

Determination of trace levels of herbicides in estuarine waters by gas and liquid chromatographic techniques

Gaël Durand, Véronique Bouvot and Damià Barceló*

Environmental Chemistry Department, CID–CSIC, c/ Jordi Girona 18–26, 08034 Barcelona (Spain)

ABSTRACT

A screening procedure based on a two-step liquid–liquid extraction with dichloromethane was used for the isolation of two fractions, one neutral containing molinate, trifluralin, atrazine, simazine, alachlor, metolachlor, isoproturon, chlortoluron and linuron and the other acidic containing bentazone, 2,4-D and 4-chloro-*o*-tolyloxyacetic acid. Recoveries varying from 60 to 100% with a relative standard deviation of 10% were achieved for most of the herbicides added to 1–4 ml water samples at levels varying from 2.5 to 25 μg/l. Exceptions were the acidic herbicides 2,4-D and MCPA, for which low recoveries up to 40% were obtained. Determinations were usually carried out by gas chromatography with nitrogen–phosphorus detection, allowing the determination of herbicides at the 5–10 ng/l level with further confirmation by gas chromatography–mass spectrometry with electron impact ionization. Liquid chromatography with diode-array detection permitted the characterization of herbicides at levels of 0.1–0.5 μg/l. Although liquid chromatography–diode-array detection was much less sensitive than gas chromatography–nitrogen–phosphorus detection determinations, its usefulness was demonstrated for direct characterization of acidic herbicides without derivatization. Illustrative examples of the determination of several herbicides in estuarine water samples from the Ebro Delta (Tarragona, Spain) are shown. Atrazine, simazine, molinate, alachlor, metolachlor and bentazone were the most common herbicides found with concentrations levels varying from 5 ng/l to 5 μg/l.

INTRODUCTION

There is a need for multi-residue analytical approaches for the trace level identification and determination of pesticides in water matrices, such as surface, estuarine, ground and sea water. Various preconcentration methods based on different physico-chemical principles are used for this purpose. Among them, liquid–liquid extraction (LLE) and off-line and on-line liquid–solid extraction (LSE) are commonly used and were recently described in a review [1].

Chlorotriazine herbicides have been extracted into dichloromethane [2–5], ethyl acetate [2] and mixtures of dichloromethane with ethyl acetate and ammonium formate [6]. For alachlor, dichloromethane has been recommended by the US EPA as an extraction solvent for waters [7]. Screening methods for different pesticide groups have been developed, generally using dichloromethane with further washing with NaOH [8,9], adding NaCl [10] or adjusting to neutral and acidic pH for the separation of two fractions [11,12]. Determinations of the different herbicides are generally carried out by gas chromatography with nitrogen–phosphorus detection (GC–NPD) [1,13,14] and by GC with mass spectrometric (MS) detection [13–19], both giving much lower detection limits than liquid chromatographic (LC) techniques. However, the use of LC facilitates the direct determination of acidic and thermally labile herbicides without the need for derivatization. This has been reported in combination with LLE [5–12], off-line LSE [8–10,20] and on-line LSE [21,22].

The aim of this work was to establish a method for the identification and confirmation of herbicides at low concentration levels and to determine the levels of molinate, trifluralin, atrazine, simazine, alachlor, metolachlor, isoproturon, chlortoluron, bentazone, 2,4-D and 4-chloro-*o*-tolyloxyacetic acid (MCPA) in estuarine water samples from the Ebro Delta (Tarragona, Spain). The choice of these her-

0021-9673/92/$05.00

bicides was agreed at a joint meeting held at the International Atomic Energy Agency laboratories in Monaco in October 1990 between the Food and Agriculture Organization of United Nations Environment Programme and representatives from France, Spain, Italy and Greece. On the basis of usage information, physico-chemical properties and persistency data, this list of priority herbicides was drawn up in order to carry out a pilot monitoring programme in estuarine areas of the mediterranean region. The analytical methodology used for achieving this purpose was decided to be liquid–liquid extraction followed by determinations using GC–NPD, GC–MS and LC–diode–array detection (DAD).

Generally sufficiently volatile herbicides can be determined in water samples by GC–NPD and GC–MS at levels of 0.01 μg/l [15,17]. As a complementary technique, LC–DAD can be employed for the determination of the more polar herbicides at this concentration level only if there is sufficient quantitative enrichment, absorption in the UV range and the compound of interest exhibits high molar absorptivity [20].

The limits of detection (L.O.D.) were determined for each of the chromatographic techniques and recommendations for the analysis of water samples for the different herbicides are discussed. Applications to the characterization of trace levels of herbicide residues in polluted estuarine water samples are presented.

EXPERIMENTAL

Chemicals

Pesticide-grade ethyl acetate, *n*-hexane, diethyl ether and dichloromethane were obtained from Merck (Darmstadt, Germany). Molinate, alachlor, metolachlor, bentazone and MCPA were obtained from Promochem (Wesel, Germany), isoproturon and chlortoluron from Riedel-de Haën (Seelze-Hannover, Germany) and 2,4-D, trifluralin, atrazine and simazine from Polyscience (Niles, IL, USA).

Sample preparation

Estuarine water samples of 1–4 l were spiked with the different herbicides giving final concentrations of 2.5 μg/l. Preliminary experiments were performed by spiking with up to 25 μg/l of each herbicide. After agitation the solutions were extracted with 50–100 ml of dichloromethane and the extract was split into two portions and evaporated to dryness. One portion was dissolved in 100–200 μl of ethyl acetate for GC–NPD and GC–MS analysis and the other portion was dissolved in 100–200 μl of methanol for LC–DAD analysis. Sulphuric acid (pH < 2) and dichloromethane (50–100 ml) were added to the water sample, which was shaken again and the dichloromethane extract was carefully evaporated to dryness and the residue dissolved in 100–200 μl of methanol for LC–DAD analysis. Recoveries obtained for the different herbicides are given in Table I.

Chromatographic analysis

GC–NPD. Following Florisil clean-up, the extracts were injected on to the column of a GC 5300 Mega Series gas chromatograph (Carlo Erba, Milan, Italy) equipped with a nitrogen–phosphorus detector. A 15 m × 0.25 mm I.D. fused-silica capillary column coated with 0.15 μm film of chemically bonded cyanopropylphenyl DB 225 (J & W Scientific, Folsom, CA, USA) was used. Hydrogen was employed as the carrier gas at 60 kPa and helium as the make-up gas at 110 kPa. The temperatures of the injector and detector were held at 270°C. The column was programmed from 60 to 90°C at 10°C/min and from 90 to 220°C at 6°C/min.

GC–MS. A Hewlett-Packard (Palo Alto, CA, USA) Model 5995 instrument interfaced to a Model 59970C data system was used for GC–electron impact (EI) ionization MS. The same fused-silica column as described above was used and directly introduced into the ion source of the mass spectrometer. Helium was used as the carrier gas at 83 kPa. Other chromatographic conditions were identical with those described for GC–NPD. The ion source and the analyser were maintained at 200°C. EI mass spectra were obtained at 70 eV.

Table II gives the main ions together with their relative abundances and retention times obtained for the different herbicides in GC–MS.

LC–DAD. Eluent delivery was provided by two Model 64 high-pressure pumps (Knauer, Bad-Homburg, Germany) coupled with a Chrom-A-Scope rapid scanning UV–VIS detector (Barspec, Rehovot, Israel). Samples were injected via a 20-μl

loop (Rheodyne, Cotati, CA, USA). The neutral fraction of the herbicides was analysed using a Serva (Heidelberg, Germany) high-performance liquid chromatographic (HPLC) column packed with 4-μm octadecyl-Daltosil 100 (250 × 4.6 mm I.D.) Gradient elution was used from methanol–acetonitrile–water (20:20:60) to methanol–acetonitrile (50:50) in 40 min at a flow-rate of 1 ml/min.

For the analysis of the acidic fraction containing bentazone, 2,4-D and MCPA, a LiChroCART cartridge column (125 × 4.0 mm I.D.) packed with 4-μm LiChrospher 100 RP-18 (Merck, Darmstadt, Germany) was used. Isocratic elution with methanol–water (60:40) containing 1% of acetic acid at a flow-rate of 1 ml/min was used.

Determination by LC–DAD was performed using UV absorption at 220 nm.

RESULTS AND DISCUSSION

LC–DAD

Most of the neutral herbicides gave recoveries up to 70%, similarly to results reported previously [2–5,8,9,15]. The phenoxy acid herbicides 2,4-D and MCPA were exceptions, with recoveries lower than 34% (see Table I), which are much lower than those reported using a similar method [11]. Such a low extraction efficiency can be explained by the low level of spiking here (2.5 μg/l) compared with that in the literature [11], so evident difficulties in determining 2,4-D and MCPA occur. In contrast, bentazone, the other acidic herbicide which exhibits a much shorter retention time (3 min) with a better peak shape under the analytical conditions, gave a much better recovery.

The best separation of the neutral fraction containing the different herbicides was achieved with a commercially available 250 × 4.6 mm I.D. HPLC column with a 4-μm particle size. The separation is shown in Fig. 1A. The only problem was the co-elution of peaks 7 and 8 (alachlor and metolachlor), which could not be overcome. However, these two compounds have very similar structures that only differ only in a CH_2 group, and would be expected to behave similarly under the conditions of analysis. It should be mentioned that the best separation reported for a variety of herbicides [8] was achieved using a 250-mm laboratory-packed HPLC column with a 3-μm particle size. As this column is not commercially available, we used that mentioned above, which gave an excellent performance. In any case, alachlor and metolachlor could be perfectly separated using GC (see Table II).

TABLE I

MEAN RECOVERIES OF HERBICIDES IN ESTUARINE WATER SAMPLES USING LIQUID–LIQUID EXTRACTION WITH DICHLOROMETHANE

Spiking level: 2.5 μg/l ($n = 6$).

Herbicide	Mean recovery (%)	Relative standard deviation (%)
Atrazine	100	9
Simazine	93	9
Alachlor	90	10
Metolachlor	90	12
Molinate	70	17
Trifluralin	85	8
Chlortoluron	100	7
Isoproturon	100	8
Linuron	100	7
Bentazone[a]	81	7
2,4-D[a]	20	20
MCPA[a]	34	20

[a] These herbicides were extracted with the same solvent after acidification to pH < 2.

In Fig. 1B, the LC–DAD trace for a water extract containing low levels of herbicides (below 0.1 μg/l) is shown. This represents the L.O.D. of the LC–DAD method. Of the different compounds examined, only atrazine (peak 3) could be unequivocally identified by its UV spectrum (see Fig. 1B). The other herbicides, such as molinate, the UV spectrum of which also shown, and alachlor–metolachlor, could not be positively identified as the UV spectra gave an absorption band that overlapped the UV spectrum of the LC eluent. This can also be observed in the UV spectrum of atrazine (peak 3), but as atrazine has its absorption maximum at 220 nm, we can still see its maximum and the characteristic spectrum, but in the other instances, with maximum absorbance at 200 nm, there is a clear interference of the spectrum of the LC eluent when working at the L.O.D. of the method. It was impossible to identify positively simazine (peak 1) as it co-eluted with a highly interfering compound from the water matrix.

Fig. 1C and D show the chromatograms of a standard sample containing the three phenoxy acid

herbicides and a positive identification of bentazone at a concentration level of 5.5 μg/l. In this instance there was no problem in the identification of this herbicide in the real sample of Ebro Delta water as the concentration found was sufficient to achieve a good UV spectrum for confirmation.

GC–NPD and GC–MS

Fig. 2 shows (A) the GC–NPD and (B) the GC–MS traces for the same extract of Ebro Delta estuarine waters containing herbicides at levels varying from 0.005 to 0.050 μg/l. The different EI mass spectra of the positively identified herbicides are shown in Fig. 3 and the main fragments obtained for each herbicide are given in Table II.

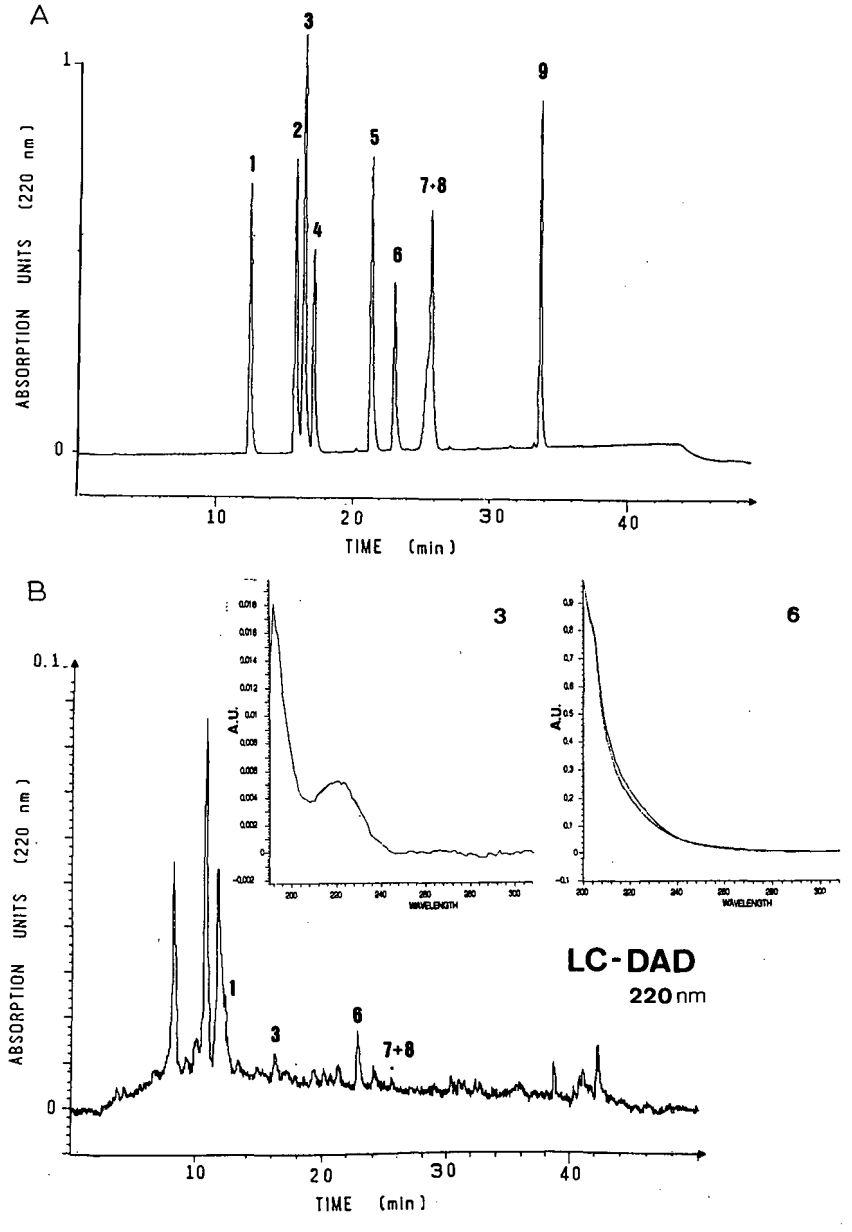

Fig. 1.

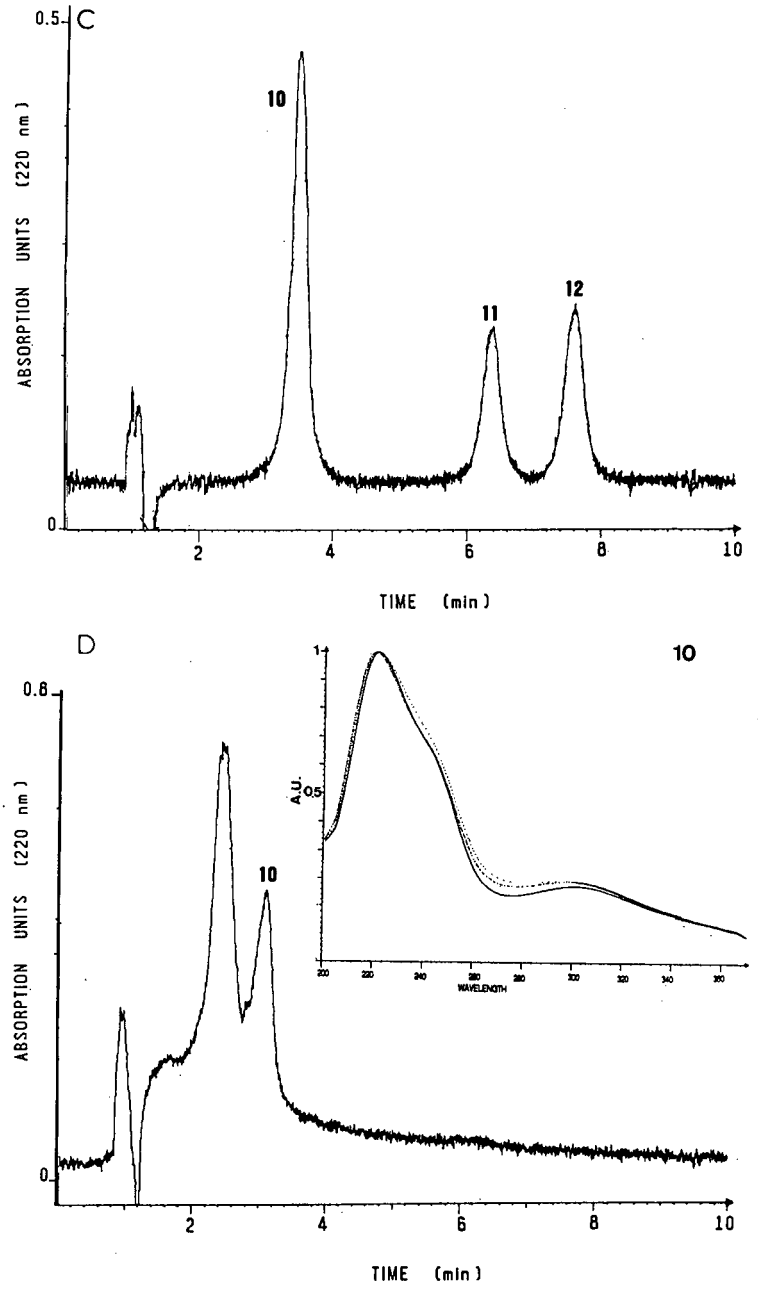

Fig. 1. (A) LC–DAD of a standard sample containing the neutral fraction. Peaks: 1 = simazine; 2 = chlortoluron; 3 = atrazine; 4 = isoproturon; 5 = linuron; 6 = molinate; 7 = alachlor; 8 = metolachlor; 9 = trifluralin. Amount of each herbicide injected: 2 μg. Serva HPLC column (250 × 4.6 mm I.D.) packed with 4-μm octadecyl-Daltosil 100. Gradient elution from methanol–acetonitrile–water (20:20:60) to methanol–acetonitrile (50:50) in 40 min at a flow-rate of 1 ml/min. (B) LC–DAD of an extract of a real water sample from the Ebro Delta containing simazine (0.040 μg/l), atrazine (0.010 μg/l) molinate (0.080 μg/l) and alachlor (0.025 μg/l). Peak purity of atrazine indicates its positive identification. The other herbicides were not positively identified owing to the low concentrations and absorption maxima at lower wavelength (200 nm), so they were determined by GC–NPD and confirmed by GC–MS. LC conditions as in (A). (C) LC–DAD of a standard sample containing the herbicides (10) bentazone, (11) 2,4-D and (12) MCPA. Amount of each herbicide injected: 2 μg. LiChroCART cartridge column (125 × 4.6 mm I.D.) packed with 4-μm LiChrospher 100 RP-18. Isocratic elution with methanol–water (60:40) containing 1% acetic acid at a flow-rate of 1 ml/min. (D) LC–DAD corresponding to an extract of a real water sample from the Erbo Delta containing 5.5 μg/l of bentazone. Peak purity of bentazone indicates its positive identification. LC conditions as in (C).

TABLE II

RETENTION TIMES AND MAIN IONS OF HERBICIDES ANALYSED BY GC–MS

Herbicide	Retention time (min)	*m/z* (relative intensity, %)
Molinate	10.5	126 (100), 187 (35)
Trifluralin	13.7	264 (80), 306 (100)
Atrazine	17.7	200 (100), 215 (60)
Simazine	18.2	186 (60), 201 (100)
Alachlor	18.5	160 (100), 188 (100)
Metolachlor	19.3	162 (100), 238 (60)

The GC–MS characterization of the chlorotriazine herbicides atrazine and simazine has been discussed previously [14]. The base peaks at *m/z* 200 and 201 corresponded to $[M - CH_3]^+$ and $[M]^{+\cdot}$ for atrazine and simazine, respectively. The second most abundant ions were obtained with *m/z* 215 and 58 and 173 and 186, corresponding to $[M]^{+\cdot}$ and $[C_3H_7NH]^+$ and $[M - C_2H_4]^+$ and $[M - CH_3]^+$ for atrazine and simazine, respectively. Molinate exhibited two main ions corresponding to the molecular mass and to the loss of $[SCH_2CH_3]^+$ at *m/z* 187 and 126, respectively. Diagnostic ions for trifluralin were at *m/z* 306 and 264, corresponding to $[M - CH_2CH_3]^+$ and $[M - (CH_2)_4CH_3]^+$, respectively. For alachlor, the two diagnostic ions at *m/z* 188 and 160 corresponded to $[M - CH_2OCH_3 - HCl]^+$ and $[M - CH_3OH - OCCH_2Cl]^+$, respectively. Other ions at *m/z* 269 and 237 corresponding to the molecular mass and $[M - CH_3OH]^+$, respectively, can also be observed in the EI mass spectrum in Fig. 3 (peak 7). Metolachlor exhibited a similar fragmentation pattern to alachlor, as these herbicides have similar structures. The main ions were at *m/z* 238 and 162, assigned to $[M - CH_2OCH_3]^+$ and $[M - CH_2OCH_3 - OCCHCl]^+$, respectively.

The various ions found for these herbicides agree with previous results obtained using EI [15,17,23]. The different ions indicated in Table II can be used as diagnostic ions for screening purposes, as they correspond to higher *m/z* values. Alachlor and metolachlor exhibit an intense peak in the EI mass spectrum corresponding to $[CH_2OCH_3]^+$ at *m/z* 45 [23], but it is not recommended as a diagnostic ion as main ions at higher *m/z* values are obtained.

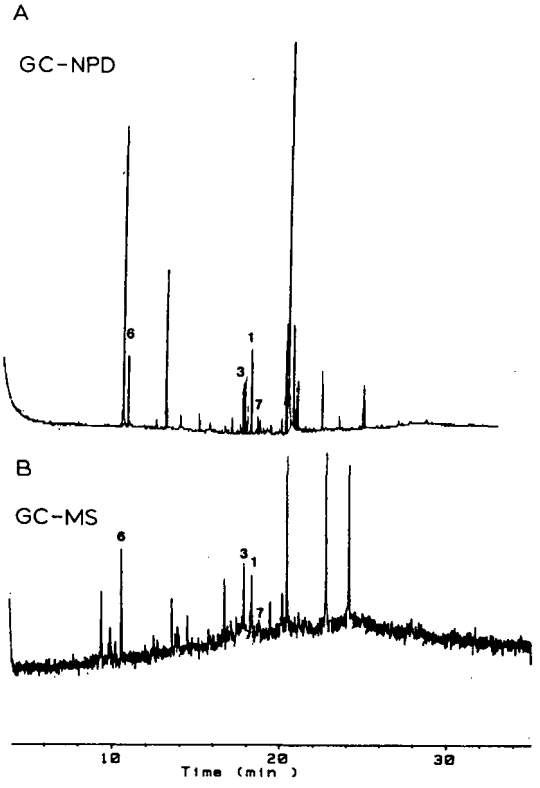

Fig. 2. (A) GC–NPD and (B) GC–MS of an extract of a real water sample from the Ebro Delta containing (6) molinate (0.050 μg/l), (3) atrazine (0.010 μg/l), (1) simazine (0.012 μg/l) and (7) alachlor (0.005 μg/l). 15 m × 0.25 mm I.D. fused-silica capillary GC column coated with chemically bonded cyanopropylphenyl DB 225, programmed from 60 to 90°C at 10°C/min and from 90 to 220°C at 6°C/min.

Performance of the analytical system

The repeatabilities of the GC–NPD and LC–DAD systems were determined after analysis of the dichloromethane extracts of the samples containing atrazine, simazine, alachlor and metolachlor at the level of 0.1 μg/l. The relative standard deviation was 2–3% ($n = 6$). The reproducibility of the same extracts was higher and varied between 3 and 5% ($n = 6$). Calibration graphs for atrazine, simazine, alachlor, metolachlor and molinate were constructed and were linear over the concentration ranges investigated, from 1 ng/l to 1 μg/l for GC–NPD. In LC–DAD, the concentration ranged from 50 ng/l to

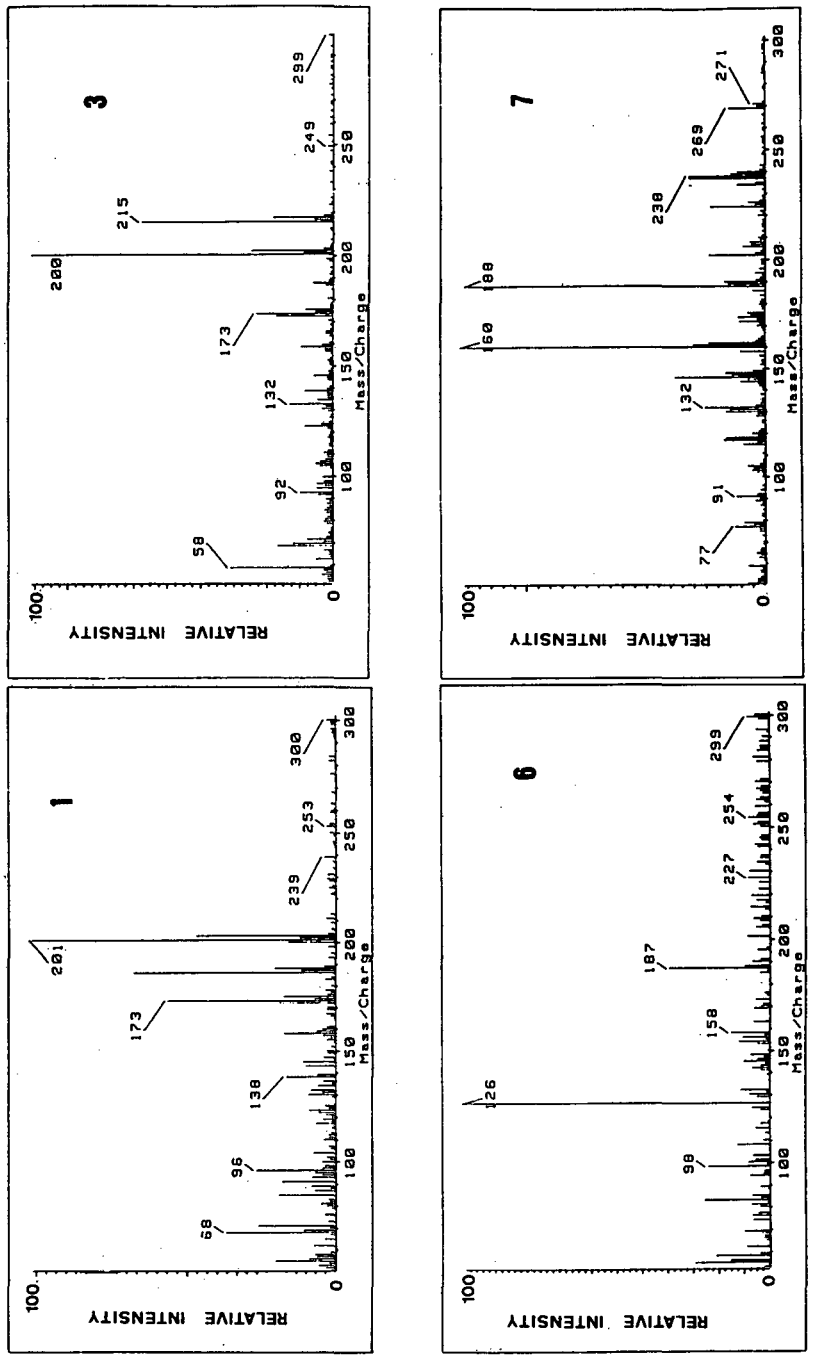

Fig. 3. EI mass spectra of the herbicides positively identified in Fig. 2. Numbers on the spectra correspond to the peaks in Fig. 2.

10 μg/l for atrazine, simazine and bentazone and from 500 ng/l to 10 μg/l for molinate, alachlor and metolachlor.

The limits of detection at a signal-to-noise ratio of 3 for the different herbicides were calculated for both GC–NPD and LC–DAD using the analytical protocol described under Experimental. For GC–NPD, the L.O.D. was calculated to be at the 0.1 ng/l level, thus allowing the application of the method to the analysis of relatively "clean" water samples. Indeed, GC–NPD will be the method of choice recommended for the determination of herbicides at trace levels, if they are sufficiently volatile. For confirmation purposes, the use of GC–MS under full-scan conditions is recommended. Quantification by GC–MS using selected ion monitoring also permits determinations at the 0.1 ng/l level [15,17].

The L.O.D. for LC–DAD was, as usual, worse than for GC–NPD. The L.O.D. was calculated to be 10 ng/l for herbicides exhibiting absorption maxima above 210 nm, such as atrazine, simazine, chlortoluron, isoproturon and bentazone, whereas for molinate, alachlor, metolachlor and trifluralin, which exhibit UV maxima below 210 nm, the L.O.D. was ten times higher, 100 ng/l. For the two chlorinated phenoxy acids 2,4-D and MCPA, although they exhibit absorption maxima at 220 nm, the L.O.D. is *ca.* 500 ng/l owing to their poor extraction efficiency and LC properties.

Environmental levels

A pilot monitoring programme was carried out in the Ebro Delta area to investigate the levels of the different herbicides. The Ebro Delta area is used mainly for rice growing but also contains other cultivations such as lettuce and corn. Of the different herbicides used in this area, molinate and bentazone, which are typical in rice cultivation, accounted 56 and 9 tons of active ingredient, respectively, during 1991, whereas the other herbicides such as alachlor, metolachlor, atrazine and simazine were used to lesser extents, *ca.* 1 ton of active compound, during the same period. Fig. 4 shows the levels of the most common herbicides found in the area at one of the stations located on the Ebro River, located betweeen the rice-growing fields and the corn fields. The concentrations of herbicides here are much lower than those in the drainage canals, which contained *ca.* ten times higher concentrations. The most common herbicides detected at almost all the stations at all periods were atrazine, simazine, alachlor and metolachlor. Most of the levels of the different herbicides were in the range 5–550 ng/l, with some exceptions, such as molinate and bentazone, which reached levels up to 3 and 5 μg/l, respectively, in one of the drainage canals.

CONCLUSIONS

A combination of LC–DAD and GC–NPD with

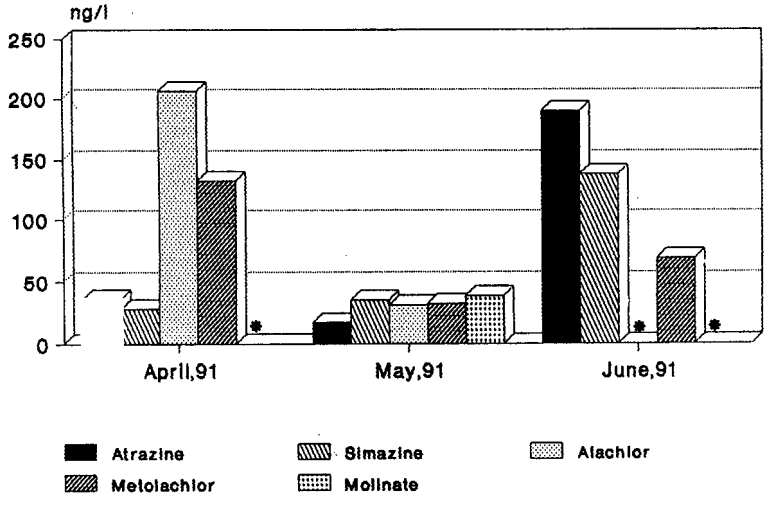

Fig. 4. Environmental levels of herbicides at a station located on the Ebro River (Tarragona, Spain) during April–June 1991. Concentration levels are indicated in ng/l (ng/l). Asterisks denote herbicides not detected.

UV and GC–MS confirmation, respectively, has been applied to the determination of trace levels of herbicides in relatively clean water samples. The reported screening method is applicable for monitoring most of the herbicides considered, with a few exceptions, in water samples under the restrictive measures (0.1 μg/l) imposed by the European Community of herbicide residues in water for human consumption.

The possibilities of peak identification in LC–DAD when working at very low detection limits were discussed. Such positive identification depends on the concentration of the analyte and on its UV spectrum. When absorption maxima in the spectra are at higher wavelengths (above 210 nm), the L.O.D. is lower (10 ng/l) than those for herbicides with absorption maxima in the region of 190–210 nm (100 ng/l).

The use of the two chromatographic methods offers a great advantage in the screeninig of trace levels of a variety of herbicides in water samples. GC–NPD allowed determinations at very low limits of detection and permitted the separation of alachlor and metolachlor, which was impossible by LC–DAD, whereas LC–DAD permitted the direct determination of bentazone without any derivatization.

ACKNOWLEDGEMENTS

This work was supported by the Food and Agriculture Organization and the United Nations Environment Programme (FAO–UNEP).

REFERENCES

1 D. Barceló, *Analyst (London)*, 116 (1991) 681.
2 A. S. Y. Chau and B. K. Afghan, *Analysis of Pesticides in Water*, Vols. I, II and III, CRC Press, Boca Raton, FL, 1982.
3 C. D. Watts, L. Clark, S. Hennings, K. Moore and C. Parker, in B. Crathorne and G. Augeletti (Editors), *Pesticides: Analytical Requirements for Compliance with EEC Directives (Water Pollution Research Report*, No. 11), Commission of the European Communities, Brussels, 1989, pp. 16–34.
4 *Chlorophenoxy Acid Herbicides, Trichlorobenzoic Acid, Chlorophenols, Triazines and Glyphosate in Water 1985*, H.M. Stationery Office, Publications Center, London, 1986, pp. 1–50.
5 W. Schüssler, *Chromatographia*, 27 (1989) 431.
6 G. Durand and D. Barceló, *Toxicol. Environ. Chem.*, 25 (1989) 1.
7 *Determination of Alachlor, Butachlor and Propachlor in Wastewater*, US Environmental Protection Agency, Washington, DC, 1983, pp. 1–12.
8 R. Reupert and E. Plöger, *Wasser*, 72 (1989) 211.
9 R. Reupert and E. Plöger, *Fresenius' Z. Anal. Chem.*, 331 (1988) 503.
10 T. A. Bellar and W. L. Budde, *Anal. Chem.*, 60 (1988) 2076.
11 W. Schüssler, *Chromatographia*, 29 (1990) 24.
12 M. Fielding, S. Gibby and K. Moore, in A. Bjørset and G. Angeletti (Editors), *Organic Micropollutants in the Aquatic Environment, Lisbon Symposium*, Kluwer, Dordrecht, 1991, pp. 142–162.
13 G. Durand, R. Forteza and D. Barceló, *Chromatographia*, 28 (1989) 597.
14 G. Durand and D. Barceló, *Anal. Chim. Acta*, 243 (1991) 259.
15 W. E. Pereira, C. E. Rostad and T. J. Leiker, *Anal. Chim. Acta*, 228 (1990) 69.
16 H.-J. Stan, *J. Chromatogr.*, 467 (1989) 85.
17 E. Benfenati, P. Tremoleda, L. Chiappetta, R. Frassanito, G. Bassi, N. Di Toro, R. Fanelli and G. Stella, *Chemosphere*, 21 (1990) 1411.
18 G. C. Mattern, Ch.-H. Liu, J. B. Louis and J. D. Rosen, *J. Agric. Food Chem.*, 39 (1991) 700.
19 L. G. M. Tuinstra, F. R. Povel and A. H. Roos, *J. Chromatogr.*, 552 (1991) 259.
20 C. Schlett, *Fresenius' Z. Anal. Chem.*, 339 (1991) 344.
21 E. A. Hogendoorn and C. E. Goewie, *J. Chromatogr.*, 475 (1989) 432.
22 V. Coquart and M. C. Hennion, *J. Chromatogr.*, 553 (1991) 329.
23 R. Hites, *CRC Handbook of Mass Spectra of Environmental Contaminants*, CRC Press, Boca Raton, FL, 1985, pp. 1–434.

Journal of Chromatography, 607 (1992) 329–338
Elsevier Science Publishers B.V., Amsterdam

CHROM. 24 149

Determination of the triglyceride composition of avocado oil by high-performance liquid chromatography using a light-scattering detector

M. T. G. Hierro*

Instituto de Fermentaciones Industriales (CSIC), Juan de la Cierva 3, 28006 Madrid (Spain)

M. C. Tomás

Centro de Investigación y Desarrollo en Criotecnología de Alimentos (CIDCA), Fac. de Cs. Exactas (UNLP), 47 y 116 La Plata (Argentina)

F. Fernández-Martín

Instituto del Frío (CSIC), Ciudad Universitaria, 28040 Madrid (Spain)

G. Santa-María

Instituto de Fermentaciones Industriales (CSIC), Juan de la Cierva 3, 28006 Madrid (Spain)

ABSTRACT

The triglyceride composition of avocado oil was determined by high-performance liquid chromatography using a light-scattering detector. Two avocado varieties, Fuerte and Hass, were analysed, and the qualitative composition of each was found to be similar, though quantitative differences were detected. The triglyceride composition was predicted using a system of equations based on the relationship between log k' and the molecular variables equivalent carbon number, chain length and number of double bonds for each of the fatty acids in the glycerides. A total of 24 molecular species of triglycerides were identified. The chromatographic system used successfully separated the critical pairs OOO–LOS, PaPaO–LnPP and PaOO–LOP (O = olein; L = linolein; S = stearin; Pa = palmitolein; Ln = linolenin; P = palmitin). Detector response was found to have a linear relationship with the amount of sample injected over the injection range 10–70 μg.

INTRODUCTION

The avocado (*Persea americana*) is a subtropical fruit of the family *Lauraceae* which is becoming increasingly common in Spain. The lipid content is very high and may attain 25% of the edible portion of the fruit. The saponifiable fraction of the lipid material in avocados is highly unsaturated [1], which makes it not only a highly esteemed food and food ingredient, but also a valuable raw material for the cosmetics industry [2].

It is normal practice to follow the avocado maturation process by monitoring the lipid content, because lipid levels are related to the ripening stages in each cultivar [3,4]. Some workers have proposed the more refined method of fatty acid profile analysis carried out by either gas chromatography (GC) or high-performance liquid chromatography (HPLC), which has the advantage of being able to monitor fruit maturity stages as well as to differentiate individual cultivars [5]. Applying the higher power of new analytical instrumentation to this same line of

0021-9673/92/$05.00

refinement, it is appropriate to examine the potential benefits of analysing the glycerides themselves.

The triglyceride (TG) composition of mesocarp lipids has been investigated by separating molecular species by thin-layer chromatography (TLC) and GC [6], silver nitrate TLC and pancreatic lipolysis [7], or HPLC [8]. Non-aqueous reversed-phase chromatography separates TGs on the basis of the number of carbon atoms and the number of double bonds [9]. Such factors as the type of stationary phase, composition of the mobile phase and column temperature have been studied with a view to enhancing the resolution of critical pairs of TGs [10–13]. The light-scattering detector [14–16] affords an advantage over refractive index detectors in that elution gradients can be used, and over ultraviolet detectors in that no baseline drift occurs and there are no limitations on the use of mobile phase solvents.

Some workers have reported that the mass detector is subject to a non-linear relationship between reponse and the amount of solute injected [14,17], *i.e.*, the response (A) is proportional to the amount (m) injected raised to a power ($A = am^x$). The exponent, x, is closely linked to the nebulizer shape (pressure and temperature conditions in the evaporator).

The identification of chromatogram peaks is difficult because of the rarity of mixed TGs in a pure state. To indentify the HPLC-separated TG molecular species, the relationships between the retention time and the partition number [18,19], the equivalent carbon number (ECN) [12,20,21], the theoretical carbon number [10], or with the equivalent chain length [22] have been studied. All are similar concepts with differences in the manner in which they relate the carbon number and the number of double bonds in the fatty acids in the glycerides. Takahashi and co-workers [23,24] suggested a matrix model relating the retention time with the chain length and number of double bonds for each fatty acid in the glyceride, giving a more accurate prediction of the TG molecular species from the retention time than if only the total carbon number and number of double bonds were used, without distinguishing the positions of the fatty acids.

The object of this paper is to report the determination of the glyceride composition of the lipid fraction extracted from the mesocarp of the two major avocado cultivars in Spain, Fuerte and Hass, performed using an HPLC technique with a light-scattering detector. The application of mathematical modelling to the retention behaviour of TGs is used to estimate the TG composition.

EXPERIMENTAL

Sample preparation

Samples of avocado pears (varieties Hass and Fuerte) from Granada (Mediterranean coastal zone, Spain) were analysed.

The avocado pear samples were freeze-dried and the oil was obtained by Sxohlet extraction with chloroform–methanol (2:1). The oil sample (1 g) was extracted with ten volumes of *n*-hexane (Panreac, Madrid, Spain) containing 0.1 mg/ml butylhydroxytoluol (Fluka, Buchs, Switzerland) as an antioxidant. The mixture was homogenized and poured into a separation funnel with a solution of ethanol (Panreac) and distilled water (80:20, v/v), in the proportion 3:2 (v/v). The mixture was shaken vigorously and then allowed to stand until separation of the upper, organic fraction from the lower, aqueous alcoholic fraction was complete. The organic fraction was filtered through 1PS filter paper (Whatman, Maidstone, UK), exposed to a stream of nitrogen for 1 min, and evaporated to dryness under low pressure at 30°C. The TG residue was redissolved in HPLC-grade chloroform (2 ml; Ferosa, Madrid, Spain) and passed through a filter with a pore size of 0.2 μm (Millipore, Milford, MA, USA). Portions of the resulting solution were used for HPLC analysis.

HPLC analysis

The HPLC equipment consisted of two pumps (Models 510 and 6000A, Waters Chromatography Division, Milfrod, MA, USA), a system controller (Model 720, Waters Chromatography Division), an injector (Model 7125, Rheodyne, Cotati, CA, USA), two 25 cm × 4.6 mm I.D. stainless-steel columns containing a bonded phase composed of Sperisorb ODS-2 (Phase Separations, Queensferry, UK and Symta, Madrid, Spain), with a particle size of 3 μm, connected in series. The column effluent was passed through a mass detector (Model 750/14, ACS, Macclesfield, UK). The mass detector oven temperature was 60°C and the inlet gas pressure

(from an air compressor) was 20 p.s.i.g.; the detector was connected to an integration system (System Gold, Beckman, San Raman, CA, USA).

The column was placed in a hot air oven (Kariba Instruments, Cardiff, UK) to keep the analysis temperature constant at 30°C. The mobile phase consisted of an elution gradient from 35 to 70% (v/v) HPLC–grade acetone (Panreac) in HPLC–grade acetonitrile (Ferosa) in two stages: a linear increase in acetone at 4.6 μl/min for the first 45 min, followed by a linear increase in acetone at 2.4 μl/min from that point to 75 min. From 75 to 120 min elution was isocratic. The flow-rate was 0.8 ml/min and the pressure 2200 p.s.i.g.

The TGs were quantified based on the percentage peak area in the HPLC chromatogram.

To calculate response factors in relation to the internal standard, trilinolein (LLL) (99% pure, 10 mg/ml, Sigma Chemical, St. Louis, MO, USA), chloroform solutions containing 10 mg/ml of the simple TGs (99% pure, Sigma Chemical) tricaproin (CoCoCo), tricaprylin (ClClCl), tricaprin (CaCaCa), trilinolein (LLL), trilinolenin (LnLnLn), trimyristin (MMM), tripalmitolein (PaPaPa), tripalmitin (PPP), triolein (OOO) and tristearin (SSS) and the mixed TGs 1,2-dimyristoyl-3-palmitoyl glycerol (MMP), 1,2-dioleoyl-3-palmitoyl glycerol (OOP), 1,2-dipalmitoyl-3-oleoyl glycerol (PPO), 1,2-dioleoyl-3-stearoyl glycerol (OOS), 1,2-distearoyl-3-oleoyl glycerol (SSO) and 1,2-stearoyl-3-myristoyl glycerol (SSM) were analysed.

Five replications of the HPLC analysis were performed for one of the avocado oil samples to determine the reproducibility of the HPLC method. All analyses were performed in triplicate.

Calculation of the random composition

The random composition of the TGs in the avocado oil was calculated from the percentage mole fractions of the main fatty acids in the total TG fraction, taking the three positions on the glycerol molecule to be equivalent [25].

The fatty acid composition of the total TG fraction was obtained from data for avocado oil (varieties Fuerte and Hass) from Granada from previously reported data [2]. The percentage mole fraction values for the main fatty acids ranged from 0.50 to 19.22%.

Calculation of the ECN

The ECN for each individual TG was calculated using the formula given by Herslöf *et al.* [20]:

$$ECN = CN - (a'ND) \quad (1)$$

where CN is the total number of carbon atoms and ND the total number of double bonds in the fatty acids attached to the glycerol molecule. The value of the constant a' was calculated by multiple linear regression analysis of the experimental values of the dependent variable, log k', on the independent variables CN and ND for the TGs available in pure form [$\log k' = q' + b'(CN + c')ND$], where a' is the quotient of the coefficient c' on the coefficient b'.

Calculation of the equations used in the identification system

Linear and multiple regression were aplied to relate the ECN to log k'; log k' to the chain length (CL) and the number of double bonds (DB) in each of the three fatty acids in the TG molecule, taking the three possible positions to be equivalent; and log k' for mixed TGs to log k' for simple TGs [26]. The equations were calculated from experimental data for the available pure mixed and simple TGs.

RESULTS AND DISCUSSION

Fig. 1 shows the HPLC profiles for the TGs in the avocado oil from the two varieties (Fuerte and Hass) studied. The Fuerte variety gave 19 peaks, whereas the Hass variety gave 24. Reproducibility of the retention times of the peaks was good, with coefficients of variation of about 1% in all instances.

The molecular species that corresponded to each of the peaks on the chromatogram was determined by applying a system that had proved effective in an earlier experiment [27]. The first step was to compare the ECN for each peak with the ECNs for the possible TGs established from the fatty acid composition of the avocado oil.

The three stereospecific positions on the glycerol molecule were assumed to be equivalent, inasmuch as the position isomers were not distinguishable with the HPLC system used. Based on the eight main fatty acids, the total possible number of molecular species was calculated to be 120. However, the maximum number of molecular species de-

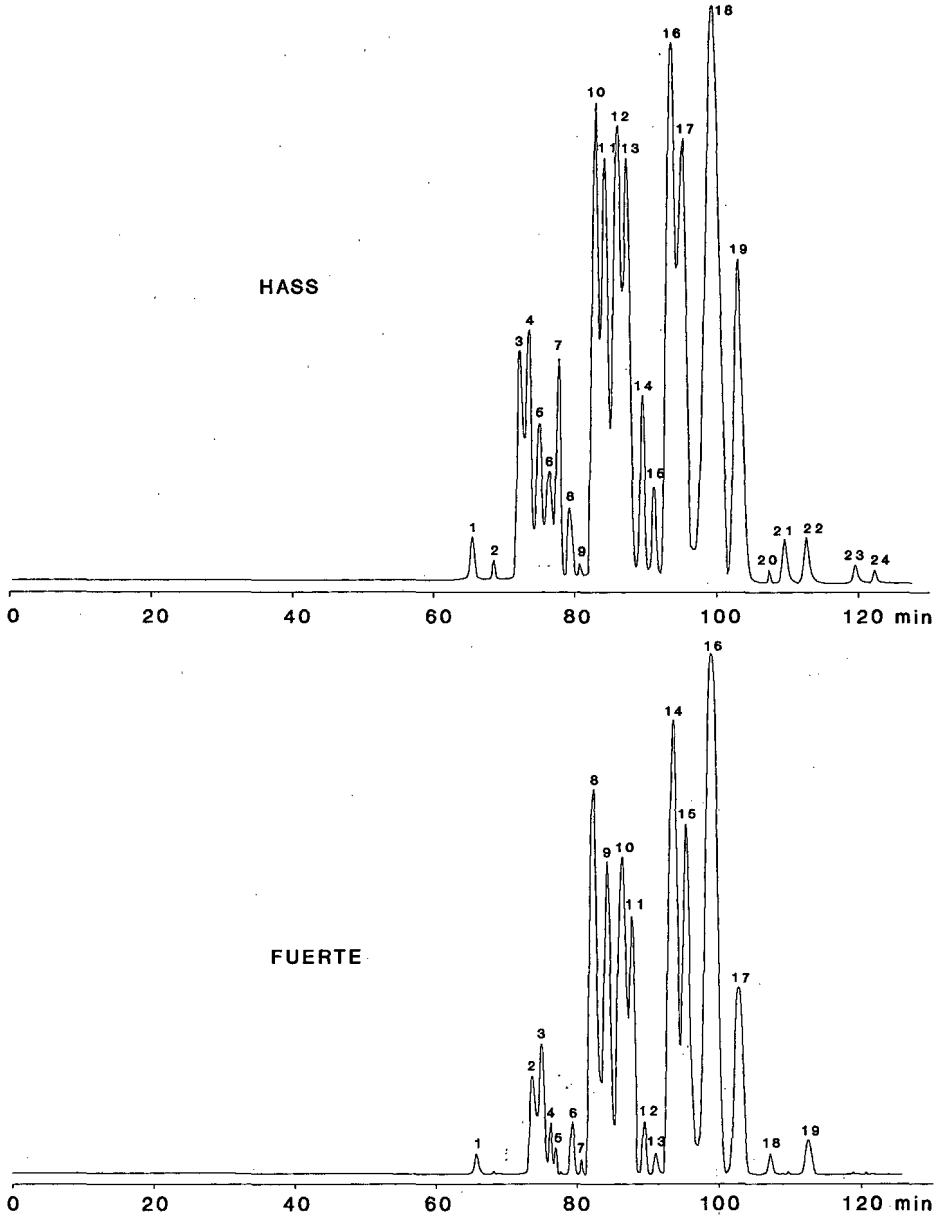

Fig. 1. HPLC analysis of avocado TGs. See Table I for identification of peak numbers.

scribed previously was 33 (28]; Lozano [8] has described 31 possible molecular species.

The usefulness of random composition in predicting the molecular species of TGs present in a fat has been shown previously [21,29]. As a result, the most probable molecular species were considered herein to be those with random composition values higher than 0.01%, which brought the number of possible TGs down to 41.

The ECN was at first calculated using eqn. 1. The value of the constant a' was calcualted to be 1.87 from the equation $\log k' = -0.7665 + 0.0426CN - 0.0797ND$ [standard error (S.E.) = 0.0553]. The TGs eluted, as expected, in ascending order of

ECN, except for certain series of critical pairs such as those with a partition number of 48, namely, OOO, OOP, OPP and PPP, for which the ECN values were 48.39, 48.26, 48.13 and 48.00, respectively, which eluted in descending order of ECN. The reason for this failure to conform to the generally accepted pattern of behaviour for TGs in non-aqueous, reversed-phase HPLC was attributed to improper estimation of the ECN by eqn. 1. The relationship between ECN and the molecular variables CN and ND may possibly be more complex than that described by the equation.

To elucidate this question, stepwise linear regression was applied, taking CN and ND and transforms thereof, as the independent variables.

$$ECN = CN(1 - 0.0062CN) - 1.1234ND(1 - 0.0256ND) \quad (2)$$

On the basis of the new ECN values calculated using eqn. 2, all the TGs eluted in ascending order of ECN.

Table I gives the ECN values for each of the peaks in the chromatogram for the total TG fraction from the sample of avocado oil from the Fuerte variety calculated using eqn. 3.

$$\log k' = -1.372 + 0.0797ECN \text{ (S.E. = 0.0152)} \quad (3)$$

Table I also gives the distribution of the 41 preselected possible TGs among the 19 peaks on the chromatogram according to their ECN calculated using eqn. 2. Theoretically, there was more than one TG for each of the peaks; and, additionally, certain molecular species could correspond to more than one peak.

In the next step the equation proposed by Takahashi *et al.* [26] was used to estimate the value of log k' for mixed TGs from the log k' values for the simple TGs composed of the appropriate fatty acids according to the composition of the mixed TGs (eqn. 4). The equation was applied to the possible TGs preselected in the preceding step.

$$\log k'_{ABC} = 1/3\log k'_{AAA} + 1/3\log k'_{BBB} + 1/3\log k'_{CCC} \text{ (S.E. = 0.0071)} \quad (4)$$

The experimental data for the mixed TGs MMP, OOP, OPP, OOS, MSS and OSS and the corresponding simple TGs confirmed the applicability of this equation to the chromatographic system used.

Table I shows that application of this equation reduced the number of possible TGs for each peak approximately by half and in some instances limited the possibility to a single TG. Thus, in step 1, six TGs (OOO, LOS, PaOS, OOP, LPS and MMP)

TABLE I

IDENTIFICATION OF TGs IN AVOCADO OIL (VARIETY FUERTE)

Peak No.	ECN (eqn. 3)	Possible TGs (eqn. 2)	Possible TGs (eqn. 4)
1	30.51	LLPa, LnOPa, LnPaP, LPaM, LnLP, LPaPa, PaPaPa	LLPa, LnOPa, LnLP, LPaPa
2	31.10	LLO, LnOO, LPaO, LLP, LnOP	LLO, LnOO, LPaOP
3	31.19	LLO, LnOO, LPaO, LLP, LnOP, PaPaO, LOM, LnPP	LLO, LPaP, LLP, PaPaO
4	31.32	LPaO, LLP, LnOP, PaPaO, LOM, LnPP, PaPaP	LPaO, LLP, LnOP, PaPaO, LOM
5	31.42	PaPaO, LOM, LnOP, PaPaP, LnPP, LLP, LPaO	LOM, LnPP, PaPaP, LnOP, LLP
6	31.45	PaPaO, LOM. LnOP, PaPaP, LnPP, LLP, LPaO	LOM, LnOP, PaPaP, LnPP, LLP
7	31.51	LOM, PaPaO, LnPP, PaPaP	LOM, PaPaP
8	31.91	LOO, LnOS, LLS, PaOO, LOP, LPaS, LnPS	LOO, PaOO
9	31.99	LOO, LnOS, LLS, PaOO, LOP, LPaS, LnPS	PaOO
10	32.11	PaOO, LOP, LPaS, LnPS, PaOP, LPP, OOM	LOP, OOM
11	32.19	PaOO, LOP, LPaS, LnPS, OOM, PaOP, LPP, PaPaS	LOP, OOM, PaOP, LPP
12	32.35	OOM, PaOP, LPP, PaPaS	PaOP, LPP
13	32.45	OOM, PaOP, LPP, PaPaS, PaPP, OMP	PaOP, LPP, PaPaS, PaPP, OMP
14	32.61	PaPP, OMP, MPP, OOO, LOS, PaOS, LPS	LPP, PaPaS, PaPP, OMP, OOO
15	32.66	PaPP, OMP, MPP, OOO, LOS, PaOS, LPS	LPP, PaPaS, OOO, PaPP, OMP
16	32.88	OOO, LOS, PaOS, OOP, LPS, MMP	OOP
17	33.17	PaPS, OPP	OPP
18	33.50	PaPS, OPP, PPP	PaPS, OPP
19	33.73	PPP, OOS	OOS

were possible for peak 16 ($\log k' = 1.249$), which had an ECN of 32.88. After application of eqn. 4, $\log k'$ for these TGs took on the values 1.237, 1.273, 1.278, 1.252. 1.284 and 1.177, respectively, hence OOP became the only possible TG for this peak.

The next step was to apply the equation put forward by Takahashi and co-workers [23,24] relating $\log k'$ for a TG to the chain length (L) and the number of double bonds (D) for the fatty acids making up the TG molecule (eqn. 5).

$$\log k' = -0.8072 + 0.0521L1 + 0.0246L2 + 0.0549L3 - 0.1479D1 - 0.08335D2 - 0.0186D3 \quad (\text{S.E.} = 0.0499) \quad (5)$$

Chain length for the acid at position 3 ($L3$) was calculated from the $\log k'$ values for each peak, using the order of fatty acids in the TGs established in Table II. Checking which of the TGs preselected using the above equation met the chain length requirement for the fatty acid at position 3 (Table II) yielded a new selection of molecular species.

Table II shows that most of the peaks on the chromatogram had only a single corresponding TG. The identification of peaks 16, 17 and 19 was confirmed by comparing the retention times with those for the mixed TGs available in the form of pure TGs, *i.e.* OOP, OPP and OOS.

TABLE II

TGs IN AVOCADO OIL (VARIETY FUERTE)

Peak no.	ECN (eqn. 3)	Possible TGs (eqn. 5)[a]
1	30.51	LLPa
2	31.10	LLO[a], LPaO
3	31.19	LLO, LPaO[a]
4	31.32	PaPaO, LLP[a]
5	31.42	PaPaO[a], LLP, LnPP
6	31.45	LnPP[a], PaPaP
7	31.51	PaPaP
8	31.91	LOO
9	31.99	PaOO
10	32.11	LOP
11	32.19	PaOP
12	32.35	LPP
13	32.45	PaPP
14	32.61	OOO[a], LOS
15	32.66	OOO, LOS[a]
16	32.88	OOP
17	33.17	OPP
18	33.50	PaPS
19	33.73	OOS

[a] TGs with greater possibility of corresponding to the particular peak.

The possible TGs for peaks 14 and 15 were the same, OOO and LOS, for both peaks. The ECN was the same (32.809) for both these TGs, hence it was difficult, in principle, to determine the order of elution. However, based on the retention time for the simple TG OOO, which was available in pure form, the TG OOO corresponded to peak 14. Therefore, it would appear that for TGs with the same ECN, the first to elute was the TG with the greatest number of unsaturated fatty acids.

According to eqn. 5, the TGs LnPP and PaPaP were the possible TGs for peak 6. LnPP was the most likely choice, because PaPaP was the only possible TG for peak 7 and hence should not be considered for peak 6. In addition, the ECN for LnPP (31.389) was lower than that for PaPaP (31.584) and thus eluted first. Consequently, the TG LnPP was disregarded for peak 5, which was thereby limited to the TGs PaPaO and LLP, which were also the most likely candidates for peak 4. The ECNs for these two TGs were 31.389 and 31.202, respectively, hence PaPaO probably corresponded to peak 5 and LLP to peak 4.

The two possible TGs for chromatographic peaks 2 and 3 were LLO and LPaO. Which of the two should elute first can be predicted from the ECN values. As the ECNs for these TGs were 31.023 for LLO and 31.202 for LPaO, the order of elution should be first LLO, then LPaO. Therefore, the likely TGs were LLO for peak 2 and LPaO for peak 3.

Based on the foregoing, it would appear that the relationship between ECN and CN or ND is not as simple as has been presumed up to now. This was to be expected, inasmuch as analytical methods developed in recent years have proved capable of resolving TGs with the same conventional ECN value.

TGs with equal ECNs eluted in ascending order of number of saturated fatty acids in the molecule. This was confirmed for the critical pairs OOO–LOS, LPaO–LLP, PaPaO–LnPP and PaOO–LOP (Table III). The behaviour of TGs in non-aqueous reversed-phase HPLC is therefore dependent not only on the CN and ND, but also on the number of unsaturated acids in the molecule.

The chromatographic peaks corresponding to the TG fraction of avocado oil from the Hass variety

TABLE III

TGs IN AVOCADO OIL (VARIETY HASS)

Peak No.	ECN	TGs
1	30.55	LLPa
2	30.60	LPaPa
3	31.16	LLO
4	31.21	LPaO
5	31.32	PaPaO
6	31.40	LLP
7	31.45	LnOP
8	31.52	LnPP
9	31.67	PaPaP
10	31.90	LOO
11	32.00	PaOO
12	32.10	LOP
13	32.19	PaOP
14	32.34	LPP
15	32.44	PaPP
16	32.60	OOO
17	32.63	LOS
18	32.85	OOP
19	33.14	OPP
20	33.39	PaPS
21	33.49	PPP
22	33.72	OOS
23	33.99	OPS
24	34.08	PPS

were identified using the same procedure described above. The TGs estimated were the same as those for the Fuerte variety, except that there were five additional TGs in the Hass variety, which corresponded to five additional chromatographic peaks.

Table III gives the TG composition of the avocado oil from the Hass variety. Peaks 2, 7, 21, 23 and 24, correspoding to the TGs LPaPa, LnOP, PPP, OPS and PPS, differentiated the oils from the two avocado varieties.

These results showed good agreement with the results reported by Lozano [8] and Gaydou *et al.* [4]. Although these workers succeeded in separating ten chromatographic peaks and estimating thirteen TGs, in the present experiment nineteen TGs were separated and estimated for the Fuerte variety and 24 for the Hass variety.

The enhanced resolution achieved with the analytical method employed here is reflected in peaks 2–7, for which Lozano [8] separated only two chromatographic peaks and described three TGs (LLO, LLP and LOPa), compared with the six peaks and TGs (LLO, LPaO, LLP, PaPaO, LnPP and PaPaP) separated here.

The resolution of peaks 8–12, which has been described previously by other workers, improved considerably in this experiment.

The differences between the TGs in the two avocado varieties considered were probably more quantitative than qualitative, because the chromatograms for the Fuerte variety displayed small traces that could not be quantified. The retention times for these trace peaks were the same as those for peaks 2, 7, 21, 23 and 24 in the Hass variety.

Quantitative analysis

As explained earlier, the response of the light-scattering detector is not dependent on the structure of the component detected but is closely related to the size of solute droplets. Therefore, response factor values should be 1 or close to 1. For TGs, the response should be independent of the number of carbon atoms and the number of unsaturated bonds.

To confirm this for the detection system used, the response factors were first calculated for each of the available pure TGs, simple or mixed, with respect to LLL, which eluted at an intermediate point on the chromatogram for the pure TGs and, moreover, was not detected in the avocado oil. The values so obtained all ranged from 0.976 to 1.043.

Next, the relationship between peak area and amount of sample injected was examined for sample amounts (pure TGs) ranging from 10 to 70 μg under the conditions already described for the system, to establish whether the relationship was linear over a smaller range than that studied by Perrin *et al.* [17] and Stolyhwo *et al.* [14]. Such a linear relationship is an esential condition if quantitative analysis is to be carried out using an integrator.

The linearity of the relationship was analysed for all the available pure TGs, simple or mixed; linear relationships were detected in all instances with coefficients of determination ranging from 0.990 to 0.999 and regression coefficients ranging from 23.91 to 25.35. The relationship between the log of the chromatographic peak area and the log of the amount of sample injected was also examined; the analysis yielded a regression coefficient of 1.001 ± 0.003, which was the value of the exponent in the

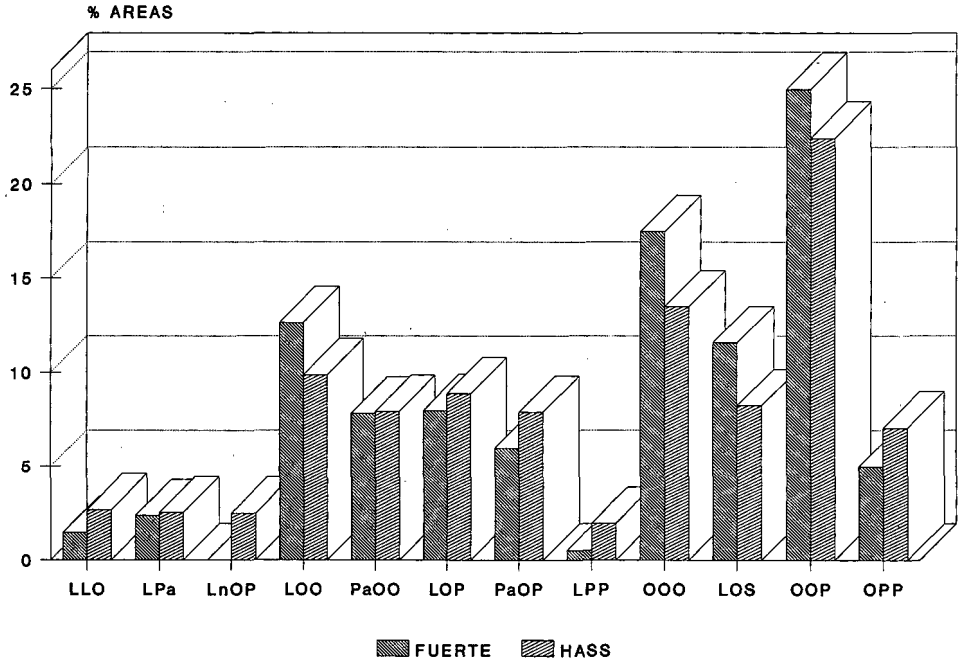

Fig. 2. Composition (%) of the major TGs in avocado oil (varieties Hass and Fuerte).

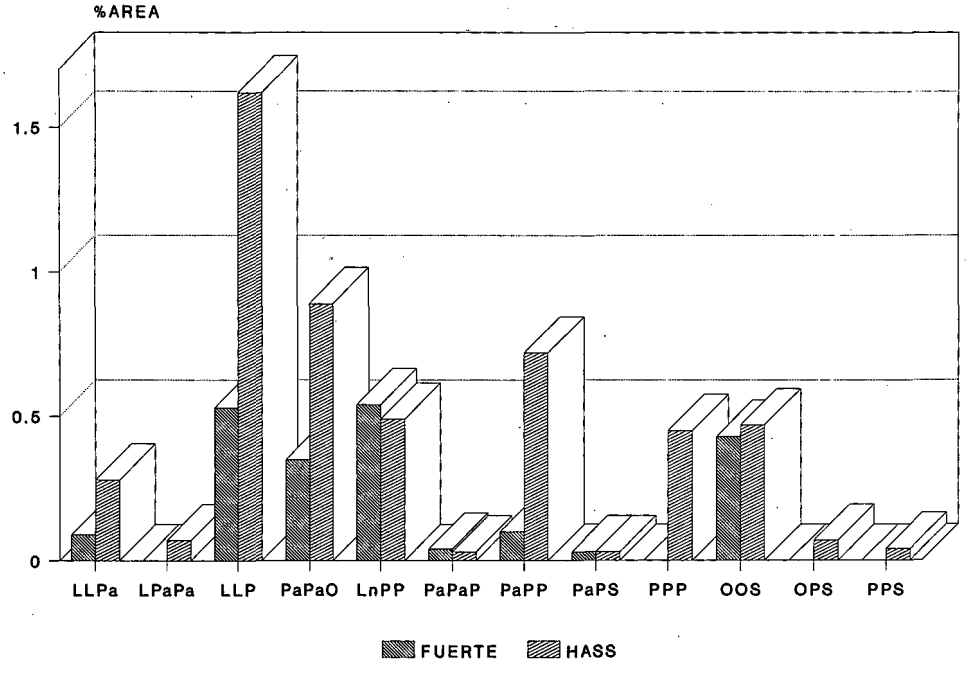

Fig. 3. Composition (%) of the minor TGs in avocado oil (varieties Hass and Fuerte).

equation $A = am^x$ mentioned previously. Thus the response can be assumed to be linear over a small interval of injection amounts, and quantfication of the components using an integrator is therefore possible.

Fig. 2 shows the percentage share of each of the main TGs in the oils of the two avocado varieties considered (Fuerte and Hass).

Fig. 2 shows that the TGs with the highest percentage shares, OOO, LOS, OOP and LOO, were present in higher amounts in the Fuerte variety than in the Hass variety. The rest of the major TGs were similar in the two varieties or lower in the Fuerte variety, whereas the shares of LnOP and PaPP in the Fuerte variety were each less than 0.5%; they were 2 and 7%, respectively, in the Hass variety. OOP was the major TG in both varieties and was present in a proportion of 22.41% in the Hass variety and 24.99% in the Fuerte variety.

Fig. 3 shows the percentages shares of the minor TGs present in the avocado oils from the Fuerte and Hass varieties. In all instances the shares were higher in the Hass variety than in the Fuerte variety, except for the TGs PaPaP and PaPS, which, with values of 0.03 and 0.04%, respectively, were similar in both varieties. In contrast, the shares of the TGs LPaPa, LnOP, PPP, OPS and PPS, which were not present in measurable amounts in the Fuerte variety, ranged between 0.04% for PPS and 2.5% for LnOP in the Hass variety.

Lozano [8] published data on the centesimal composition of major TGs, and the reported values were similar to the values reported here. By way of example, the percentage share values for the major TGs OOO, OOP and OPP reported by Lozano [8] were 18.6, 24.5 and 6.2, respectively, whereas the results recorded in this study were 14.5, 24.9 and 5.0 respectively. For the TGs LOP and PaOO, which Lozano [8] was unable to resolve chromatographically, the reported combined value was 16.2% [8], approximately equal to the sum of the percentages recorded in the present analysis (7.97% for LOP and 7.83% for PaOO), in which both these TGs were resolved.

The differences between the two varieties may have been due either to differing degrees of ripening of the fruit or to varietal differences, two factors which have been considered for various avocado varieties by other workers [4,30].

ABBREVIATIONS

Ca	Caprin
Cl	caprylin
Co	caproin
L	linolein
Ln	linolenin
M	mysristin
O	olein
P	palmitin
Pa	palmitolein
S	stearin

ACKNOWLEDGEMENTS

Thanks are due to C.I.C.Y.T. for the Project grant ALI88-0171. M.C.T. thanks the C.S.I.C. for a postdoctoral fellowship of the CONICET (Argentina)–CSIC (Spain) cooperation programme.

REFERENCES

1 C. Petrocini, E. Bazán, M. Panno and V. Averna, *Riv. Ital. Sostanze Grasse*, 4 (1978) 260.
2 L. M. Nieto, F. C. Rubio, S. R. Vives and M. V. M. Romero, *Grasas Aceites*, 39 (1988) 272.
3 J. V. Ratovohery, Y. F. Lozano and E. M. Gaydou, *J. Agric. Food Chem.*, 36 (1988) 287.
4 E. M. Gaydou, Y. Lozano and J. Ratovohery, *Phytochemistry*, 26 (1987) 1595.
5 Y. Lozano, J. Ratovohery and E. M. Gaydou, *Rev. Fr. Corps Gras*, 32 (1985) 377.
6 E. Bazán, M. Panno, C. Petrocini and V. Averna, *Riv. Ital. Sostanre Grasse*, 58 (1981) 571.
7 Ch. B. Sharma and G. C. Martinez, *J. Am. Oil Chem. Soc.*, 49 (1972) 229.
8 Y. Lozano, *Rev. Fr. Corps Gras*, 30 (1983) 333.
9 L. J. R. Barrón and G. Santa-María. *Chromatographia*, 23 (1987) 209.
10 A. H. El-Hamdy and E. H. Perkins, *J. Am. Oil Chem. Soc.*, 58 (1981) 867.
11 J. A. Singleton and H. W. Patee, *J. Am. Oil Chem. Soc.*, 61 (1984) 761.
12 E. Frede, *Chromatographia*, 21 (1986) 29.
13 L. J. R. Barrón, G. Santa-María and J. C. Diez Masa, *J. Liq. Chromatogr.*, 10 (1987) 3193.
14 A. Stolyhwo, H. Colin, M. Martin and G. Guiochon, *J. Chromatogr.*, 288 (1984) 253.
15 A. Stolyhwo, H. Colin and G. Guiochon, *Anal. Chem.*, 57 (1985) 1342.
16 M. Lafosse, M. Dreux and L. L. Morin-Allory, *J. Chromatogr.*, 404 (1987) 95.
17 J. L. Perrin, A. Prévot, A. Stolyhwo and G. Guiochon, *Rev. Fr. Corps Gras*, 31 (1984) 495.
18 S. Wada, C. Koizumi and J. Nonaka, *Yukagaku*, 26 (1977) 95.

19 S. Wada, C. Koizumi, A. Takiguchi and J. Nonaka, *Yukagaku,* 27 (1978) 579.
20 B. Herslöf, O. Podlaha and B. Töregard, *J. Am. Oil Chem. Soc.,* 56 (1979) 864.
21 L. J. R. Barrón, M. T. G. Hierro and G. Santa-María, *J. Dairy Res.,* 57 (1990) 517.
22 J. P. Goiffon, C. Reminiac C. and D. Furon, *Rev. Fr. Corps Gras,* 28 (1981) 199.
23 K. Takahashi, T. Hirano and K. Zama, *J. Am. Oil Chem. Soc.,* 61 (1984) 1226.
24 K. Takahashi, T. Hirano, M. Egi and K. Zama, *J. Am. Oil Chem. Soc.,* 62 (1985) 1489.
25 A. E. Bailey, *Industrial Oil and Fat Production,* Interscience, New York, 2nd ed., 1951, p. 834.
26 K. Takahashi, T. Hirano and M. Saito, *Nippon Suisan Gakkaishi,* 54 (1988) 523.
27 L. J. R. Barrón and G. Santa-María, *Chromatographia,* 28 (1989) 183.
28 C. B. Sharma and G. C. Martinez, *J. Am. Chem. Soc.,* 49 (1971) 229.
29 K. V. V. Nurmela and L. T. Satama, *J. Chromatogr.,* 435 (1988) 139.
30 Y. F. Lozano, J. V. Ratovohery and E. M. Gaydou, *Lebensm-Wiss. Technol.,* 24 (1991) 46.

Journal of Chromatography, 607 (1992) 339–347
Elsevier Science Publishers B.V., Amsterdam

CHROM. 24 087

Determination of additives in wine by high-performance liquid chromatography

M. Calull*, R. M. Marcé, G. Sánchez and F. Borrull

Departament de Química, Universitat de Barcelona, Plaça Imperial Tárraco 1, 43005 Tarragona (Spain)

ABSTRACT

Two methods for determining additives in wine samples by reversed-phase high-performance liquid chromatography using UV–visible detection were studied. One method used gradient elution for the separation of the different additives in a short time (less than 12 min). Before the injection of the sample, a solid-phase extraction was applied to obtain better results when a red wine was analysed. The other method effected the separation of these compounds by isocratic elution using cetyltrimethylammonium bromide (CTAB) as an ion-pair reagent, without sample pretreatment.

INTRODUCTION

Different methods have been developed for the determination of food additives, including UV spectrophotometry [1,2], thin-layer chromatography [3,4], gas chromatography [5–7] and high-performance liquid chromatography (HPLC) [8–16]. The HPLC technique is the most commonly used method for the determination of possible additives in different foods, *e.g.*, cheese [13], mayonnaise [10], yoghurt [14,16], cosmetic products [11], liquid foods [15], powdered milk [15], sauces, mustard and coconut cream [15].

The control of different additives is important owing to the strict control of wine quality. Among different additives, antiseptics and antioxidants are commonly used in wine treatment, and their addition is regulated. Only the addition of sulphur dioxide, sorbic acid and ascorbic acid is permitted, and only up to a certain concentration. The Office International de la Vigne et du Vin (OIV) established two HPLC methods to determine different possible compounds by isocratic elution (one allowed the separation of the most polar and the other the least polar compounds) [17].

In this work, two methods to determine a group of antiseptics (sorbic acid, benzoic acid, *p*-chlorobenzoic acid, salicylic acid, *p*-hydroxybenzoic acid, ethyl *p*-hydroxybenzoate), an antioxidant (ascorbic acid) and a sweetener (saccharin) by reversed-phase HPLC using UV–VIS detection were developed, one involving gradient elution and the other isocratic elution. Simultaneous separation of these additives by isocratic elution is difficult because of their different polarities. For this reason ion-pair chromatography was used.

In the gradient elution method, the determination of saccharin and ascorbic acid was not possible because of their high polarity and their co-elution with other polar compounds in the wine sample at the beginning of the chromatogram.

When the gradient method was applied to determine these compounds in red wine samples, pretreatment of the sample was needed to decrease the interference of the matrix. In this work, a solid-phase extraction with strong anion exchange (LC-SAX) cartridges was applied, and the different conditions of treatment were optimized.

Although good resolution can be obtained in a short time when a gradient of solvent strength is used, isocratic elution has some advantages in routine analysis. In this work, an isocratic method to determine all compounds, including ascorbic acid and saccharin, was also optimized using ion-pair

0021-9673/92/$05.00

chromatography. Using this method, salicylic acid could not be determined because a peak distortion appeared.

When the ion-pair method was used, different variables influencing the separation were taken into account and their influence was studied to obtain the optimum conditions.

EXPERIMENTAL

Equipment

A Hewlett-Packard (Avondale, PA, USA) liquid chromatograph with an HP 1040M diode-array detector was used. Separation was carried out using a 5-μm Spherisorb ODS-2 column (250 × 4.6 μm I.D.) with a precolumn (30 × 3.9 mm I.D.) packed with μBondapack C_{18}/Corasil (particle size 37–50 μm) (Teknokroma, Barcelona, Spain). Chromatographic data were collected and recorded using an HP 7999A workstation.

Reagents and standards

In both methods studied, acetic acid, phosphoric acid, sulphuric acid and 0.05 *M* acetate–0.05 *M* phosphate buffer solution (Merck, Darmstadt, Germany) were used as modifiers of the pH, acetonitrile (HPLC quality from Merck) as organic modifier and cetyltrimethylammonium bromide (CTAB) (Sigma, St.Louis, MO, USA) and tetrabutylammonium bromide (Fluka, Buchs, Switzerland) as ion-pair reagents. Water was purified in a Milli-Q water purification system (Millipore, Bedford, MA, USA).

The additives studied were ascorbic acid, benzoic acid, salicylic acid, sorbic acid, *p*-chlorobenzoic acid, *p*-hydroxybenzoic acid, ethyl *p*-hydroxybenzoate and saccharin (Sigma). The study was carried out with a standard solution of additives at a concentration of 10 ppm in water–acetonitrile (50:50).

Chromatographic conditions

Gradient elution. The chromatographic conditions adopted were as follows: flow-rate, 1 ml/min; detection, UV absorption at 240 nm; volume injected, 5 μl; temperature, constant at 60°C; and mobile phase, acetic acid at pH 3 as solvent A and acetonitrile as solvent B with a gradient programme (Table I).

Isocratic elution. The chromatographic conditions were as follows: flow-rate, 1 ml/min; detection, UV absorption at 235 nm; volume injected, 5 μl; and temperature, constant at 40°C. The mobile phase composition was optimized and the best conditions obtained were 2 m*M* CTAB, 35% of acetonitrile and 10% of buffer solution (0.05 *M* H_3PO_4– and 0.05 *M* acetic acid adjusted with 2 *M* NaOH at pH 5.5).

TABLE I

GRADIENT ELUTION PROGRAMME

Time (min)	Solvent A (%)	Solvent B (%)
0	85	15
2	85	15
8	60	40
15	0	100
20	85	15
30	Next injection	

Sample preparation

All wine samples were filtered with a 0.45-μm nylon membrane. When the gradient elution method was applied to a red wine, a solid-phase extraction to remove the coloured compounds and decrease the interference of the matrix with the anion exchange LC-SAX cartridges (quaternary amine-bonded silica, strong anion exchanger) (Supelco, Bellefonte, PA, USA) was necessary. The cartridge was conditioned with 5 ml of Milli-Q purified water and then 1 ml of sample diluted 1:2 was slowly passed through the extraction tube. In order to obtain a good recovery of additives, it was necessary to pass 1.5 ml of 0.5 *M* sulphuric acid through the cartridge. After homogenization of the two fractions the sample can be injected.

RESULTS AND DISCUSSION

Gradient elution

Simultaneous separation of some of these compounds using gradient elution have been reported [10,11,14–16]. In this work, a preliminary study was carried out to determine sorbic acid, salicylic acid, benzoic acid, *p*-hydroxybenzoic acid, *p*-chlorobenzoic acid and ethyl *p*-hydroxybenzoate with gra-

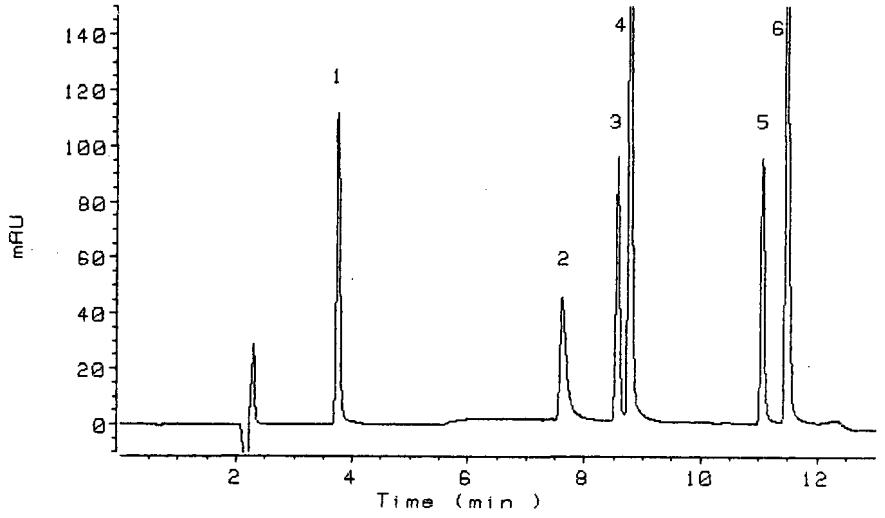

Fig. 1. Chromatogram of standards obtained by gradient elution. Peaks: 1 = *p*-hydroxybenzoic acid; 2 = salicylic acid; 3 = benzoic acid; 4 = sorbic acid; 5 = ethyl *p*-hydroxybenzoate acid; 6 = *p*-chlorobenzoic acid.

dient elution. The mobile phase was acetic acid (pH 3) with acetonitrile as organic modifier.

Different acids were used to adjust the pH of solvent A to 3. When sulphuric or phosphoric acid was used, distortion of the peaks occurred. A good baseline in wine analysis was obtained when acetic acid was used. The pH was established at 3 because higher values increased peak distortion and shoulders on the peaks appeared; on the other hand, low values increased absorption of the mobile phase.

Fig. 1 shows a chromatogram of a standard mixture of compounds obtained with the above experimental conditions. Under these conditions a good separation of the different compounds was obtained within 12 min.

In all the experiments carried out to obtain the optimum conditions in the gradient elution, ascorbic acid and saccharin eluted with short retention times, owing to the high polarity of these compounds. When a wine sample spiked with a standard solution was analysed, these compounds coeluted with other compounds present and for this reason the determination of these two additives was not possible by the gradient elution method. Under the experimental conditions chosen, only six of the eight additives studied appeared in the chromatogram.

Fig. 2 shows the chromatogram obtained when a red wine sample spiked with a standard solution was analysed. A baseline distortion can be observed caused by the large number of compounds present in wine and which absorb at this wavelength when the gradient elution method is used. This distortion of the baseline can cause difficulties with determinations, mainly for salicylic acid.

Solid-phase extraction can be used to clean up the sample before injection. The great difference in the polarities of the compounds studied made it difficult to carry out this extraction with a Sep-Pak C_{18} cartridge. Only Terada and Sakabe [12] used this method after the formation of an ion pair with CTAB. In this study, the clean-up of the sample was carried out with LC-SAX tubes. The chromatogram of the same red wine spiked with the standard solution after solid-phase treatment is shown in Fig. 3.

In order to optimize the extraction conditions with the SAX cartridge, after 1 ml of the sample spiked with the standard solution had passed through the cartridge, different volumes of sulphuric acid were tested to elute the compounds; 1, 1.5 and 2 ml of 0.5 *M* sulphuric acid were compared (Table II), and good results were obtained with 1.5 ml. Higher elution volumes involved greater dilu-

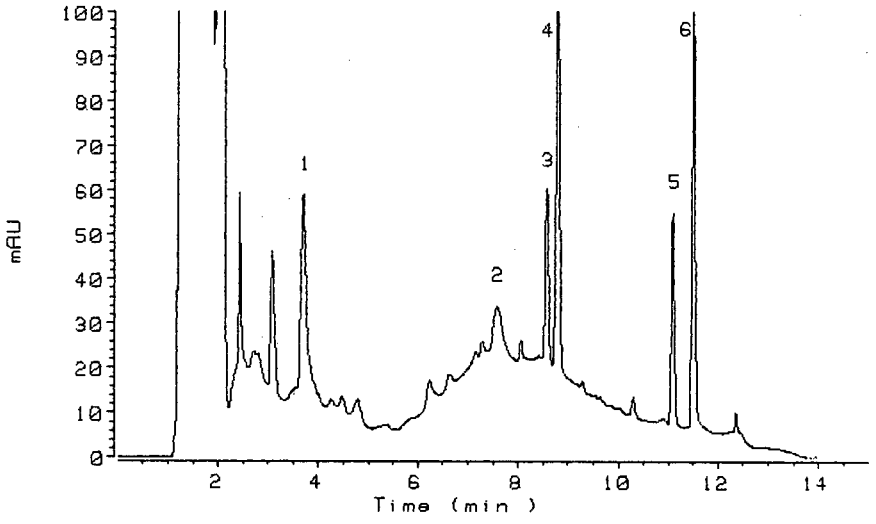

Fig. 2. Chromatogram of red wine spiked with standards obtained by gradient elution without SAX extraction. Peaks as in Fig. 1.

tion of the sample, and the results were not improved. A concentration of sulphuric acid lower than 0.5 *M* did not elute compounds with good recoveries.

The purity of the peaks was checked with the HP 1040 diode-array detector. The peaks for a wine sample were compared with those for the standard and the match factor was determined. In all instances the match factors were higher than 990, indicating that the peaks were pure.

Before this method can be applied to real samples it is necessary to validate the method and determine the recovery, repeatability, reproducibility, linearity and detection limit. To determine the recovery of the method, including SAX treatment, a red wine sample was spiked with different concentrations of

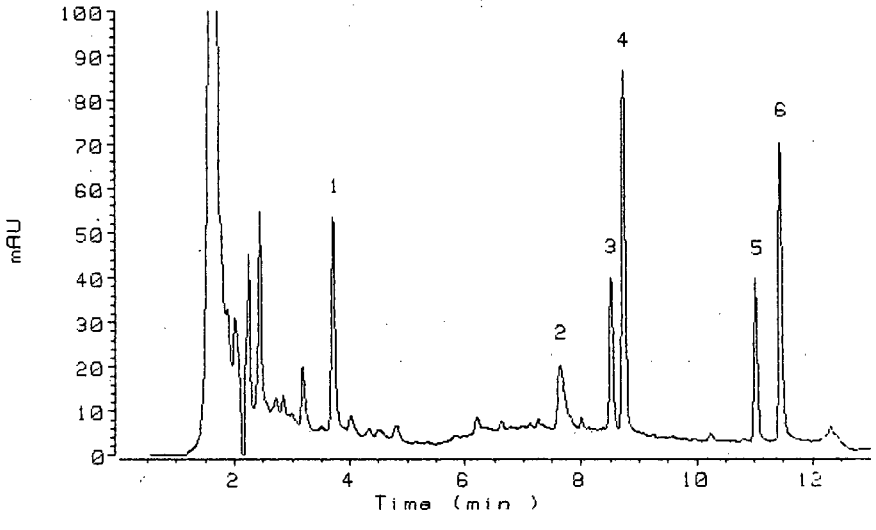

Fig. 3. Chromatogram of the same red wine as in Fig. 2 spiked with a solution of standards obtained by gradient elution after SAX extraction. Peaks as in Fig. 1.

TABLE II

EFFECT OF THE VOLUME OF 0.5 *M* SULPHURIC ACID IN THE SAX TREATMENT

Compound	Volume of H_2SO_4 (ml)	Amount added (ppm)	Found (ppm)	Recovery (%)
p-Hydroxybenzoic acid	1	10.41	9.50	91.3
	1.5		9.30	89.3
	2		9.23	88.7
Salicylic acid	1	10.07	7.75	77.2
	1.5		9.38	93.2
	2		9.24	91.8
Benzoic acid	1	10.51	9.76	92.9
	1.5		10.76	102.4
	2		11.24	107.0
Sorbic acid	1	10.80	8.89	83.1
	1.5		9.13	84.5
	2		9.44	87.4
Ethyl *p*-hydroxybenzoate	1	9.90	8.74	88.3
	1.5		8.94	90.3
	2		8.97	90.6
p-Chlorobenzoic acid	1	10.33	7.01	67.9
	1.5		8.96	86.7
	2		9.35	90.5

the standard solution and the results are given in Table III.

A study of the repeatability of the method and its reproducibility between days was performed. The results for repeatability showed a relative standard deviation ($n = 10$) ranging from 1.8 to 4% and those for reproducibility between days from 2.5 to 5%.

Good linearity of response was obtained for all the compounds studied between 5 and 50 ppm. For sorbic acid, whose addition is allowed up to 200 ppm, linearity was studied from 5 to 300 ppm.

The detection limit of the method was 0.5 ppm. However, this could be enhanced for a particular analysis by using the wavelengths of maximum absorption (benzoic acid, 225 nm; sorbic acid, *p*-hydroxybenzoic acid and its ethyl ester, 260 nm; and salicylic acid and *p*-chlorobenzoic acid , 235 nm). In this work a wavelength of 240 nm chosen for the simultaneous detection of all these compounds.

Isocratic elution

The different polarities among the additives requires ion-pair formation in order to determine them by isocratic elution. As a preliminary step, it was necessary to select the ion-pair reagent. Two ion-pair reagents, CTAB and tetrabutylammonium bromide, were studied. After preliminary experiments, CTAB was chosen because it was not possible to determine sorbic acid with tetrabutylammonium bromide under the conditions chosen for this study.

Different variables influencing the separation were studied. In the first step, pH was optimized because it had the greater influence on the resolution, especially in the separation of sorbic and benzoic acids.

The influence of pH on k' is shown in Fig. 4. The influence of pH was similar for all the acids but different from that observed for saccharin and ethyl *p*-hydroxybenzoic acid. Fig. 4 shows the different k' values of *p*-chlorobenzoic acid at different pH values and its high value with respect to the others. After different experiments a pH of 5.5 was chosen.

The concentration of the buffer solution was studied. Fig. 5 shows a decrease in k' at higher percentages of buffer for all the compounds except of ethyl *p*-hydroxybenzoate, which showed a different

TABLE III

STUDY OF THE RECOVERY WITH SAX TREATMENT

Compound	Amount added (ppm)	Found (ppm)	Recovery (%)
p-Hydroxybenzoic acid	5.20	5.18	99.7
	10.41	9.30	89.3
	31.23	27.67	88.6
	52.05	46.06	88.5
Salicylic acid	5.04	3.97	78.7
	10.07	9.38	93.2
	30.21	27.58	91.3
	50.35	46.22	91.8
Benzoic acid	5.26	6.00	114.1
	10.51	10.76	102.4
	31.53	31.40	99.6
	52.55	52.34	99.6
Sorbic acid	5.40	5.02	92.9
	10.80	9.13	84.5
	32.40	27.67	85.4
	54.00	45.74	84.7
Ethyl *p*-hydroxybenzoate	4.95	5.00	100.9
	9.90	8.94	90.3
	29.70	26.05	87.7
	49.50	43.31	87.5
p-Chlorobenzoic acid	5.16	4.99	96.7
	10.33	8.96	86.7
	30.99	26.90	86.8
	51.65	45.19	87.5

behaviour. The best separation was obtained at 10%, as the separation between ascorbic, *p*-hydroxybenzoic acid and ethyl *p*-hydroxybenzoate was better than that obtained at 5%, and *p*-hydroxybenzoic acid and its ester overlapped at 15%.

Fig. 6 shows the effect of CTAB concentration on the capacity factors. An increase in k' is observed with increase in CTAB concentration, except for ethyl *p*-hydroxybenzoate, which showed only a slight increase. Overlapping of different peaks appeared at CTAB concentrations less than 2 m*M* but concentrations higher than 2 m*M* resulted in higher k' values. Therefore, a concentration of 2 m*M* was chosen as the optimum.

The effect of the percentage of acetonitrile was studied and the results are shown in Fig. 7. A value

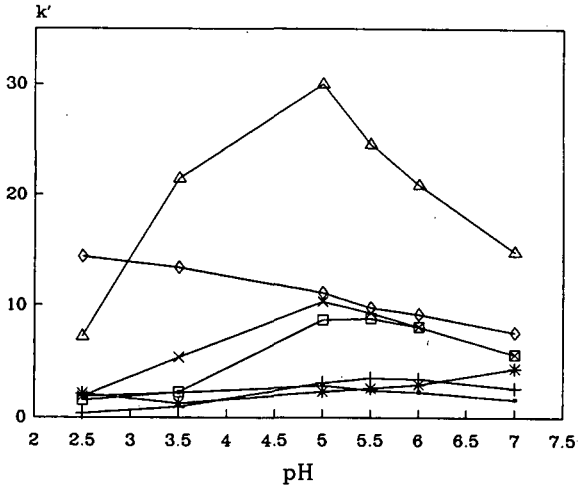

Fig. 4. Effect of the pH of the buffer solution added to the mobile phase containing 2 m*M* CTAB as an ion-pair reagent, 5% of buffer solution and 35% of acetonitrile on the k' of the additives. ● = Ascorbic acid; + = *p*-hydroxybenzoic acid; * = ethyl *p*-hydroxybenzoate; □ = sorbic acid; × = benzoic acid; ◇ = saccharin; △ = *p*-chlorobenzoic acid.

of 35% was chosen because this is the maximum concentration that involved no co-elution of peaks and gave an acceptable analysis time.

From the different experiments carried out, the optimum conditions chosen were 35% of acetoni-

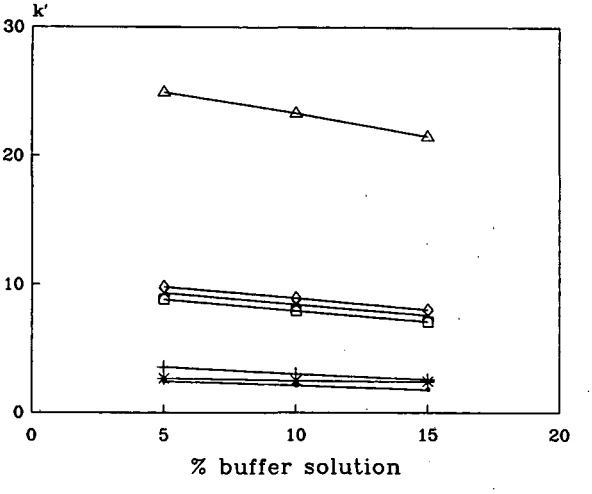

Fig. 5. Effect of the concentration of buffer solution (pH 5.5) on the k' of the additives. Mobile phase containing 2 m*M* of CTAB and 35% of acetonitrile. Symbols as in Fig. 4.

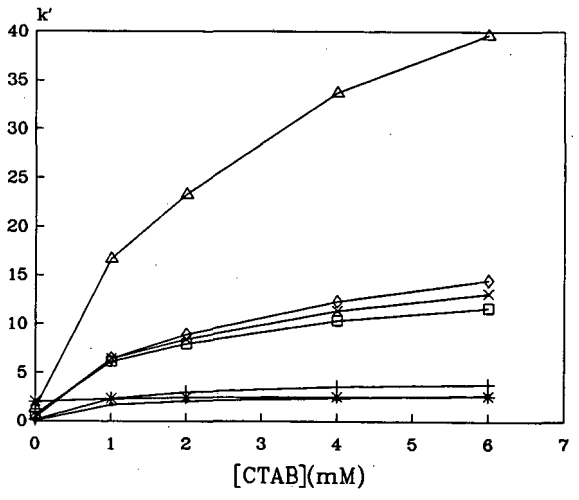

Fig. 6. Effect of the concentration of CTAB on k' of the additives. Mobile phase, acetonitrile–water–buffer (pH 5.5) (35:55:10). Symbols as in Fig. 4.

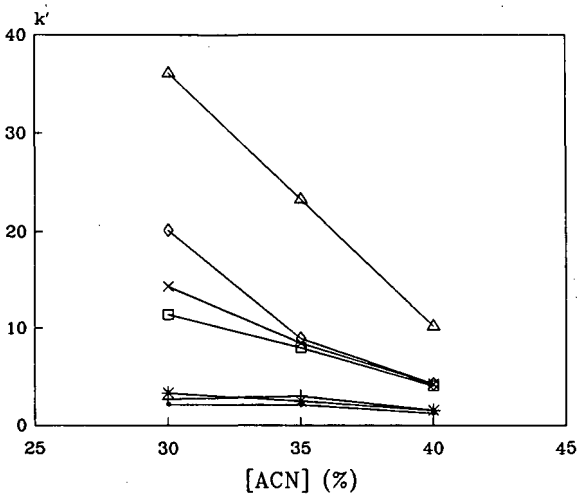

Fig. 7. Effect of the concentration of acetonitrile on the k' of the additives. Mobile phase containing 2 mM CTAB and 10% of buffer solution at pH 5.5. Symbols as in Fig. 4.

trile, 10% of buffer solution at pH 5.5 and an ion-pair concentration of 2 mM. The analysis time under these conditions was 40 min and good resolution between the different peaks was obtained. A chromatogram of a standard solution is shown in Fig. 8. As can be seen, the long analysis time is due to the determination of *p*-chlorobenzoic acid. This is not, however, the most important additive, and when its determination is not required, the analysis time decreases to 18 min.

Salicylic acid could not be determined by this method because of the distortion of the peak and its low sensitivity under the conditions adopted.

The optimization of the mobile phase was carried

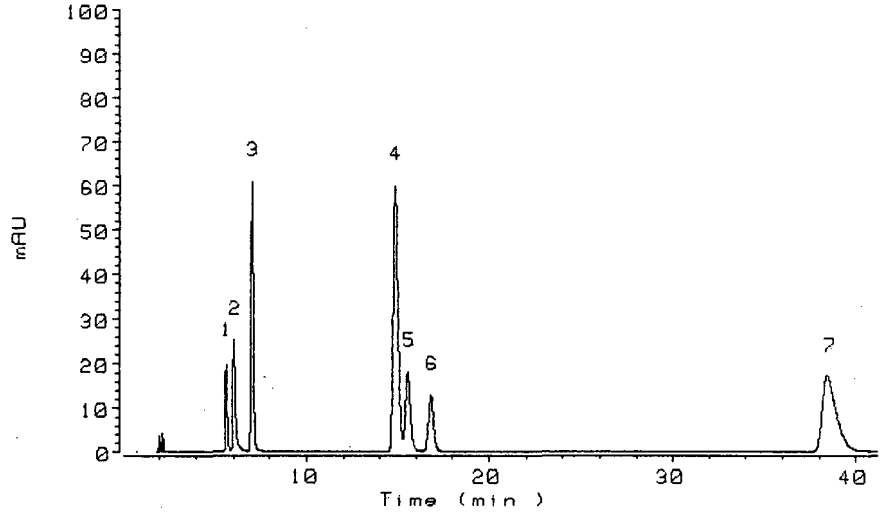

Fig. 8. Chromatogram of standards obtained under the optimum experimental conditions. Peaks: 1 = ascorbic acid; 2 = ethyl *p*-hydroxybenzoate; 3 = *p*-hydroxybenzoic acid; 4 = sorbic acid; 5 = benzoic acid; 6 = saccharin; 7 = *p*-chlorobenzoic acid.

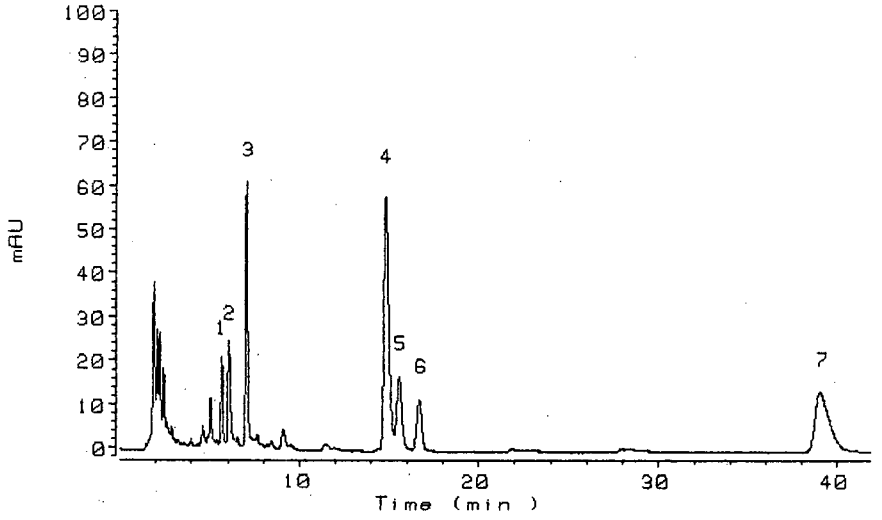

Fig. 9. Chromatogram of a red wine spiked with standards. Peaks as in Fig. 8.

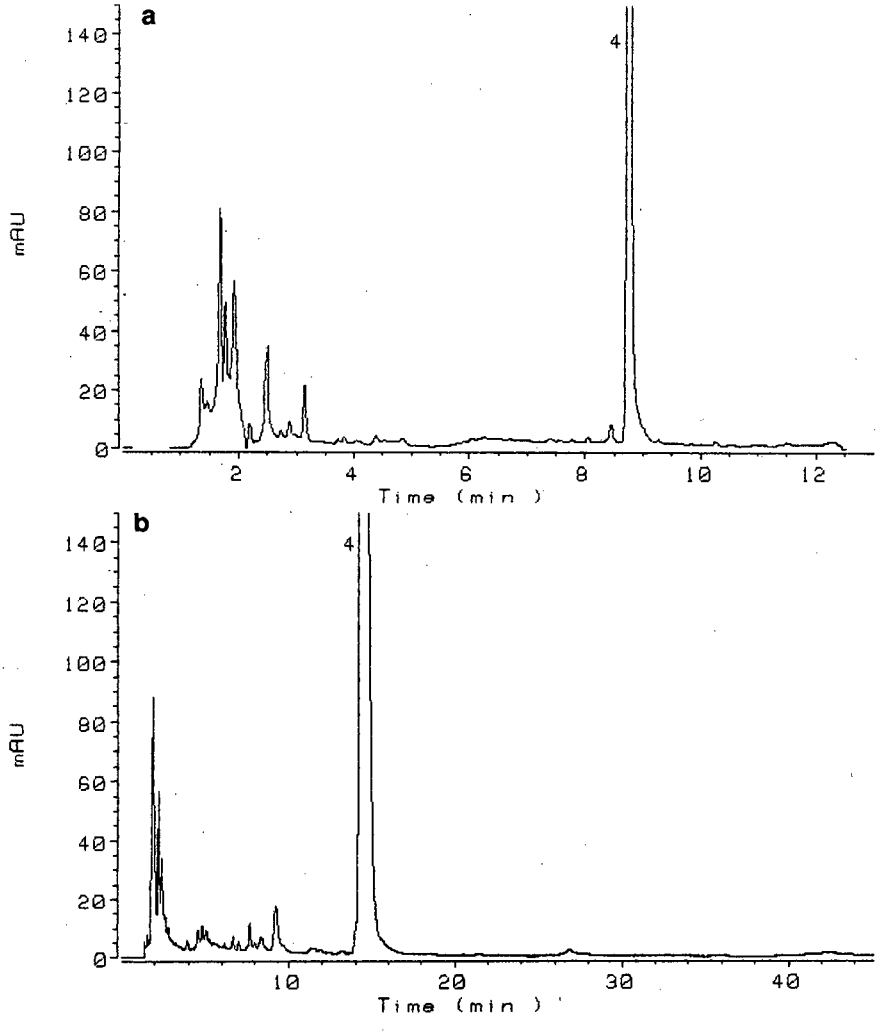

Fig. 10. Chromatogram of a white wine in which sorbic acid was detected (peak 4). (a) Gradient elution method; (b) isocratic method.

out taking into account the possible co-elution of other substances when a wine is analysed. The elution of a red wine sample spiked with a standard solution is shown in Fig. 9.

Similar studies carried out with the gradient method were applied to validate this isocratic method. Matrix interference was studied and no interference was obtained with either by red wine or white wine, so no sample pretreatment is necessary. The repeatability of the method showed a relative standard deviation ($n = 10$) between 2.0% and 4.2% and the reproducibility between days was between 2.7% and 6.1%.

The detection limit of the method was established as 0.5 ppm for all the substances except ascorbic acid (3 ppm). Good linearity of response was obtained between the same range of concentrations. Linearity for ascorbic acid was obtained from 5 to 300 ppm and for saccharin from 5 to 50 ppm.

After both methods had been validated, several wine samples were analysed to determine these compounds. Only in some of them was sorbic acid detected, at a very low concentration. The chromatograms obtained by the two methods for one of the white wines analysed, in which sorbic acid was detected, are shown in Fig. 10. The result obtained by the gradient method was 170 ppm and by the isocratic method 162 ppm.

The purity of the sorbic acid peak was checked and factors of 995 and 994 were obtained for the peak obtained by the gradient method and the isocratic method, respectively. To confirm the identification, each spectrum was compared with one recorded in a UV–VIS spectral library and factors of 992 and 994 were obtained.

CONCLUSIONS

Two methods for determining additives in wine samples were developed. The gradient method showed good results and a short analysis time, but no determination of the most polar compounds was possible under the conditions studied. In this event, if a red wine is analysed, pretreatment of the sample is required to obtain good results. On the other hand, ion-pair chromatography allows the separation of the additives, including saccharin and ascorbic acid, by isocratic elution with no pretreatment of the sample, but the analysis time is longer if *p*-chlorobenzoic acid is to be determined.

REFERENCES

1 H. Sokol, *Drug Stand.*, 20 (1972) 89.
2 D.W. Fink, H.C. Fink, J.W. Tolan and J. Blodinger, *J. Pharm. Sci.*, 67 (1978) 837.
3 C. Gertz and J. Hild, *Z. Lebensm.-Unters.-Forsch.*, 170 (1980) 103.
4 J. Sherma and S. Zorn, *Int. Lab.*, 12 (1982) 68.
5 A. Geahchan, M. Pierson and P. Chambon, *J. Chromatogr.*, 176 (1979) 123.
6 G.B. Cox, C.R. Lascombé and K. Sugden, *Anal. Chim. Acta*, 92 (1977) 345.
7 B.K. Larsson, *J. Assoc. Off. Anal. Chem.*, 66 (1983) 775.
8 F. Eisenbeiss, M. Weber and S. Ehlerding, *Chromatographia*, 10 (1977) 262.
9 M.A. McCalla, F.Mark and W.H. Kipp, *J. Assoc. Off. Anal. Chem.*, 60 (1977) 71.
10 A. Collinge and A. Noirfalise, *Anal. Chim. Acta*, 132 (1981) 201.
11 L. Gagliardi, A. Amato, A. Basili, G. Cavazzutti, E. Gattavecchia and D. Tonelli, *J. Chromatogr.*, 315 (1984) 465.
12 H. Terada and Y. Sakabe, *J. Chromatogr.*, 346 (1985) 333.
13 I. Saito, H. Oshima, N. Kawamura, K. Uno and M. Yamada, *J. Assoc. Off. Anal. Chem.*, 70 (1987) 507.
14 M.L. Puttemans, C. Branders, L. Dryon and D.L. Massart, *J. Assoc. Off. Anal. Chem.*, 68 (1985) 80.
15 L.V. Bui and C. Cooper, *J. Assoc. Off. Anal. Chem.*, 70 (1987) 892.
16 F. Olea, I. Sánchez and G. Noguera, *J. Liq. Chromatogr.*, 14 (1991) 709.
17 *Recueil des Méthodes Internationals d'Analyse des Vins et des Moûts*, Office International de la Vigne et du Vin, Paris, 1990.

Journal of Chromatography, 607 (1992) 349–352
Elsevier Science Publishers B.V., Amsterdam

CHROM. 24 077

Effect of germination on the oligosaccharide content of lupin species

M. Muzquiz*, C. Rey and C. Cuadrado

Departamento de Producción y Tecnología de Alimentos, Instituto Nacional de Investigaciones Agrarias, Apartado 8111, Madrid (Spain)

G. R. Fenwick

AFRC Institute of Food Research, Norwich Laboratory, Colney Lane, Norwich NR4 7UA (UK)

ABSTRACT

The effect of germination on the oligosaccharide content of two lupin species (*Lupinus albus* and *Lupinus luteus*) was determined with an extraction method, using aqueous methanol and purification through ion-exchange minicolumns. The quantification was carried out using high-performance liquid chromatography and showed that during germination of both species there was a clear reduction in the levels of raffinose family oligosaccharides.

INTRODUCTION

Legumes are well known inducers of intestinal gas (flatulence) because of the presence of oligosaccharides of the raffinose family. These sugars are characterized by the presence of α-D-galactopyranosyl residues bound to the glucose moiety of sucrose [1]. Animals and man are not able to digest such oligosaccharides because of the absence of α-1,6-galactosidase in their intestinal mucosa. Consequently the raffinose oligosaccharides pass into the colon and, as they are unable to be transported across the intestinal wall, are fermented by intestinal bacteria with considerable production of gas, mainly carbon dioxide [2]. It is clearly desirable to decrease the oligosaccharide content of legumes if they are to be most efectively exploited as inexpensive sources of protein.

A number of studies have indicated that the content of raffinose oligosaccharides in a range of legumes decreases during germination [3–5]. This could consequently increase the nutritional value of these foods, since there is evidence that protein content and quality are unaffected [6,7].

Lupin seed represents a potentially important source of protein for animal and human consumption. The utilization of this crop has been limited for some years as a result of the presence of toxic alkaloids [8], but low-alkaloid, "sweet" varieties are now available for cultivation. The present study was initiated to examine the effect on oligosaccharide content of germination of two species of lupin, *Lupinus albus* and *Lupinus luteus*.

EXPERIMENTAL

Seeds of two species of bitter lupin (*L. albus* from Badajoz and *L. luteus* from Huelva) were used in the present study. The surface of the seeds was sterilized with 6% calcium hypochlorite and washed repeatedly with deionized water prior to germination.

Chemicals

Water purified with a Milli-Q system (Millipore, Bedford, MA, USA) was used throughout.

High-performance liquid chromatography (HPLC)-grade acetonitrile and methanol were purchased from Scharlau (Barcelona, Spain). Other

0021-9673/92/$05.00

chemicals, all of analytical or reagent grade, were supplied by Prolabo, Merck or Fluka (Buchs, Switzerland).

Germination

The washed seeds were soaked in water for 3 h and germination was effected in a dark chamber at 29°C, water being added as necessary. Samples of 400 seeds were removed at 24, 48, 72, 96 and 120 h, dried and ground to pass through a 100-mesh sieve. Samples of the dry, non-germinated seeds were ground and homogenized. Chromatographic analysis was carried out four times on each sample, the germination procedure being repeated in triplicate.

Extraction

Two extraction methods were used:

(a) Finely ground material (2 g) was treated with aqueous methanol (60% methanol, 40 ml). The suspension was boiled at 92°C under reflux for 2 h, cooled and centrifuged at 700 *g* for 5 min. The supernatant was removed and the residue extracted twice more with boiling aqueous methanol and finally washed with water (40 ml). The combined extracts and washings were evaporated to dryness *in vacuo* below 50°C [9]. The residue was dissolved in water (25 ml) and an aliquot of 3.5 ml was transferred into a glass-stoppered test tube; acetonitrile (6.5 ml) was added with shaking and the mixture allowed to stand at 5°C for 1 h [10]. After filtering (Millipore, 0.45 μm), the sample (20 μl) was injected into the HPLC system.

(b) Ground material (0.5 g) was homogenized with aqueous methanol (70% methanol, 5 ml) for 1 min at room temperature. The mixture was centrifuged for 5 min (700 *g*) and the supernatant decanted. The procedure was repeated twice more and the combined supernatants evaporated *in vacuo* at 35°C. The product was dissolved in double-deionized water (1 ml) and passed through Dowex (Dow

TABLE I

RECOVERY OF OLIGOSACCHARIDES USING EXTRACTION METHODS a AND b

Oligosaccharide	Amount added (mg)	Total amount found (mg)	Recovery (%)
Method a (in 2 g of flour)			
Sucrose	0.00	29.29	–
	20.21	46.15	83.42
	40.08	69.29	99.80
	80.23	101.43	89.84
Raffinose	0.00	21.64	–
	20.14	37.15	77.01
	40.25	56.43	86.43
	80.20	98.22	95.49
Stachyose	0.00	120.36	–
	20.07	137.86	87.19
	40.06	157.15	91.84
	80.21	187.72	83.98
Method b (in 500 mg of flour)			
Sucrose	0.00	8.10	–
	5.21	13.70	107.49
	10.30	18.26	98.64
	20.18	27.32	95.24
Raffinose	0.00	2.48	–
	5.22	7.30	92.34
	10.19	11.36	87.14
	20.36	20.38	87.92
Stachyose	0.00	27.38	–
	5.04	34.06	132.54
	10.19	37.46	98.92
	20.09	45.52	90.29

Chemical) 50W-X8 (200–400 mesh) and Waters QMA minicolumns with a Supelco vacuum system (Bellefonte, PA, USA). Water (three 1-ml portions) was added to flush the columns and the combined extracts and washings were collected and injected (20 μl) into the HPLC system.

HPLC analysis

Samples (20 μl) were analysed using a Konik chromatograph fitted with an ERMA 7520 refractive index detector (Barcelona, Spain). A Spherisorb-5-NH_2 column (250 × 4.6 mm I.D.) (Teknokroma, Bellefonte, PA, USA) was employed with acetonitrile–water (1 ml/min^{-1}) in two different proportions [72:28 (v/v) in method a and 65:35 (v/v) in method b] as the mobile phase. Individual sugars were quantified by comparison with external standards of sucrose, raffinose, stachyose (Sigma, St. Louis, MO, USA) and a standard sample of verbascose that was obtained from *Vicia faba* (cv. Alameda) seeds, as described below.

Extraction of verbascose

The ground *V. faba* flour was extracted according to method b above, and the residue dissolved in water (1 ml). Individual sugars were separated by preparative thin-layer chromatography on silica gel plates (Whatman's PLK 5F, 20 × 20 cm, 1000 μm). The solvent system was butanol–acetic acid–water (12:3:5), colour development being achieved by aniline–diphenylamine–phosphoric acid [11]. The verbascose band was removed and dissolved in water and the mixture centrifuged at 700 *g* for 10 min; the supernatant was removed and the water evaporated *in vacuo*.

Statistical analysis

The data were analysed for variance using a BMDP-2V ANOVA programme (W. J. Dixon, BMDP Statistical Software, Software Release, 1988) and the mean values compared using Duncan's multiple range test.

RESULTS AND DISCUSSION

HPLC was used to quantify the individual sugars, sucrose, raffinose, stachyose and verbascose. Calibration curves were constructed for all four sugars; a linear response was evident for the range 0–5 mg/ml^{-1}, correlation coefficients being 0.99. The recoveries of oligosaccharides using methods a and b are presented in Table I. The results of this study show satisfactory recoveries using both methods, but higher values were found with method b. Because of these results, quantification of the effect of germination on oligosaccharides was carried out using method b.

Fig. 1 shows HPLC patterns for the dry (non-germinated) seeds of *L. albus* and *L. luteus*. The α-galactoside contents in these seeds before and during germination are listed in Tables II and III. In *L. albus*, stachyose was originally present in much larger amounts than raffinose or verbascose, whilst in *L. luteus* the contents of stachyose and verbascose were approximately the same and greatly in excess of the amount of raffinose. The values obtained for the dry beans agree with figures reported for these species by other authors [9,12]. Trials on animals have shown that the molecular mass of these oligosaccharides has an influence on flatus formation. Stachyose, the tetrasaccharide, and verbascose, the pentasaccharide, have marked effects, while raffinose, the trisaccharide, has an insignificant effect [9].

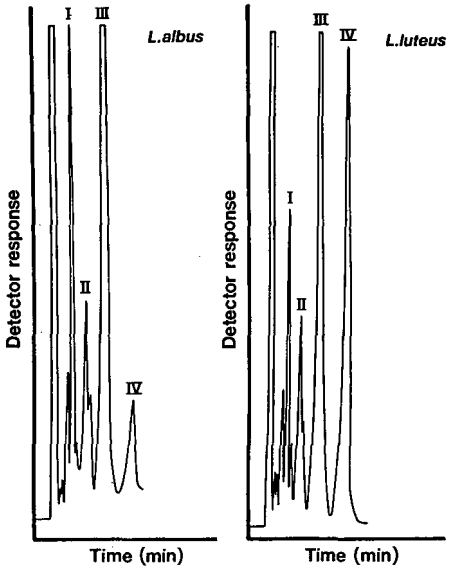

Fig. 1. HPLC patterns of α-galactosides from an aqueous extract for dry (non-germinated) seeds of *L. albus* and *L. luteus* oligosaccharides numbered as sucrose (I), raffinose (II), stachyose (III) and verbascose (IV). A Spherisorb-5-NH_2 column (250 × 4.6 mm I.D.) was employed with 65:35 (v/v) acetonitrile–water (1 ml/min^{-1}) as the mobile phase.

TABLE II

COMPOSITION OF α-GALACTOSIDES OF *LUPINUS ALBUS* SEEDS DURING GERMINATION

Time (h)	Concentration (mean ± S.D.) (g per 100 g of dry matter)			
	Sucrose	Raffinose	Stachyose	Verbascose
0	2.0±0.07	1.0±0.01	7.1±0.13	1.0 ±0.10
24	3.7±0.43	0.8±0.08	2.9±0.31	0.6 ±0.09
48	4.5±0.15	0.2±0.01	0.6±0.02	0.1 ±0.01
72	4.3±0.02	0.2±0.01	0.6±0.02	0.08±0.001
96	4.1±0.28	0.2±0.01	0.4±0.03	0.04±0.002
120	3.5±0.04	0.1±0.04	0.3±0.008	Trace
	(33.87)[a]	(200.38)	(704.74)	(6.10)

[a] Figures in parentheses are *F*-values from variance analysis of individual sugars over the time course (from 0 to 120 h) of the germination. All values are significant at the 0.1% level.

TABLE III

COMPOSITION OF α-GALACTOSIDES IN *LUPINUS LUTEUS* DURING GERMINATION

Time (h)	Concentration (mean ± S.D.) (g per 100 g of dry matter)			
	Sucrose	Raffinose	Stachyose	Verbascose
0	0.9±0.01	0.9 ±0.03	6.1±0.14	5.6 ±0.29
24	1.9±0.03	0.6 ±0.04	3.1±0.21	3.5 ±0.03
48	2.2±0.12	0.5 ±0.03	2.3±0.12	2.8 ±0.20
72	2.2±0.05	0.1 ±0.06	0.6±0.08	1.0 ±0.09
96	2.4±0.04	0.1 ±0.06	0.6±0.03	0.7 ±0.02
120	1.2±0.04	0.01±0.001	0.1±0.01	0.05±0.01
	(205.91)[a]	(106.59)	(723.96)	(347.59)

[a] Figures in parentheses are *F*-values from variance analysis of individual sugars over the time course (from 0 to 120 h) of the germination. All values are significant at the 0.1% level.

Variance analysis revealed significant trends during germination, since there is a clear reduction in the levels of raffinose, stachyose and verbascose throughout the period of germination. The greatest rate of loss, for both species, is noted during the first 48 h, with a slower decrease in *L. luteus*. The results obtained here are in agreement with the findings of other authors on other species [5,13]. Sucrose contents increase until 48 h in *L. albus* and until 96 h in *L. luteus*. Saini [12] and Kuo *et al.* [13] have suggested that during germination raffinose oligosaccharides present in the cotyledons are initially hydrolysed to the next lower homologue of the series yielding finally sucrose, apparently as a result of the presence of α-galactosidase in the seeds.

In the light of these results it can be concluded that, during germination of *Lupinus* species, raffinose oligosaccharides decrease. From the nutritional standpoint, it would be of interest to examine the variation of protein content and quality, and alkaloid content, throughout the germination process. This would be enable the germination conditions to be optimized so as to minimize levels of antinutrients, most notably alkaloids and α-galactosides.

ACKNOWLEDGEMENT

The authors are grateful to Professor H. Sorensen, Department of Chemistry, Royal Veterinary and Agricultural University, Copenhagen, for assistance and encouragement.

REFERENCES

1 O. Kandler and H. Hopf, *The Biochemistry of Plants*, Vol. 3, Academic Press, New York, 1980, p. 221.
2 K. R. Price, J. Lewis, G. M. Wyatt and G. R. Fenwick, *Nahrung*, 32 (1988) 609.
3 N. K. Matheson and H. S. Saini, *Phytochemistry*, 16 (1977) 59.
4 P. Aman, *J. Sci. Food Agric.*, 30 (1979) 869.
5 A. R. El-Madhy and L. A. El-Sebaig, *J. Sci. Food Agric.*, 34 (1983) 951.
6 M. Duranti, E. Cucchetti and P. Cerletti, *J. Agric. Food Chem.*, 32 (1984) 490.
7 C. Rey and M. Muzquiz, *Proceedings of the VIIIth Reunión Nacional de la S.E.F.V., Barcelona, 12–15 September 1989*, Universidad de Barcelona, Barcelona, 1989, p. 57.
8 L. López Bellido and M. Fuentes, *Adv. Agron.*, 40 (1986) 239.
9 R. Macrae and A. Zand-Moghaddam, *J. Sci. Food Agric.*, 29 (1978) 1083.
10 I. M. Knudsen, *J. Sci. Food Agric.*, 37 (1986) 560.
11 R. W. Bailey, S. E. Mills and E. L. Hove, *Thin Layer Chromatography*, Springer, Berlin, 1969, p. 856.
12 H. S. Saini, in J. Huisman, T. F. B. van der Poel and I. E. Liener (Editors), *Recent Advances of Research in Antinutritional Factors in Legume Seeds*, Pudoc, Wageningen, 1989, p. 329.
13 T. M. Kuo, J. F. Van Middlesworth and W. J. Wolf, *J. Agric. Food Chem.*, 36 (1988) 32.

Journal of Chromatography, 607 (1992) 353–360
Elsevier Science Publishers B.V., Amsterdam

CHROM. 24 296

Isolation of the phenolic fraction of coal pyrolysis tars by ion-exchange chromatography

Marisa Díaz, Rafael Moliner and José V. Ibarra*

Instituto de Carboquímica, CSIC, P.O. Box 589, 50080 Zaragoza (Spain)

ABSTRACT

The isolation of the phenolic fraction from coal pyrolysis tars by ion-exchange chromatography is reported. Tars were obtained from low temperature pyrolysis (600°C) of four coals varying in rank from lignite to bituminous. The phenolic fraction was extracted from tars using an anion-exchange resin (Amberlyst A-26, OH-form) activated by consecutive treatments in a column with 2 *M* HCl, 2 *M* NaOH and isopropanol–water (1:1). Tar samples dissolved in dichloromethane–diethyl ether (5:1) were shaken with the resin (10 cm^3/g sample) for 30 min. The resin was then separated by filtration and the acid fraction was quantitatively eluted from the resin with chlorotrimethylsilane–dichloromethane. The acid fraction extracted in this way represented between 46 and 58% (w/w) of the whole tar for the analysed samples. The efficiency of the separation was tested by enthalpimetric titration, gas chromatography, Fourier transform (FT) IR spectroscopy and ^1H NMR. The residual fraction obtained after removal of the acid fraction has no acid character and does not contain hydroxyl groups. In contrast, phenolic structures are concentrated in the acid fraction. The main compounds in the acid fraction were identified and quantified by wide-bore gas chromatography using external standards. Several structural parameters of the fractions were deduced from FT-IR and ^1H NMR data. The acid fraction is mainly aromatic in nature whereas the aliphatic structures tend to concentrate in the residue.

INTRODUCTION

Coal-derived liquids (CDLs) are complex mixtures of widely varying, predominantly aromatic compounds. The development of coal conversion processes such as liquefaction and pyrolysis has created the need for analytical methodologies of fractionation and characterization of CDLs to understand conversion mechanisms.

The fractionation of CDLs is usually carried out by distillation, solvent extraction or by chromatographic methods based on sorption, steric exclusion or ion-exchange processes. Separation methods and the characterization of CDLs have been reviewed by Poirier and George [1]. The development of non-aqueous ion-exchange resins has initiated the development of separation schemes for CDLs into discrete compound classes giving fractions based on chemical functionality differences (acids, bases and neutral compounds) [2–5].

Tars from the low temperature pyrolysis of coal have a large content of phenolic compounds especially when low rank coals are processed. This acid fraction is useful as a chemical feedstock but it is undesirable when CDL are used to produce synthetic fuels. Therefore fractionation schemes which allow an easy and large scale separation of the phenolic fraction are required.

Fractionation of pyrolysis tars by ion-exchange chromatography (Amberlyst A-27 and A-15) followed by extrography of the neutral fraction according to the separation scheme of Strachan and Johns [5] has been carried out with unsatisfactory results [6]. Loss of material and the presence of hydroxyl groups in basic and neutral fractions were found. Zanella has reported [7] satisfactory results for the separation of the phenolic fraction of low temperature tars using Amberlyst A-26 and batch procedures instead of column chromatography. This procedure simplifies the fractionation schemes proposed by other workers and can be applied on a large scale to isolate the acid fraction of tars for character-

0021-9673/92/$05.00

ization and use as chemical feedstocks or for upgrading CDLs.

In this work the isolation of the acid fraction of low temperature pyrolysis tars using an anion-exchange resin (Amberlyst A-26) was studied. Four tars obtained from coals varying in rank from lignite to bituminous were fractionated and the phenolic fractions obtained were characterized by enthalpimetric titration, gas chromatography and spectroscopic techniques [Fourier transform (FT) IR and ^{1}H NMR].

EXPERIMENTAL

Starting materials

Tars were obtained from the low temperature pyrolysis of four coals varying in rank: a brown coal (Mequinenza), two subbituminous coals from Teruel (AA1, EL3) and a bituminous coal from Asturias (Hu). Pyrolysis was carried out in a fluidized bed at 600°C under nitrogen and tars were extracted with dichloromethane which was then removed by distillation.

Ion-exchange separation

The resin used was Amberlyst A-26 (Fluka, Buchs, Switzerland), a strong anion-exchange resin which was carefully activated to prevent artifacts arising from the incorrect preparation of non-aqueous ion-exchange resins [8]. A column (50 × 2 cm I.D.) packed with 100 g of the resin was eluted with 2 *M* HCl (2 l) and distilled water until free of chloride ions. It was subsequently activated by washing with 2 *M* NaOH (2.5 l) followed by distilled water until a neutral pH was reached and then isopropanol–water (1:1; 2.5 l).

Finally the resin was conditioned by Soxhlet extraction with isopropanol (24 h) and then diethyl ether (24 h). The resin was stored in diethyl ether to prevent absorption of CO_2.

The tar sample was disolved in a mixture of dichloromethane–diethyl ether (5:1, v/v) in a ratio of 60 ml/g sample. The solution was treated with the resin (10 ml/g sample) in an Erlemeyer flask and the system mechanically shaken for 30 min. The resin was separated from solution by filtration and then washed with dichloromethane until colourless washings were seen. These washings were combined with the non-retained solution and the solvent was eliminated by distillation. This residue consists of the basic and neutral fractions of tar.

The acid fraction was recovered from the resin by treating in a flask with a solution of chlorotrimethylsilane (Aldrich Chemie) in diethyl ether ($1.8 \cdot 10^{-4}$ *M*) for 30 min. The resin was then washed with dichloromethane until a colourless liquid was obtained. For tars with high contents of phenol compounds it may be necessary to repeat the elution process. Solvents were then removed by distillation.

Analytical methods

Elemental analyses (C, H, N, S) were carried out using Leco (St. Joseph, MI, USA) elemental analysers (CHN-600, SC-32). The amount of phenolic compounds in various fractions was determined by enthalpimetric titration according to the following procedure [7].

The sample (0.1–0.3 g) was dissolved in anhydrous acetone (100 ml) and accurately titrated with KOH (0.5 *M*) in isopropanol. The end-point was indicated by an increase in temperature of 2°C, which was detected by a thermocouple. The KOH solution was previously titrated with acetic acid. The standard deviation (σ) found for this method was $1 \cdot 10^{-4}$ for model compounds (phenols) and $1 \cdot 10^{-2}$ for tars from different coal pyrolysis processes.

Gas chromatography (GC) of tars and their fractions was carried out on a Varian 3400 system (Walnut Creek, CA, USA) using a wide-bore (0.53 mm, 25 m) CP Sil 5B wall-coated column from Chrompack (Middelburg, Netherlands). The chromatographic conditions are given in Fig. 1. GC–mass spectrometry (MS) was carried out on a Varian 3300 system linked to a Finnigan ion trap detector (ITD 800; San Jose, CA, USA). The chromatographic conditions were the same than those used for GC unless a splitless injection mode was used. The National Bureau of Standards (USA) computerized library was used for identification.

^{1}H NMR spectra of tars were obtained in a Bruker (Karlsruhe, Germany) WP80 CW system, 80 MHz, with samples solved in C^2HCl_3 using trimethylsilane (TMS) as a reference. FT-IR spectra were determined on a Nicolet 10 DX instrument (Madison, WI, USA) with tars on KBr windows.

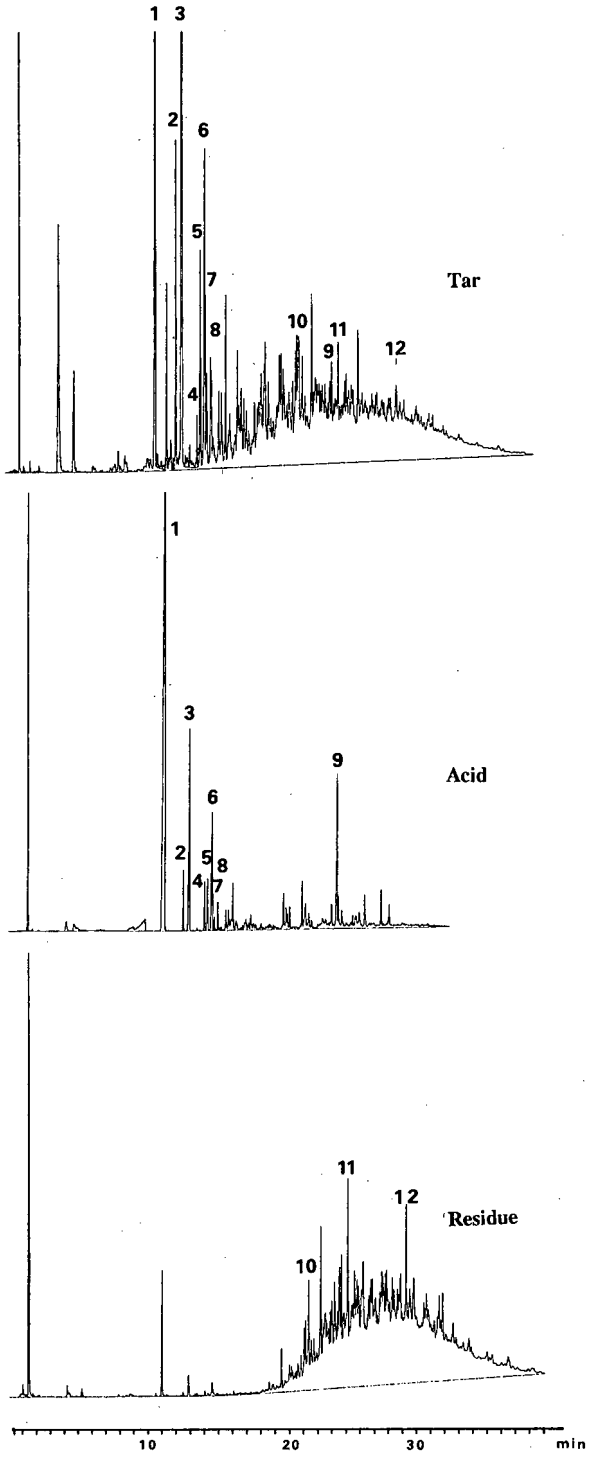

Fig. 1. Gas chromatograms of the tar, acid fraction and residual fraction from AA1 coal. Column, 0.53 mm × 25 m, CP Sil 5B WCOAT; sample, $1 \cdot 10^{-6}$ l, split, 1:30; detector, flame ionization; temperature, 350°C; injector, 350°C; temperature programme, 50°C, 5 min hold, 10°C/min to 300°C; carrier gas, helium. Peaks 1–9 are identified in Table II. Peak 10 = n-C_{16}; 11 = n-C_{18}; and 12 = n-C_{22}.

RESULTS AND DISCUSSION

Table I shows the main characteristics of the starting tars and their acid and residue fractions. The important contribution of the acid fraction, which represents the 50% or more of the tar, is noted. Losses less than 0.1 wt% were found in all instances.

The phenolic content of tars, determined by enthalpimetric titration, tends to increase with increasing rank of the starting coals. However, it remains constant, in practice, in all acid fractions independent of the origin of the tar. No acid functions were found in the residue (basic plus neutral) by enthalpimetric titration. The elemental analysis data show that the oxygen contained in tars is mainly recovered in the acid fraction, so that the oxygen content of the residue is low. This fact could be used for upgrading liquids from low quality coals.

Gas chromatography

Fig. 1 shows the chromatograms obtained for the whole tar and the acid and residual tar fractions. It is noted that the chromatogram of the whole tar splits into two chromatograms corresponding to the acid and the residual fractions. Peaks that correspond to the lightest phenolic compounds appear in the acid fraction and not in the residual fractions, with the except of the phenol (0.35%, w/w, in the residual fraction against 52.32% (w/w) in the acid fraction). On the other hand, the peaks with longer elution times appear in the residual fraction and not in the acid fraction, with except of anthracene (6.58% in the acid fraction).

Peaks in the acid fraction have been identified by their relative retention times (RRT) referred to phenol. A set of external standards was used for identification. A difference $\leqslant 0.005$ between the RRT of the standard and the identified peak was accepted.

Peak abundances were calculated from the normalized areas of peaks which were corrected by a relative response factor according to the equations:

$$A_i = NA_i \cdot RRF_i \tag{1}$$

$$RRF_i = RF_i/(RF)_{\text{phenol}} \tag{2}$$

$$RF_i = \frac{\text{mass of external standard}}{\text{peak area}} \tag{3}$$

$$(\text{Abundance})_i\ (\%) = \frac{A_i}{\sum A_i} \times 100 \tag{4}$$

TABLE I

MAIN CHARACTERISTICS OF THE TARS AND THEIR FRACTIONS

Sample	Fraction	% (w/w) of fraction	OH content (%, w/w)	Elemental analysis (wt%)			
				C	H	N	O+S_{diff}
Mequinenza	Tar	100	3.6	78.5	7.5	0.5	13.5
	Acid	51.4	11.0	75.2	7.4	0.6	16.8
	Residue	48.5	–	80.6	8.0	0.6	10.8
AA1	Tar	100	4.9	75.3	7.6	0.8	16.3
	Acid	47.8	11.0	68.0	6.8	0.5	24.7
	Residue	52.1	–	77.4	8.5	0.6	13.5
EL3	Tar	100	5.0	77.9	7.2	0.7	14.2
	Acid	46.4	10.9	74.6	7.7	0.4	17.3
	Residue	53.5	–	83.0	8.8	0.3	7.9
Hu	Tar	100	5.7	81.6	8.0	1.2	9.2
	Acid	57.8	11.5	74.1	7.6	1.1	17.3
	Residue	42.1	–	86.2	9.3	1.4	3.1

where A_i = corrected area of compound i; NA_i = normalized area of compound i from chromatogram; RRF_i = relative response factor of compound i; RF_i = response factor of compound i; and $(RF)_{phenol}$ = response factor of phenol.

A quantitative test mixture was used to calculate the response factors of the identified compounds.

Table II shows the compounds identified in the acid fraction, which represent 84% of the total weight. All of them, with the except of the anthracene, are phenolic compounds. The presence of anthracene in the acid fraction could be explained in terms of the affinity of polyaromatic compounds towards the resin matrix.

TABLE II

COMPOUNDS IDENTIFIED BY GC IN THE ACID FRACTION OF THE AA1 COAL

RRT = Relative retention time; RRF = relative response factor (see details in text).

Peak No.	Compound	RRT	RRF	Abundance (%)
1	Phenol	1.000	1.000	52.32
2	*o*-Cresol	1.173	1.026	1.74
3	*m*/*p*-Cresol	1.223	1.043	10.97
4	*o*-Ethylphenol	1.365	1.025	1.64
5	2,4-Dimethylphenol	1.389	1.054	1.59
6	*p*-Ethylphenol	1.426	1.025	4.43
7	2,3-Dimethylphenol	1.431	1.054	3.61
8	3,4-Dimethylphenol	1.483	1.054	1.18
9	Anthracene	2.558	0.760	6.58
–	Unidentified	–	0.768	15.94

Unidentified peaks were supposed to be polyaromatic hydrocarbons (PAHs) and heavy aliphatic hydrocarbons. This assumption was confirmed by GC–MS. The response factor for unidentified peaks has been calculated as an average from a standard mixture containing several PAHs and paraffinic compounds.

Some peaks have been identified in the residual fraction by their relative retention times. GC–MS confirmed that most of them correspond to aliphatic compounds which are eluted over a non-resolved background. Scanning of this background looking for mass spectra of phenolic compounds did not yield positive results and confirmed the absence of this type of compound in the residual fraction.

The results show that the method used extracts the acid compounds quantitatively, although it is not entirely selective as some PAHs can be also extracted in the acid fraction.

^1H *NMR spectroscopy*

Table III gives the hydrogen distribution for tars

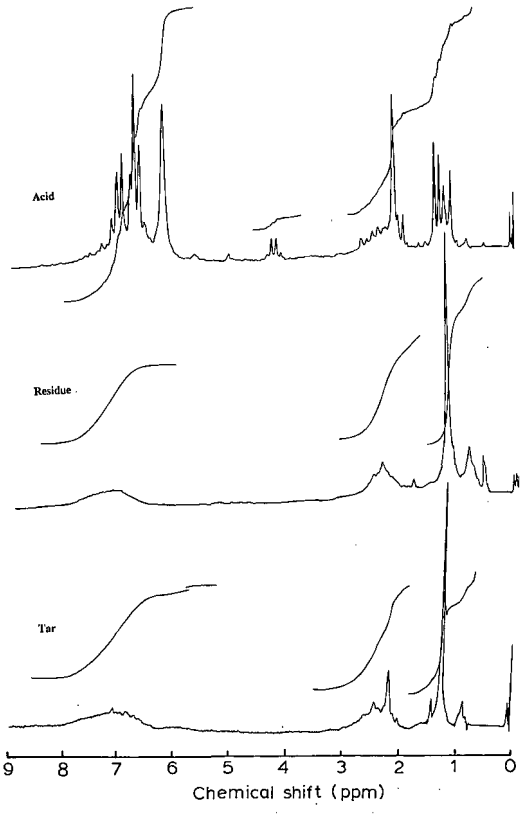

Fig. 2. ^{1}H NMR spectra of tar Hu and its fractions.

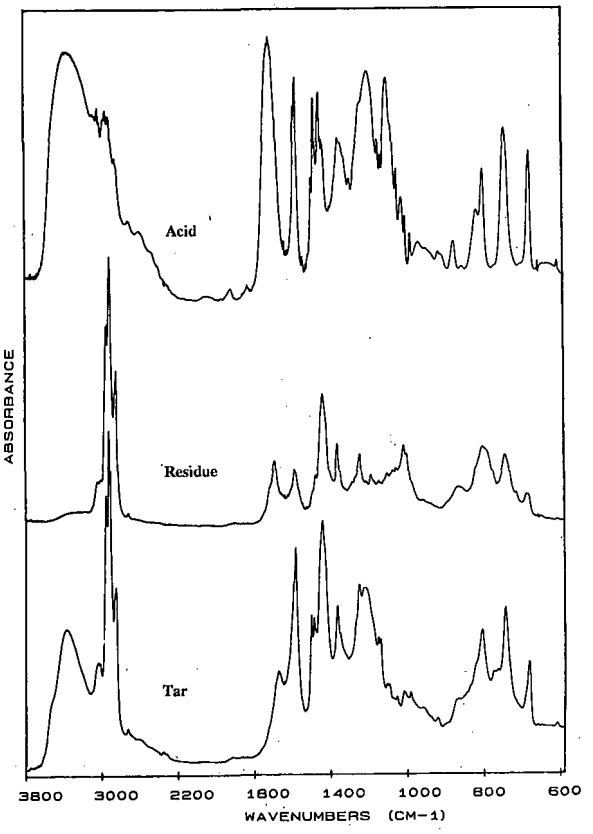

Fig. 3. FT-IR spectra of tar AA1 and its fractions.

and their fractions evaluated by ^{1}H NMR. Spectra were divided for integration in specific zones according to Stompel and Bartle [9] and Ibarra *et al.* [10]. It is observed that the acid fraction has a higher aromatic hydrogen content than the starting tar in all instances whereas the residue is more aliphatic. The variation of the aromatic to aliphatic hydrogen ratio (H_{ar}/H_{al}) reflects this trend. The higher hydrogen content in the phenolic structures of the acid fraction is also revealed by ^{1}H NMR (Fig. 2 and Table III). Owing to the high sensitivity of the chemical shift of phenolic protons to experimental conditions (such as concentration and solvent) NMR has not been used for quantitative purposes.

FT-IR spectroscopy

Fig. 3 shows the FT-IR spectra of the whole tar, the acid and the residue fractions corresponding to sample AA1. Similar spectra were obtained for the other samples. The total disappearance of the hydroxyl band (3375 cm^{-1}) in the residue after the acid fraction removal from tar can be seen. The acid fraction has a markedly increased content of phenolic compounds (3375 and 1124 cm^{-1}), other acidic groups such as C=O (1734 and 1225 cm^{-1}) and aromatic structures (several bands at 1600 and 1500 cm^{-1}). The residue shows, in addition to the disappearance of hydroxyl bands, a higher aliphatic character than the tar and the persistance of C=O structures (1685 cm^{-1}, aromatic ketones and quinones). This band should be related to the presence of polar structures in the residue [2,11].

Fig. 4 shows expanded FT–IR spectra corresponding to aliphatic and aromatic zones of tar AA1 and its fractions. The appearance in the acid fraction of two aromatic hydrogen bands at 3054 cm^{-1} (benzenic structures) and 3020 cm^{-1} (more condensed aromatic structures) can be observed, which

TABLE III

HYDROGEN DISTRIBUTION (%) FOR TARS AND THEIR FRACTIONS

H_f = ring-joining methylene; H_α = CH_3, CH_2 and CH α to an aromatic ring; H_n = CH_2 and CH β to an aromatic ring (naphthenic); H_β = β-CH_3, CH_2 and CH γ or further from an aromatic ring; H_γ = CH_3 γ or further from an aromatic ring.

Type of hydrogen	Hydrogen concentration (ppm)	Mequinenza			AA1			EL3			Hu		
		Tar	Acid	Residue	Tar	Acid	Residue	Tar	Acid	Residue	Tar	Acid	Residue
H_{ar}	9.0–6.5	26.0	39.5	20.1	36.3	39.5	24.4	36.3	39.7	27.9	26.6	41.8	21.2
H_{OH}	6.5–5.5	5.9	9.1	–	5.7	9.1	–	5.2	10.6	–	3.1	16.9	–
H_f	4.5–3.3	–	1.8	–	–	1.8	–	–	–	–	–	3.0	–
H_α	3.3–2.0	30.1	22.3	28.3	30.0	22.3	34.6	31.5	18.2	29.5	34.7	16.9	24.6
H_n	2.0–1.6	8.3	4.1	11.0	4.6	4.1	4.7	4.5	5.0	6.2	3.0	4.2	5.9
H_β	1.6–1.0	19.5	15.9	32.7	14.4	15.9	23.5	15.5	16.6	27.9	26.5	15.4	38.1
H_γ	1.1–0.5	10.2	7.3	7.9	10.0	7.3	12.8	7.0	8.9	8.5	6.1	1.8	10.2
H_{ar}/H_{al}		0.38	0.8	0.25	0.6	0.8	0.32	0.62	0.82	0.4	0.4	1.1	0.3

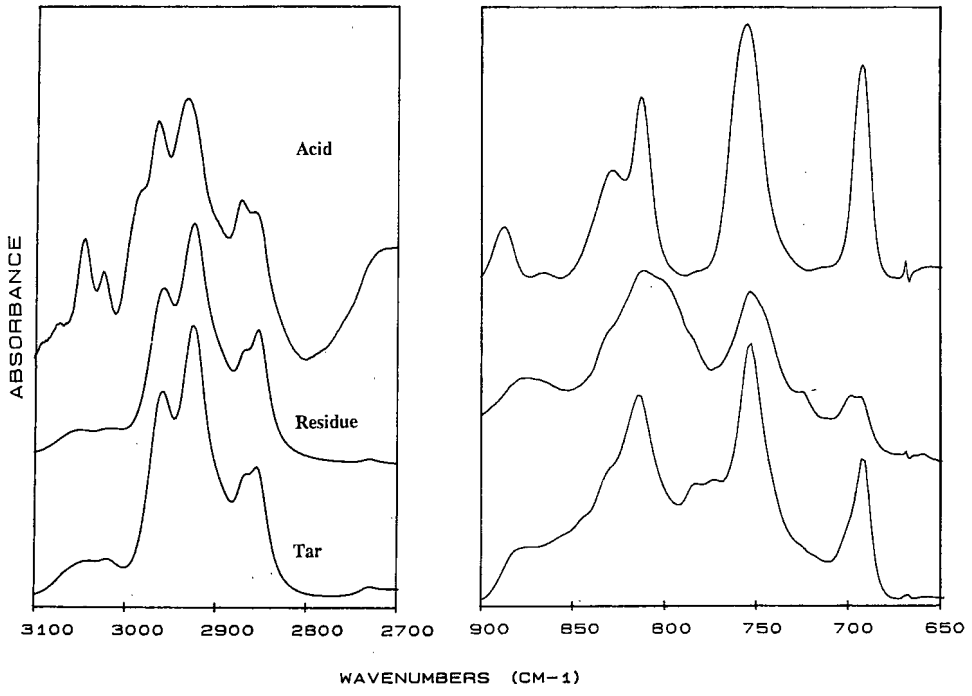

Fig. 4. Expanded spectra in the aliphatic and aromatic zone of tar AA1 and its fractions.

denotes its higher aromatic character in relation to the starting tar. The increase in the acid fraction of the 690 cm^{-1} band (monosubstituted aromatic structures) and the 825 and 890 cm^{-1} bands (more substituted aromatic rings) also confirms this fact. Likewise the increase in the 2960 and 2870 cm^{-1} bands (asymmetric and symmetric CH_3 stretching modes) in relation to the band at 2924 and 2856 cm^{-1} (asymmetric and symmetric CH_2 stretching modes) indicates shorter aliphatic chains for the acid fraction and thus a lower aliphatic character.

Evidence for the confirmation of these facts will be deduced from the structural parameters presented in the following section.

Structural parameters

On the basis of the elemental analysis and ^{1}H-NMR data some structural parameters as defined by Brown and Ladner [12] can be easily deduced according to the following equations:

$$f_a = 1 - C_{al}/C \quad (5)$$

where f_a is the aromaticity or aromatic carbon content and C_{al} the carbon in aliphatic structures which calculated from the eqn. (6):

$$C_{al}/C = (H_{al}/H) \cdot (H/C)/(H_{al}/C_{al}) \quad (6)$$

where H_{al}/H is the fraction of total hydrogen present as aliphatic hydrogen, H/C is the atomic hydrogen to carbon ratio calculated from elemental analysis and H_{al}/C_{al} is an atomic hydrogen to carbon ratio for aliphatic chains which is generally taken to be 2.3 for tars derived from coal [13]. H_{al} is usually derived from NMR or FTIR data [14]. In this paper H_{al} (H_α, H_β, H_γ) has been calculated using the H_{ar}/H_{al} ratio deduced from ^{1}H-NMR data and the following equation:

$$H_T = H_{al} + H_{ar} + H_{acid} \quad (7)$$

where H_T is the total hydrogen content determined by elemental analysis and H_{acid} is the hydrogen in acid structures determined by enthalpimetric titration. The H/C ratio has also been corrected for the hydrogen in acid structures.

The results obtained in this way are shown in Table IV. It can be observed that the aromatic

TABLE IV

STRUCTURAL PARAMETERS OF TARS AND THEIR FRACTIONS

Sample	Fraction	H/C	H_{ar}/H_{al}	H_{al} (%, w/w)	H_{ar} (%, w/w)	H_{al}/H	C_{al} (%, w/w)	C_{ar} (%, w/w)	f_a	H_{ar}/C_{ar}
Mequinenza	Tar	1.18	0.38	5.36	2.03	0.73	27.9	47.4	0.63	0.51
	Acid	1.10	0.79	3.49	2.75	0.56	18.4	49.6	0.73	0.67
	Residue	1.32	0.25	6.79	1.70	0.80	41.8	35.6	0.54	0.57
AA1	Tar	1.10	0.61	4.47	2.73	0.62	23.5	55.0	0.70	0.60
	Acid	1.09	0.80	3.78	3.02	0.56	19.6	55.6	0.74	0.65
	Residue	1.19	0.32	6.04	1.93	0.76	31.4	49.2	0.61	0.47
EL3	Tar	1.06	0.62	4.23	2.63	0.62	22.6	55.3	0.71	0.57
	Acid	1.15	0.82	3.92	3.22	0.55	20.1	54.5	0.73	0.71
	Residue	1.27	0.39	6.34	2.47	0.72	33.2	49.8	0.60	0.59
Hu	Tar	1.12	0.38	5.53	2.10	0.72	28.6	53.0	0.65	0.48
	Acid	1.13	1.09	3.34	3.65	0.48	17.8	56.3	0.76	0.78
	Residue	1.30	0.27	7.32	1.98	0.79	38.8	47.4	0.55	0.50

hydrogen and carbon content of the acid fraction increased in all instances in relation to the whole tar and the residue. The acid fraction also has a higher aromaticity (f_a). Whereas the residue has a higher aliphatic character. The degree of aromatic substitution evaluated from the aromatic hydrogen to aromatic carbon ratio (H_{ar}/C_{ar}) denotes a lower degree of substitution for the acid fraction.

CONCLUSIONS

The acid fraction of low temperature pyrolysis tars can be succesfully separated by ion-exchange chromatography on Amberlyst A-26 and later elution with chlorotrimethylsilane. Hydroxyl groups have not been detected by FT-IR and enthalpimetric titration in the residual fractions, although some aromatic compounds have been detected in the acid fraction. The acid fraction represents 50% or more of all studied samples. It has a higher aromatic character than the original tar whereas the aliphatic structures tend to be concentrated in the residue. An important removal heterograms (O + S) from the tar can be achieved by the separation of the acid fraction.

REFERENCES

1 M. A. Poirier and A. E. George, *Energy Sources*, 5 (1981) 339.
2 P. V. Webster, J. N. Wilson and M. C. Franks, *Anal. Chem. Acta*, 38 (1967) 193.
3 S. E. Scheppele, P. A. Benson, G. J. Greenwood, Q. Grindstaff, T. Aczel and B. Bieber, *Prepr. Am. Chem. Soc. Div. Petroleum Chem.*, 24(4) (1979) 963.
4 J. B. Green, R. J. Hoff, P. W. Woodward and L. L. Stevens, *Fuel*, 63 (1984) 1920.
5 M. G. Strachan and R. B. Johns, *Anal. Chem.*, 58 (1986) 312.
6 A. C. Gracia, *Degree disertation*, University of Zaragoza, Zaragoza, 1987.
7 I. Zanella, *Ph. Thesis*, University of Metz, Metz, 1987.
8 M. G. Strachan and R. B. Johns, *Anal. Chem.*, 59 (1987) 636.
9 Z. Stonpel and K. D. Bartle, *Fuel*, 62 (1983) 900.
10 J. V. Ibarra, I. Cervero and R. Moliner, *Fuel Process. Technol.*, 22 (1989) 135.
11 J. V. Ibarra, R. Moliner and A. C. Gracia, presented at the *XVII Meeting on Chromatography and Related Techniques, Reus, November 1989.*
12 J. K. Brown and W. R. Ladner, *Fuel*, 39 (1960) 87.
13 C. Snape, W. R. Ladner and K. D. Bartle, in H. D. Schultz (Editor), *Coal Liquefaction*, Wiley, New York, 1984, Chapter 4.
14 J. V. Ibarra and R. Moliner, *J. Anal. Appl. Pyrol.*, 20 (1991) 171.

Journal of Chromatography, 607 (1992) 361–376
Elsevier Science Publishers B.V., Amsterdam

CHROM. 24 401

Molecular analysis of sulphur-rich brown coals by flash pyrolysis–gas chromatography–mass spectrometry

The Type III-S kerogen☆

Jaap S. Sinninghe Damsté*, F. Xavier C. de las Heras☆☆ and Jan W. de Leeuw

Organic Geochemistry Unit, Delft University of Technology, de Vries van Heystplantsoen 2, 2628 RZ Delft (Netherlands)

ABSTRACT

The molecular composition of five brown coals from three different basins (Maestrazgo, Mequinenza and Rubielos) in Spain was investigated by flash pyrolysis–gas chromatography and flash pyrolysis–gas chromatography–mass spectrometry. In these techniques, the macromolecular material is thermally degraded in an inert atmosphere and the compounds formed are on-line separated, identified and quantified. This information provided insight into the macromolecular structure of the coals which was inaccessible by other means. The composition of the pyrolysates is described in detail with emphasis on the distributions and relative abundance of *n*-alkanes, *n*-1-alkanes, (alkyl)phenols, sulphur compounds [(alkyl)thiophenes and (alkyl)benzothiophenes], (alkyl)benzenes and (alkyl)naphthalenes. These compound classes represent the major pyrolysis products of the samples analysed and were used to assess the contributions of specific biomacromolecules mainly originating from higher plants. One of the five brown coal samples investigated is so rich in organic sulphur (one sulphur atom for every 9–15 carbon atoms as determined by elemental analysis) that a new kerogen type (Type III-S) describing the kerogen contained in this coal is defined. Type III-S kerogen is defined as a kerogen with high atomic $S_{org.}/C$ (>0.04) and O/C (>0.20) ratios. Two of the five brown coals samples investigated contain a series of long-chain alkylbenzenes with an unprecedented carbon number distribution pattern with a second maximum at C_{18}. This unusual distribution pattern is thought to originate from the presence of long-chain alkylbenzene moieties bound via a heteroatom (presumably an ether bond) to the macromolecular coal matrix preferentially at position 12 in the alkyl side-chain of these moieties.

INTRODUCTION

Coal is predominantly a macromolecular organic substance mainly derived from specific tissues of higher plants such as woody tissue, cuticles, spores, pollen, seeds and corkified cell walls which have undergone chemical alterations by the coalification process [1]. To some extent remains of these tissues can still be recognized by light microscopic investigation of coal. This type of recognition has led to the maceral concept: macerals are defined as microscopically recognizable entities in the coal matrix and shed light on the composition of coal and its original precursors.

Apart from this microscopic approach coal has also been analysed chemically for more than a century [2]. Elemental analysis and other bulk chemical analyses have been and still are important analytical techniques for characterizing coals. There is, however, increasing interest in the characterization of the structure of coal at the molecular level. Because of the macromolecular, insoluble nature of coal such a molecular characterization is more difficult than that of the other major fossil fuels, petroleum and natural gas. Spectroscopic techniques such as Fourier transform infrared and solid-state ^{13}C NMR spectroscopy have been used but do not

☆ Delft Organic Geochemistry Unit Contribution 277.

☆☆ Present address: Escola Universitària Politècnica de Manresa, UPC, Av. Bases de Manresa 61-73, 08240 Manresa, Spain.

0021-9673/92/$05.00

provide information on the arrangement of atoms. Specific chemical degradation reactions have also been applied to coals to identify the structures of released moieties (*e.g.*, [3,4]). However, the yields are relatively low or the information is limited owing to less specific chemical reagents. Analytical pyrolysis (controlled thermal degradation in an inert atmosphere) in combination with gas chromatography, mass spectrometry and gas chromatography–mass spectrometry can supply detailed molecular information on coal [5–8] and isolated maceral fractions [9–11]. These pyrolysis approaches in combination with spectroscopy have led to the recognition of resistant, selectively enriched biomacromolecules in coal derived from plant cuticles (cutan [12–15]), corkified cell walls (suberan [16]), spores and pollen (sporopollenin [17,18]), seed coats [19], woody tissues [20] and resins [21].

Organic sulphur in coal is not derived from the biomacromolecules present in plant tissues. It is formed by syndepositional incorporation of reduced inorganic sulphur species formed by microbial reduction of sulphate into the organic matrix (for reviews see [22,23]) which leads to the formation of organically bound sulphur. It is therefore that marine-influenced depositional environments generate coals which generally have a higher sulphur content. Since the presence of organic sulphur is of major environmental concern in the utilization of this fossil fuel resource, a better understanding of the formation, forms and distribution of organic sulphur in coal is required [22–24].

In this paper, the results of analysis by flash pyrolysis–gas chromatography (Py–GC) and flash pyrolysis–gas chromatography–mass spectrometry (Py–GC–MS) of five sulphur-rich brown coals from Spain are reported. The results indicate that under specific conditions the organic sulphur content can become so high (one sulphur atom for every 9–14 carbon atoms) that it is appropriate to define a new type of kerogen, Type III-S.

EXPERIMENTAL

Coal samples

Five brown coal samples were selected from three different sedimentary basins in Spain. Three samples were taken from the Maestrazgo basin, which is located in the Iberian mountain chain and the southern sector of the Catalan coastal range in NE Spain. Two of these samples (Estercuel and Portalrubio) are from the Utrillas formation and were both deposited in proximal areas of a delta estuary during the middle Albian (upper Lower Cretaceous, *ca.* 105 Ma). These coals have high sulphur contents (see Table I). This is possibly due to an influx of sulphate resulting from weathering of gypsum of the evaporitic Keuper formation in the catchment area into the delta estuary [25]. This resulted in significant sulphate reduction which, in turn, led to reaction of organic matter with reduced forms of inorganic sulphur. It is noteworthy that these conditions have led to a higher sulphur content of the coals deposited in proximal areas than in coals from the same basin derived from marine influenced depositional environments [25]. The Paula lignite was collected from sediments of the same basin and is thought to be of Tertiary age.

One sample was taken from the Mequinenza subbasin which is located in the SE margin of the large Catalan Ebre (Ebro) basin. The Mequinenza basin is mainly filled with carbonate sediments deposited in an extensive, shallow, open palaeolake. The coal-bearing carbonate sequences were deposited in the open lacustrine zones closer to marginal evaporitic and marsh environments in the Oligocene (*ca.* 35 Ma) [26,27].

The Rubielos coal is from a basin located in the SE part of the Iberian mountain chain (NE Spain), which belongs to a Miocene (*ca.* 14 Ma) lacustrine system where lignites were deposited in the middle unit and are interbedded with lacustrine limestones which contain significant amounts of immature organic matter [28,29].

Sample treatment

Two coal samples (Mequinenza and Rubielos) were Soxhlet extracted with dichloromethane–methanol (2:1, v/v) for 36 h. The other three were analysed as such.

Elemental analysis

Elemental analysis (C, H, N, $S_{tot.}$) were performed on Carlo Erba Model 1106 and 1500 elemental analysers. Duplicate analyses indicated good reproducibility. Ash contents were determined gravimetrically by heating the sample at 900°C for 2 h. Pyrite and $S_{org.}$ were determined according to ASTM methods.

Curie-point pyrolysis–gas chromatography

The brown coals were thermally degraded using a non-commercial Curie-point pyrolyser and ferromagnetic wires with a Curie temperature of 610°C. The brown coals were applied to the wire by pressing the samples on the wire [30]. The pyrolyser was mounted on the injection port of a Varian Model 3700 gas chromatograph. On-line separation of the flash pyrolysate was accomplished by using a fused-silica capillary column (25 m × 0.32 mm I.D.) coated with CP Sil-5 CB (film thickness 0.40 μm) (Chrompack, Middelburg, Netherlands). The oven of the gas chromatograph was temperature programmed from 0°C to 300°C at 3°C min^{-1} using a cryogenic unit. The oven was first held at 0°C for 5 min and finally at 300°C for 15 min. Helium was used as the carrier gas. Pyrolysis products were detected by simultaneous flame ionization detection (FID) and sulphur-selective flame photometric detection (FPD) using a stream splitter (SGE) at the end of the capillary column.

Curie-point pyrolysis–gas chromatography–mass spectrometry

The coal samples were thermally degraded using a Curie-point pyrolyser (FOM-3LX [31]) and ferromagnetic wires with a Curie temperature of 610°C. The pyrolyser was connected directly to a gas chromatograph (Hewlett-Packard Model 5890) in tandem with a magnetic sector mass spectrometer (VG-70S) by direct insertion of the capillary column into the ion source. The gas chromatograph was fitted with a fused-silica capillary column (25 m × 0.32 mm I.D.) coated with CP Sil-5 CB (film thickness 0.40 μm) in an oven that was temperature programmed from 0°C to 300°C at 3°C min^{-1}. The oven was first held at 0°C for 5 min and finally at 300°C for 15 min. Helium was used as the carrier gas. The mass spectrometer was set at an ionizing voltage of 70 eV and operated at a cycle time of 1.8 s over the mass range m/z 40–800 at a resolution of 1000. Date acquisition was started 1 min after pyrolysis.

RESULTS AND DISCUSSION

The five selected coal samples were thermally degraded using ferromagnetic wires with a Curie temperature of 610°C. The pyrolysates of the coals were analysed on-line by GC–MS. Compounds were identified by comparison of mass spectral and relative retention time data with literature data [32–36]. The total ion currents (TICs; Figs. 1A–5A) reveal the general composition of the pyrolysates. Although (alkyl)phenols, (alkyl)benzenes, (alkyl) naphthalenes, 1-pristene and *n*-alkanes and *n*-1-alkenes are major components in all pyrolysates, significant differences between the coals are observed. Large variations in the relative amounts of sulphur compounds (mainly alkylated thiophenes and benzo[*b*]thiophenes) are also noted. Hopanes and a series of higher-molecular-mass alkylbenzenes are only present in significant amounts in the Estercuel

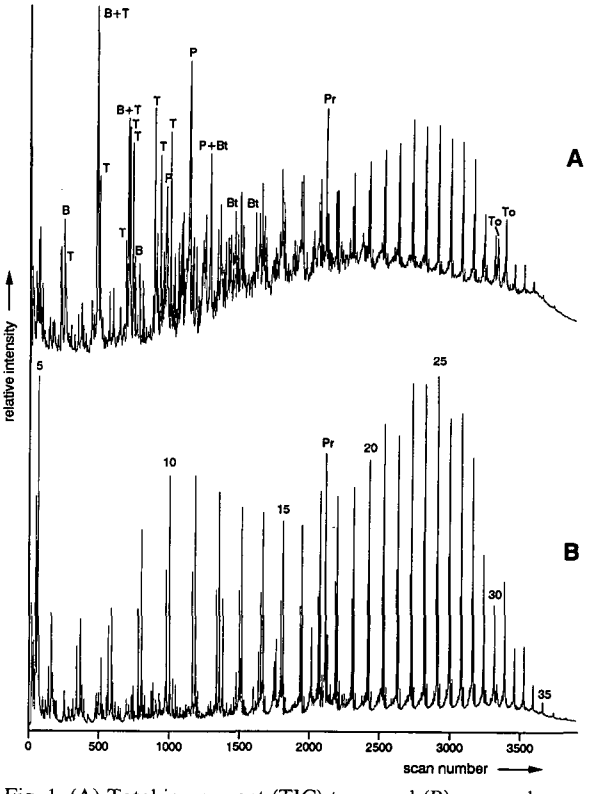

Fig. 1. (A) Total ion current (TIC) trace and (B) summed mass chromatogram of m/z 55 + 57 of the flash pyrolysate (Curie temperature 610°C) of the Mequinenza coal. Key for the TIC: B = (alkyl)benzenes; T = (alkyl)thiophenes; P = (alkyl)phenols; N = (alkyl)naphthalenes; Bt = (alkyl)benzothiophenes; D = 1,2-dihydroxybenzene; Pr = 1-pristene; To = tocopherols; H = hopanes. The number of carbon atoms of several members of the homologous series of *n*-1-alkenes and *n*-alkanes (series of doublets) in the m/z 55 + 57 mass chromatogram are indicated.

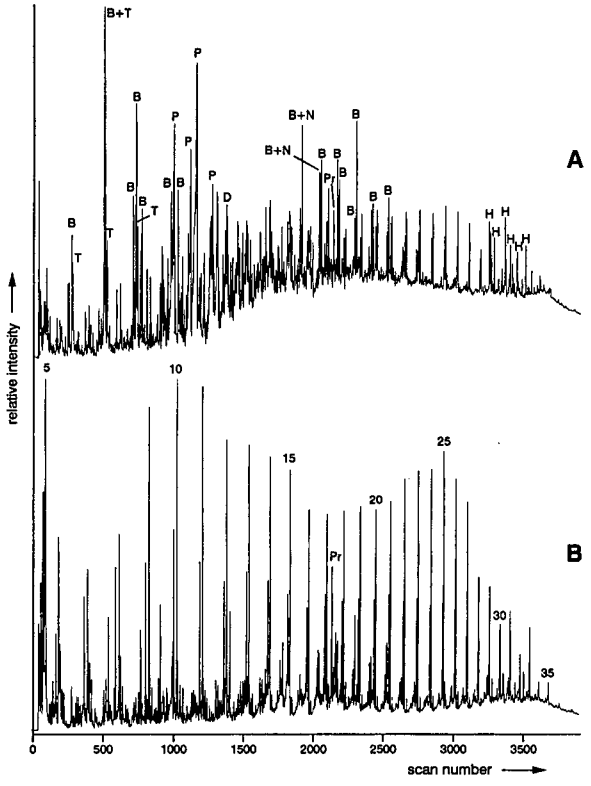

Fig. 2. (A) Total ion current (TIC) trace and (B) summed mass chromatogram of *m/z* 55 + 57 of the flash pyrolysate (Curie temperature 610°C) of the Estercuel coal. For the key to the symbols and numbers, see Fig. 1.

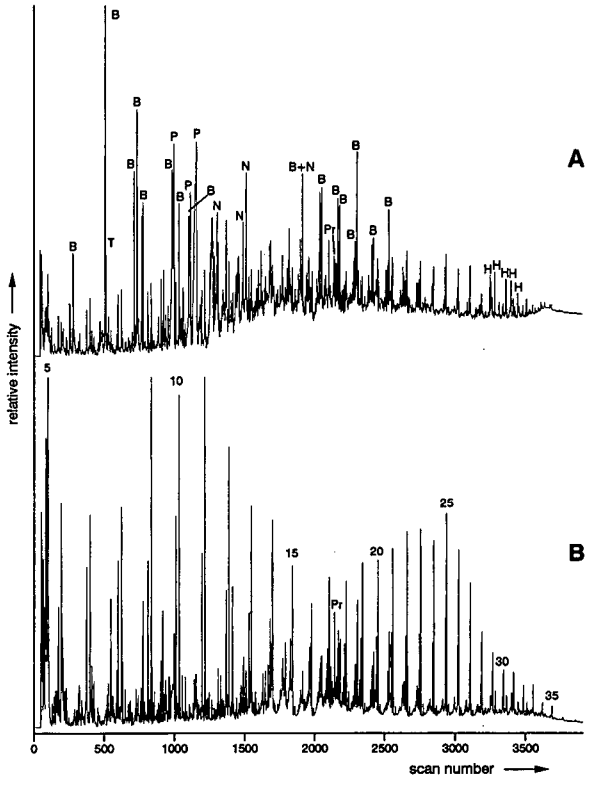

Fig. 3. (A) Total ion current (TIC) trace and (B) summed mass chromatogram of *m/z* 55 + 57 of the flash pyrolysate (Curie temperature 610°C) of the Portalrubio coal. For the key to the symbols and numbers, see Fig. 1.

and Portalrubio coal pyrolysates. Tocopherols are only abundant in the Mequinenza coal pyrolysate.

Aliphatic hydrocarbons

The distribution of the series of *n*-alkanes and *n*-1-alkenes are illustrated with the summed mass chromatogram of *m/z* 55 + 57 (Figs. 1B–5B), two major ions in the mass spectra of alkanes and alkenes. The abundance of these two homologous series of pyrolysis products in the TIC (Figs. 1A–5A) varies: they are the most abundant relative to the other, aromatic pyrolysis products in the pyrolysates of the Paula and, to a lesser extent, Mequinenza coals. As expected, these coals also have the highest atomic H/C ratios (Table I).

In four of the five pyrolysates (*i.e.*, those of the Estercuel, Portalrubio, Mequinenza and Paula coals) a clear bimodal distribution of the *n*-alkanes and *n*-1-alkenes is observed with maxima around C_{10} and C_{25}. It should be noted that in case of the unextracted coals (*i.e.*, Portalrubio, Estercuel and Paula) *n*-alkanes present as such in the coals are released in addition to the *n*-alkanes generated on thermal breakdown of the macromolecular matrix. This is especially evident in the pyrolysate of the Paula coal in which the C_{22}–C_{32} *n*-alkanes (the latter eluting compounds of the doublets) show an odd-over-even carbon number predominance which can be ascribed to the presence of epicuticular waxes [37].

The bimodal distribution of the *n*-alkanes and *n*-1-alkenes indicates the presence of at least two different macromolecular fractions in the coals. One of these is probably cutan, the highly aliphatic biomacromolecule present in the cuticules of higher plant leaves which on pyrolysis generates mainly a series of *n*-alkanes and *n*-1-alkenes optimizing in the C_{20}–C_{30} chain length range [12–15,38–40]. This

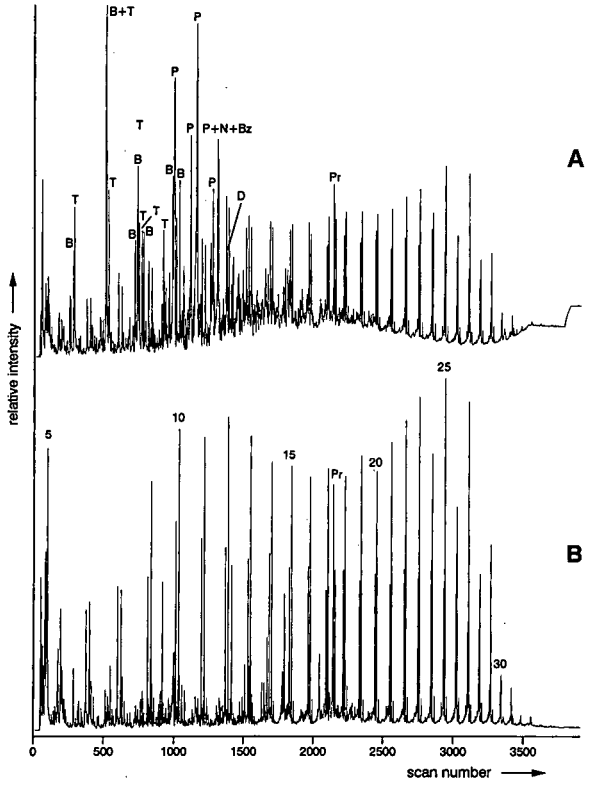

Fig. 4. (A) Total ion current (TIC) trace and (B) summed mass chromatogram of *m/z* 55 + 57 of the flash pyrolysate (Curie temperature 610°C) of the Paula coal. For the key to the symbols and numbers, see Fig. 1.

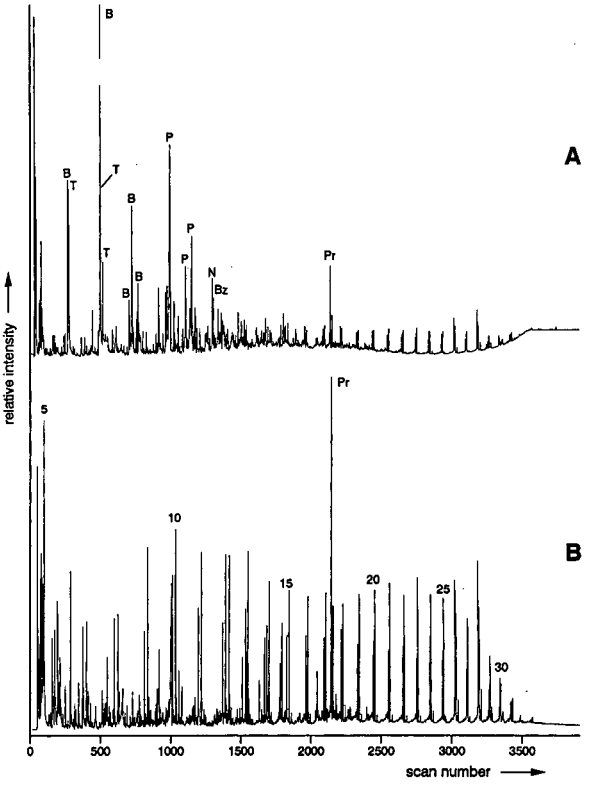

Fig. 5. (A) Total ion current (TIC) trace and (B) summed mass chromatogram of *m/z* 55 + 57 of the flash pyrolysate (Curie temperature 610°C) of the Rubielos coal. For the key to the symbols and numbers, see Fig. 1.

highly resistant biomacromolecule is selectively preserved during diagenesis and is, in case of coal formation, concentrated in the coal maceral cutinite [9–11]. In extant cuticles and in immature sediments these series of *n*-alkanes and *n*-1-alkenes are accompanied by a series of mainly long-chain methyl ketones [14]. The latter were found in the pyrolysate of the Paula coal but were below the detection limit in the other coal pyrolysates.

Other highly aliphatic biomacromolecular fractions which can be present in coal are suberan [16] and algaenan [40–45]. Suberan is a highly aliphatic biomacromolecule present in the outer bark tissue and explains the liptinitic nature of the coal maceral suberinite [16]. Algaenan is also a highly aliphatic biomacromolecule and is a major constituent of the outer cell walls of certain types of freshwater algae [40–45]. Alginite-rich coals probably contain these highly resistant algaenans. Recently, two other highly aliphatic biomacromolecules have been described in fossil spore walls (massulae) of water ferns [40] and in the inner coat (tegmen) of seeds of water plants [46]. These biomacromolecules can also explain, at least in part, the series of *n*-alkanes and *n*-1-alkenes in coal pyrolysates. Since all these different types of highly aliphatic biomacromolecules generate the same suite of compounds with distribution patterns depending on actual precursor organisms and stage of diagenesis, it is at present not possible to relate more specifically the series of *n*-alkanes and *n*-1-alkenes to one or more of the above-mentioned plant organs.

1-Pristene is a major component in all coal pyrolysates indicating the low stage of thermal maturity of the coals [47]. In the three unextracted coal samples it was possible to determine the pristane forma-

TABLE I

ELEMENTAL ANALYSIS, OPTICAL MEASUREMENT AND PYROLYSIS DATA FOR THE BROWN COALS STUDIED

Coal	Elemental analysis[a]											Pyrolysis			
	C (%)	H (%)	N (%)	$S_{org.}$ (%)	O[b] (%)	H/C	$S_{org.}/C$	O/C	Ash (%)	$S_{tot.}$ (%)	Pyrite (%)	$\bar{R}_o$[f] (%)	TR[c]	$S_{org.}/C$ (estimated)	PFI[d]	$\bar{R}_o$ (%)[f] (estimated)
Mequinenza	60.6	5.3	1.0	10.1	23.0	1.05	0.062	0.28	13.9	11.5	1.2	0.31	1.60	0.11	nd	nd
Estercuel	73.2	5.8	0.7	3.2	17.1	0.95	0.016	0.18	19.2	4.4	2.3	0.39	0.44	0.03	0.19	0.42
Portalrubio	73.5	4.4	0.8	1.3	20.0	0.72	0.007	0.20	17.4	3.0	1.7	0.47	0.13	0.01	0.32	0.46
Paula	51.8	5.3	1.2	5.2	36.5[e]	1.23	0.037	0.53[e]	40.0	10.3	5.0	0.35	0.57	0.04	0.09	<0.04
Rubielos	45.6	3.8	1.5	3.2	45.9[e]	1.00	0.026	0.75[e]	15.4	4.2	0.8	0.34	0.24	0.02	nd	nd

[a] On a dry and ash-free basis except for ash, total sulphur and pyrite contents, which are on a dry weight basis.
[b] By difference.
[c] TR = Thiophene ratio = (2,3-dimethylthiophene)/[(1,2-dimethylbenzene)+(*n*-1-nonene)].
[d] PFI = Pristane formation index = (pristane)/[(pristane)+(prist-1-ene)+(prist-2-ene)].
[e] These values are extremely high and probably erratic. Interpretation of these values should be performed with great caution.
[f] $\bar{R}_o$ = Mean random vitrinite reflectance (oil).

tion index (PFI), which is defined as [pristane]/{[pristane]+[1-pristene]+[2-pristene]} [47] and was measured from peak-height data in the *m/z* 55 + 57 mass chromatograms (Table I). Comparison with literature data of the Mahakam coal sequence [47] led to an estimate of the thermal maturity level in terms of vitrinite reflectance values (Table I). In the Estercuel, Portalrubio and Paula coals the calculated values agree surprisingly well with the measured values of vitrinite reflectance. These data confirmed the relatively low level of thermal maturity. Interestingly, the coals which yielded very similar pyrolysates (Estercuel and Portalrubio; *cf.*, Figs. 2A and 3A; see also later) do not have the same level of thermal maturity; the Portalrubio coal is more mature than the Estercuel coal.

It is thought that 1-pristene (and 2-pristene) are derived from thermal breakdown of macromolecularly bound tocopherols [48]. The abundance of tocopherols in the extracted Mequinenza coal (Figs. 1A and 6) support this idea. It is not completely understood why in the other coal pyrolysates tocopherols are much lower whereas 1-pristene is still a significant pyrolysis product (Figs. 2A–5A).

Hopanes are significantly present in the pyrolysates of the Estercuel and Portalrubio coals (Figs. 2A and 3A). Fig. 7 shows a partial accurate mass chromatogram of *m/z* 191 revealing the distribution of the triterpanes in the Portalrubio coal pyrolysate. The distribution in the Estercuel coal pyrolysate is very similar to that shown in Fig. 7. All identified triterpanes belong to the hopane family; no triterpanes characteristic of higher land plants, such as oleananes or ursanes, were found. The abundance of hopanes relates to a contribution from bacteria to the coals.

Phenols and benzenediols

All pyrolysates contain abundant phenol and C_1–C_3 alkylated phenols. No major differences in their distribution patterns were observed with the exception of the Rubielos coal pyrolysate where phenol is the most abundant component whereas in the other pyrolysates 3- and 4-methylphenol (which co-elute on the stationary phase used) are the most abundant. In addition 1,2-benzenediol and C_1-alkylated 1,2-benzenediols are important pyrolysis products in the pyrolysates. The well known pyrolysis products of lignin, 4-alkyl-2-methoxyphenols and 4-alkyl-2,6-dimethoxyphenols [49], are not important pyrolysis products in these brown coals.

Similar distributions of phenols and benzenediols have been reported for pyrolysates of fossil outer seed walls (testae) of water plants and the Beulah

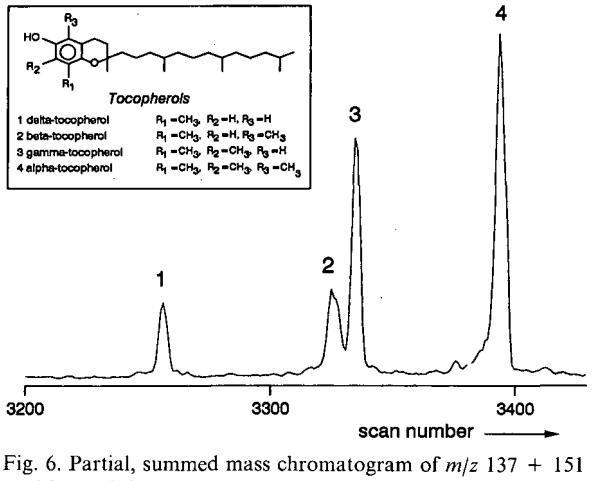

Fig. 6. Partial, summed mass chromatogram of *m/z* 137 + 151 + 165 + 402 + 416 + 430 showing the distribution of the tocopherols in the flash pyrolysate (Curie temperature 610°C) of the Mequinenza coal. The inset shows the structures of the tocopherols.

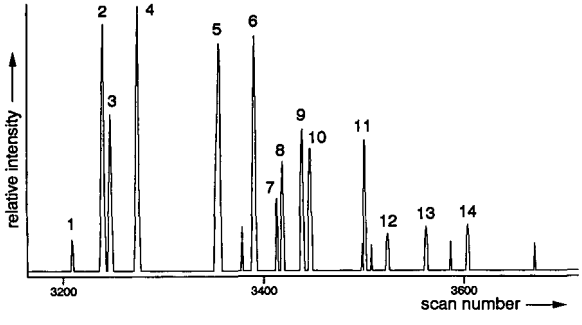

Fig. 7. Partial, accurate (mass window 0.04 dalton) mass chromatogram of *m/z* 191.22 revealing the distribution of the hopanes in the flash pyrolysate of the Portalrubio coal. Key: 1 = trisnorhopene; 2 = 22,29,30-trisnorhop-17,21-ene; 3 = 17α(H)-22,29,30-trisnorhopane; 4 = 17β(H)-22,29,30-trisnorhopane; 5 = 17α(H),21β(H)-30-norhopane; 6 = 17β(H),21α(H)-30-norhopane; 7 = hopene; 8 = 17α(H),21β(H)-hopane; 9 = 17β(H),21β(H)-30-norhopane; 10 = 17β(H),21α(H)-hopane; 11 = 17α(H),21β(H)-homohopane; 12 = 17β(H),21α(H)-homohopane; 13 = unknown hopane; 14 = 17β(H),21β(H)-homohopane.

Zap lignite [19]. At present, it is not clear whether the phenols encountered are derived from highly degraded lignin [20] or from a novel biomacromolecule, a polyphenol [19]. The first hypothesis is deemed unlikely by Van Bergen *et al.* [19] since the morphology of the testae of the fossil seeds is perfectly preserved. Such a preservation is unlikely if the underlying chemistry has been modified considerably. On the other hand, pyrolysates of recent angiosperm or gymnosperm wood, the major source of lignin-like materials in coal, contain only low relative amounts of phenols, which weakens the second hypothesis. Therefore, a straightforward interpretation of the origin of phenols in lignites and more mature coal pyrolysates cannot be made.

Sulphur compounds

The sulphur compounds present in the pyrolysates of the coals studied are dominated by hydrogen sulphide (as revealed by the FPD chromatograms) and (alkyl)thiophenes, although (alkyl)benzothiophenes were also present in all pyrolysates. Hydrogen sulphide is formed by thermal degradation of (poly)sulphide linkages in the macromolecular coal matrix whilst alkylthiophenes and -benzothiophenes are produced from sulphur-containing aromatic units [50].

The dominance of alkylthiophenes over alkylbenzothiophenes is consistent with the low level of thermal maturity of the brown coal samples [51]. The distribution patterns of the C_1–C_4 alkylthiophenes in the pyrolysates are relatively similar (Fig. 8). 2-Methylthiophene is in all cases the most abundant thiophene present. A difference is observed in the abundance of the C_{2+} alkylthiophenes relative to 2-methylthiophene: in the pyrolysate of the Mequinenza coal the C_{2+} alkylthiophenes are more abundant than in the pyrolysate of the Rubielos coal (*cf.*, Fig. 8A and C). In the latter pyrolysate C_4 alkylthiophenes are difficult to identify because of their low concentrations. In the C_2-cluster 2,4-dimethylthiophene is the most dominant component. This is a characteristic pattern for coal pyrolysates [23,50–53]. In kerogen pyrolysates 2,5- and 2,3-dimethylthiophene (compounds 4 and 6 in Fig. 8) are always more abundant than 2,4-dimethylthiophene [50–53]. The abundance of 3-isopropyl-2-methylthiophene (compound 14 in Fig. 8), especially in the Mequinenza coal pyrolysate, is noteworthy. This is

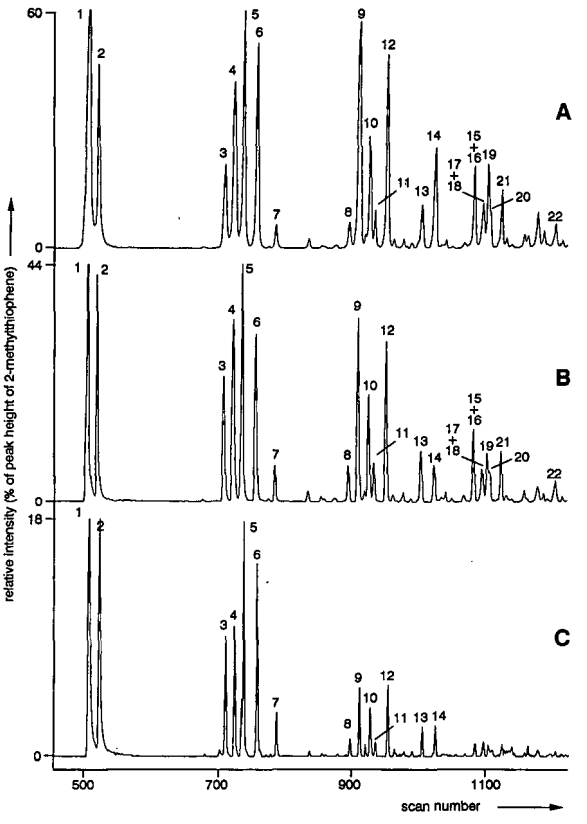

Fig. 8. Partial, accurate (mass window 0.02) summed mass chromatogram of *m/z* 97.01 + 98.01 + 111.03 + 112.03 + 125.03 + 126.03 + 139.03 + 140.03 illustrating the distribution of the C_1–C_4 alkylated thiophenes in the flash pyrolysates of the (A) Mequinenza, (B) Estercuel and (C) Rubielos coals. Key: 1 = 2-methylthiophene; 2 = 3-methylthiophene; 3 = 2-ethylthiophene; 4 = 2,5-dimethylthiophene; 5 = 2,4-dimethylthiophene; 6 = 2,3-dimethylthiophene; 7 = 3,4-dimethylthiophene; 8 = 2-propylthiophene; 9 = 2-ethyl-5-methylthiophene; 10 = 2-ethyl-4-methylthiophene; 11 = ethylmethylthiophene; 12 = 2,3,5-trimethylthiophene; 13 = 2,3,4-trimethylthiophene; 14 = 3-isopropyl-2-methylthiophene; 15 = 2-methyl-5-propylthiophene; 16 = 2,5-diethylthiophene; 17 = 2-butylthiophene; 18 = methylpropylthiophene; 19 = 2-ethyl-3,5-dimethylthiophene; 20 = ethyldimethylthiophene; 21 = 5-ethyl-2,3-dimethylthiophene; 22 = 2,3,4,5-tetramethylthiophene. Mass chromatograms are normalized on peak 5.

the first coal sample in which this compound is the most abundant C_4 alkylthiophene. 3-Isopropyl-2-methylthiophene has also been encoutered as a major compound in flash pyrolysates of kerogens from the Monterey Formation [54]. The structure of 3-isopropyl-2-methylthiophene suggests that it is

formed during pyrolysis via β-cleavage of macromolecular moieties in the coal matrix which were formed by incorporation of sulphur into 24-ethyl steroids [51]. The predominance of this compound in all coal pyrolysates can be rationalized by the fact that the major steroids biosynthesized by higher plants are compounds with an ethyl at C_{24} [55].

Although qualitatively no major differences were observed in thiophene composition, large variations in abundance relative to other pyrolysis products are evident (Figs. 1A–5A). The Mequinenza coal pyrolysate (Fig. 1) contains the highest amounts of alkylthiophenes relative to the other pyrolysis products. This is also reflected by the very high thiophene ratio (1.60, Table I), which is defined as [2,3-dimethylthiophene]/{[1,2-dimethylbenzene] + [*n*-1-nonene]} [52]. This ratio is obtained by integration of the appropriate peaks in the FID chromatogram of the pyrolysate. The thiophene ratio can be used to obtain an idea of the organic sulphur content of the samples pyrolysed [52]. Using the plot of the thiophene ratio *versus* atomic $S_{org.}/C$ ratios determined for a whole suite of samples as reported by Eglinton *et al.* [52], the $S_{org.}/C$ ratio of the Mequinenza coal can be estimated to be 0.11. Elemental analysis indicates an atomic $S_{org.}/C$ ratio of 0.062 (Table I), which suggests that the concentration of organic sulphur is overestimated by this approach. However, these measurements both indicate that this coal is extremely rich in organic sulphur (for every 9–14 carbon atoms it contains one sulphur atom). In this context, it should be noted that Orr [56] has defined organic sulphur-rich Type II kerogens as Type II-S kerogens when their atomic $S_{org.}/C$ ratios were larger than 0.04. Following the same definition, we propose here to classify the Mequinenza coal as a Type III-S kerogen characterized by a low atomic H/C and a high atomic $S_{org.}/C$ (>0.04) and O/C (>0.20) ratios. The other coal pyrolysates contain less abundant sulphur compounds (Figs. 2A–5A) as is also evident from their thiophene ratios (Table I). The Paula coal is, however, still fairly sulphur-rich and its estimated $S_{org.}/C$ ratio (Table I) indicate that it is has a composition close to that of a Type III-S kerogen, as confirmed by the elemental analysis data (Table I). The organic sulphur data obtained by Py–GC–MS show the same trends as the elemental composition data (Table I), although some discrepancies exist in absolute values.

An interesting observation is the significant difference in the abundance of alkylthiophenes in the pyrolysates of the Estercuel and Portalrubio coals, whereas the distribution of other pyrolysis products is very similar (see also the later discussion of extended alkylbenzenes), suggesting a very similar contribution of organic matter to these coals. This can be explained by the availability of inorganic sulphur species which are capable of reacting with the organic matter to form thiophene moieties in the coal matrix in the palaeodepositional environment. In the case of the depositional environment of the Portalrubio coal less inorganic sulphur species were available than in the case of the Estercuel depositional environment. A second explanation is the slightly higher level of thermal maturity of the Portalrubio coal; it is known that on increasing thermal stress organic sulphur is preferentially removed [51,57].

In the Rubielos coal pyrolysate a series of as yet unrecognized sulphur compounds were identified. Their presence was evident from the FPD chromatogram of the pyrolysate (Fig. 9), which contains a large peak not previously noted in other analyses of coal and kerogen samples [50–52]. The mass spectrum of this component (Fig. 9, inset) indicates that it is dimethyl tetrasulphide. The presence of four sulphur atoms in this molecule explains why the presence of this component in the pyrolysate leads to such a large peak in the FPD chromatogram (note also that the FPD instrument has a quadratic response). Dimethyl trisulphide and dimethyl disulphide were also identified in the pyrolysate. It was not possible to determine whether dimethyl sulphide was also present in the pyrolysate since the acquisition of mass spectra starts 1 min after pyrolysis. The geochemical significance of these dimethyl polysulphides in pyrolysates is as yet unknown but their formation by secondary reactions is unlikely because primary pyrolysis products are removed very rapidly from the heated zone. The presence of these dimethyl polysulphides may explain the discrepancy between the $S_{org.}/C$ ratio as estimated by the thiophene ratio and the higher atomic $S_{org.}/C$ ratio as determined by elemental analysis because the former determination takes only relative thiophene abundance into consideration which in case of the Rubielos coal will lead to an underestimation owing to the presence of dimethyl polysulphides in the pyrolysate.

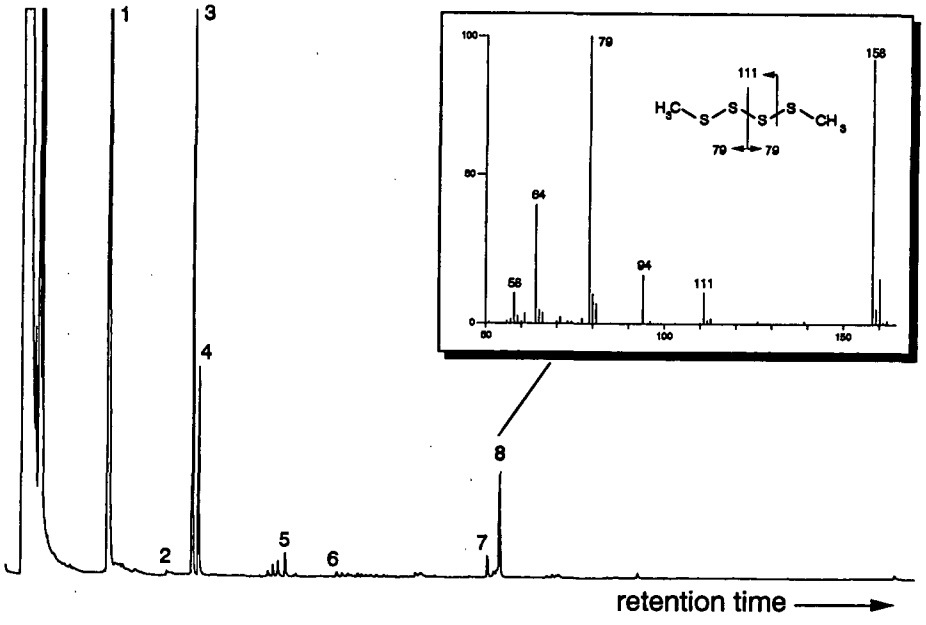

Fig. 9. Partial (0–90 min) FPD chromatogram (normalized on compound 3) of the pyrolysate of the Rubielos coal. Key: 1 = thiophene; 2 = dimethyl disulphide; 3 = 2-methylthiophene; 4 = 3-methylthiophene; 5 = 2,3-dimethylthiophene; 6 = dimethyl trisulphide; 7 = benzo[*b*]thiophene; 8 = dimethyl tetrasulphide. The inset shows the mass spectrum (corrected for background) of dimethyl tetrasulphide.

Alkylbenzenes

The C_1–C_4 alkylated benzenes are dominant pyrolysis products in all coal pyrolysates but no major differences were observed in their distribution patterns. Fig. 10 illustrates this statement; it shows the distributions in two coal pyrolysates in which some variation can be observed. For example, ethylbenzene (compound 2 in Fig. 10), propylbenzene (compound 7) and butylbenzene (compound 21) are relatively higher in the Portalrubio coal pyrolysate than in the Paula coal pyrolysate. In general, the alkylbenzene distributions are typical for those observed in coal pyrolysates [58]. The relatively low amounts of 1,2,3,4-tetramethylbenzene reveals that photosynthetic sulphur bacteria are not major contributors of organic matter to these coals [58–61]. In case of the Rubielos coal pyrolysate a substantial reduction in the abundance of C_2–C_4 alkylbenzenes relative to toluene is observed, an observation also made in case of the alkylthiophenes.

Striking differences between the coal pyrolysates were observed in the distributions of long-chain alkylbenzenes. In most samples these compounds are dominated by monoalkylbenzenes; only the pyrolysates of Paula and Rubielos coals contain a series of 2-alkyltoluenes with a concentration of the same order of magnitude as the monoalkylbenzenes. The distributions of the monoalkylbenzenes in three representative pyrolysates are shown by partial mass chromatograms of m/z 91 + 92, the two most abundant ions in the mass spectra of monoalkylbenzenes (Fig. 11). In case of the Mequinenza and Rubielos coal pyrolysates (Fig. 11B and C), the concentration of the higher members of this series of compounds is only a few percent of the first member (*i.e.*, toluene). However, in case of the Estercuel (Fig. 11A) and Portalrubio (not shown but identical with that of Estercuel) coal pyrolysates, a second maximum is observed at C_{18}. Further, a second series of compounds eluting just before the monoalkylbenzenes is apparent in Fig. 11A. This second series has a maximum at C_{17} and a slight odd-over-even carbon number predominance in the C_{16}–C_{20} range, whereas the monoalkylbenzenes possess an even-over-odd carbon number predominance in this range. Mass spectra of the C_{17} mem-

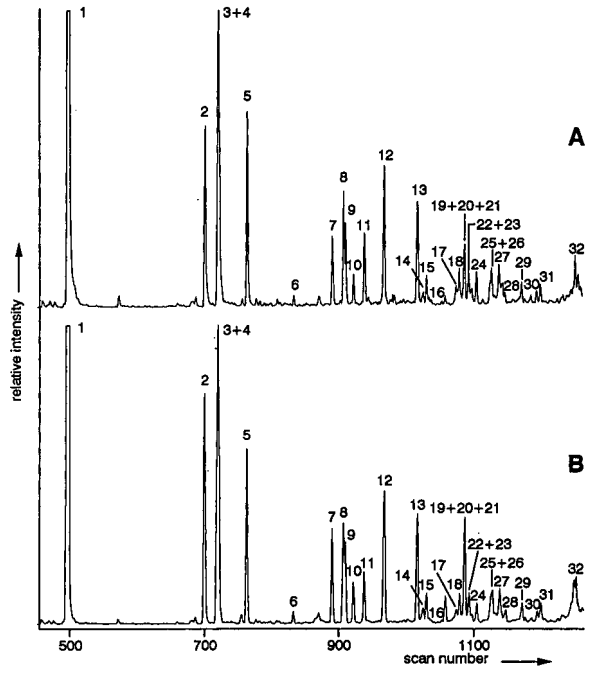

Fig. 10. Partial summed mass chromatograms of m/z 91 + 92 + 105 + 106 + 119 + 120 + 133 + 134 revealing the distributions of the C_1–C_4 alkylated benzenes in the flash pyrolysates of the kerogens of (A) Paula and (B) Portalrubio coal. Key: 1 = toluene; 2 = ethylbenzene; 3 = *m*-xylene; 4 = *p*-xylene; 5 = *o*-xylene; 6 = isopropylbenzene; 7 = propylbenzene; 8 = 1-ethyl-3-methylbenzene; 9 = 1-ethyl-4-methylbenzene; 10 = 1,3,5-trimethylbenzene; 11 = 1-ethyl-2-methylbenzene; 12 = 1,2,4-trimethylbenzene; 13 = 1,2,3-trimethylbenzene; 14 = 1-isopropyl-3-methylbenzene; 15 = 1-isopropyl-4-methylbenzene; 16 = 1-isopropyl-2-methylbenzene; 17 = 1,3-diethylbenzene; 18 = 1-methyl-3-propylbenzene; 19 = 1-methyl-4-propylbenzene; 20 = 1,4-diethylbenzene; 21 = butylbenzene; 22 = 1,2-diethylbenzene; 23 = 1-ethyl-3,5-dimethylbenzene; 24 = 1-methyl-2-propylbenzene; 25 = 2-ethyl-1,4-dimethylbenzene; 26 = 1-ethyl-2,4-dimethylbenzene; 27 = 1-ethyl-3,4-dimethylbenzene; 28 = 2-ethyl-1,3-dimethylbenzene; 29 = 1-ethyl-2,3-dimethylbenzene; 30 = 1,2,4,5-tetramethylbenzene; 31 = 1,2,3,5-tetramethylbenzene; 32 = 1,2,3,4- tetramethylbenzene. Mass chromatograms are normalized on peak 3 + 4. Semi-quantitative determination of the alkylbenzene abundances indicated that the concentration of 1,3- and 1,4-dimethylbenzene is 30% and 8% of the toluene concentration in the pyrolysates of the Paula and Portalrubio coal, respectively.

bers of these series (Fig. 12) indicated that the second (earlier eluting) series is most likely a linear alkylbenzene with an unsaturation in the side-chain. The characteristic fragment of m/z 104, which is present in all the mass spectra of this series, indicates that the double bond is not conjugated with the aromatic ring but reference mass spectra indicated that this fragment cannot be used to further assess the double bond position [62]. The formation of this ion is most likely induced by an α-hydrogen transfer. Mass chromatography of m/z 91 + 92, 104 and 230 of the C_{17} cluster (Fig. 13) reveals that, in addition to the major series described above, other minor components (compounds 1, 4 and 5 in Fig. 13) are present which possess similar mass spectra, suggesting that they are isomers of the major "104" component. This can be rationalized by the presence of isomers with the double bond in

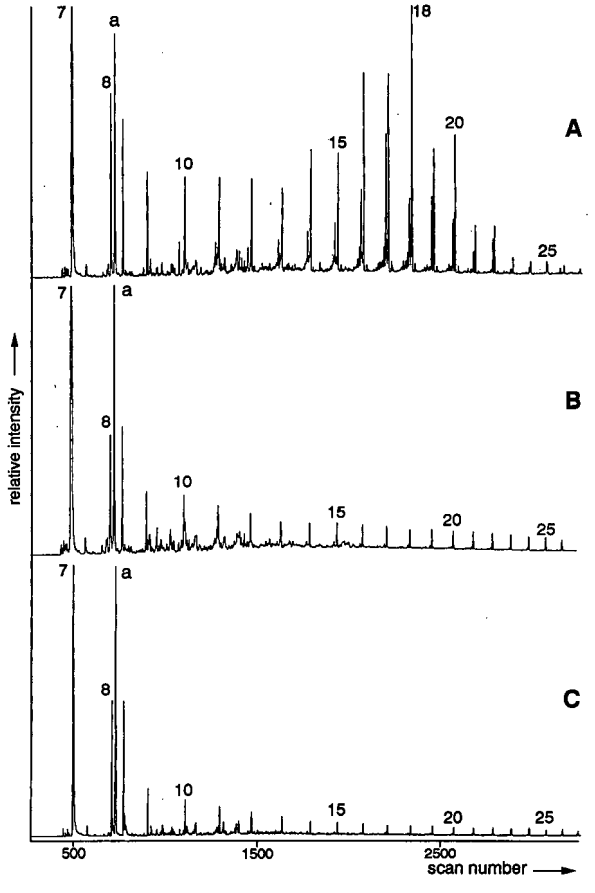

Fig. 11. Partial, summed mass chromatograms of m/z 91 + 92 revealing the distributions of alkylbenzenes in the flash pyrolysates of (A) Estercuel, (B) Mequinenza and (C) Rubielos coals. Numbers indicate total number of carbon atoms of this series of compounds. Mass chromatograms are normalized on 1,3- and 1,4-dimethylbenzene (peak a) in case of the Mequinenza and Rubielos coal pyrolysates and on dodecylbenzene in case of the Estercuel coal pyrolysate.

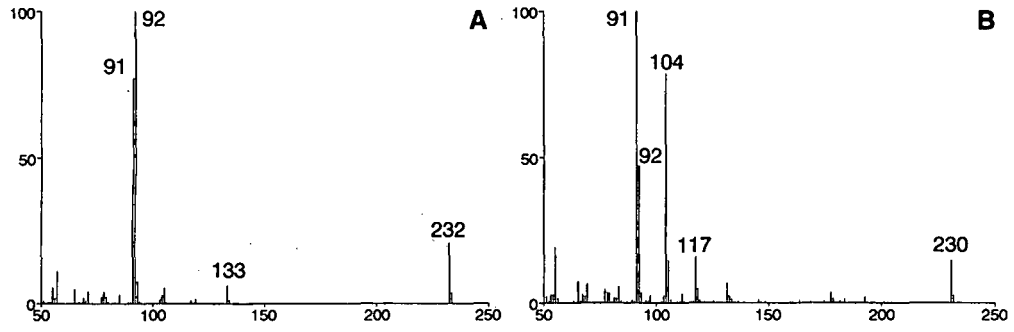

Fig. 12. Mass spectra (subtracted for background) of (A) *n*-undecylbenzene and (B) *n*-undec-11-enylbenzene obtained from the Py–GC–MS analysis of the Estercuel coal.

different positions and in different stereochemical configurations (*cis* and *trans*). By analogy with the retention behaviour of *n*-alkenes relative to *n*-alkanes [63], compound 2 in Fig. 13 is tentatively identified as undec-10-enylbenzene, compounds 3 and 4 as *cis*- and *trans*-undec-9-enylbenzene and the cluster of compounds indicated by 1 as monounsaturated undecylbenzenes with the double bond position at ω^3–ω^9.

To the best of our knowledge, a distribution of monoalkylbenzenes as observed in the Estercuel and Portalrubio coal pyrolysates has not yet been reported. This phenomenon probably indicates that the Estercuel and Portalrubio coals contain specific moieties from which these long-chain monoalkylbenzenes are generated. Similar distributions have been observed for homologous series of pyrolysis products generated from aromatic moieties (which preferentially cleave at the β-carbon–carbon bond of the alkyl side-chain): 2-alkyltoluenes, 2-alkyl-5-methylthiophenes and 2-alkyl-5-ethylthiophenes in the pyrolysate of the kerogen of the Guttenberg Oil Rock [59] and for 5-alkyl-1,3-benzenediols and mono- and dimethyl-5-alkyl-1,3-benzenediols in the pyrolysate of the kerogen of the Estonian kukersite [64]. In both studies these distributions were interpreted as caused by thermal degradation of a moiety (toluene, 2-methylthiophene, 2-ethylthiophene, 1,3-benzenediol and methylated 1,3-benzenediol) with a long alkyl chain bound to the macromolecular matrix via a heteroatom. The second maximum in the distribution can then be used to assess the position in the alkyl side-chain at which most of the moieties are bound to the macromolecular matrix. These interpretations are, to some extent, supported by pyrolysis of model compounds [60]. For example, flash pyrolysis of the sodium salt of 16-(4'-methylphenyl)hexadecanoic acid generates a suite of 4-alkyltoluenes with a maximum at C_{22}. Further, unsaturated counterparts are also formed and show

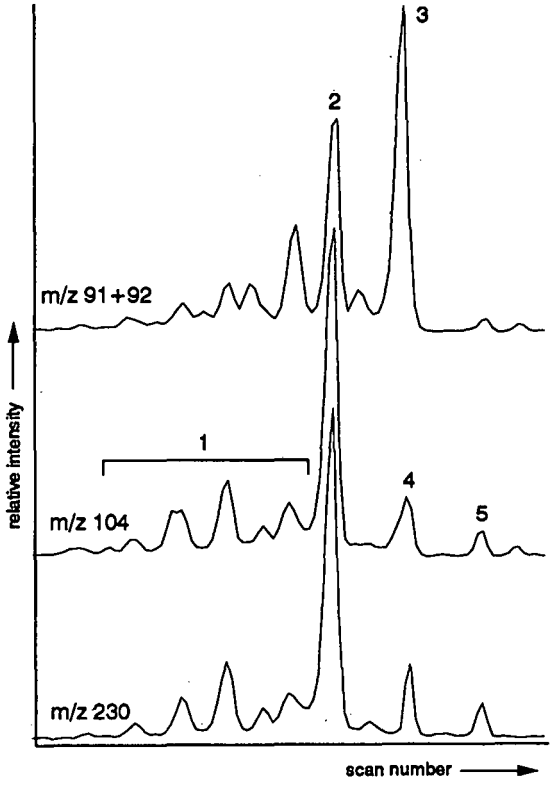

Fig. 13. Partial mass chromatograms of *m/z* 91 + 92, *m/z* 104 and *m/z* 230 of the pyrolysate of the Portalrubio coal.

a shift in their carbon number distribution by one carbon atom [60]. These data suggest that in case of the Estercuel and Portalrubio coal long-chain alkylbenzenes are present and are preferentially bound at position 12 in the alkyl side-chain of these moieties. At present we can only speculate on the heteroatom involved in the bonding of these moieties but on basis of the significant differences in organic sulphur content between the two coals (see above) and the abundance of oxygen (Table I), ether bonds are not unlikely.

Alkylnaphthalenes

Naphthalene and alkylated naphthalenes are important compounds in all pyrolysates, but are especially abundant in the Estercuel and Portalrubio coal pyrolysates. Fig. 14 (left panels) shows the distribution of naphthalene and its C_1–C_3 alkylated derivatives by summed mass chromatograms of m/z 128 + 141 + 142 + 155 + 156 + 169 + 170 (the major ions in the mass spectra of these compounds) in the pyrolysates of the Mequinenza, Estercuel, Paula and Rubielos coals. The distribution of the (alkyl)naphthalenes in the Estercuel and Portalrubio coals pyrolysates is virtually identical, illustrating again the similar composition of these two samples. Substantial differences are observed in the carbon number distributions of the naphthalenes: naphthalene is the most dominant component in the Rubielos coal pyrolysate whereas the C_1 and the C_3 alkylnaphthalenes dominate in the pyrolysates of the Mequinenza and Paula coals and Estercuel coal, respectively.

Significant differences are also observed in the internal distribution patterns. For example, the distribution of the C_2 alkylated naphthalenes (Fig. 14, middle panels) is similar for the Estercuel, Paula and Rubielos coal pyrolysates but substantially different from that of the Mequinenza coal pyrolysate. In the latter pyrolysate, 1,5-dimethylnaphthalene (compound 12 in Fig. 14) dominates whereas in the other pyrolysates 1,7-dimethylnaphthalene and/or 1,6-dimethylnaphthalene (compounds 9 and 10) are the most abundant C_2 alkylnaphthalene(s).

The distribution of the C_3 alkylnaphthalenes (Fig. 14, right panels) in the Estercuel, Portalrubio and Paula coal pyrolysates is similar and is dominated by 1,2,5-trimethylnaphthalene (compound 27). In case of the Estercuel and Portalrubio pyrolysates this compound is prominent in the TIC. The C_3 alkylnaphthalene distributions in the pyrolysates of the other two coals are not dominated by a specific isomer. It is worth noting that although the C_2 alkylnaphthalene distribution of the pyrolysate of the Rubielos coal is similar to that observed in the Paula and Estercuel coal pyrolysates, the C_3 alkylnaphthalene distribution is completely different (Fig. 14). In the pyrolysates where the C_3 alkylnaphthalenes are dominated by 1,2,5-trimethylnaphthalene the C_4 alkylnaphthalenes are also dominated by one specific isomer, 1,2,5,6-tetramethylnaphthalene (not shown). The concentration of this component is *ca.* 50% of the concentration of 1,2,5-trimethylnaphthalene. The co-occurrence of 1,2,5-trimethylnaphthalene and 1,2,5,6-tetramethylnaphthalene as major alkylnaphthalenes has been described before in extracts of coal and shale samples [65]. Püttmann and Villar [65] and De las Heras [66] attributed the predominance of these two specific polymethylnaphthalenes in the coal extracts to their diagenetic derivation from pentacyclic triterpenoids via 8,14-*seco*-triterpenoids. Such a derivation is in agreement with the abundance of hopanes in two of the three samples (*i.e.*, Estercuel and Portalrubio) with these characteristics. The coal samples examined by Püttmann and Villar [65] had a slightly higher level of thermal maturity (random vitrinite reflectance 0.58–0.83%) than the brown coals studied in this work. In the case of the brown coals these specific naphthalenes are probably generated mainly via thermal breakdown of the macromolecular matrix, suggesting that macromolecularly bound aromatized 8,14-*seco*-triterpenoids are the precursors of these compounds.

In the pyrolysates of the Estercuel and Portalrubio coals cadalene (4-isopropyl-1,6-dimethylnaphthalene) is an important component and the dominant C_5 alkylnaphthalene. Its co-occurrence with 1,6-dimethylnaphthalene as a major C_2 alkylnaphthalene can be ascribed to the presence of resin-derived material (resinite) in the coal samples [67].

CONCLUSIONS

The pyrolysates of the five brown coals all contain abundant *n*-alkanes, *n*-1-alkenes, (alkyl)phenols and alkyl(benzenes). The *n*-alkanes and *n*-1-

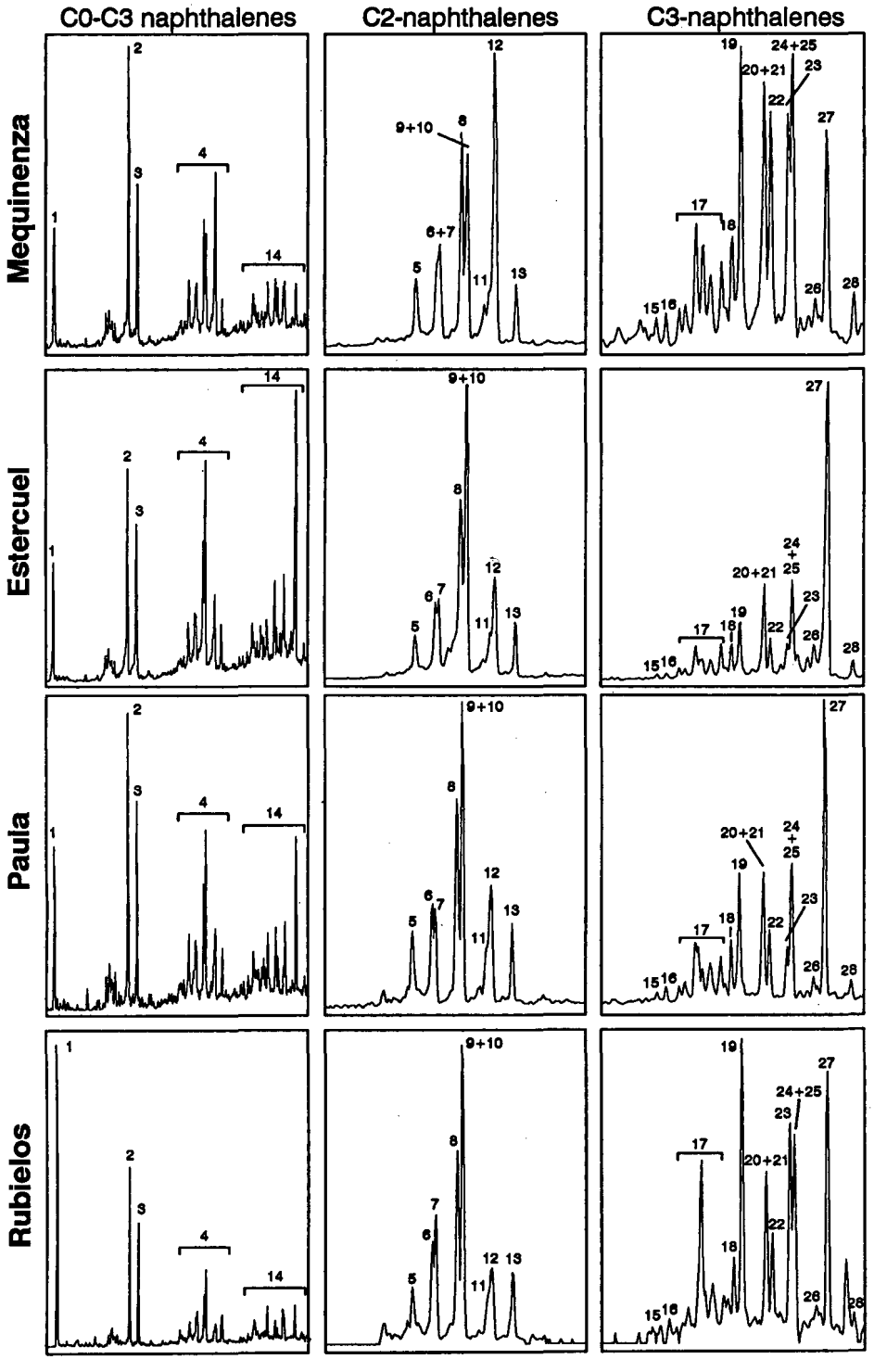

Fig. 14. Partial summed mass chromatograms of *m/z* 128 + 141 + 142 + 155 + 156 + 169 + 170 and *m/z* 156 and 170 illustrating the distribution of naphthalene and C_1–C_3 alkylated naphthalenes and the C_2 and C_3 naphthalenes, respectively, in the pyrolysates of the Mequinenza, Estercuel, Paula and Rubielos coals. Keys: 1 = naphthalene; 2 = 2-methylnaphthalene; 3 = 1-methylnaphthalene; 4 = C_2 naphthalenes; 5 = 2-ethylnaphthalene; 6 = 2,5-dimethylnaphthalene; 7 = 2,7-dimethylnaphthalene; 8 = 1,3-dimethylnaphthalene; 9 = 1,7-dimethylnaphthalene; 10 = 1,6-dimethylnaphthalene; 11 = 2,3- and 1,4-dimethylnaphthalene; 12 = 1,5-dimethylnaphthalene; 13 = 1,2-dimethylnaphthalene; 14 = C_4-naphthalenes; 15 = 2-propylnaphthalene; 16 = 1-propylnaphthalene; 17 = ethylmethylnaphthalenes; 18 = 1,3,7-trimethylnaphthalene; 19 = 1,3,6-trimethylnaphthalene; 20 = 1,4,6-trimethylnaphthalene; 21 = 1,3,5-trimethylnaphthalene; 22 = 2,3,6-trimethylnaphthalene; 23 = 1,2,7-trimethylnaphthalene; 24 = 1,6,7-trimethylnaphthalene; 25 = 1,2,6-trimethylnaphthalene; 26 = 1,2,4-trimethylnaphthalene; 27 = 1,2,5-trimethylnaphthalene; 28 = 1,2,3-trimethylnaphthalene.

alkenes are derived from thermal breakdown of aliphatic biomacromolecules such as cutan, algaenan and/or suberan whereas the (alkyl)phenols reflect the presence of highly degraded lignin or a polyphenol biomacromolecule. The short-chain alkylbenzenes cannot be ascribed to a specific source material in the brown coals. All pyrolysates contain 1-pristene as a major pyrolysis product. This probably reflects the presence of macromolecularly bound tocopherols. This was confirmed by the presence of significant amounts of a series of tocopherols in the pyrolysate in one extracted brown coal.

One of the five brown coal samples investigated is so rich in organic sulphur (one sulphur atom for every 9–14 carbon atoms) that it is appropriate to define a new kerogen type describing the kerogen contained in this coal. Type III-S kerogen is defined as a kerogen with high atomic $S_{org.}/C$ (> 0.04) and O/C ratios (> 0.20). The flash pyrolysates of such samples are dominated by sulphur compounds [mainly (alkyl)thiophenes and (alkyl)benzothiophenes] and (alkyl)phenols.

Two of the five brown samples investigated contain a series of long-chain alkylbenzenes with an unprecedented carbon number distribution pattern with a second maximum at C_{18}. This unusual distribution pattern is thought to originate from the presence of long-chain alkylbenzene moieties bound via a heteroatom (presumably an ether bond) to the macromolecular coal matrix preferentially at position 12 in the alkyl side-chain of these moieties. The origin of such moieties is unknown.

The (alkyl)naphthalene distributions in the pyrolysates of the brown coals show a large variation both in carbon number distribution and in predominance of specific isomers. The predominance of 1,2,5-trimethylnaphthalene together with 1,2,5,6-tetramethylnaphthalene is ascribed to the presence of macromolecularly bound, aromatized 8,14-*seco*-triterpenoids. The co-occurrence of 1,6-dimethylnaphthalene and cadalene as major naphthalene reveals the contribution of resin-derived material in some of the brown coals.

ACKNOWLEDGEMENTS

The authors thank Drs. P. Anadón, L. Cabrera and X. Querol for samples and geological data and H. Veld for vitrinite reflectance measurements. F. X. C. d.l. H. thanks la Caixa de Manresa for the fellowship "Beca Viatge de Recera a l'Europa Comunitària".

REFERENCES

1 E. Stach, G. H. Taylor, M. Th. Mackowsky, D. Chandra, M. Teichmüller and R. Teichmüller, *Stachs Textbook of Coal Petrology*, Gebrüder Borntraeger, Berlin, 3rd ed., 1982.
2 D. W. van Krevelen, *Coal. Typology, Chemistry, Physics and Constitution*, Elsevier, Amsterdam, 1961.
3 N. C. Deno, K. W. Curry, D. Jones, K. R. Keegan, W. G. Rakitsky, C. A. Richter and R. D. Minard, *Fuel*, 60 (1981) 210–212.
4 Ph. Blanc and P. Albrecht, *Org. Geochem.*, 17 (1991) 913–918.
5 G. van Graas, J. W. de Leeuw and P. A. Schenck, *J. Anal. Appl. Pyrol.*, 2 (1980) 265–276.
6 G. van Graas, J. W. de Leeuw and P. A. Schenck, in A. G. Douglas and J. R. Maxwell (Editors), *Advances in Organic Geochemistry 1979*, Pergamon Oxford, 1980, pp. 211–217.
7 M. Nip, J. W. de Leeuw, P. A. Schenck, H. L. C. Meuzelaar, S. A. Stout, P. H. Given and J. J. Boon, *J. Anal. Appl. Pyrol.*, 8 (1985) 221–239.
8 M. Nip, W. Genuit, J. J. Boon, J. W. de Leeuw, M. Blazlo and T. Szekely, *J. Anal. Appl. Pyrol.*, 11 (1987) 125–147.
9 M. Nip, J. W. de Leeuw and P. A. Schenck, *Geochim. Cosmochim. Acta*, 52 (1988) 637–648.
10 M. Nip, J. W. de Leeuw, P. A. Schenck, W. Windig, H. L. C. Meuzelaar and J. C. Crelling, *Geochim. Cosmochim. Acta*, 53 (1989) 671–683.
11 M. Nip, J. W. de Leeuw, P. A. Schenck and J. C. Crelling, *Energy Fuels*, 6 (1992) 125–136.
12 M. Nip, E. W. Tegelaar, J. W. de Leeuw, P. A. Schenck and P. J. Holloway, *Naturwissenschaften*, 73 (1986) 579–585.
13 M. Nip, E. W. Tegelaar, H. Brinkhuis, J. W. de Leeuw, P. A. Schenck and P. J. Holloway, *Org. Geochem.*, 10 (1986) 769-778.
14 E. W. Tegelaar, J. W. de Leeuw, C. Largeau, S. Derenne, H.-R. Schulten, R. Müller, J. J. Boon, M. Nip and J. C. M. Sprenkels, *J. Anal. Appl. Pyrol.*, 15 (1989) 29–54.
15 E. W. Tegelaar, J. H. F. Kerp, H. Visscher, P. A. Schenck and J. W. de Leeuw, *Palaeobiology*, 17 (1991) 133–144.
16 E. W. Tegelaar, *Ph.D. Thesis*, Delft University of Technology, Delft, 1990, pp. 115–134.
17 P. A. Schenck, J. W. de Leeuw, G. van Graas, J. Haverkamp and M. Bouman, in J. Brooks (Editor), *Organic Maturation Studies and Fossil Fuel Exploration*, Academic Press, New York, 1981, pp. 225–237.
18 W. J. Guilford, D. M. Schneider, J. Labovitz and S. J. Opella, *Plant Physiol.*, 86 (1988) 134–136.
19 P. F. van Bergen, M. E. Collinson, J. S. Sinninghe Damsté and J. W. de Leeuw, *Am. Chem. Soc. Div. Fuel Chem. Prepr.*, 36 (1991) 698–701.
20 P. G. Hatcher, *Org. Geochem.*, 16 (1990) 959–968.
21 B. G. K. van Aarssen, H. C. Cox, P. Hoogendoorn and J. W. de Leeuw, *Geochim. Cosmochim. Acta*, 54 (1990) 3021–3031.
22 D. J. Casagrande, in A. C. Scott (Editor), *Coal and Coal-bearing Strata: Recent Advances*, Publication No. 32, Geological Society London, 1987, pp. 87–105.

23 J. S. Sinninghe Damsté and J. W. de Leeuw, *Fuel Process. Technol.*, 30 (1992) 109–178.
24 L. M. Stock, R. Wolny and B. Bal, *Energy Fuels*, 3 (1989) 651–661.
25 X. Querol, R. Salas, G. Pardo and L. Ardevol, *Int. J. Coal Geol.*, 11 (1989) 171–189.
26 L. Cabrera and A. Saez, *J. Geol. Soc. London*, 144 (1987) 451–461.
27 L. Cabrera, F. Colombo and S. Robles, in M. Misla and S. Rosell (Editors), *Excursion Guide Book of the 6th European Regional Meeting of the International Association of Sedimentologist*, Excursion No. 10, 1985, pp. 394–492.
28 P. Anadón, L. Cabrera, R. Julia, E. Roca and L. Rosell, *Palaeogeogr. Palaeoclimat. Palaeoecol.*, 70 (1989) 7–28.
29 P. Anadón, L. Cabrera and R. Julia, in A. J. Fleet, K. Kelts and M. R. Talbot (Editors), *Lacustrine Petroleum Source Rocks*, Special Publication No. 40, Geological Society London, 1988, pp. 353–367.
30 A. Venema and J. Veurink, *J. Anal. Appl. Pyrol.*, 7 (1985) 207–213.
31 J. J. Boon, A. D. Pouwels and G. B. Eijkel, *Biochem. Soc. Trans.*, 15 (1987) 251–258.
32 M. L. Lee, D. L. Vassilaros, C. M. White and M. Novotny, *Anal. Chem.*, 51 (1980) 768–774.
33 S. J. Rowland, R. Alexander and R. I. Kagi, *J. Chromatogr.*, 294 (1984) 407–412.
34 J. S. Sinninghe Damsté, A. C. Kock-van Dalen, J. W. de Leeuw and P. A. Schenck, *J. Chromatogr.*, 435 (1988) 435–452.
35 P. G. Forster, R. Alexander and R. I. Kagi, *J. Chromatogr.*, 483 (1989) 384-389.
36 W. A. Hartgers, J. S. Sinninghe Damsté and J. W. de Leeuw, *J. Chromatogr.*, 606 (1992) 211–220.
37 G. Eglinton and R. J. Hamilton, in T. Swain (Editor), *Chemical Plant Taxonomy*, Academic Press, New York, 1963, pp. 187–217.
38 M. Nip, J. W. de Leeuw, P. J. Holloway, J. P. T. Jensen, J. C. M. Sprenkels, M. de Pooter and J. J. M. Sleeckx, *J. Anal. Appl. Pyrol.*, 11 (1987) 287–295.
39 E. W. Tegelaar, J. Wattendorf and J. W. de Leeuw, *Rev. Palaeobot. Palynol.*, in press.
40 J. W. de Leeuw, P. F. van Bergen, B. G. K. van Aarssen, J.-P. L. A. Gatellier, J. S. Sinninghe Damsté and M. E. Collinson, *Proc. R. Soc. London, Ser. B.*, 333 (1991) 329–337.
41 C. Largeau, S. Derenne, E. Casadevall, E. Kadouri and N. Sellier, *Org. Geochem.*, 10 (1986) 1023–1032.
42 A. Kadouri, S. Derenne, C. Largeau, E. Casadevall and C. Berkaloff, *Phytochemistry*, 27 (1988) 551–557.
43 K. Goth, J. W. de Leeuw, W. Püttmann and E. W. Tegelaar, *Nature (London)*, 336 (1989) 759–761.
44 E. W. Tegelaar, J. W. de Leeuw, S. Derenne and C. Largeau, *Geochim. Cosmochim. Acta*, 53 (1989) 3103–3106.
45 J.-P. L. A. Gatellier, J. W. de Leeuw, J. S. Sinninghe Damsté, S. Derenne, C. Largeau and P. Metzger, *Geochim. Cosmochim. Acta*, submitted for publication.
46 P. van Bergen, unpublished results.
47 H. Goossens, A. Due, J. W. de Leeuw, B. van der Graaf and P. A. Schenck, *Geochim. Cosmochim. Acta*, 52 (1988) 1189–1193.
48 H. Goossens, J. W. de Leeuw, P. A. Schenck and S. C. Brassell, *Nature (London)*, 312 (1984) 440–442.
49 C. Saiz-Jimenez and J. W. de Leeuw, *Org. Geochem.*, 6 (1984) 417–422.
50 J. S. Sinninghe Damsté, T. I. Eglinton, J. W. de Leeuw and P. A. Schenck, *Geochim. Cosmochim. Acta*, 53 (1989) 873–889.
51 T. I. Eglinton, J. S. Sinninghe Damsté, M. E. L. Kohnen, J. W. de Leeuw, S. R. Larter and R. L. Patience, in W. L. Orr and C. M. White (Editors), *Geochemistry of Sulfur in Fossil Fuels (ACS Symposium Series*, Vol. 429), American Chemical Society, Washington, DC, 1989, pp. 529–565.
52 T. I. Eglinton, J. S. Sinninghe Damsté, M. E. L. Kohnen and J. W. de Leeuw, *Fuel*, 69 (1990) 1394–1404.
53 T. I. Eglinton, J. S. Sinninghe Damsté, W. Pool, J. W. de Leeuw, G. Eijkel and J. J. Boon, *Geochim. Cosmochim. Acta*, 56 (1992) 1545–1560.
54 J. S. Sinninghe Damsté, T. I. Eglinton, W. I. C. Rijpstra and J. W. de Leeuw, in W. L. Orr and C. M. White (Editors), *Geochemistry of Sulfur in Fossil Fuels (ACS Symposium Series*, Vol. 429), American Chemical Society, Washington, DC, 1989, pp. 486–528.
55 W. R. Nes and M. L. McKean, *Biochemistry of Steroids and Other Isopentenoids*, University Park Press, Baltimore, 1977.
56 W. L. Orr, *Org. Geochem.*, 10 (1986) 499–516.
57 J. A. Gransch and J. Posthuma, in B. Tissot and F. Bienner (Editors), *Advances in Organic Geochemistry 1973*, Editions Technip, Paris, 1974, pp. 727–739.
58 W. A. Hartgers, J. S. Sinninghe Damsté and J. W. de Leeuw, *Geochim. Cosmochim. Acta*, submitted for publication.
59 A. G. Douglas, J. S. Sinninghe Damsté, M. G. Fowler, T. I. Eglinton and J. W. de Leeuw, *Geochim. Cosmochim. Acta*, 55 (1991) 275–291.
60 W. A. Hartgers, J. S. Sinninghe Damsté and J. W. de Leeuw, *Am. Chem. Soc. Div. Fuel Chem. Prep.*, 36 (1991) 790–795.
61 A. G. Requejo, J. Allan, S. Creaney, N. R. Cray and K. S. Cole, *Org. Geochem.*, in press.
62 F. W. McLafferty and D. B. Stauffer, *The Wiley/NBS Registry of Mass Spectral Data*, Wiley, New York, 1989.
63 J. S. Sinninghe Damsté, F. X. de las Heras, P. F. van Bergen and J. W. de Leeuw, *Geochim. Cosmochim. Acta*, 55 (1991) 3379–3385.
64 S. Derenne, C. Largeau, E. Casadevall, J. S. Sinninghe Damsté, E. W. Tegelaar and J. W. de Leeuw, *Org. Geochem.*, 16 (1990) 873–888.
65 W. Püttmann and H. Villar, *Geochim. Cosmochim. Acta*, 51 (1987) 3023–3029.
66 F. X. de las Heras, J. O. Grimalt, J. Albaiges, *Geochim. Cosmochim. Acta*, 55 (1991) 3387–3390.
67 B. G. K. van Aarssen, J. W. de Leeuw and B. Horsfield, *J. Anal. Appl. Pyrol.*, 20 (1991) 125–139.

Journal of Chromatography, 607 (1992) 377–379
Elsevier Science Publishers B.V., Amsterdam

CHROM. 24 381

Extraction of bituminous material from fossil organic matter using liquid carbon dioxide under liquid–vapour equilibrium conditions

F. Martin*, T. Verdejo and F. J. González-Vila

Instituto de Recursos Naturales y Agrobiologia, C.S.I.C., Apartado 1052, 41080 Seville (Spain)

ABSTRACT

Extracts from a peat, a low-rank coal and a bituminous oil shale obtained with liquid carbon dioxide were studied by capillary gas chromatography–mass spectrometry and compared with those obtained by Soxhlet extraction with *n*-hexane. Although the extraction yields with liquid carbon dioxide were lower, the composition of the extracts, comprising mainly a large variety of linear and cyclic hydrocarbons, was similar in both cases. Owing to the advantages of the liquid carbon dioxide extraction regarding speed, cleanliness and mildness of the extraction conditions, it seems to be an adequate procedure, coupled with gas chromatography–mass spectrometry, to study the biomarker composition of sedimentary organic matter.

INTRODUCTION

Soxhlet and sonication techniques have until now been the most widely used methods for extracting the bituminous fractions of sedimentary organic matter. The study of these extracts by chromatographic methods is the basis of the "biomarker technique", *i.e.* the isolation and characterization of biochemical products in geological samples, which can be related to data on the deposition medium and thermal history of the sediment. For such studies the selectivity is obviously the main concern if the extract amounts are sufficient to be studied by gas chromatography–mass spectrometry (GC–MS).

However, obtaining the extracts using the above procedures is time-consuming and requires the use of large volumes of flammable solvents, which creates disposal problems. Therefore, the use of supercritical fluids and liquids with higher than normal vapour pressures as extractants has opened up a new dimension in separation science (refs. 1 and 2 and references therein). Those fluids are faster, more economical and usually more efficient.

Supercritical carbon dioxide extraction (SFE) of coals and source rocks and its comparison with other conventional methods have been reported in the literature [3]. The advantages of the SFE are obvious and have often been described, but the availability of the necessary instrumentation still prevents the wider use of this technique.

As an alternative to extracting semivolatile and high-molecular-mass organic compounds from similar raw materials, we have used in our work a single and cost-effective apparatus that permits the use of liquid carbon dioxide under liquid–vapour conditions, previously used for extracting plant materials [1]. Both the yields of the extractions and the composition of the extracts as determined by GC–MS were compared with those obtained by extraction in Soxhlet with *n*-hexane (Merck, Darmstadt, Germany).

EXPERIMENTAL

The samples of peat and coal were taken from two closely sited deposits at Padul and Arenas del Rey (Granada, Spain), and the bituminous oil shale was from the Puertollano Basin (Ciudad Real,

0021-9673/92/$05.00

Spain). The main geological characteristics of the deposits, as well as the geochemical features of the samples, have been published elsewhere [4,5]. Before extraction, the samples were dried, milled and weighed in extraction cartridges.

An apparatus of the Jennings type [6] modified by Lentz [7] was used for the carbon dioxide extraction. The most important technical features have been described elsewhere [1]. Briefly, the high-pressure part consisted of a cylindrical autoclave of stainless steel. The top enclosure contained a cooling finger, a gauge and a valve for loading and discharging the carbon dioxide. The inner extraction apparatus consisted of a glass extraction thimble with a siphon and a separate glass vessel serving as reservoir for the evaporating extractant and for the storage of the extract. The apparatus has to operate in the two-phase region below the critical temperature. Hence temperature and pressure have to be below the critical values of 31.3°C and 7.39 MPa. As the temperature is influenced by the temperature of the coolant circulating in the cooling finger, we had to use cooling equipment. To ensure evaporation of the extractant, the bottom of the apparatus was kept in a water bath at 40°C. Carbon dioxide (Sociedad Española de Oxigeno, Spain) of 99.98% purity was transferred as a liquid from the storage vessel to the autoclave. The amount (around 180 g) was controlled by weighing the whole autoclave on normal scales.

The Soxhlet extraction was carried out with *n*-hexane, which is a solvent similar to the carbon dioxide in terms of solubility parameters [3] under the above working conditions (critical density of 0.468 g/cm^3).

GC–MS analysis was performed with a Hewlett-Packard (Palo Alto, CA, USA) 5988A interfaced to an HP 59979 data system. A 25 × 0.32 mm HPSE-52 capillary column was used with temperature programming to separate the extracted analytes.

RESULTS AND DISCUSSION

As shown in Fig. 1 the total ion chromatograms (TICs) of the carbon dioxide extracts of the oil shale (Fig. 1b), the peat (Fig. 1c) and the low-rank coal (Fig. 1d) are very complex, as is usual for the bituminous fraction from this type of sample. Greater

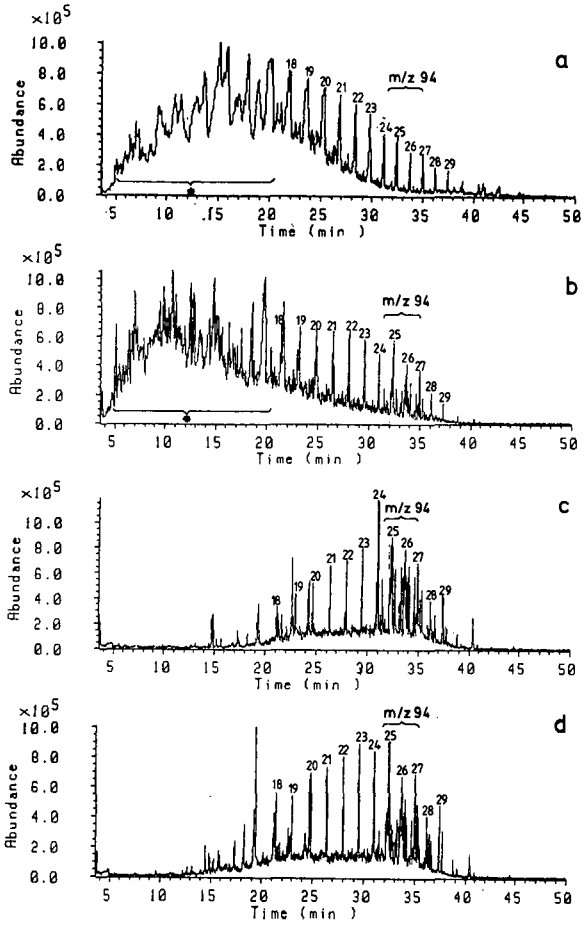

Fig. 1. Total ion chromatograms (TICs) of the *n*-hexane extraction of an oil shale (a) and the liquid carbon dioxide extracts from the same oil shale (b), a peat (c) and a low-rank coal (d). Peaks at *m/z* 94 represent artefacts introduced by the carbon dioxide. Numbers correspond to the chain lengths of *n*-alkanes. Most of the compounds marked with asterisks in (a) and (b) have been identified as series of alkyl cyclohexanes and bicyclic hydrocarbons.

similarity is apparent between the patterns of the samples of peat and low-rank coal than between these and that of the oil shale sample, in agreement with data previously obtained [5].

For comparative purposes the TICs of the Soxhlet *n*-hexane extract of the oil shale have been also included in the same figure (Fig. 1a). No great differences (less than 10%) in extraction yield were observed considering the same extraction time (1 h). Furthermore, the hydrocarbon patterns were equiv-

alent for both methods, although some differences were apparent. Thus, the recovery of light hydrocarbons is better by liquid carbon dioxide extraction, and some individual components are present in different amounts in each chromatogram.

Most of the peaks in each TIC could be identified by different procedures, including the monitoring of single diagnostic ions (SIMs) for some series present in small amount. The chemical nature of the most important homologous series detected is described in the caption to Fig. 1.

The most prominent peaks were series of *n*-alkanes in the range C_{14}–C_{32} for all the samples, although with different distributions. They are well-known biomarkers for evaluating the degree of maturity and the redox conditions during the diagenesis of the sediments.

In all the samples, series of branched alkanes of isoprenoid type in the range C_{14}–C_{18}, as well as polycyclic hydrocarbons from sesquiterpanes to tricyclic terpanes, were also detected. Only in the oil shale extracts, both with *n*-hexane and liquid carbon dioxide, were alkyl cyclohexanes (C_4–C_{10}) and some single aromatic compounds (mono- and dimethylbenzenes) found in the zone marked with asterisks in the TICs.

The distributions of all these compounds have also been widely used for the organic geochemical characterization of recent and ancient sediments.

Some dialkyl phthalates, well-known ubiquitous contaminants, were also detected in all the extracts. In addition, the carbon dioxide used introduced some artefacts (marked with their typical base peak at *m/z* 94 on the TICs), tentatively identified as benzyl derivatives of the carbonic acid. One representative mass spectrum is shown in Fig. 2. In any case, these compounds did not interfere in the detection of biomarker hydrocarbons.

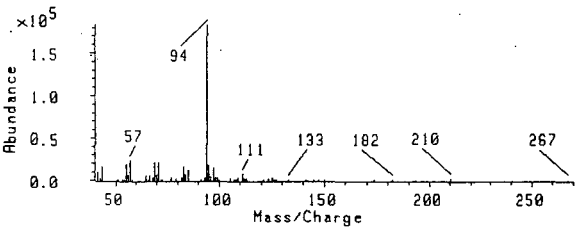

Fig. 2. Representative mass spectrum of one of the artifacts introduced by the carbon dioxide.

CONCLUSIONS

Although the organic geochemical significance of the differences found by comparing the different chromatographic extraction patterns, particularly the modifications of well-known compound ratios, should be evaluated with a wider set of samples, we can conclude that extraction with liquid carbon dioxide is a rapid, mild and clean procedure to study the biomarker composition of sedimentary organic matter.

ACKNOWLEDGEMENT

We thank the Spanish CICyT (Project PB 87/0277) for financial support.

REFERENCES

1 S. N. Naik, H. Lenz and R. C. Maheshwari, *Fluid Phase Equilib.*, 49 (1989) 115.
2 M. Richards and R. M. Campbell, *LC · GC Int.*, 4, No. 7 (1991) 33.
3 J. C. Monin, D. Barth, M. Perrut, M. Espitalié and B. Durand, *Org. Geochem.*, 13 (1988) 1079.
4 J. C. del Rio, F. J. Gonzalez-Vila and F. Martin, *Org. Geochem.*, 18 (1992) 67.
5 J. C. del Rio, J. Garcia-Molla, F. J. Gonzalez-Vila and F. Martin, *Org. Geochem.*, 1992, submitted for publication.
6 W. G. Jennings, *US Pat. 4.265.860* (1981).
7 H. Lentz, *German Utility Pat. G 8810 807.4* (1988).

Author Index

PUBLICATION SCHEDULE FOR 1992

Journal of Chromatography and *Journal of Chromatography, Biomedical Applications*

MONTH	O 1991–M 1992	J	J	A	S	O	N	D
Journal of Chromatography	Vols. 585–600	602/1 + 2 603/1 + 2 604/1	604/2 605/1 605/2 606/1	606/2 607/1 607/2	608/1 + 2 609/1 + 2			
Cumulative Indexes, Vols. 551–600		[a]						
Bibliography Section	610/1	610/2			611/1			611/2
Biomedical Applications	Vols. 573–577/1	577/2	578/1 578/2	579/1	579/2 580/1 + 2	[b]		

[a] Cumulative Indexes will be Vol. 601, to appear early 1993.
[b] The publication schedule for further issues will be published later.

INFORMATION FOR AUTHORS

(Detailed *Instructions to Authors* were published in Vol. 558, pp. 469–472. A free reprint can be obtained by application to the publisher, Elsevier Science Publishers B.V., P.O. Box 330, 1000 AH Amsterdam, The Netherlands.)

Types of Contributions. The following types of papers are published in the *Journal of Chromatography* and the section on *Biomedical Applications:* Regular research papers (Full-length papers), Review articles and Short Communications. Short Communications are usually descriptions of short investigations, or they can report minor technical improvements of previously published procedures; they reflect the same quality of research as Full-length papers, but should preferably not exceed five printed pages. For Review articles, see inside front cover under Submission of Papers.

Submission. Every paper must be accompanied by a letter from the senior author, stating that he/she is submitting the paper for publication in the *Journal of Chromatography*.

Manuscripts. Manuscripts should be typed in double spacing on consecutively numbered pages of uniform size. The manuscript should be preceded by a sheet of manuscript paper carrying the title of the paper and the name and full postal address of the person to whom the proofs are to be sent. As a rule, papers should be divided into sections, headed by a caption (*e.g.*, Abstract, Introduction, Experimental, Results, Discussion, etc.). All illustrations, photographs, tables, etc., should be on separate sheets.

Introduction. Every paper must have a concise introduction mentioning what has been done before on the topic described, and stating clearly what is new in the paper now submitted.

Abstract. All articles should have an abstract of 50–100 words which clearly and briefly indicates what is new, different and significant.

Illustrations. The figures should be submitted in a form suitable for reproduction, drawn in Indian ink on drawing or tracing paper. Each illustration should have a legend, all the *legends* being typed (with double spacing) together on a *separate sheet*. If structures are given in the text, the original drawings should be supplied. Coloured illustrations are reproduced at the author's expense, the cost being determined by the number of pages and by the number of colours needed. The written permission of the author and publisher must be obtained for the use of any figure already published. Its source must be indicated in the legend.

References. References should be numbered in the order in which they are cited in the text, and listed in numerical sequence on a separate sheet at the end of the article. Please check a recent issue for the layout of the reference list. Abbreviations for the titles of journals should follow the system used by *Chemical Abstracts*. Articles not yet published should be given as "in press" (journal should be specified), "submitted for publication" (journal should be specified), "in preparation" or "personal communication".

Dispatch. Before sending the manuscript to the Editor please check that the envelope contains four copies of the paper complete with references, legends and figures. One of the sets of figures must be the originals suitable for direct reproduction. Please also ensure that permission to publish has been obtained from your institute.

Proofs. One set of proofs will be sent to the author to be carefully checked for printer's errors. Corrections must be restricted to instances in which the proof is at variance with the manuscript. "Extra corrections" will be inserted at the author's expense.

Reprints. Fifty reprints of Full-length papers and Short Communications will be supplied free of charge. Additional reprints can be ordered by the authors. An order form containing price quotations will be sent to the authors together with the proofs of their article.

Announcement from the Publisher

ELSEVIER SCIENCE PUBLISHERS

prefers the submission of electronic manuscripts

Electronic manuscripts have the advantage that there is no need for the rekeying of text, thereby avoiding the possibility of introducing errors and resulting in reliable and fast delivery of proofs.

The preferred storage medium is a $5\frac{1}{4}$ or $3\frac{1}{2}$ inch disk in MS-DOS format, although other systems are welcome, e.g. Macintosh.

Your disk and (**exactly matching**) printed version (printout, hardcopy) should be submitted together to the accepting editor. In case of revision, the same procedure should be followed such that, on acceptance of the article, the file on disk and the printout are **identical**. Both will then be forwarded by the editor to Elsevier.

Please follow the general instructions on style/arrangement and, in particular, the reference style of this journal as given in 'Instructions to Authors'.

Please label the disk with your name, the software & hardware used and the name of the file to be processed.

Further information can be found under 'Instructions to Authors - Electronic manuscripts'.

Contact the Publisher for further information.

ELSEVIER SCIENCE PUBLISHERS B.V.
P.O. Box 330, 1000 AH Amsterdam
Netherlands
Fax: (+31-20) 5862-304

4/92